FINAL REPORT

APPENDIX A - K

Field Testing and Adaptation of a Methodology to Measure "In-Stream" Values in the Tongue River, Northern Great Plains (NGP) Region

by

Ken Bovee
James Gore
Dr. Arnold Silverman
University of Montana
Missoula, Montana

for the

U.S. Environmental Protection Agency
Rocky Mountain-Prairie Region
Office of Energy Activities
Contract No. 68-01-2653

OEA Coordinator: Denis Nelson
Project Officer: Loys Parrish

March, 1977

2\

R8
179

APPENDIX A

HYDROLOGIC CONTOUR MAPS

REARING AREAS

1. Direction of flow is from top of page to bottom

2. For easier interpretation, depth contours are indicated by vertical typeface. Velocity contours are indicated by slanting typeface.

3. Hatchered areas on contour maps indicate isolated areas of reduced depth or velocity, depending on the type of map.

4. Dashed lines indicate edge of water, either at banks or on exposed bars.

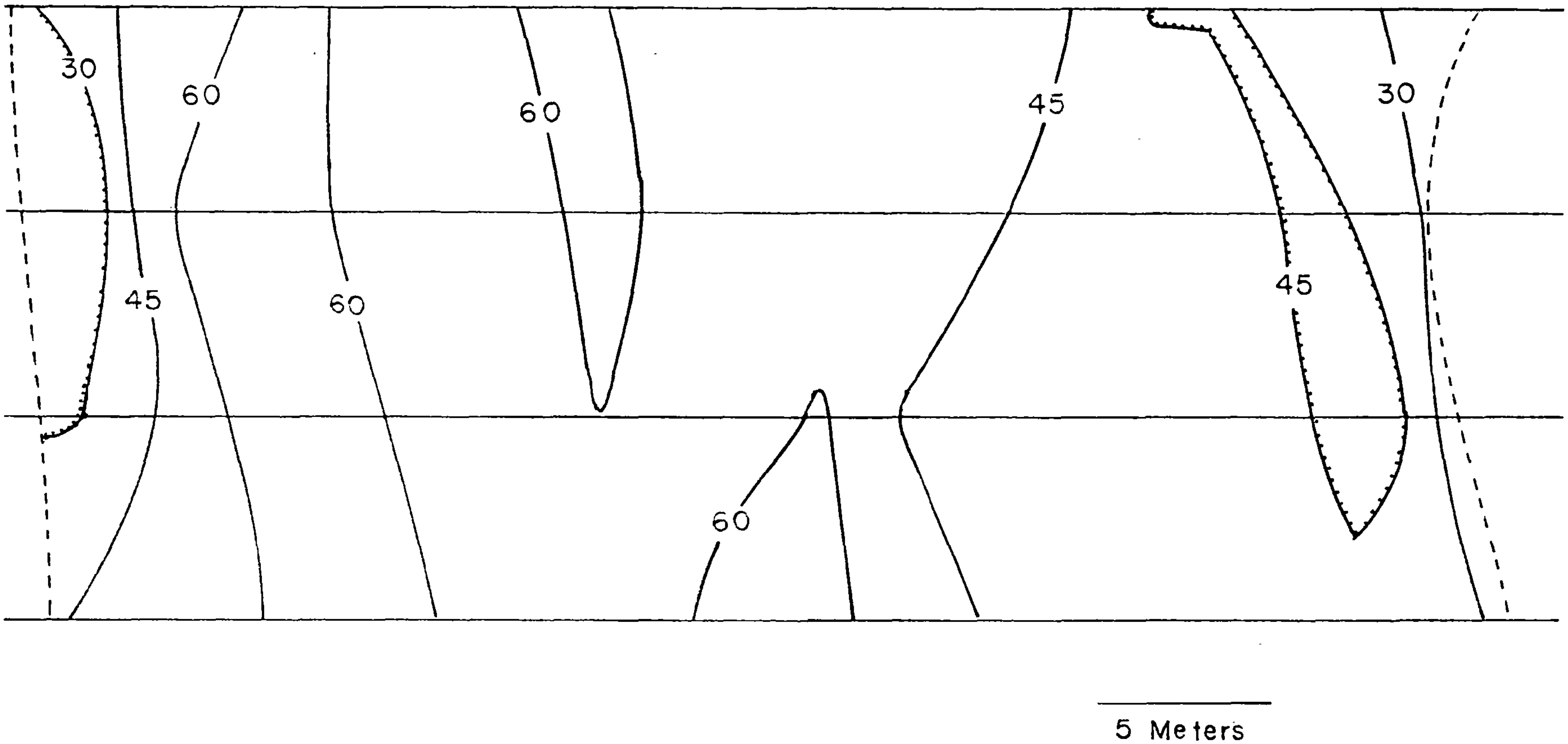

Figure A-1: Depth Contour Map from the Viall Mapping Section. Depths in cm.
Discharge = 19.4 cms.

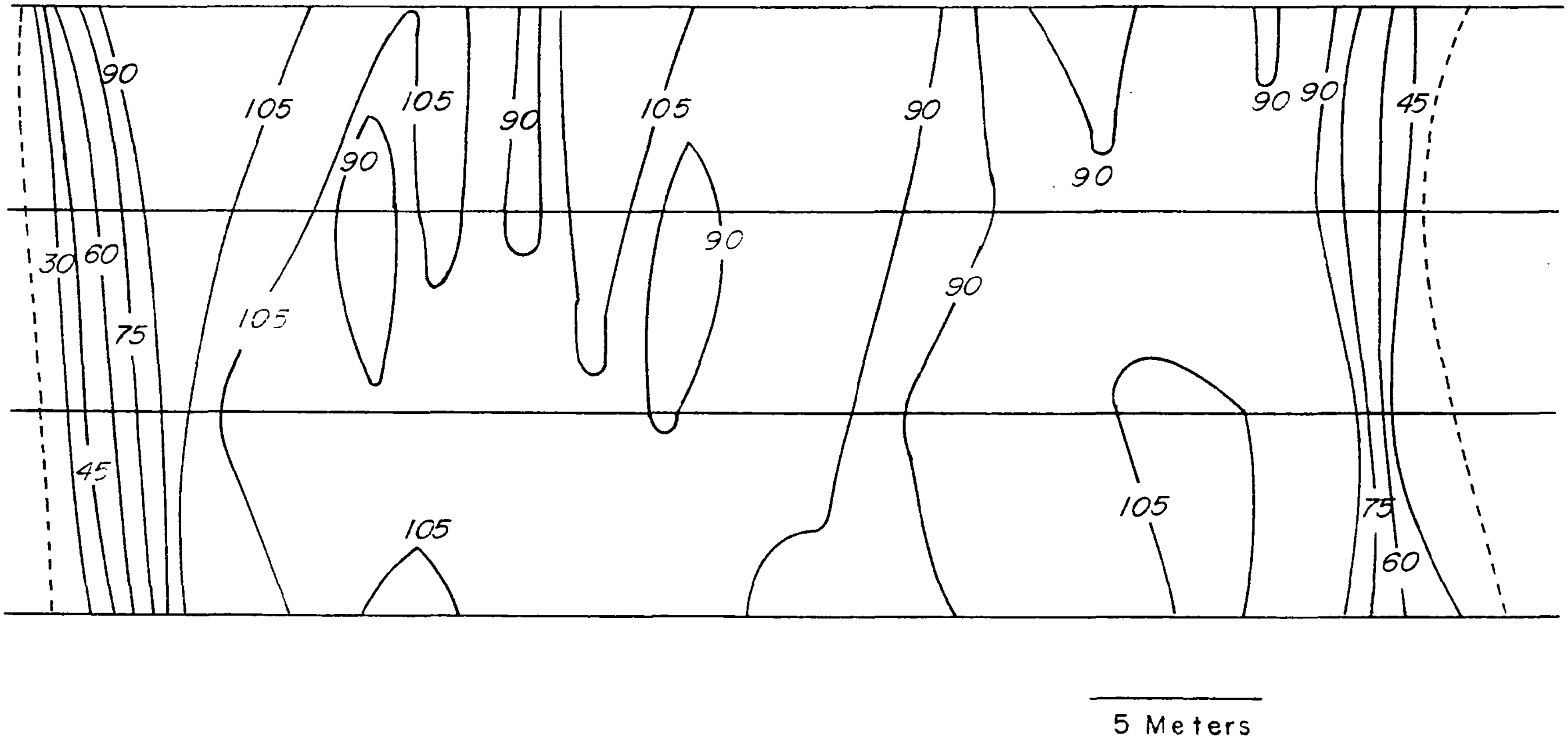

Figure A-2: Velocity Contour Map from the Viall Mapping Section. Velocities in cm./sec. Discharge = 19.4 cms.

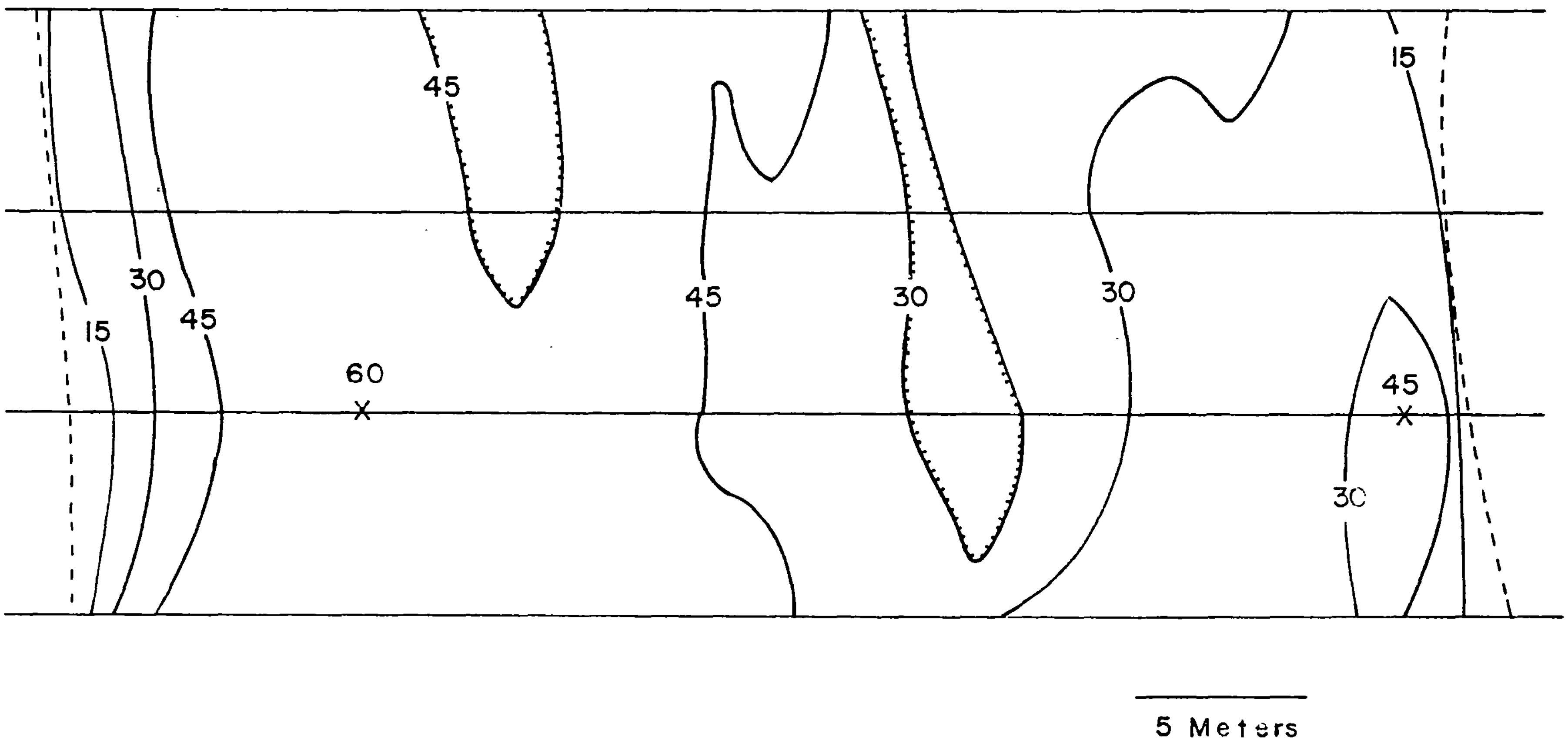

Figure A-3: Depth Contour Map from the Viall Mapping Section. Depths in cm.
Discharge = 12.0 cms.

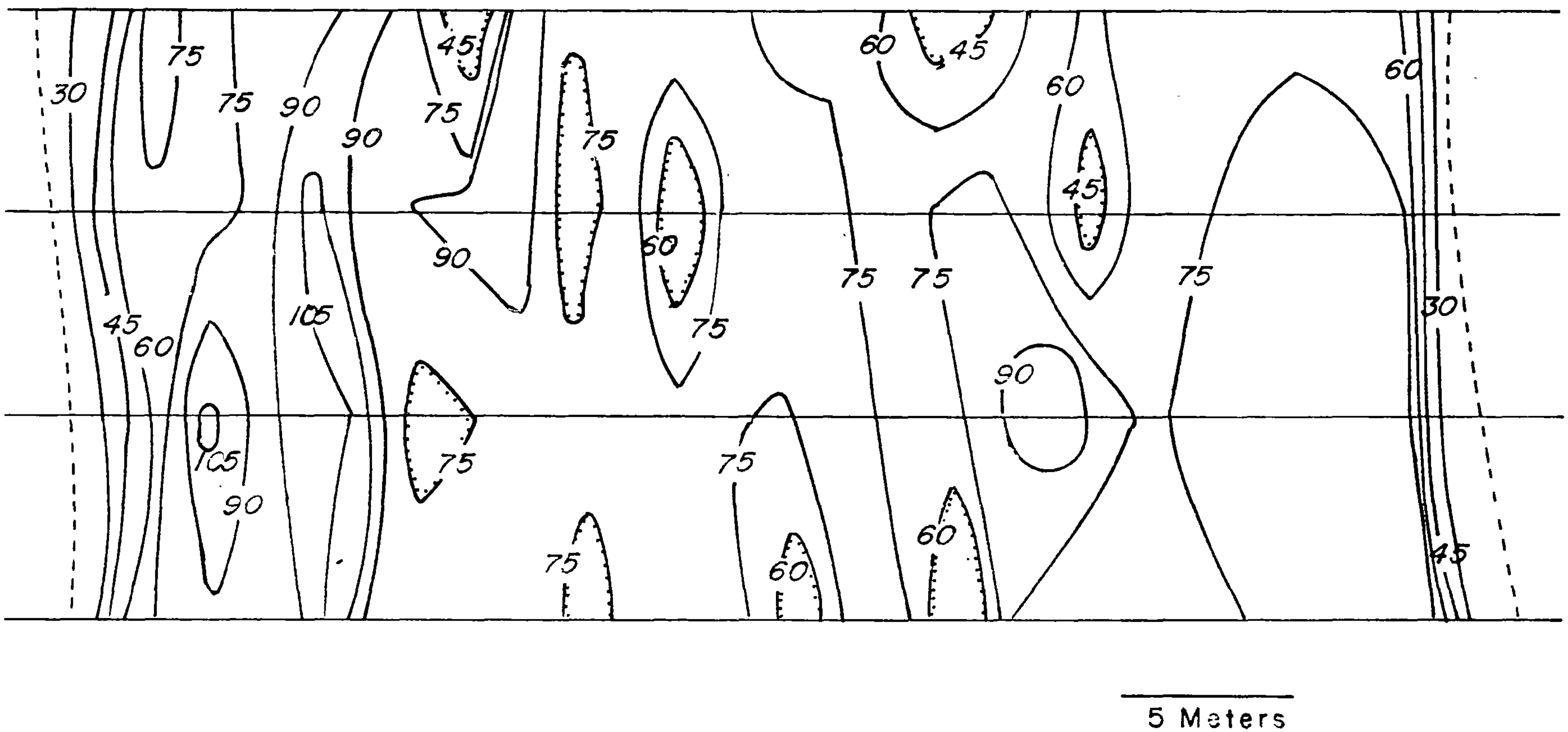

Figure A-4: Velocity Contour Map from the Viall Mapping Section. Velocities in cm./sec. Discharge = 12.0 cms.

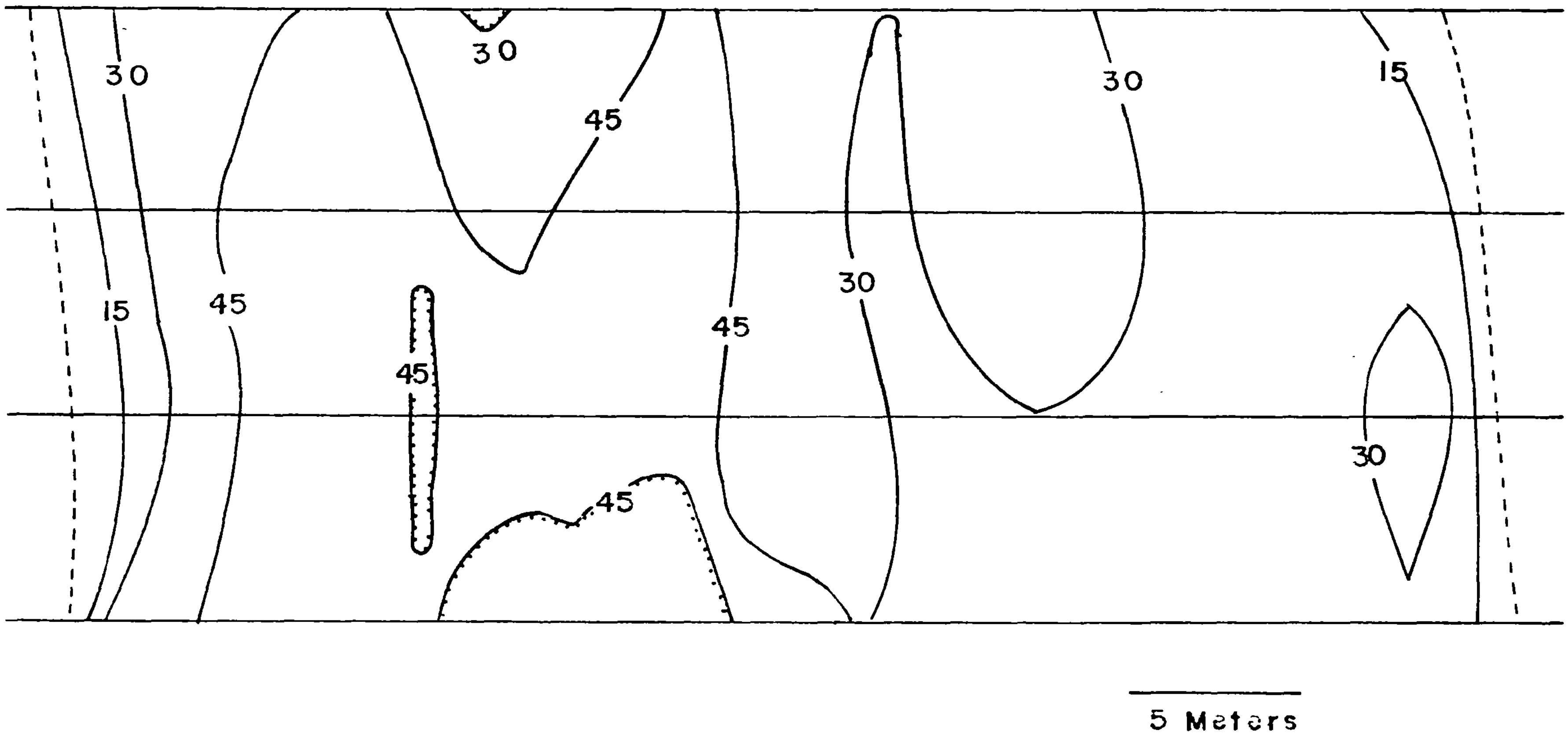

Figure A-5: Depth Contour Map from the Viall Mapping Section. Depths in cm.
Discharge = 10.2 cms.

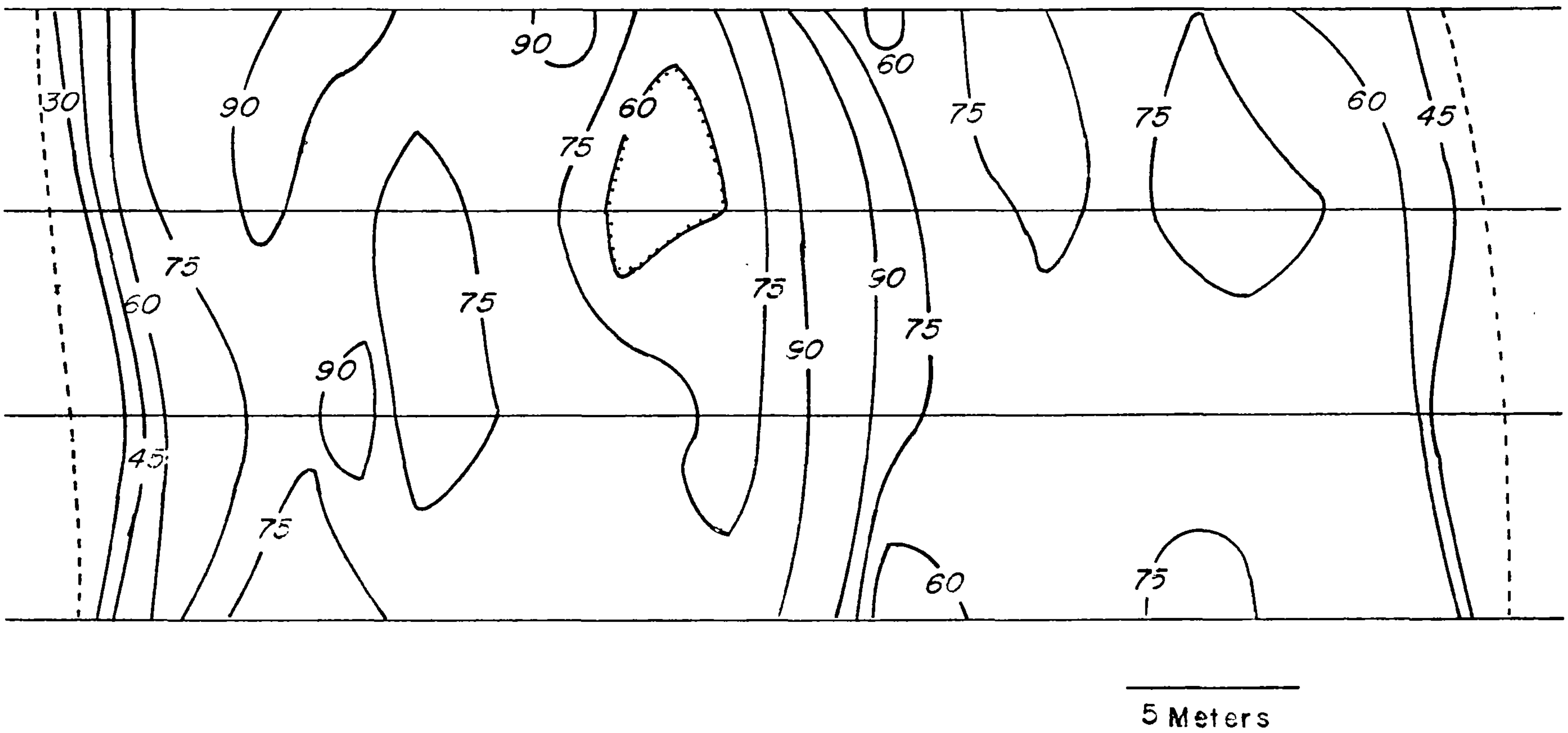

Figure A-6: Velocity Contour Map from the Viall Mapping Section. Velocities in cm./sec. Discharge = 10.2 cms.

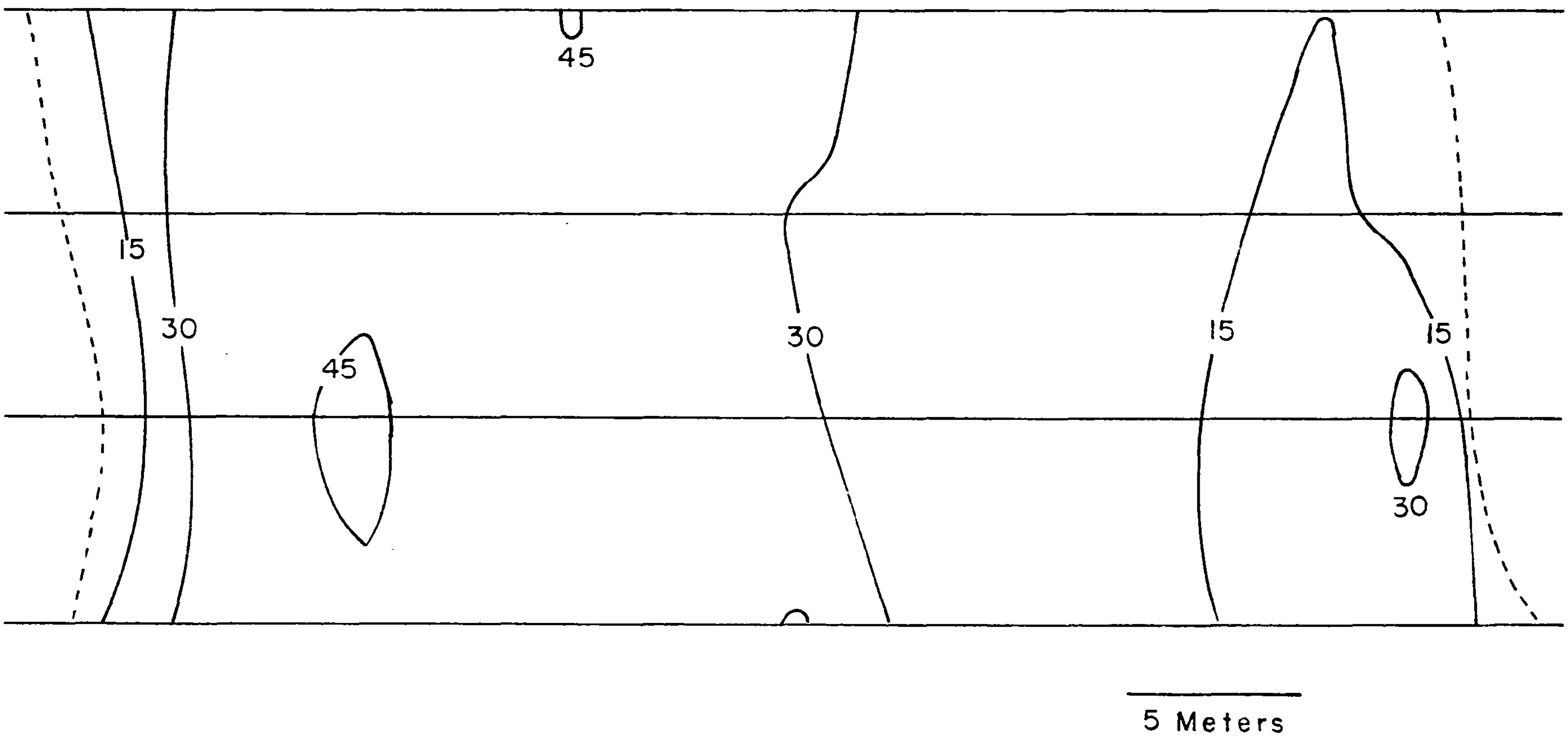

Figure A-7: Depth Contour Map from the Viall Mapping Section. Depths in cm. Discharge = 6.3 cms.

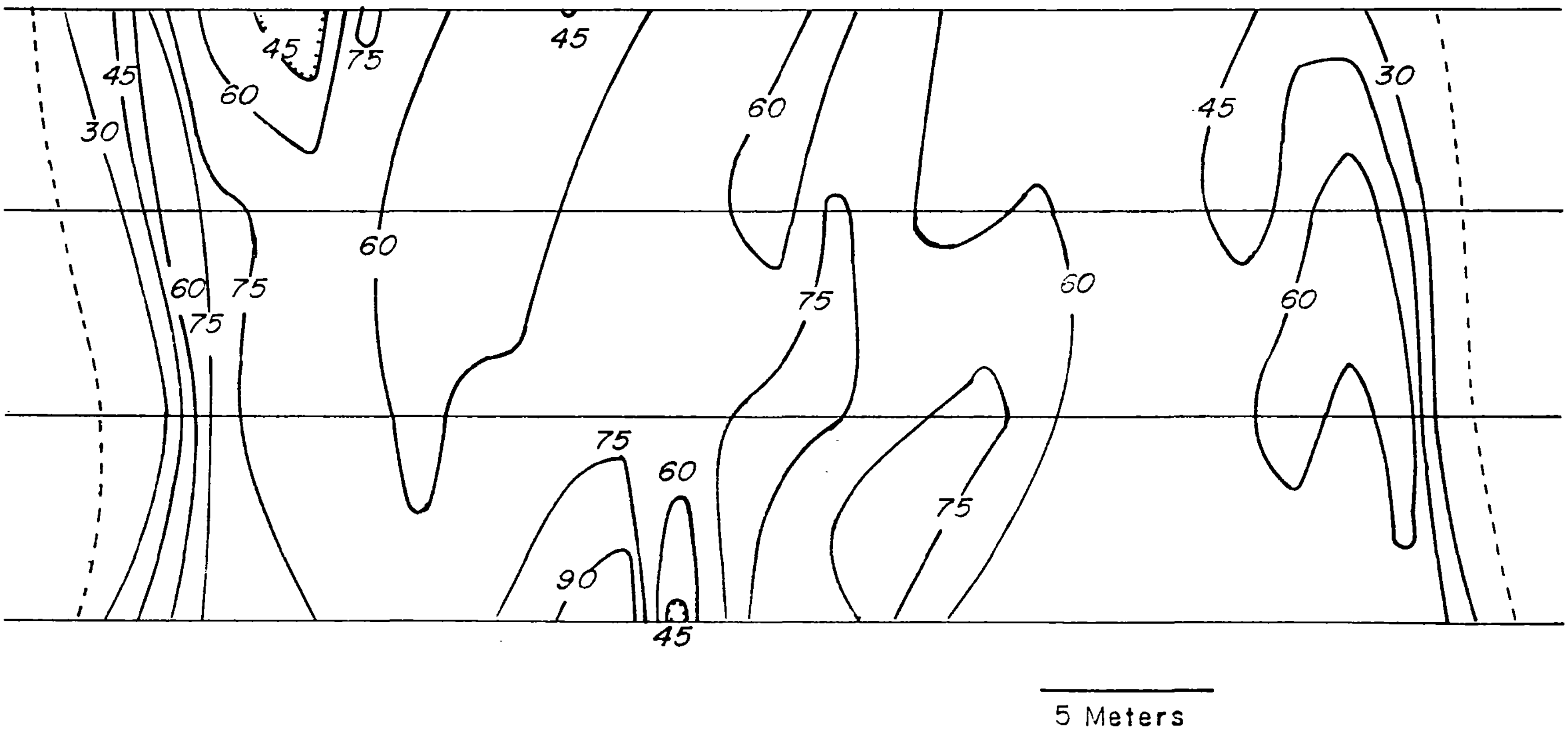

Figure A-8: Velocity Contour Map from the Viall Mapping Section. Velocities in cm./sec. Discharge = 6.3 cms.

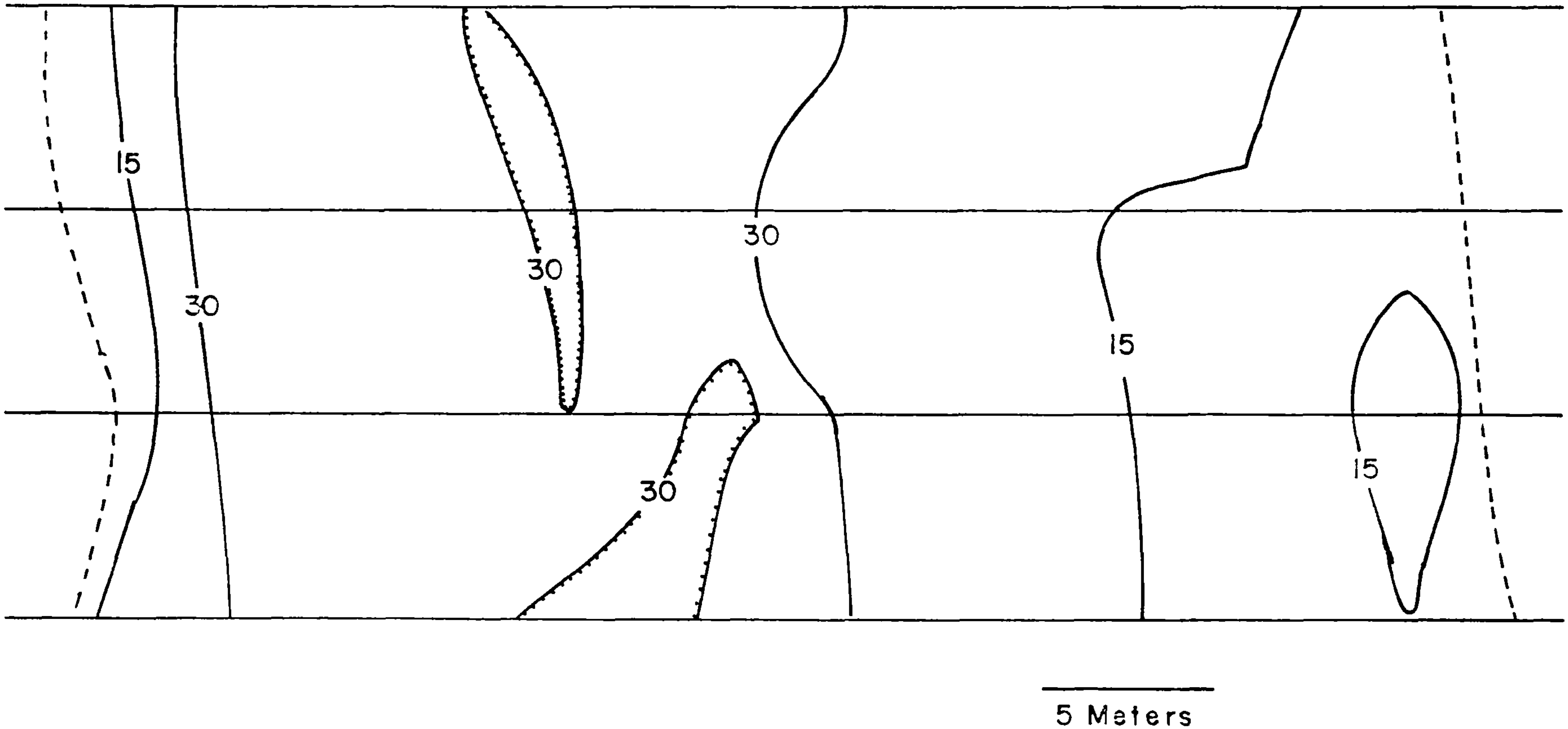

Figure A-9: Depth Contour Map from the Viall Mapping Section. Depths in cm.
Discharge = 5.6 cms.

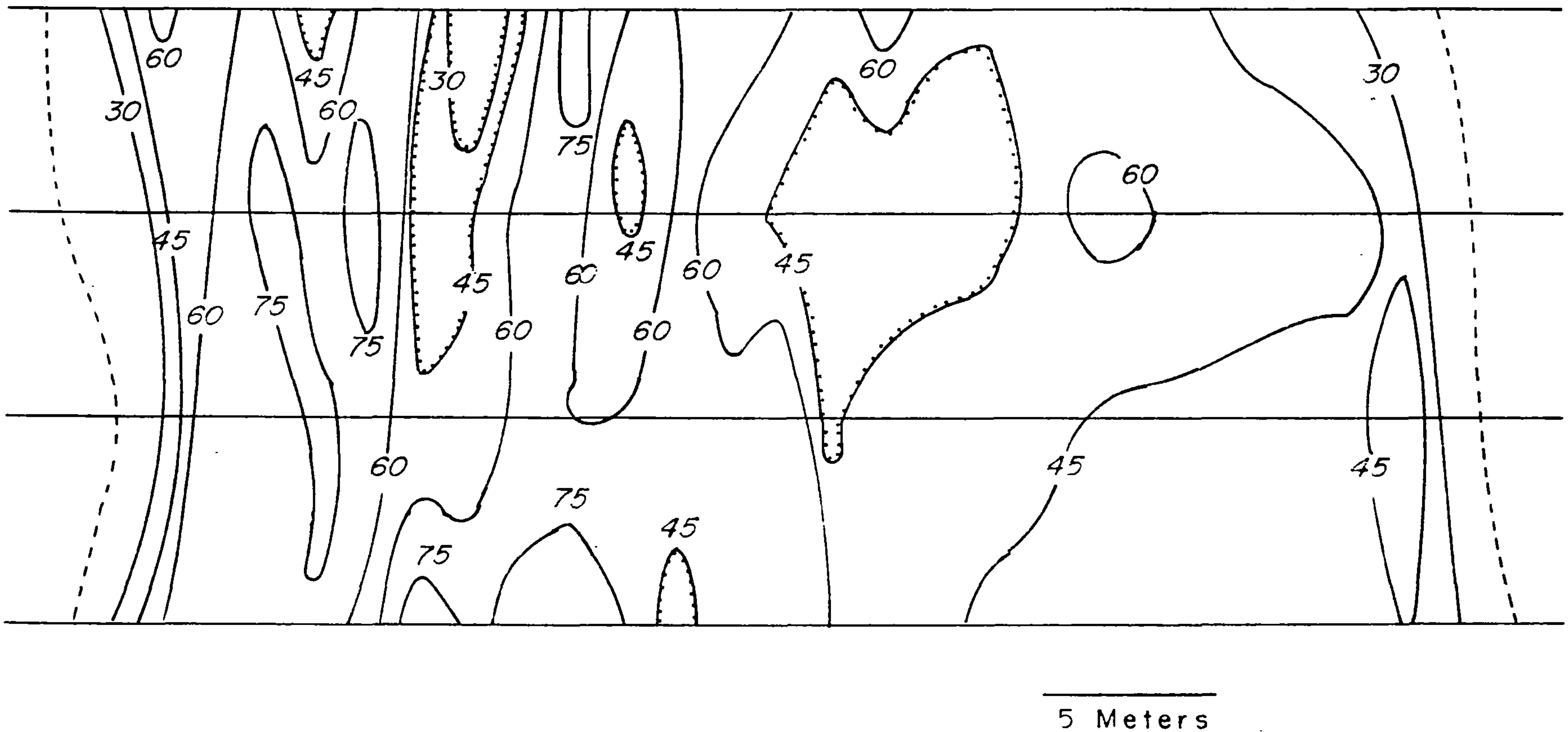

Figure A-10: Velocity Contour Map from the Viall Mapping Section. Velocities in cm./sec. Discharge = 5.6 cms.

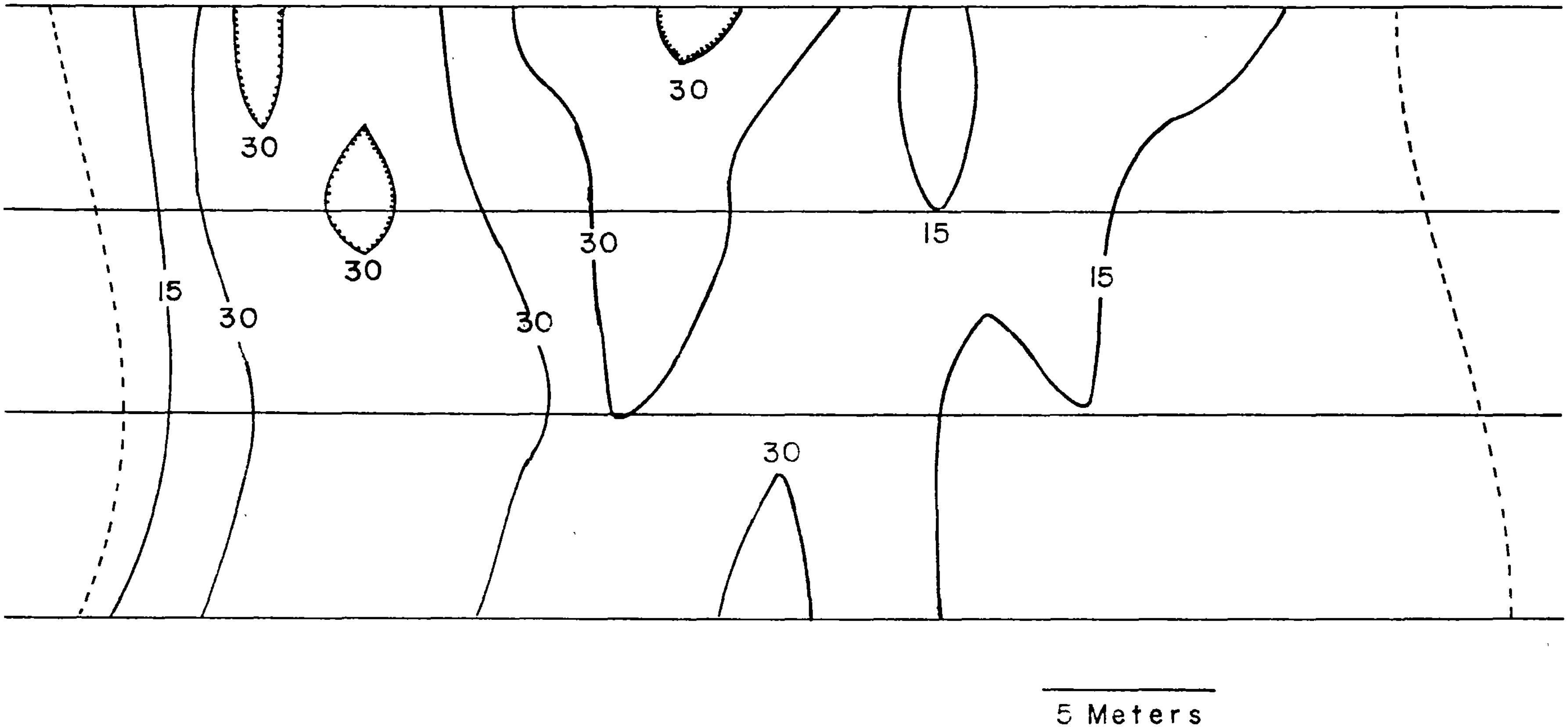

Figure A-11: Depth Contour Map from the Viall Mapping Section. Depths in cm.
Discharge = 4.0 cms.

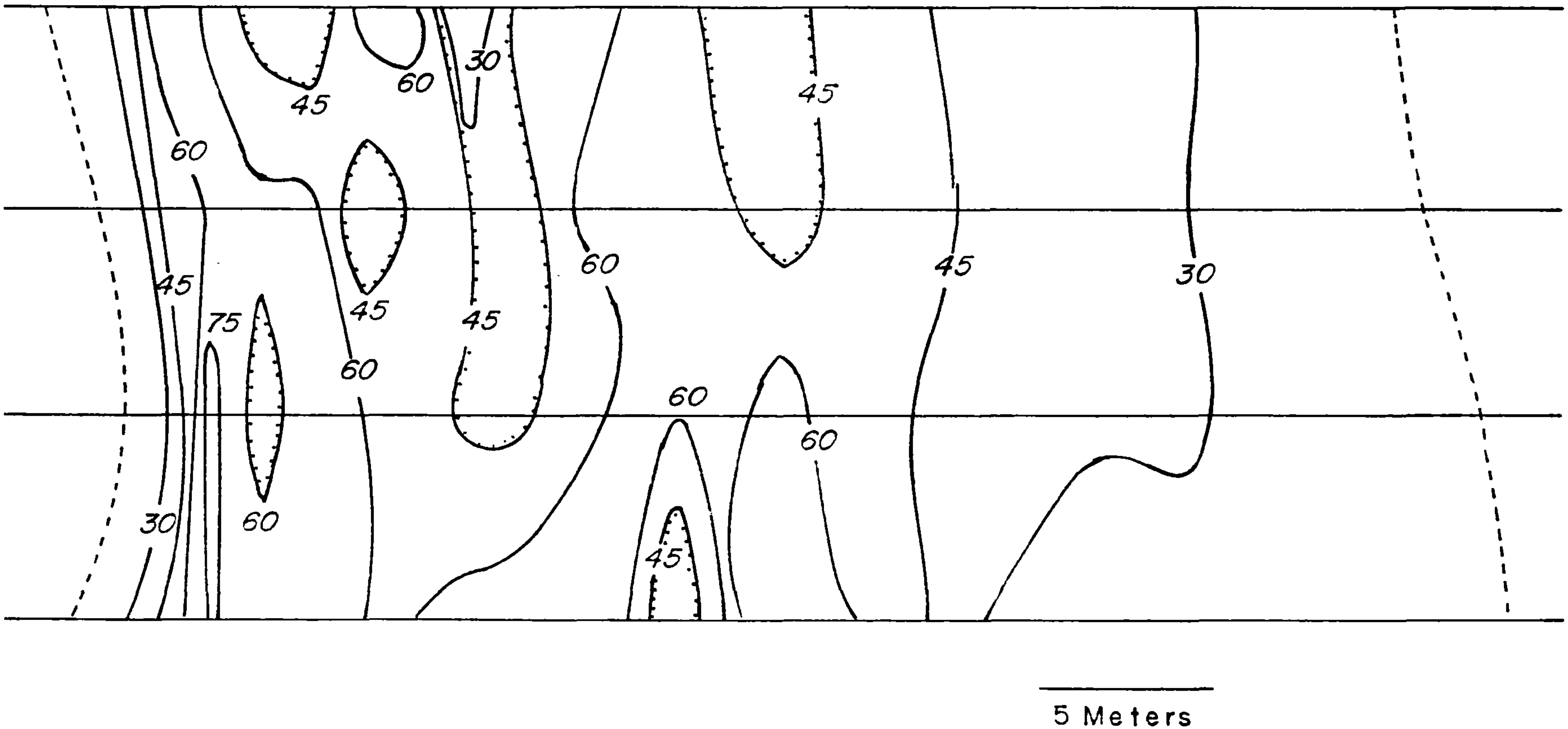

Figure A-12: Velocity Contour Map from the Viall Mapping Section. Velocities in cm./sec. Discharge = 4.0 cms.

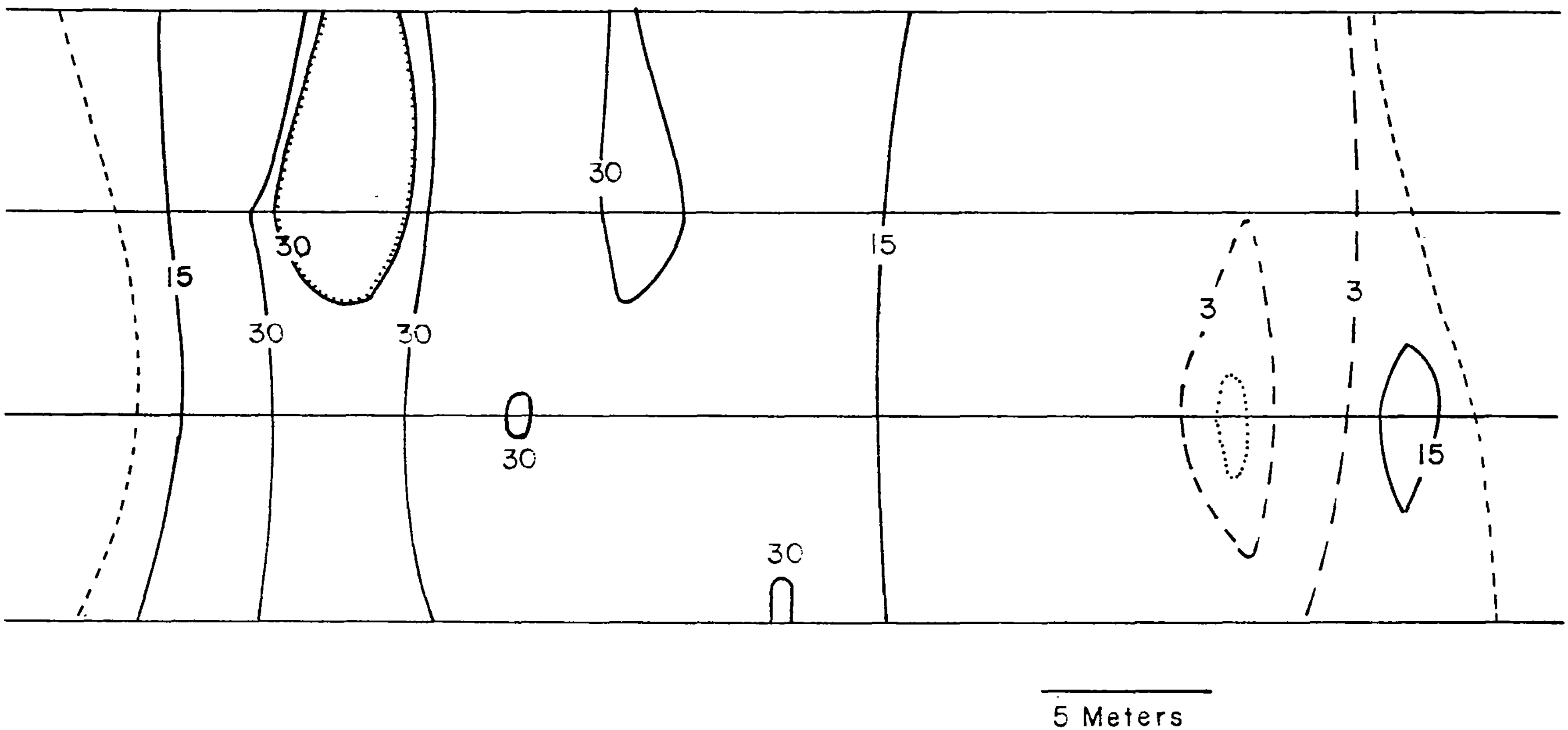

Figure A-13: Depth Contour Map from the Viall Mapping Section. Depths in cm.
Discharge = 2.83 cms.

A-14

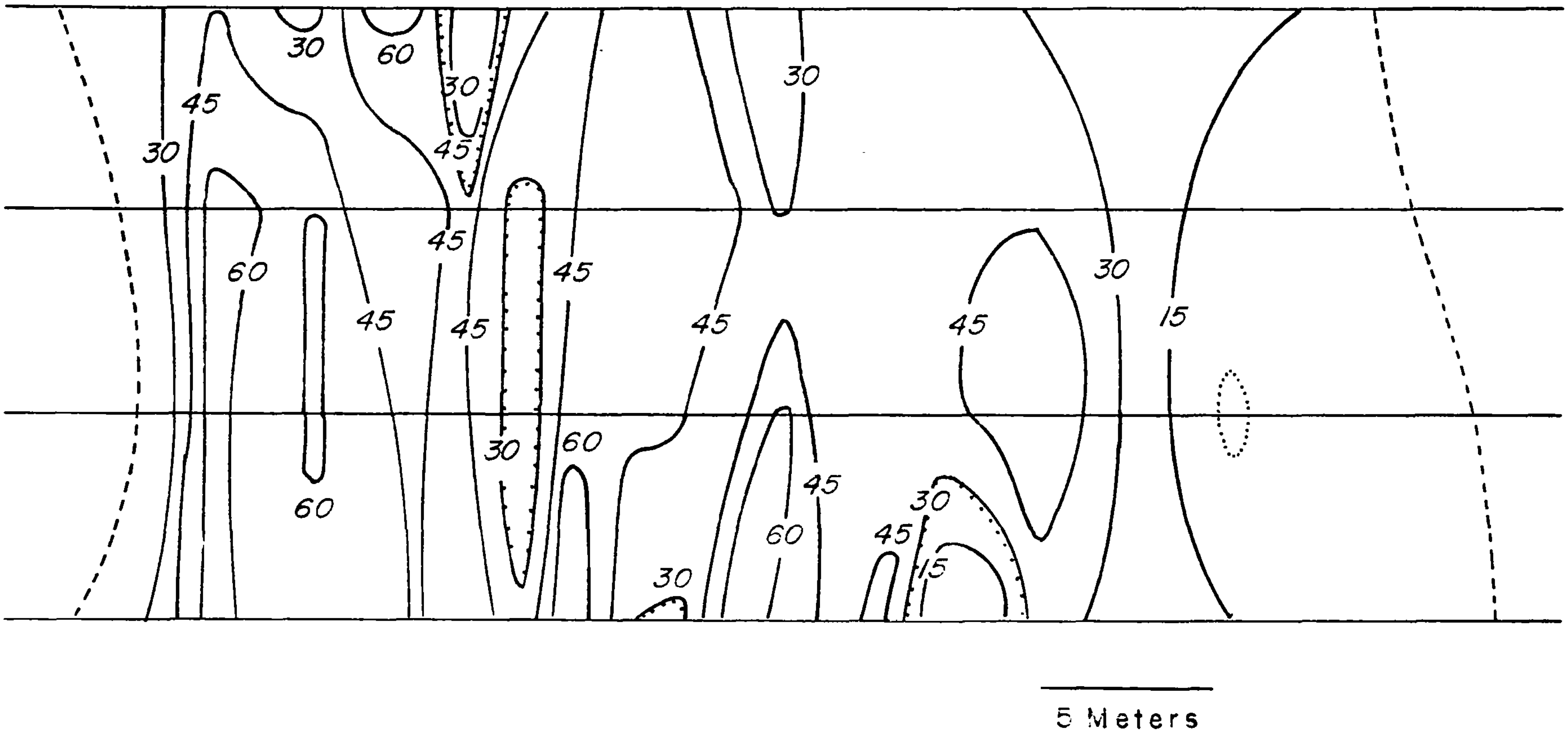

Figure A-14: Velocity Contour Map from the Viall Mapping Section. Velocities in cm./sec. Discharge = 2.83 cms.

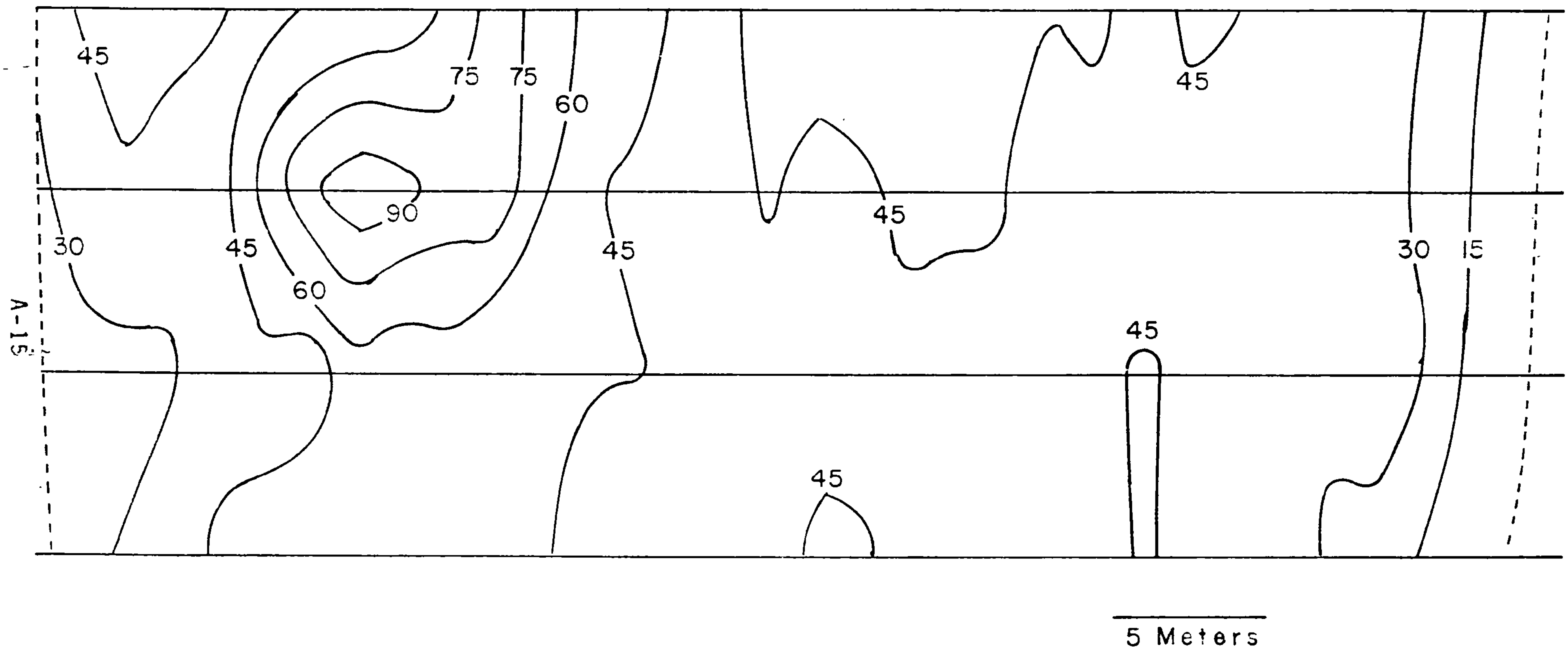

Figure A-15: Depth Contour Map from the Orcutt Mapping Section. Depths in cm.
Discharge = 18.63 cms.

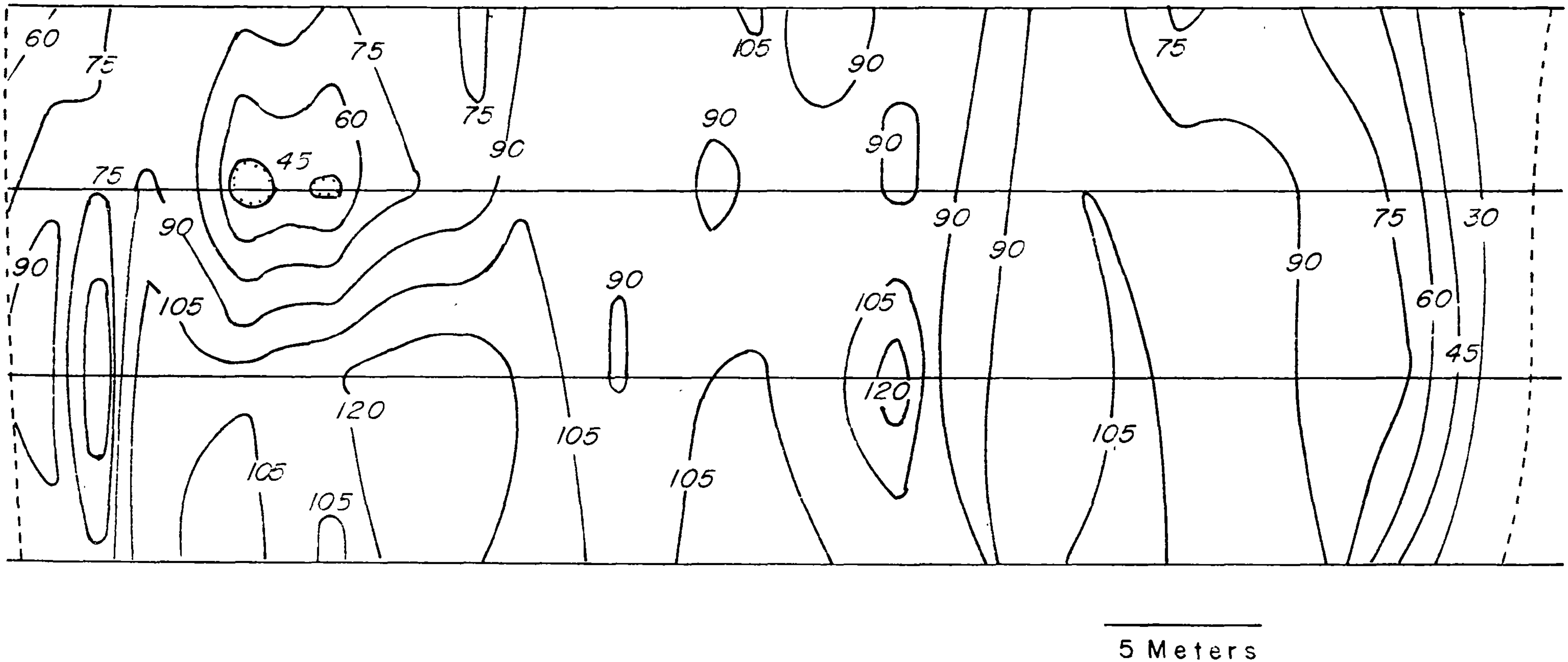

Figure A-16: Velocity Contour Map from the Orcutt Mapping Section. Velocities in cm./sec. Discharge = 18.63 cms.

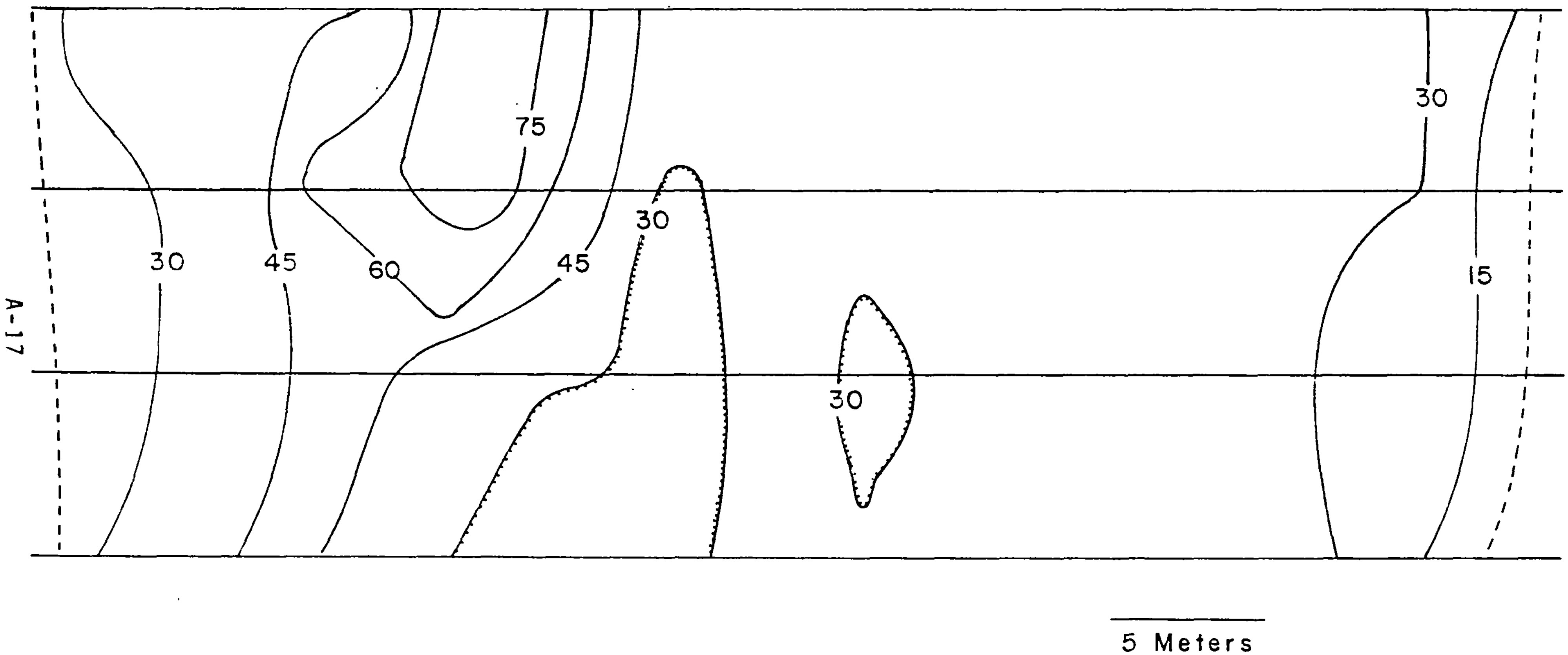

Figure A-17: Depth Contour Map from the Orcutt Mapping Section. Depths in cm.
Discharge = 11.14 cms.

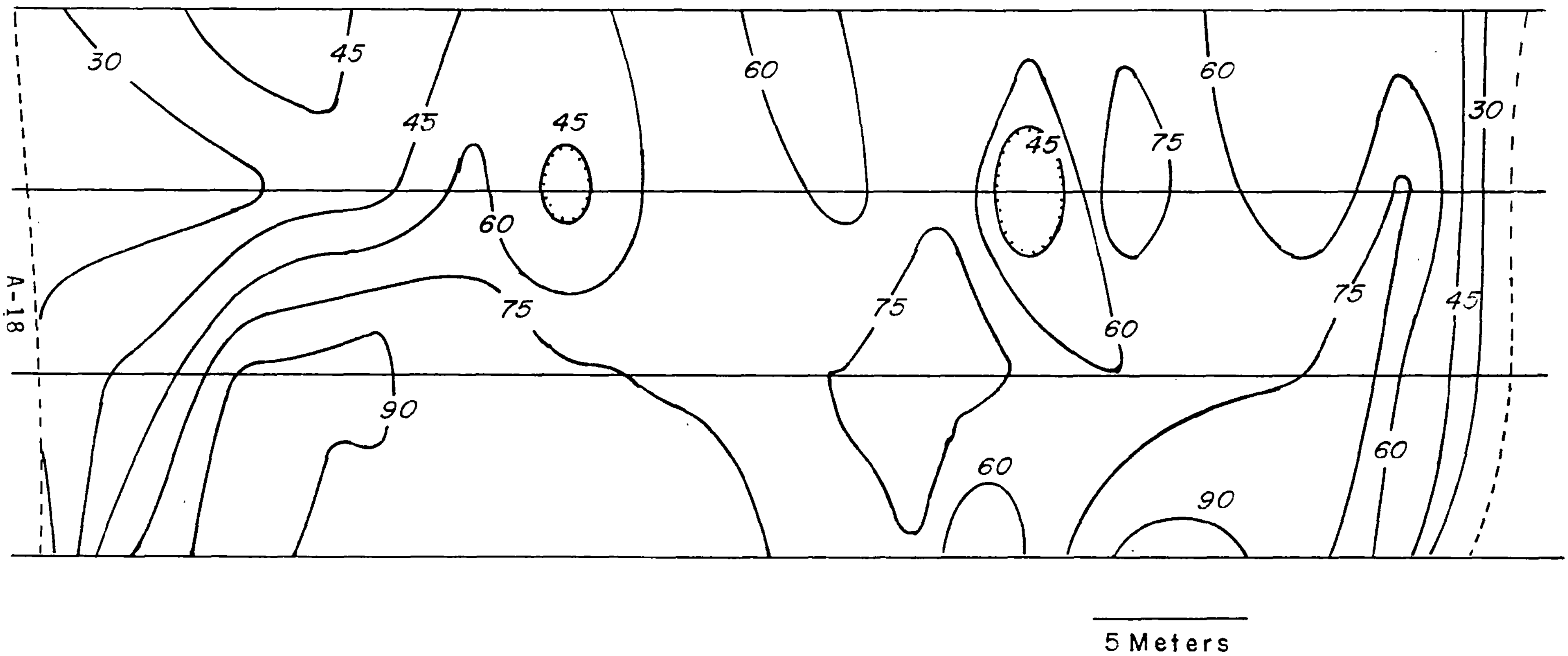

Figure A-18: Velocity Contour Map from the Orcutt Mapping Section. Velocities in cm./sec. Discharge = 11.14 cms.

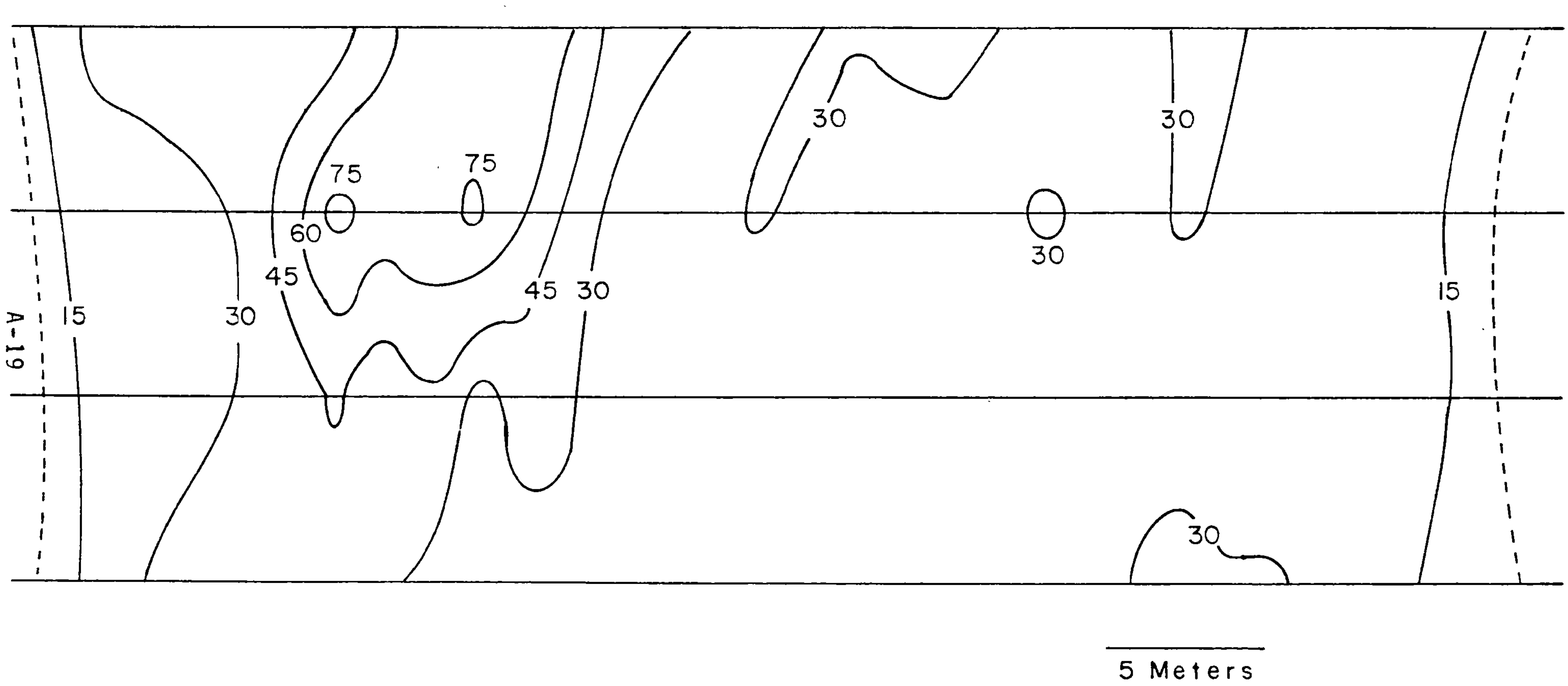

Figure A-19: Depth Contour Map from the Orcutt Mapping Section. Depths in cm. Discharge = 7.58 cms.

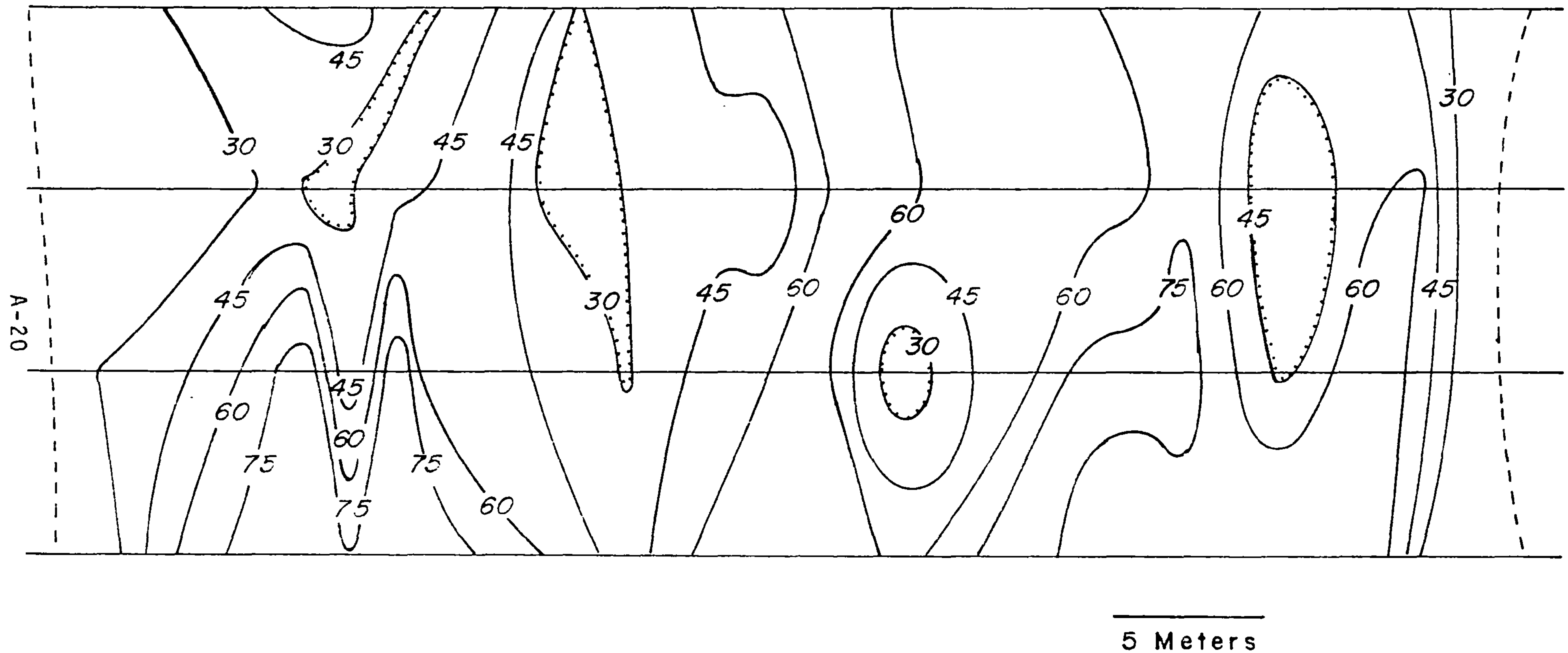

Figure A-20: Velocity Contour Map from the Orcutt Mapping Section. Velocities in cm./sec. Discharge = 7.58 cms.

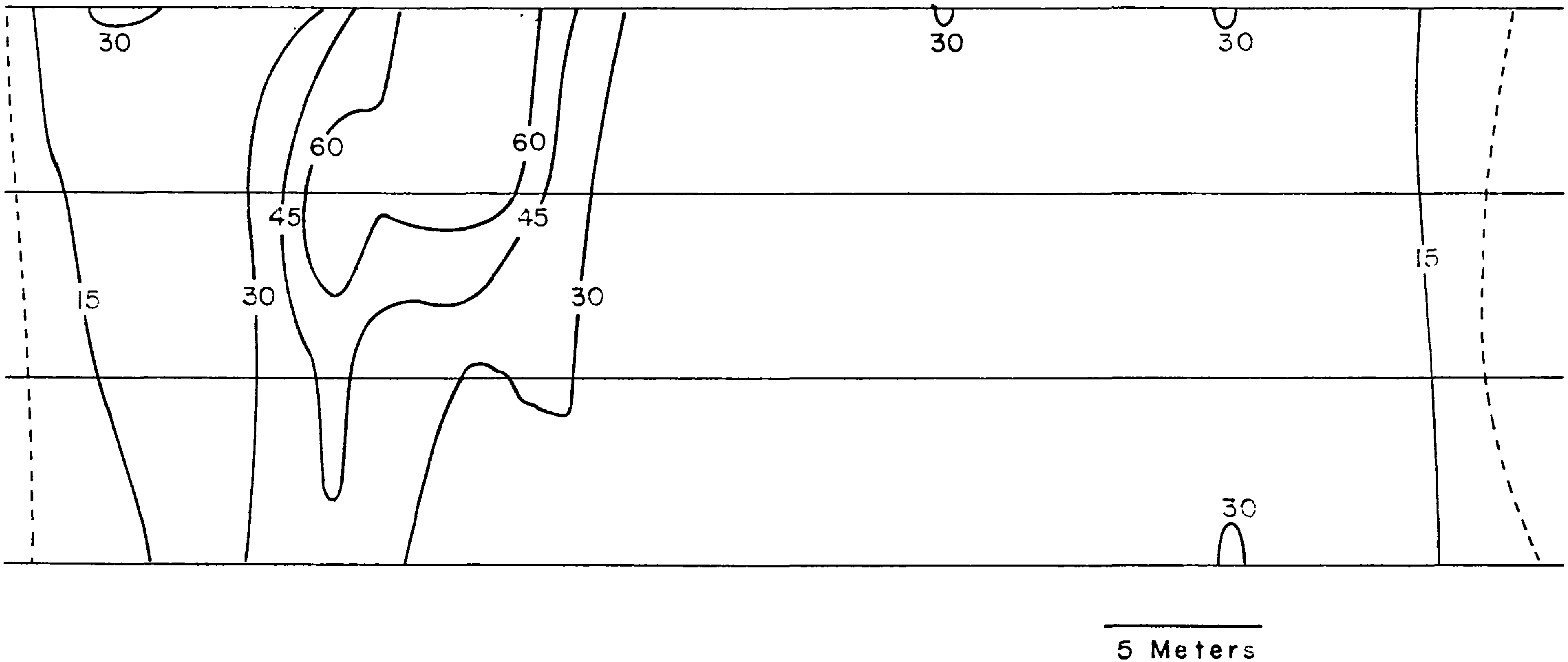

Figure A-21: Depth Contour Map from the Orcutt Mapping Section. Depths in cm.
Discharge = 5.43 cms.

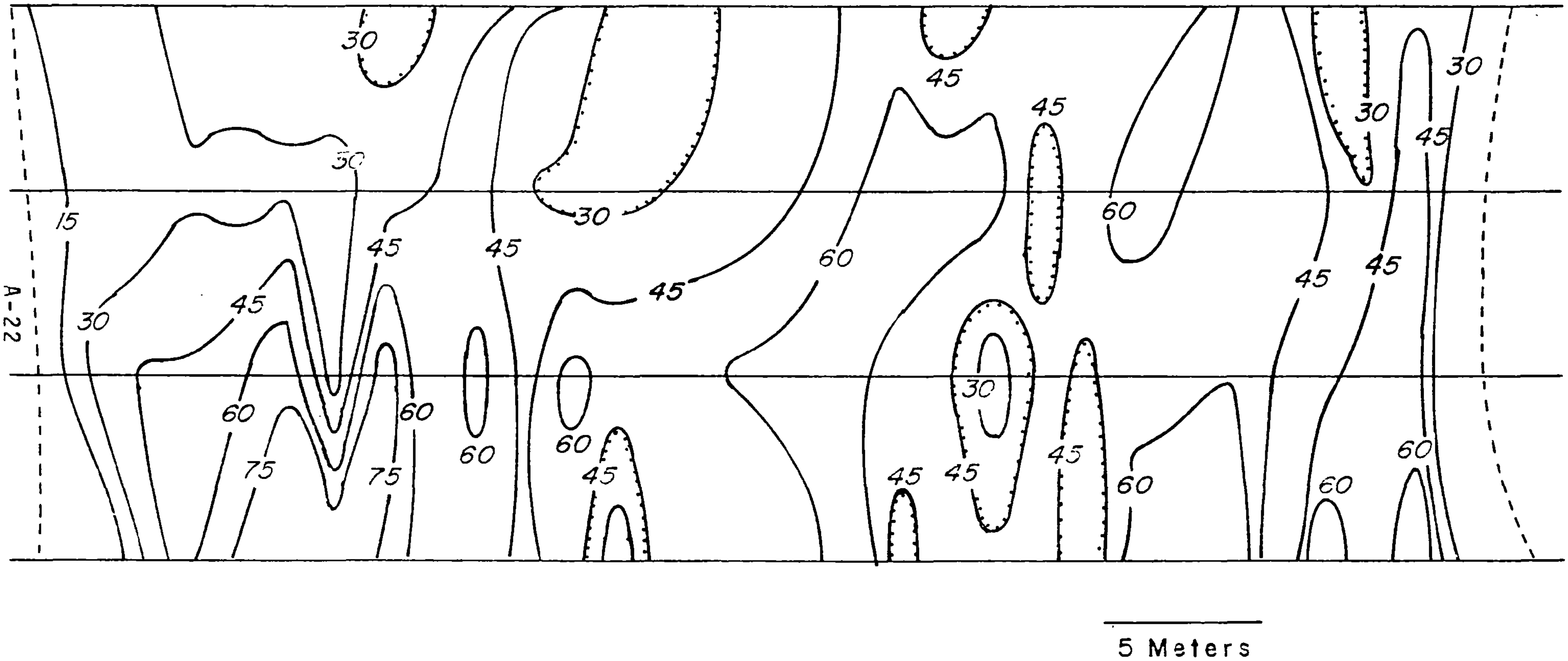

Figure A-22: Velocity Contour Map from the Orcutt Mapping Section. Velocities in cm./sec. Discharge = 5.43 cms.

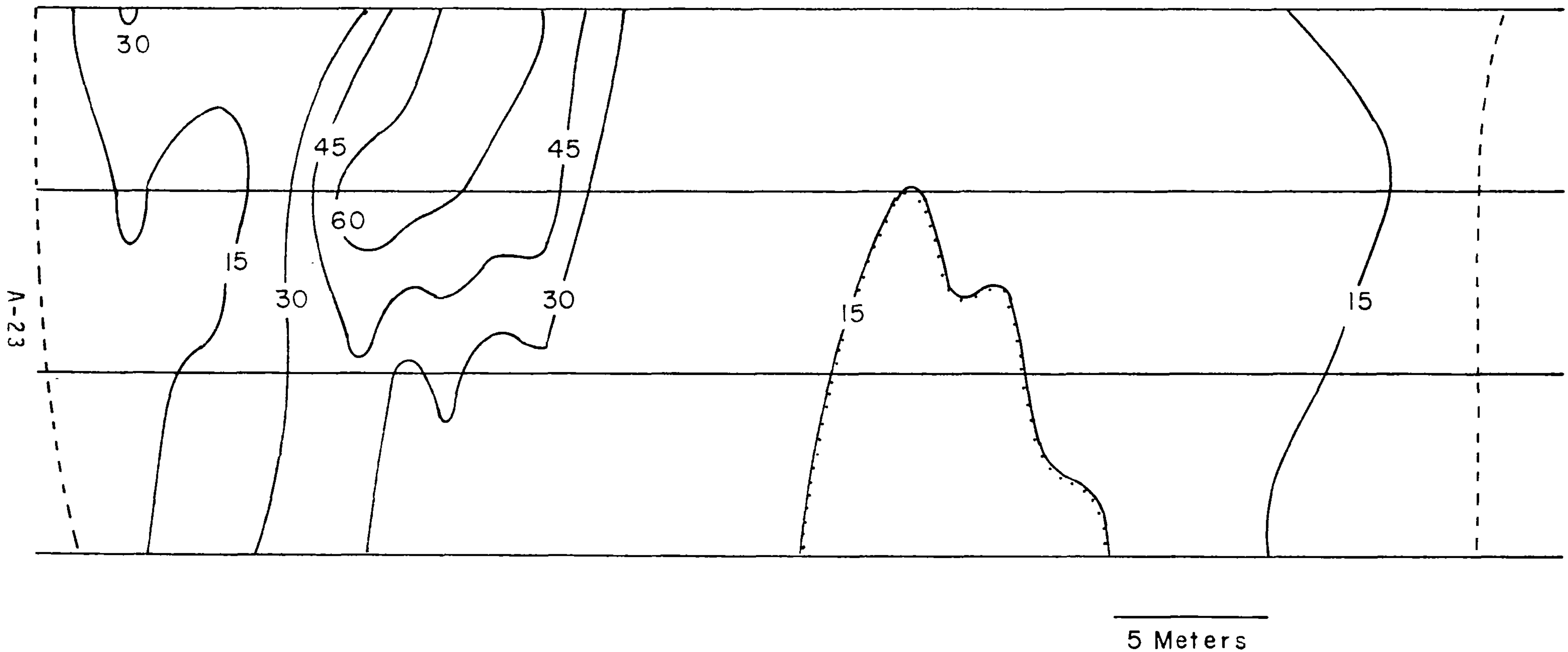

Figure A-23: Depth Contour Map from the Orcutt Mapping Section. Depths in cm.
Discharge = 3.85 cms.

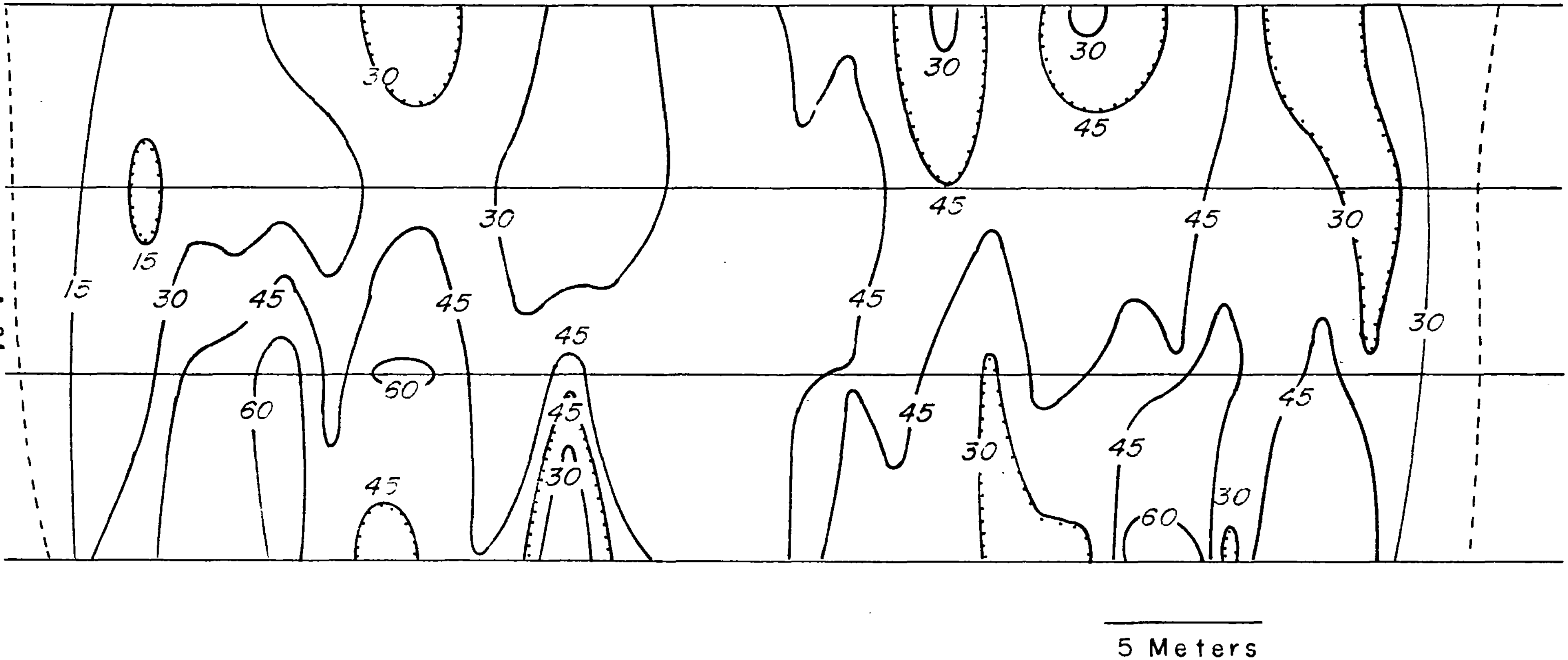

Figure A-24: Velocity Contour Map from the Orcutt Mapping Section. Velocities in cm./sec. Discharge = 3.85 cms.

APPENDIX B

COMPOSITE MAPS

REARING AREAS

1. Direction of flow is from top of page to bottom.

2. These maps indicate areas meeting preferred conditions of depth, velocity, and substrate, for the stonecat.

3. For easier interpretation, depth contours are indicated by vertical typeface. Velocity contours are indicated by slanting typeface.

4. Cross-hatched areas on composite maps indicate areas which do not meet flow criteria for the stonecat. Only those stream areas without cross-hatching meet flow criteria.

5. Dashed lines indicate water's edge, either at stream banks or on exposed bars.

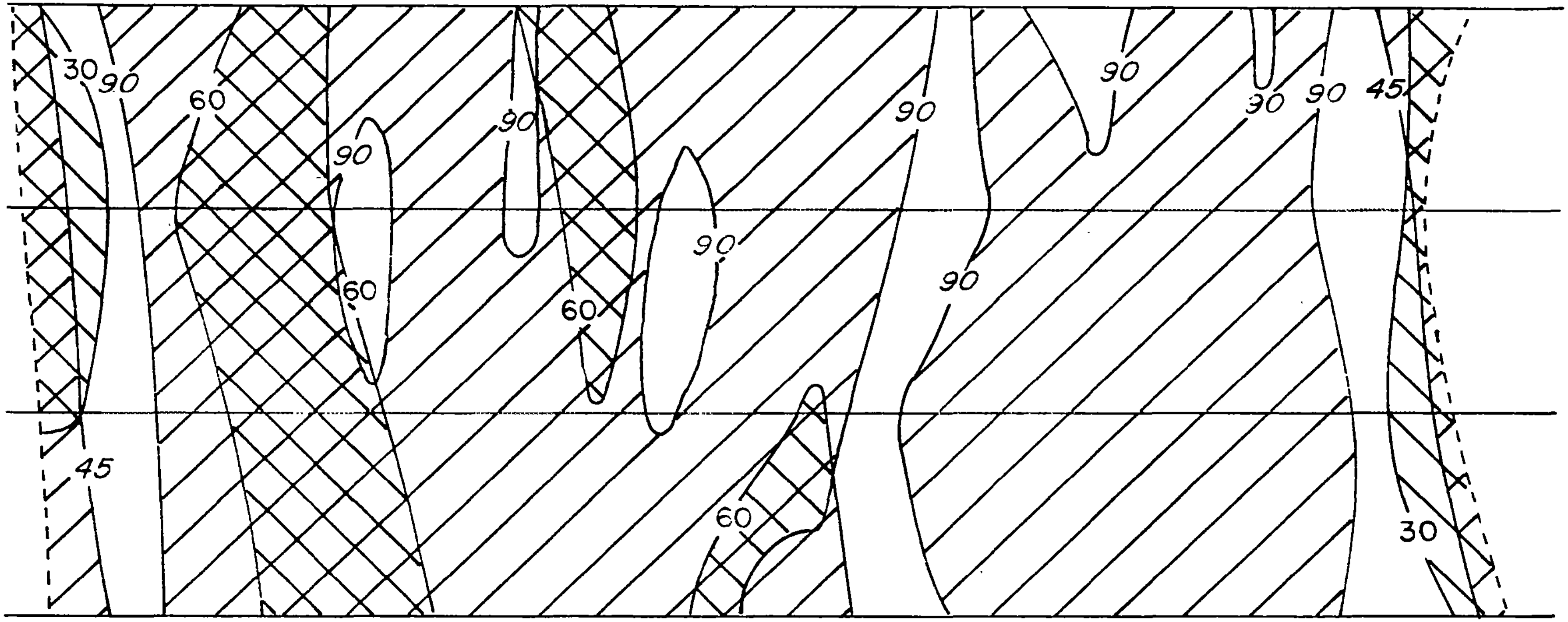

Figure B-1: Composite Map for the Viall Mapping Section, Showing Areas Meeting Flow Criteria for the Stonecat. Discharge: 19.4 cms.

Area Meeting Criteria: 116 m^2

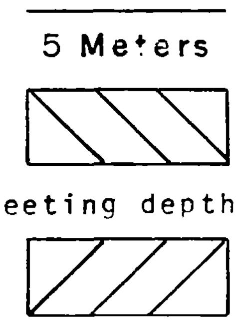

Area not meeting depth criteria

Area not meeting velocity criteria

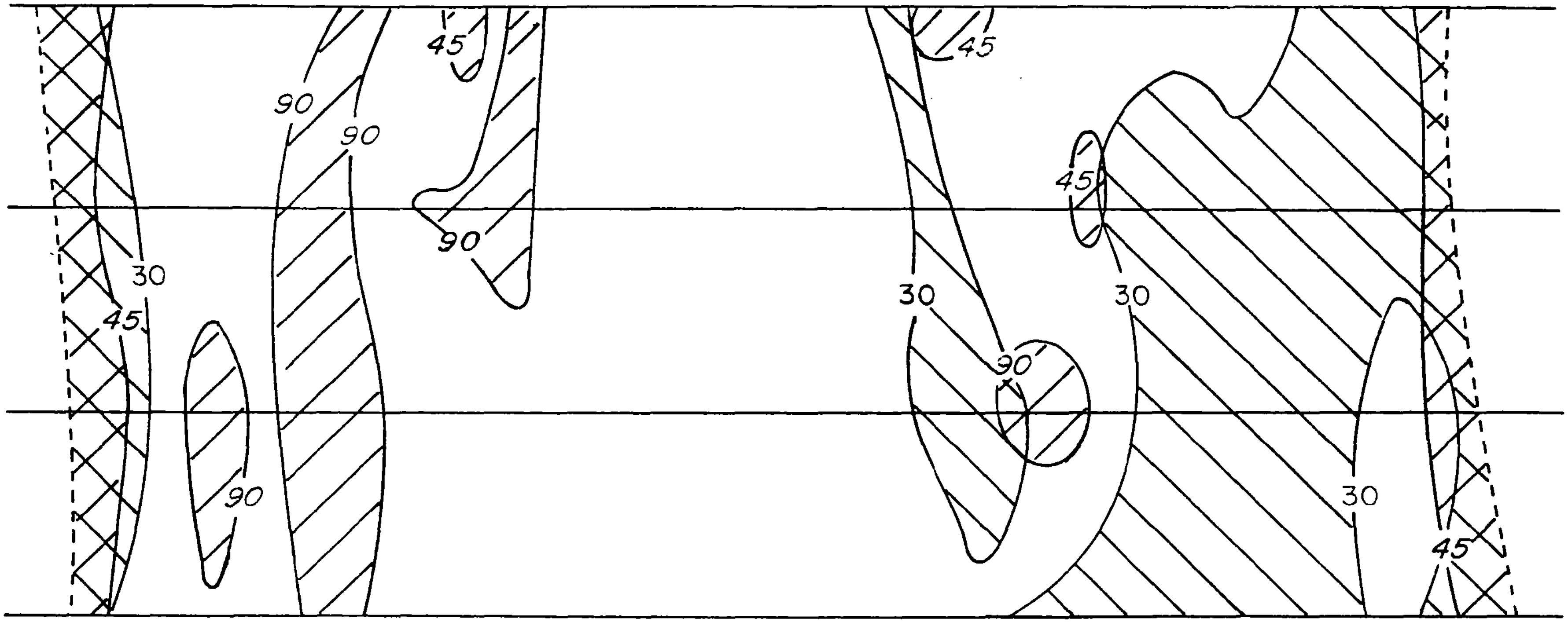

Figure B-2: Composite Map for the Viall Mapping Section, Showing Areas Meeting Flow Criteria for the Stonecat. Discharge: 12.0 cms.

Area Meeting Criteria: 425 m^2

5 Meters

Area not meeting depth criteria

Area not meeting velocity criteria

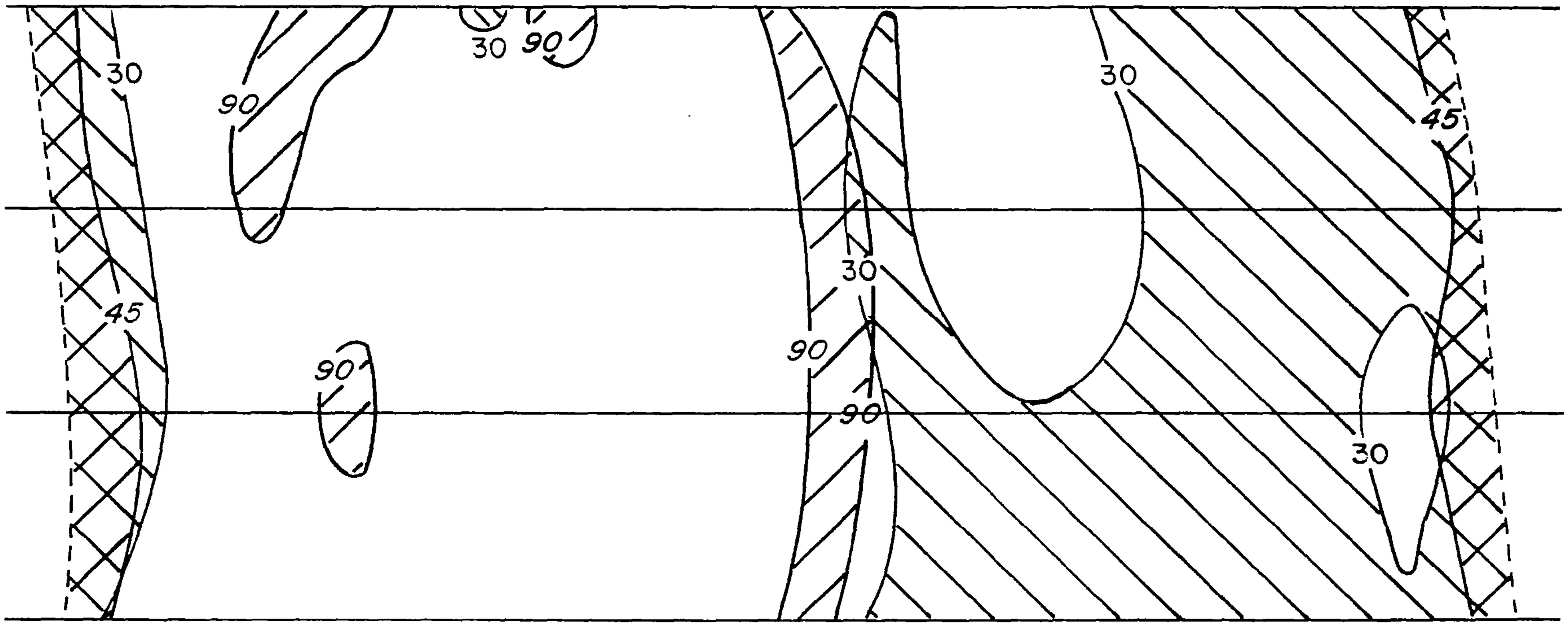

Figure B-3: Composite Map for the Viall Mapping Section, Showing Areas Meeting Flow Criteria for the Stonecat. Discharge: 10.2 cms.

Area Meeting Criteria: 401 m^2

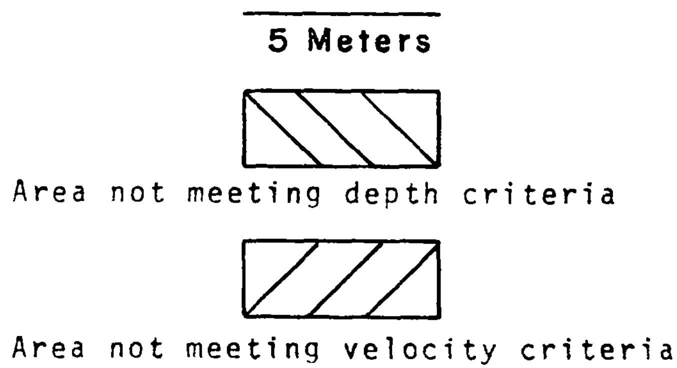

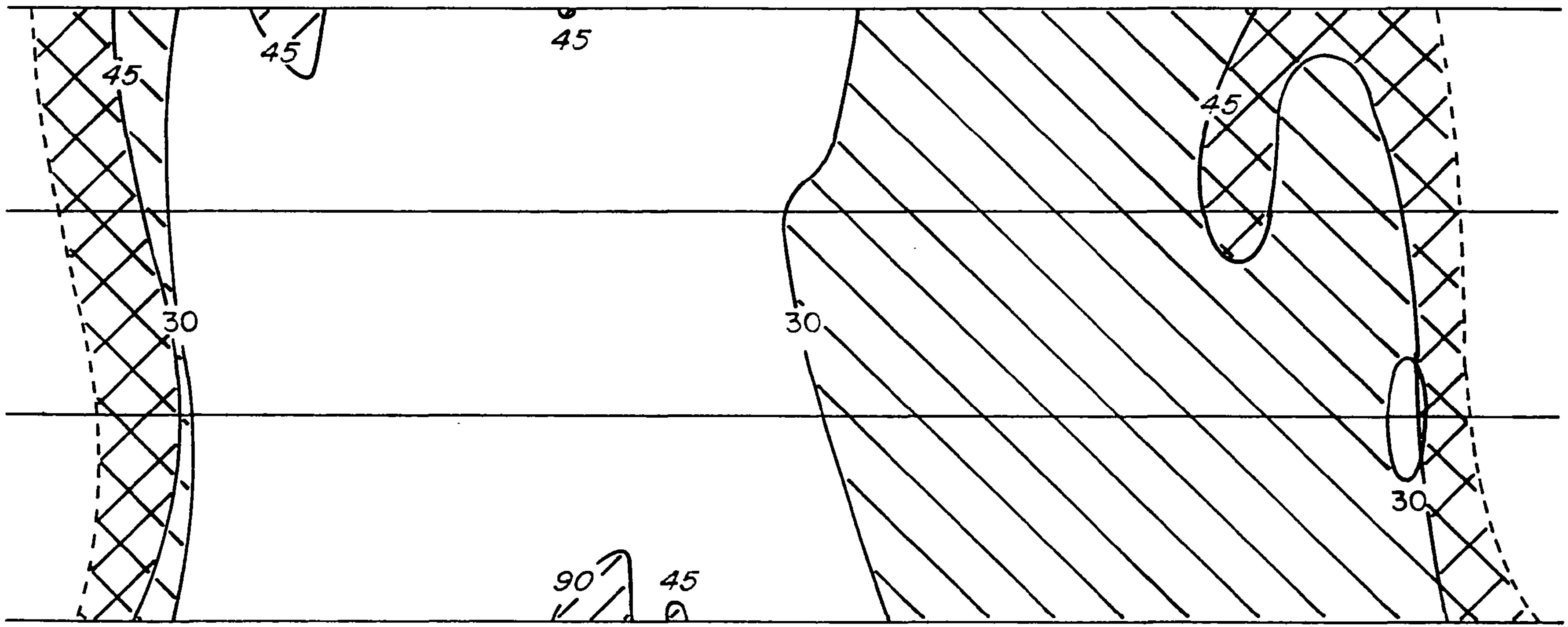

Figure B-4: Composite Map for the Viall Mapping Section, Showing Areas Meeting Flow Criteria for the Stonecat. Discharge: 6.30 cms.

Area Meeting Criteria: 335 m^2

5 Meters

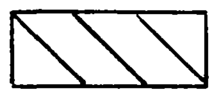

Area not meeting depth criteria

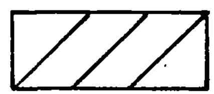

Area not meeting velocity criteria

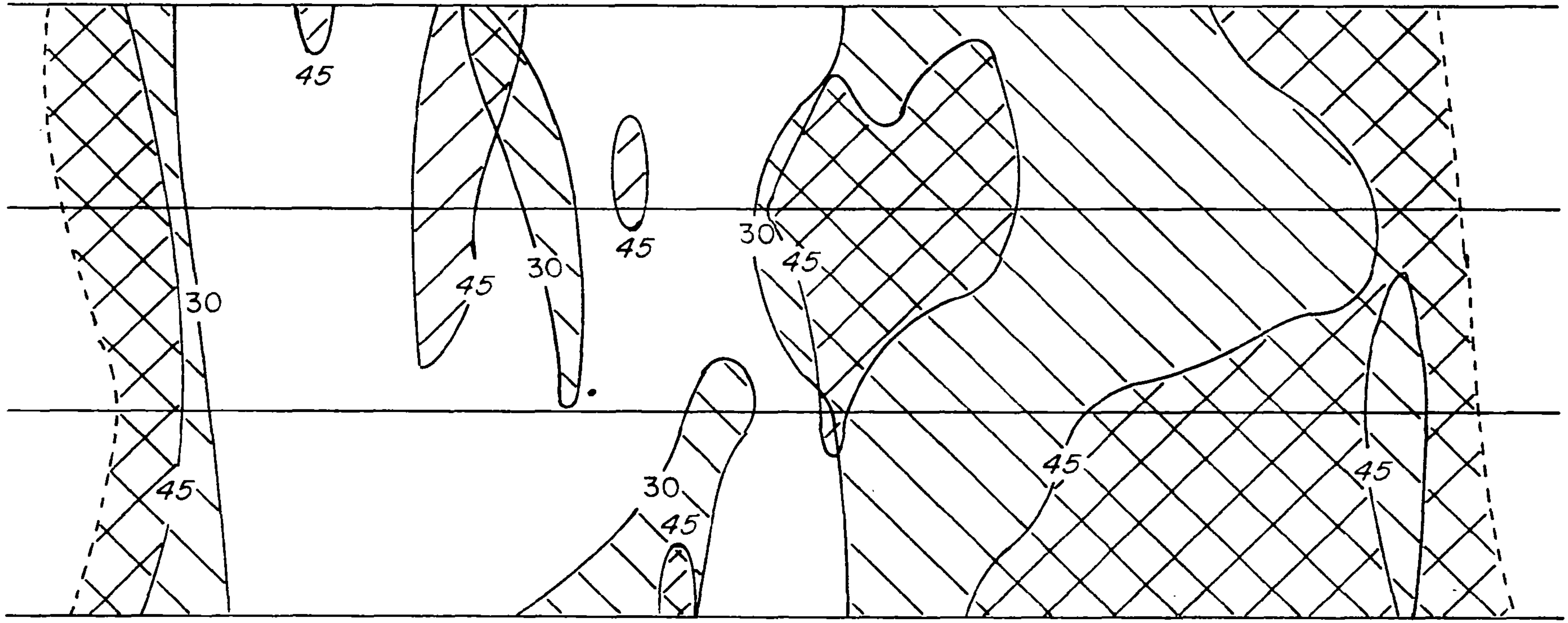

Figure B-5: Composite Map for the Viall Mapping Section, Showing Areas Meeting Flow Criteria for the Stonecat.

Discharge: 5.58 cms.

Area Meeting Criteria: 264 m^2

5 Meters

Area not meeting depth criteria

Area not meeting velocity criteria

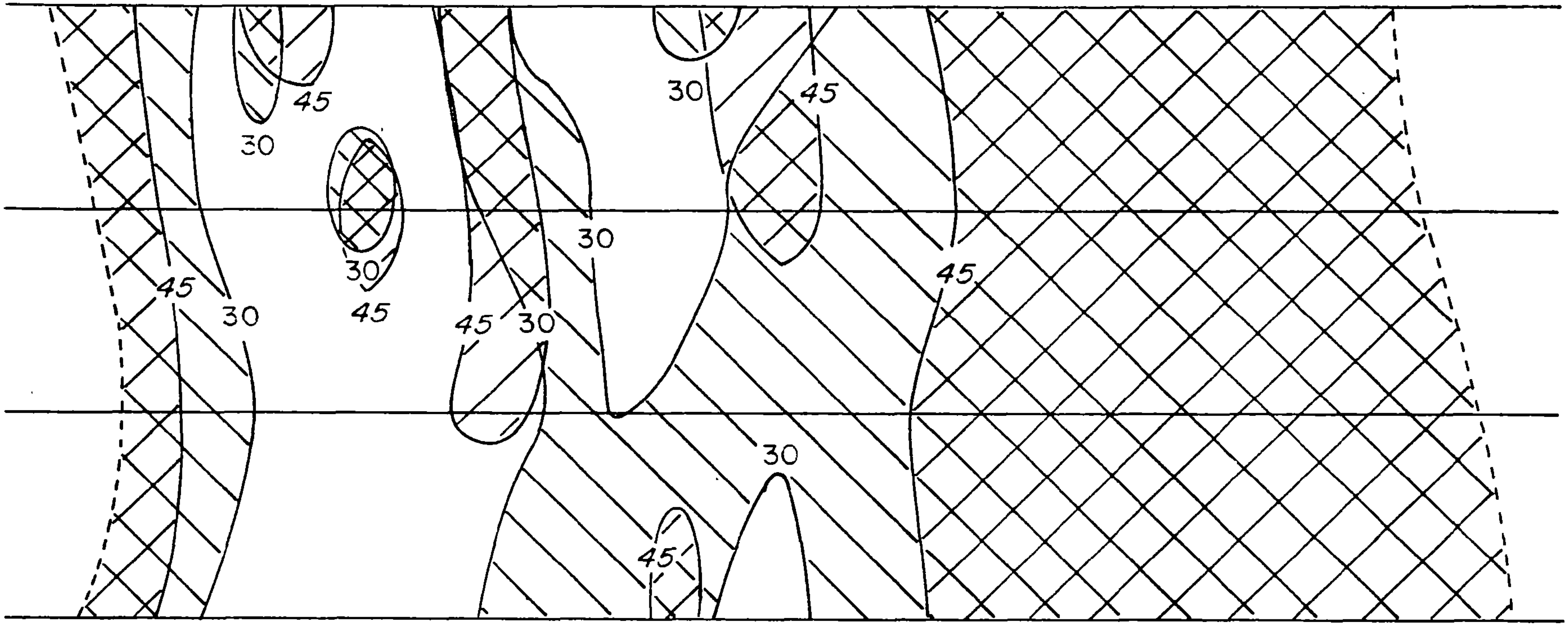

Figure B-6: Composite Map for the Viall Mapping Section, Showing Areas Meeting Flow Criteria for the Stonecat.

Discharge: 4.02 cms.

Area Meeting Criteria: 171 m^2

5 Meters

Area not meeting depth criteria

Area not meeting velocity criteria

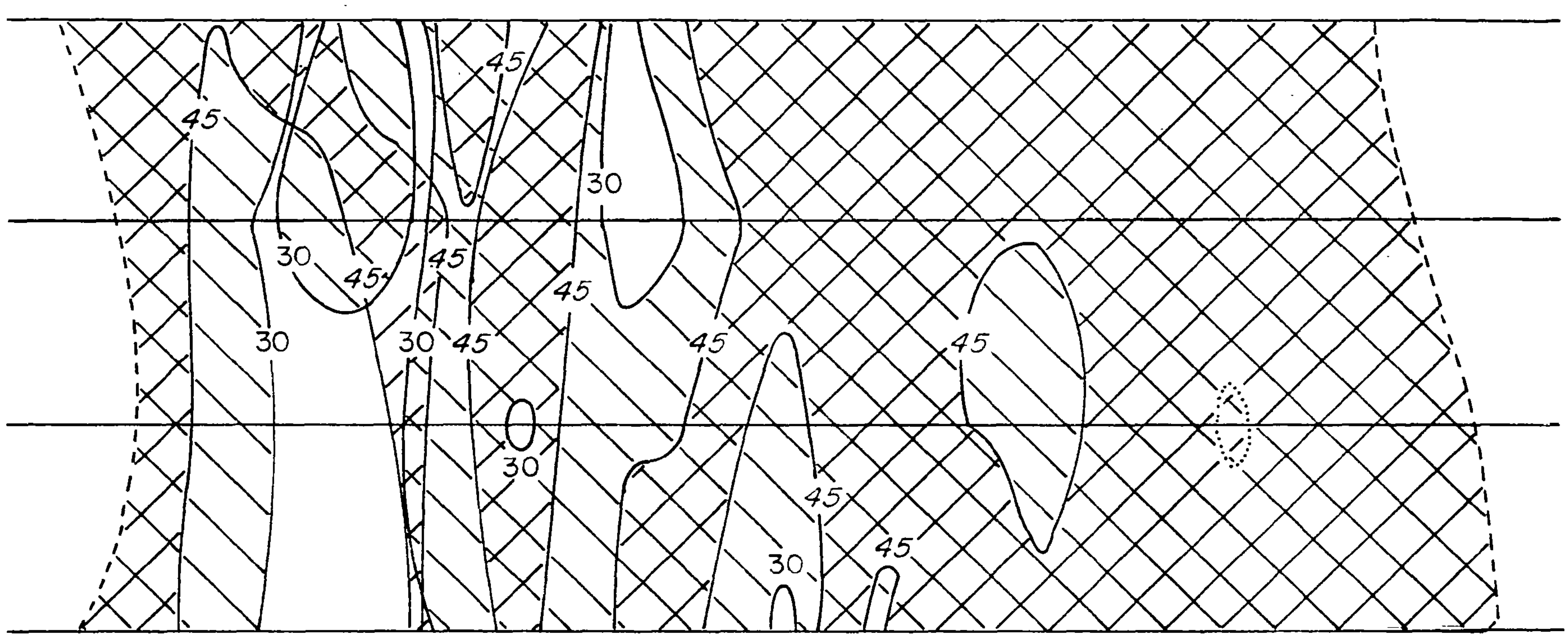

Figure B-7: Composite Map for the Viall Mapping Section, Showing Areas Meeting Flow Criteria for the Stonecat.

Discharge: 2.83 cms.

Area Meeting Criteria: 54 m^2

5 Meters

Area not meeting depth criteria

Area not meeting velocity criteria

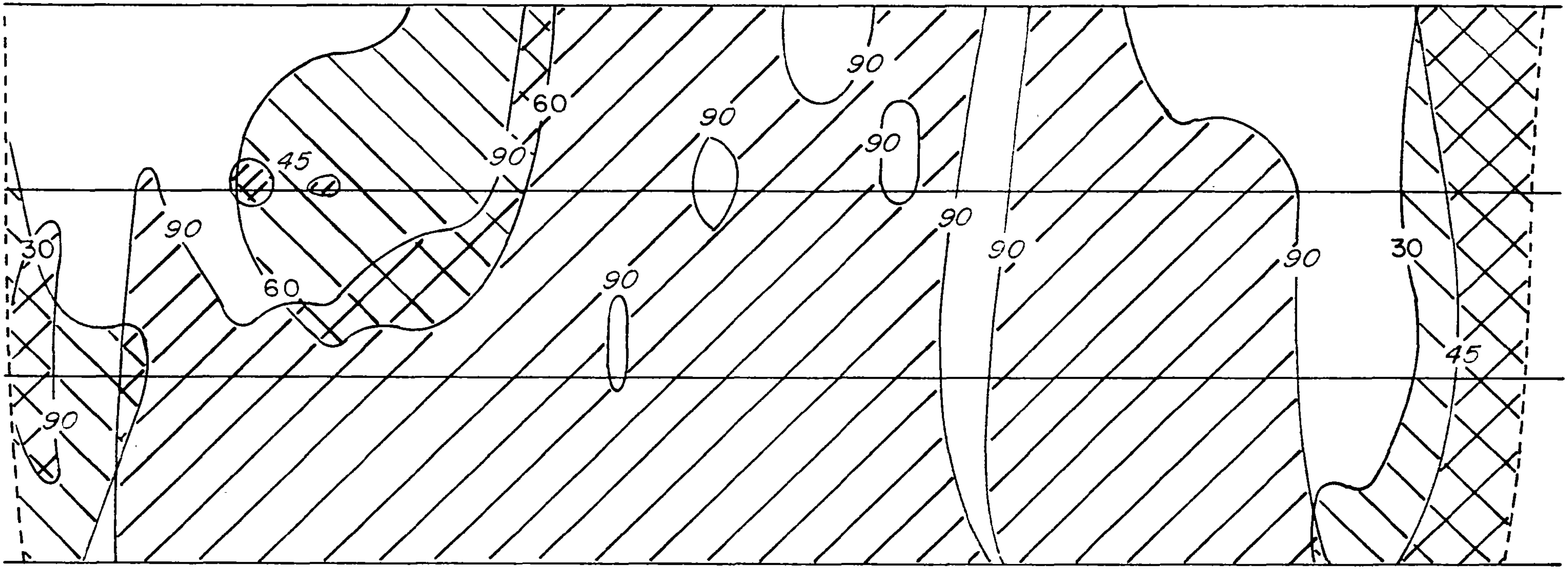

Figure B-8: Composite Map for the Orcutt Mapping Section, Showing Areas Meeting Flow Criteria for the Stonecat.

Discharge: 18.63 cms.

Area Meeting Criteria: 197 m^2

5 Meters

Area not meeting depth criteria

Area not meeting velocity criteria

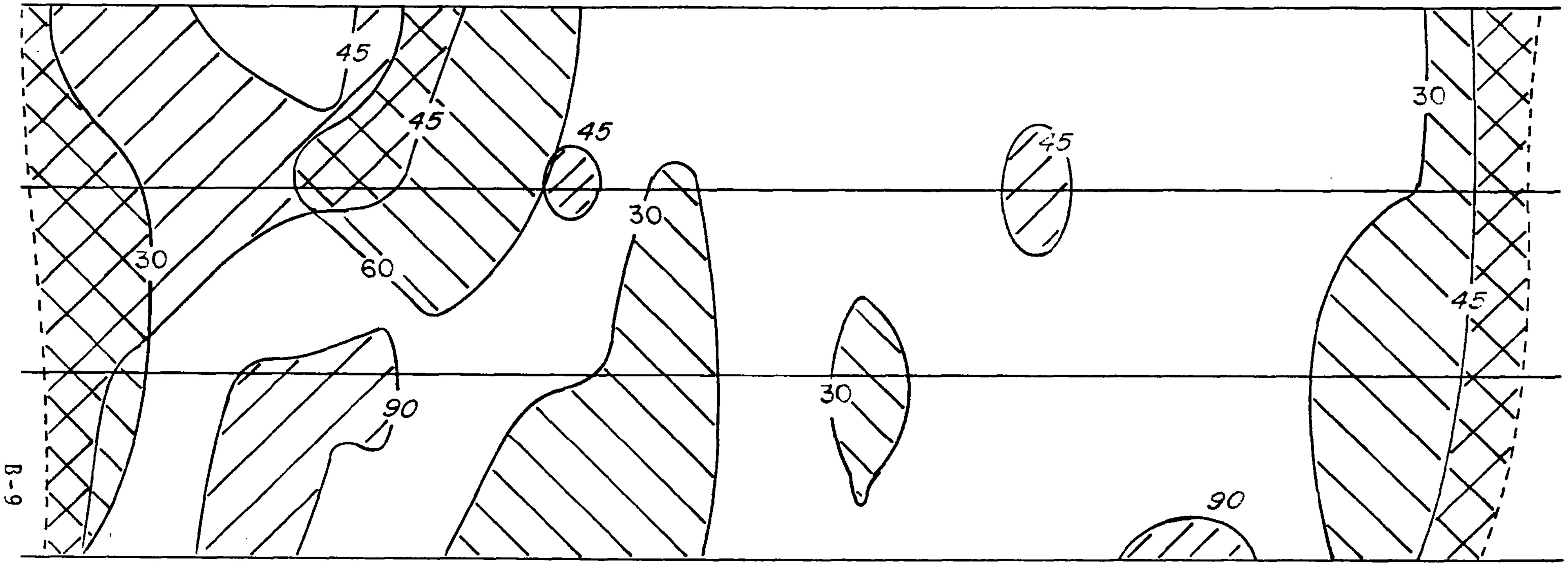

Figure B-9: Composite Map for the Orcutt Mapping Section, Showing Areas Meeting Flow Criteria for the Stonecat.

Discharge: 11.14 cms.

Area Meeting Criteria: 499 m^2

5 Meters

Area not meeting depth criteria

Area not meeting velocity criteria

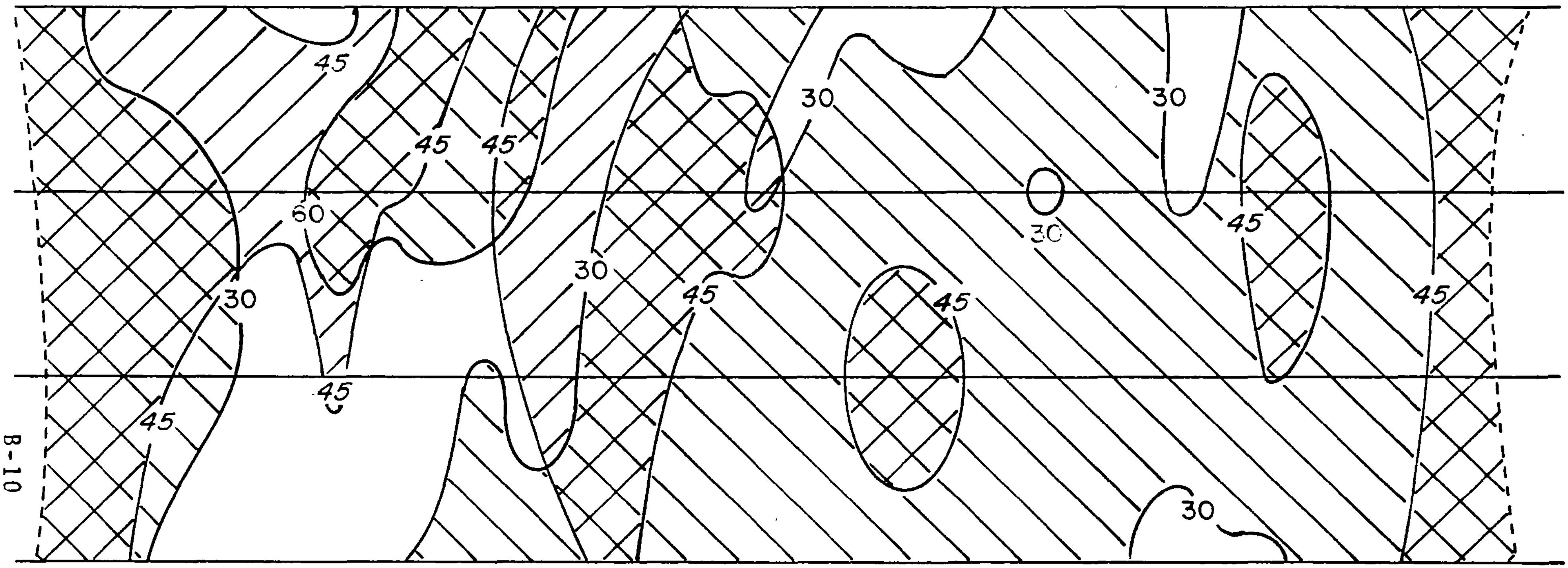

Figure B-10: Composite Map for the Orcutt Mapping Section, Showing Areas Meeting Flow Criteria for the Stonecat.

Discharge: 7.58 cms.

Area Meeting Criteria: 113 m^2

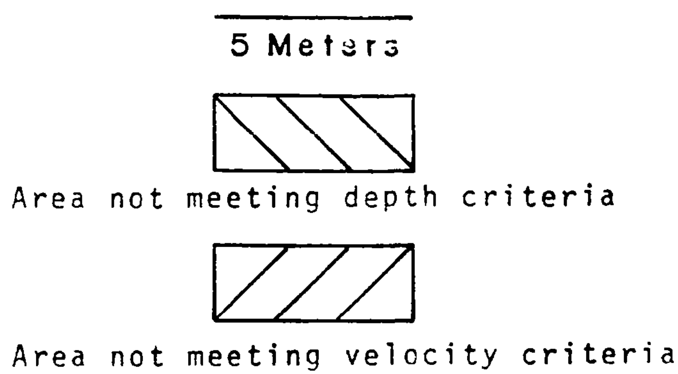

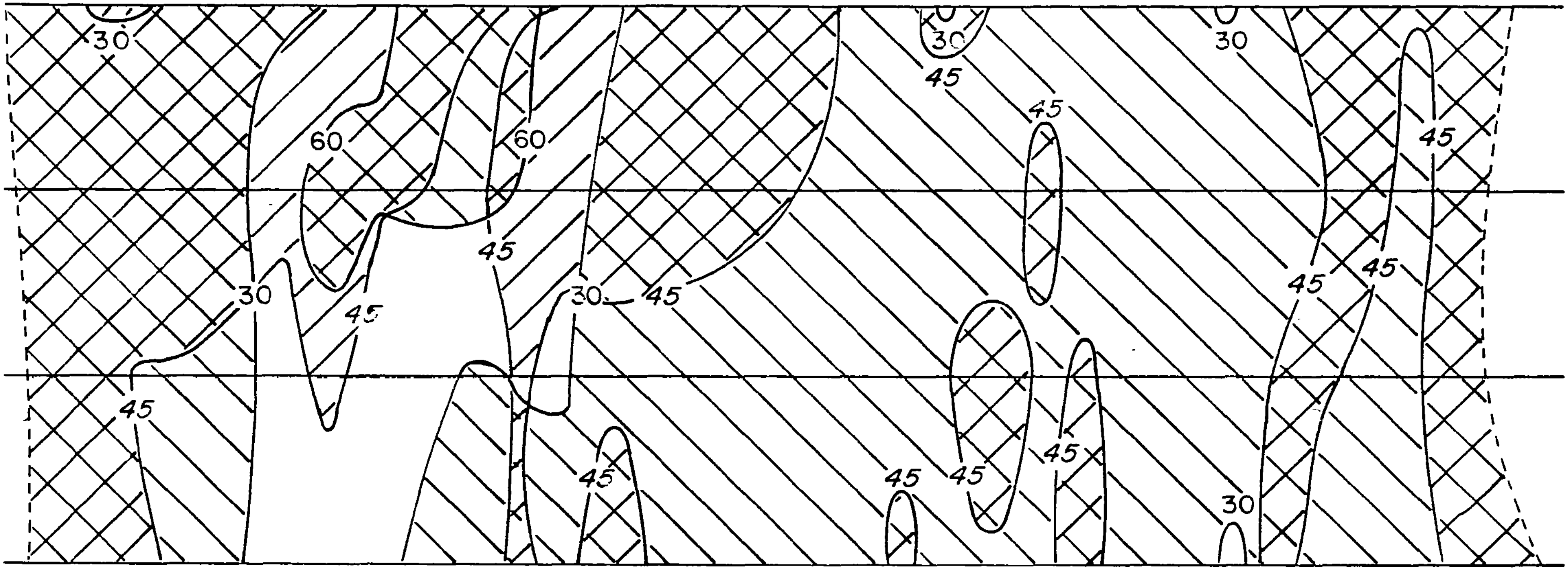

Figure B-11: Composite Map for the Orcutt Mapping Section, Showing Areas Meeting Flow Criteria for the Stonecat.

Discharge: 5.43 cms.

Area Meeting Criteria: 59 m^2

5 Meters

Area not meeting depth criteria

Area not meeting velocity criteria

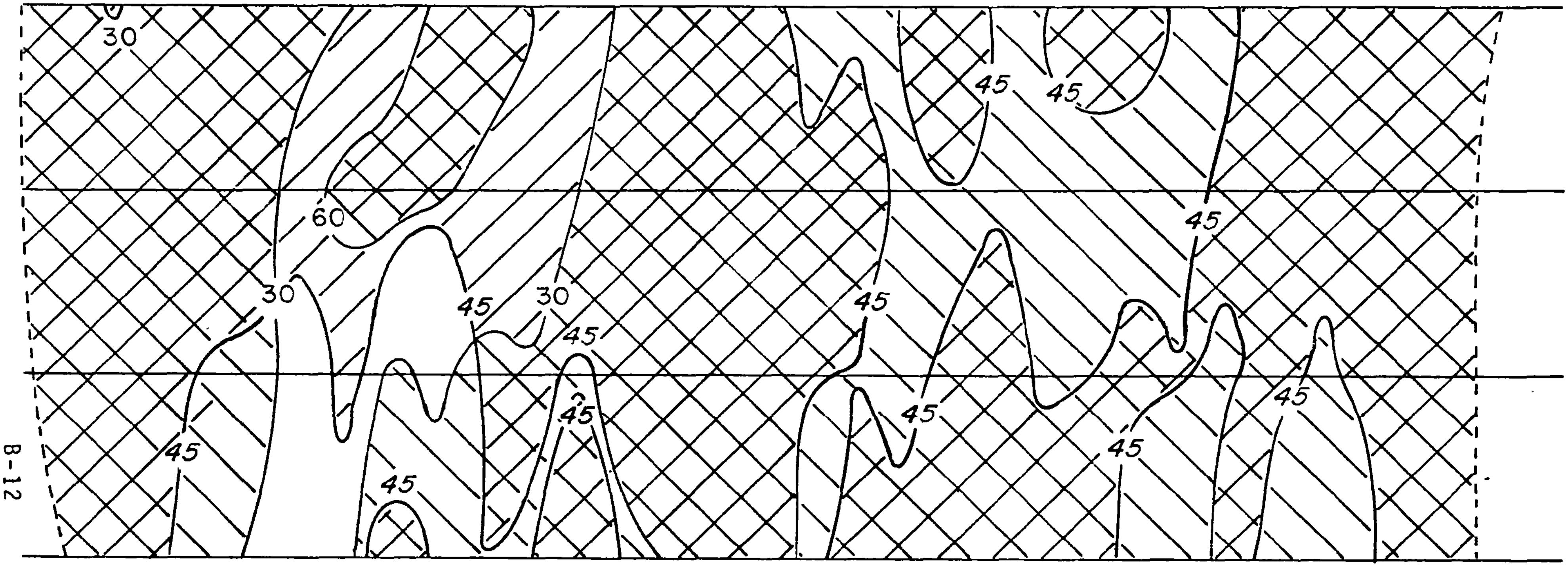

Figure B-12: Composite Map for the Orcutt Mapping Section, Showing Areas Meeting Flow Criteria for the Stonecat.

Discharge: 3.85 cms.

Area Meeting Criteria: 36 m^2

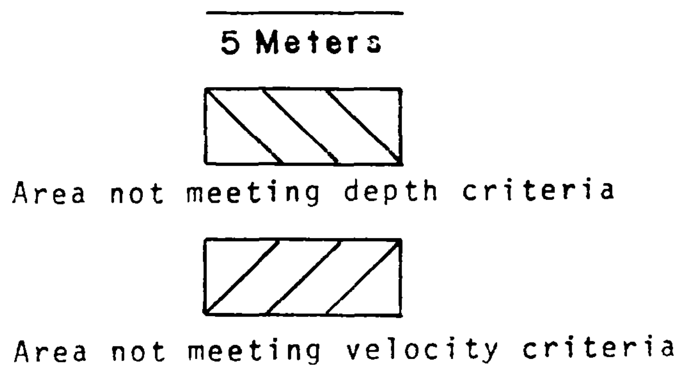

APPENDIX C

COMPOSITE MAPS

INSECT PRODUCTIVITY AREAS

1. Direction of flow is from top of page to bottom.

2. These maps indicate areas meeting preferred conditions of depth, velocity, and substrate, for optimum diversity and productivity of aquatic insects, as determined using _Rhithrogena hageni_ as the indicator species.

3. For easier interpretation, depth contours are indicated by vertical typeface. Velocity contours are indicated by slanting typeface.

4. Cross-hatched areas on composite maps indicate areas which do not meet flow criteria for _Rhithrogena hageni_. Only those areas withcut cross-hatching meet flow criteria.

5. Dashed lines indicate water's edge, either at banks or on exposed bars.

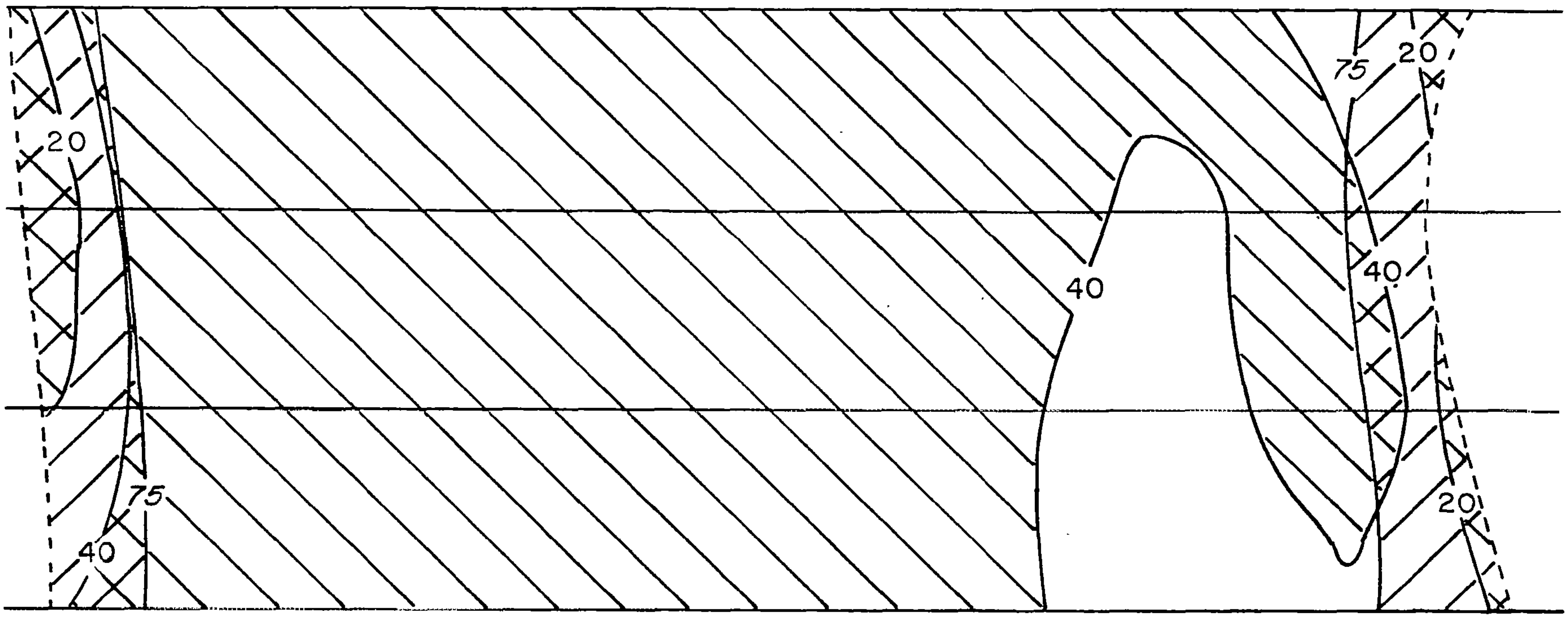

Figure C-1: Composite Map of the Viall Mapping Section Showing Areas Meeting Flow Criteria, Using *Rhithrogena hageni* as the Indicator Species.

Discharge: 19.4 cms.

Area Meeting Criteria: 92 m^2

5 Meters

Area not meeting depth criteria

Area not meeting velocity criteria

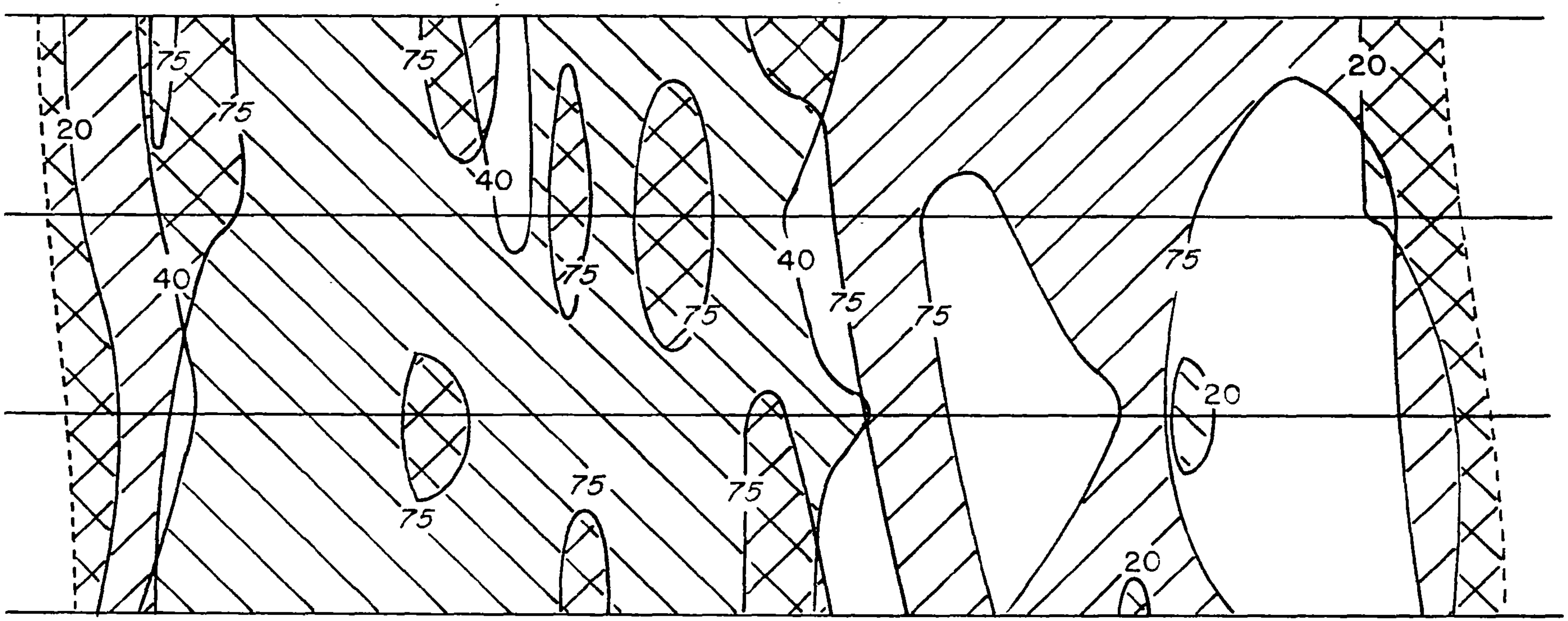

Figure C-2: Composite Map of the Viall Mapping Section, Showing Areas Meeting Flow Criteria, Using Rhithrogena hageni as the Indicator Species.

Discharge: 12.0 cms.

Area Meeting Criteria: 163 m^2

5 Meters

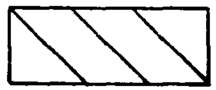

Area not meeting depth criteria

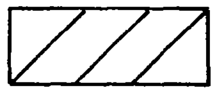

Area not meeting velocity criteria

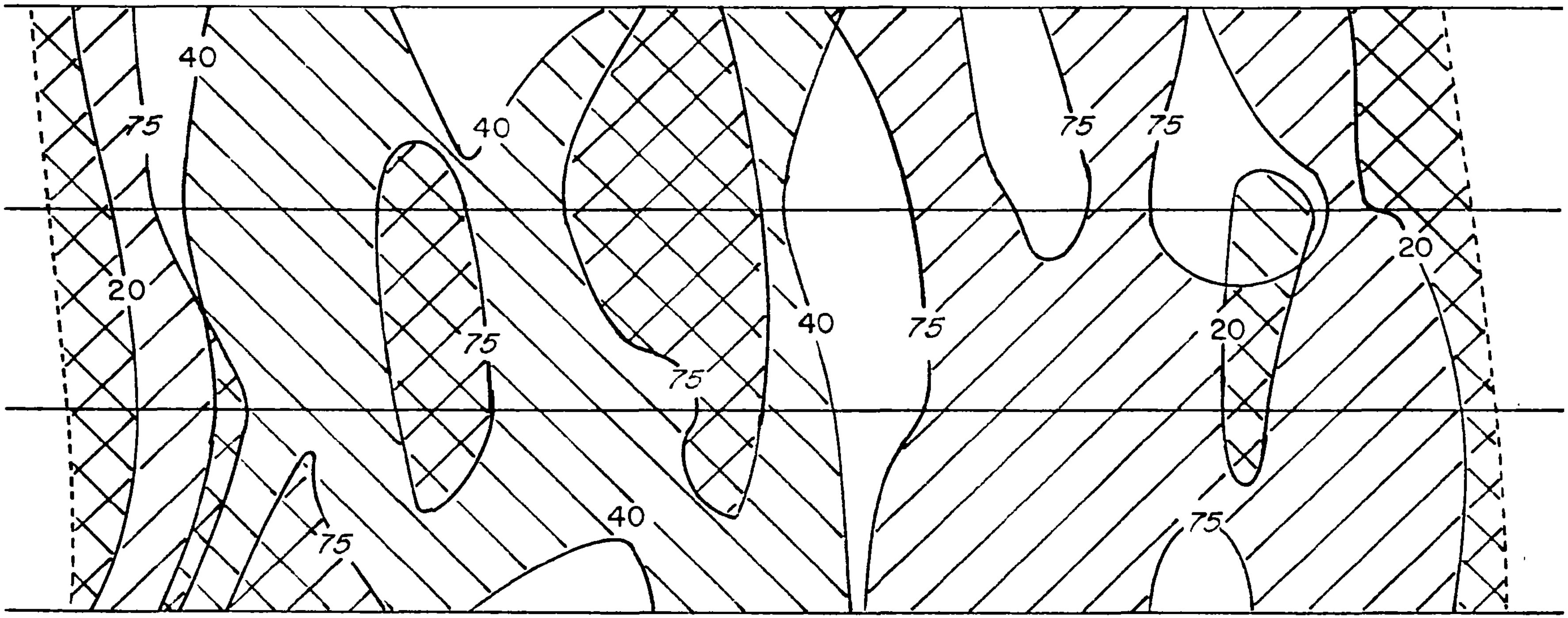

Figure C-3: Composite Map of the Viall Mapping Section, Showing Areas Meeting Flow Criteria, Using _Rhitnrogena hageni_ as the Indicator Species.

Discharge: 10.2 cms.

Area Meeting Criteria: 73 m^2

5 Meters

Area not meeting depth criteria

Area not meeting velocity criteria

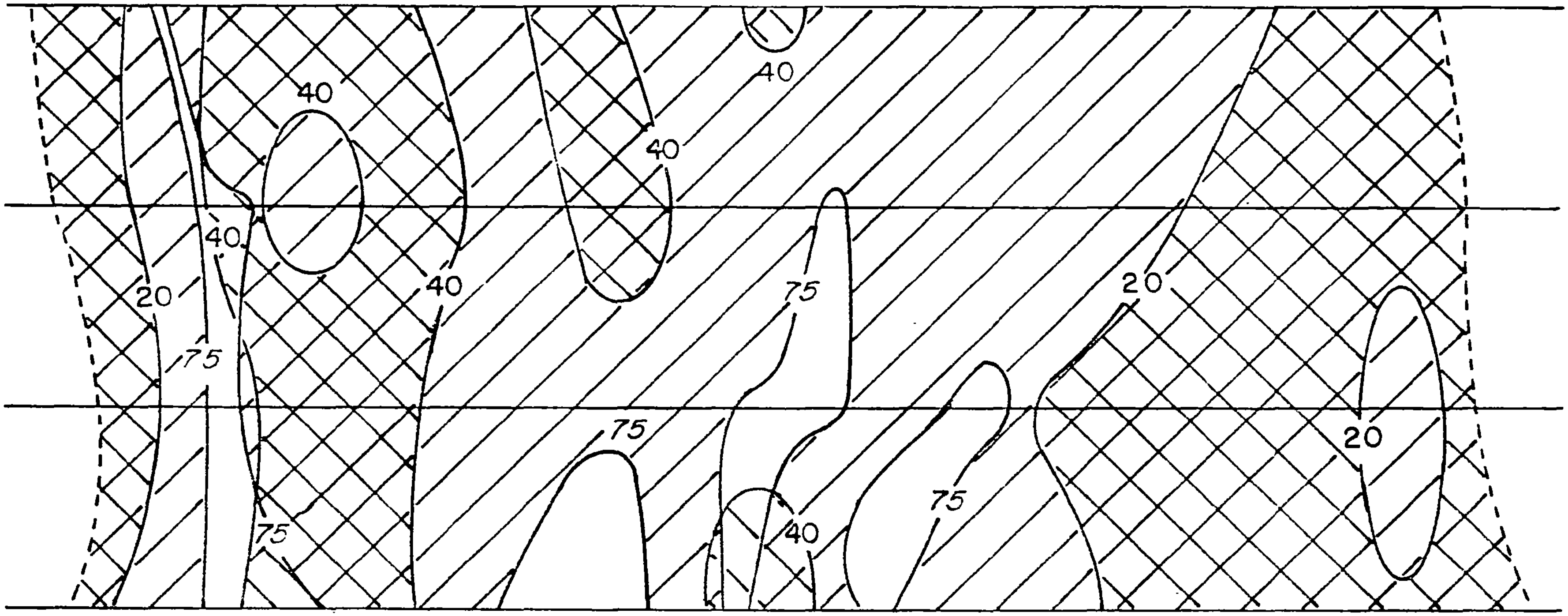

Figure C-4: Composite Map of the Viall Mapping Section, Showing Areas Meeting Flow Criteria, Using Rhithrogena hageni as the Indicator Species.

Discharge: 6.3 cms.

Area Meeting Criteria: 60 m^2

5 Meters

Area not meeting depth criteria

Area not meeting velocity criteria

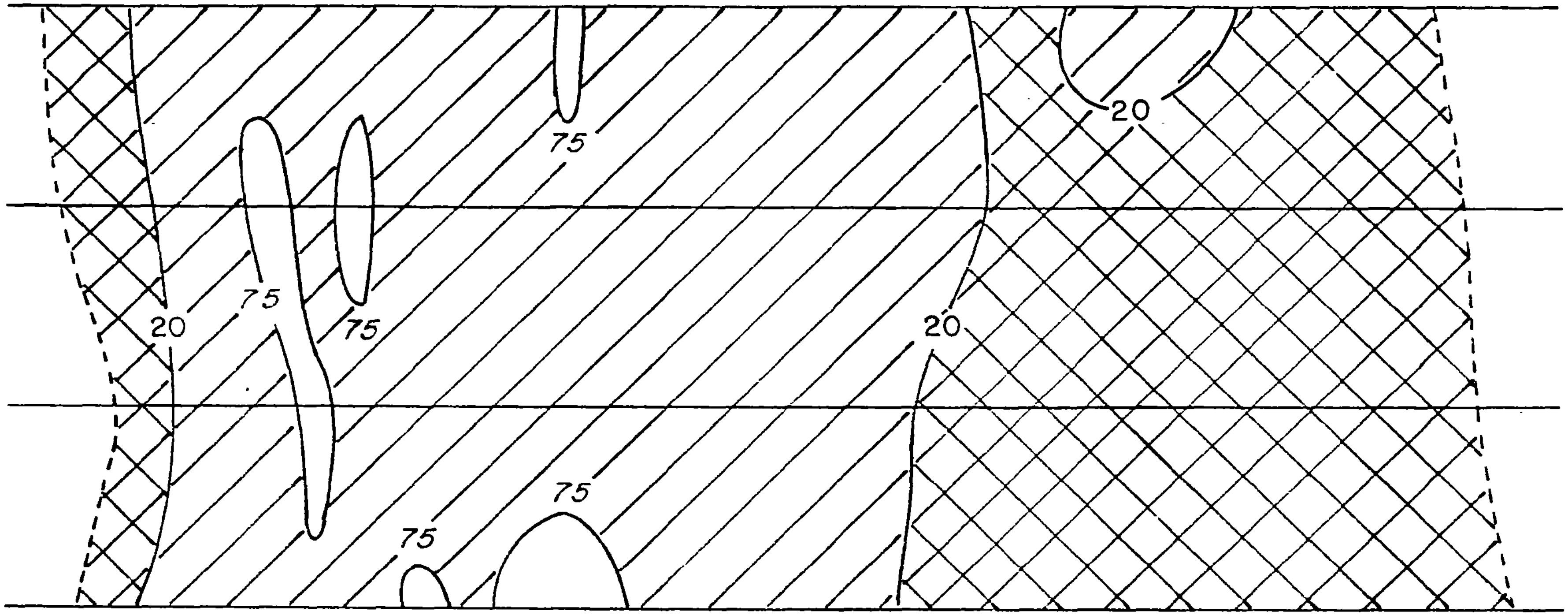

Figure C-5: Composite Map of the Viall Mapping Section, Showing Areas Meeting Flow Criteria, Using <u>Rhithrogena</u> <u>hageni</u> as the Indicator Species.

Discharge: 5.58 cms.

Area Meeting Criteria: 23 m^2

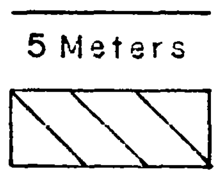

Area not meeting depth criteria

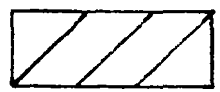

Area not meeting velocity criteria

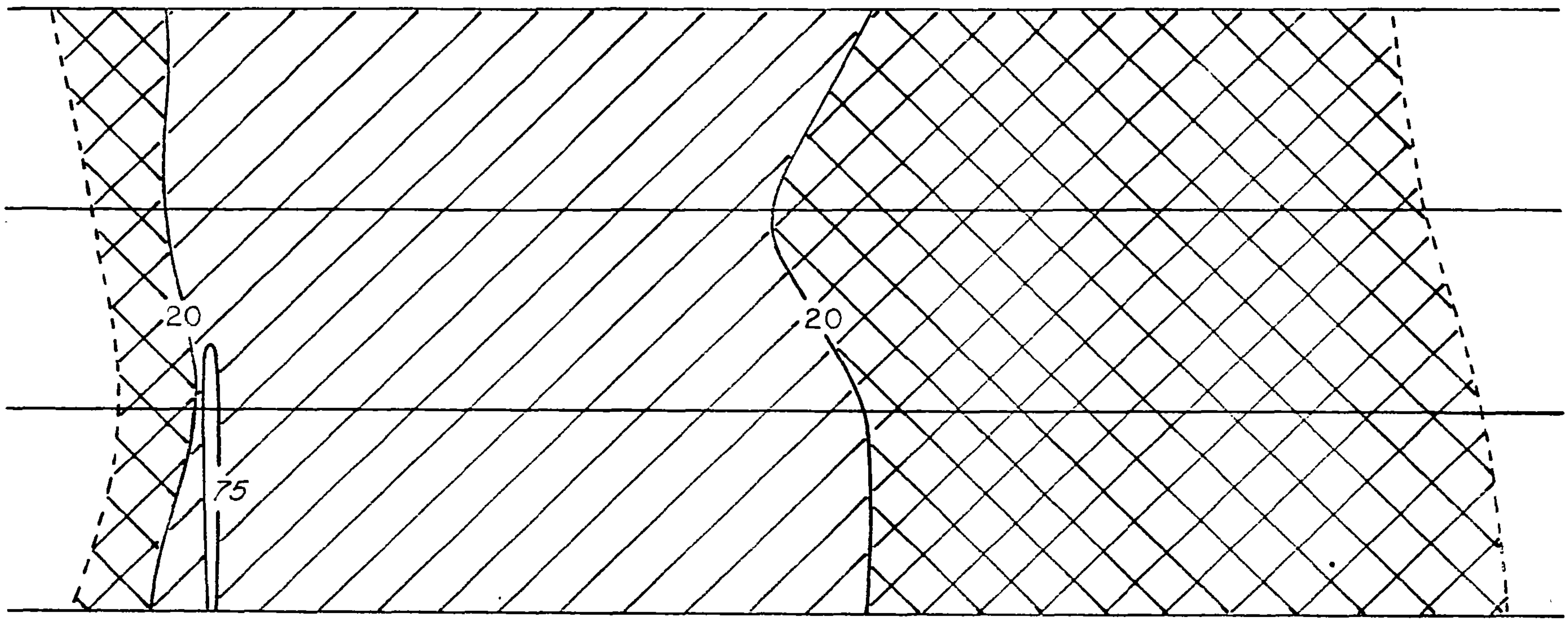

Figure C-6: Composite Map of the Viall Mapping Section, Showing Areas Meeting Flow Criteria, Using <u>Rhithrogena</u> <u>nageni</u> as the Indicator Species.

Discharge: 4.02 cms.

Area Meeting Criteria: 3 m^2

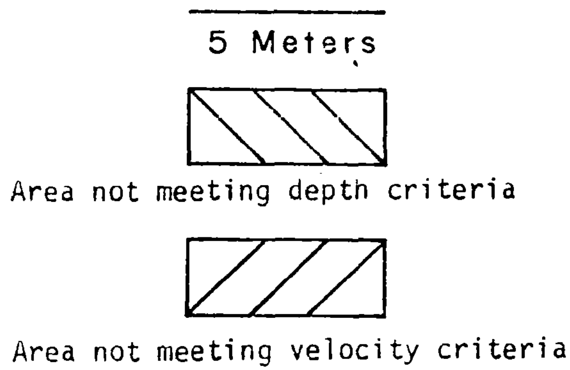

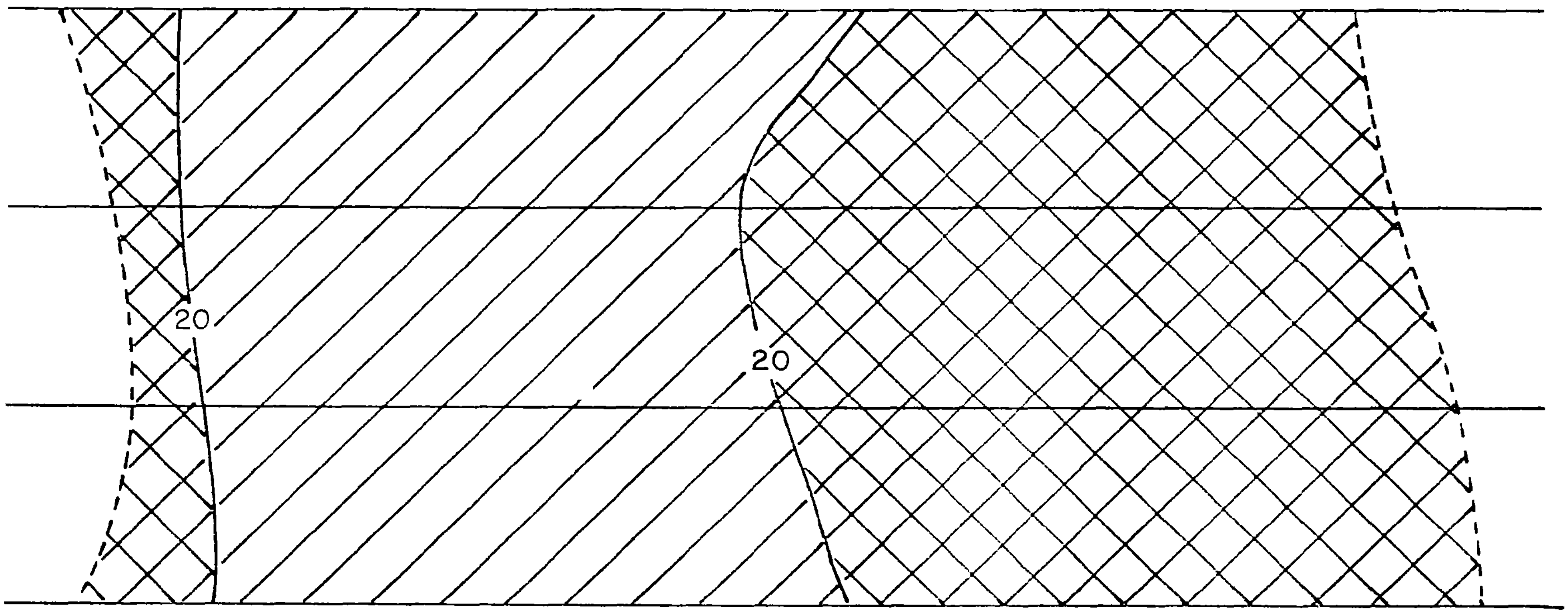

Figure C-7: Composite Map of the Viall Mapping Section, Showing Areas Meeting Flow Criteria, Using <u>Rhitnrogena hageni</u> as tne Indicator Species.

Discharge: 2.83 cms.

Area Meeting Criteria: 0 m^2

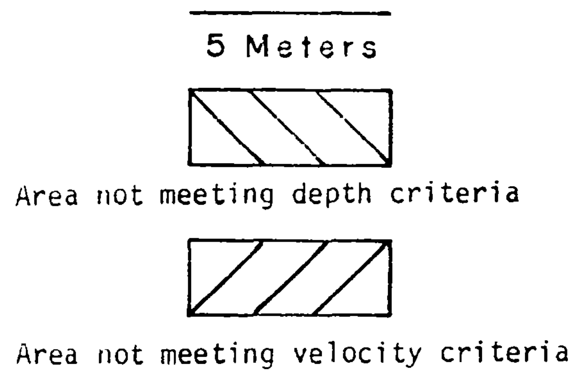

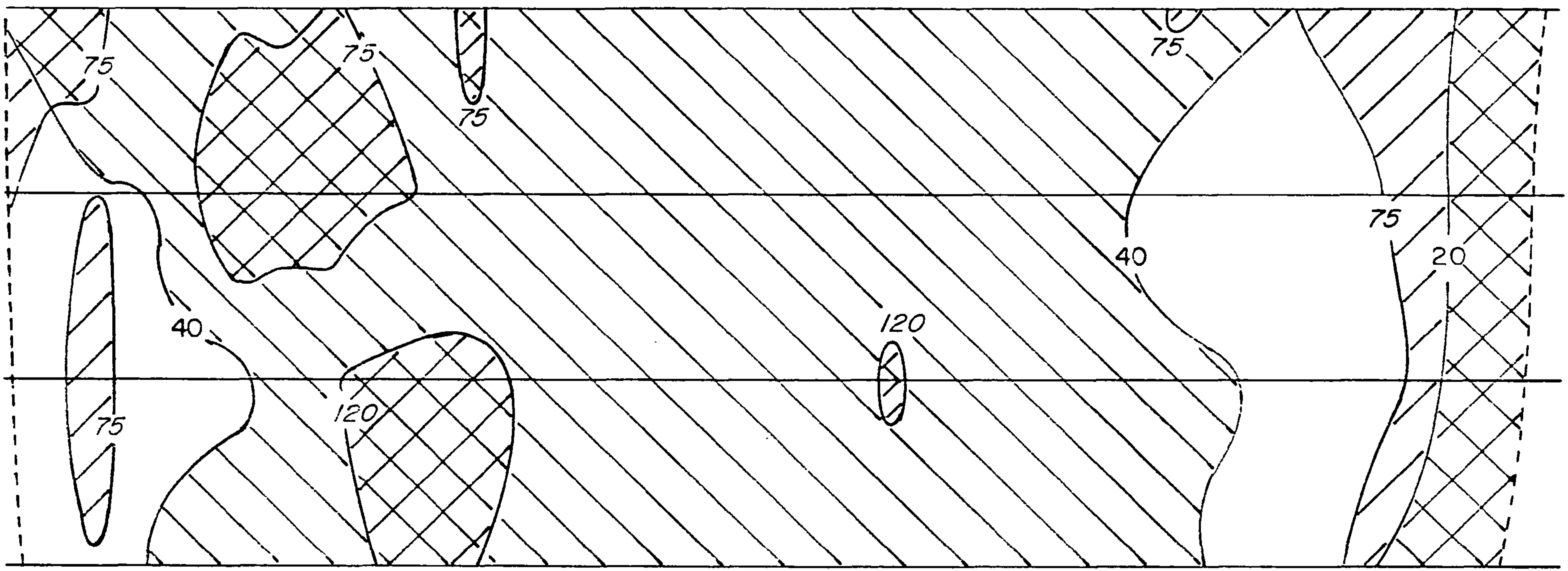

Figure C-8: Composite Map of the Orcutt Mapping Section, Showing Areas Meeting Flow Criteria, Using _Rhithrogena hageni_ as the Indicator Species.

Discharge: 18.63 cms.

Area Meeting Criteria: 147 m^2

5 Meters

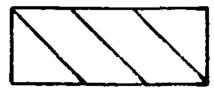

Area not meeting depth criteria

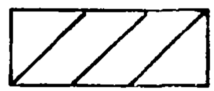

Area not meeting velocity criteria

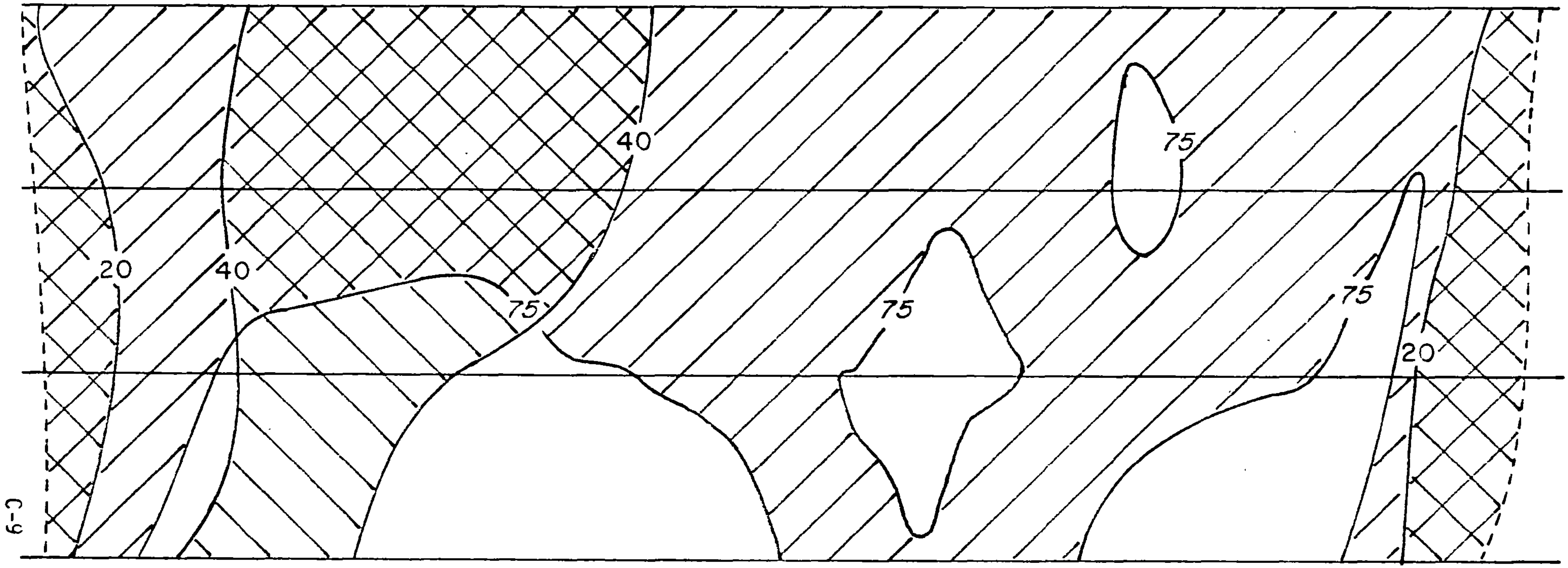

Figure C-9: Composite Map of the Orcutt Mapping Section Showing Areas Meeting Flow Criteria, Using <u>Rhitnrogena</u> <u>hageni</u> as the Indicator Species.

Discharge: 11.14 cms.

Area Meeting Criteria: 177 m^2

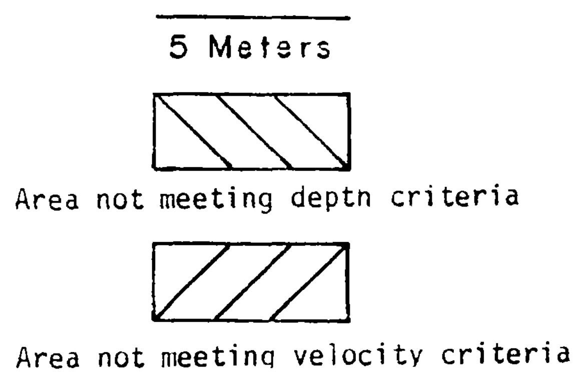

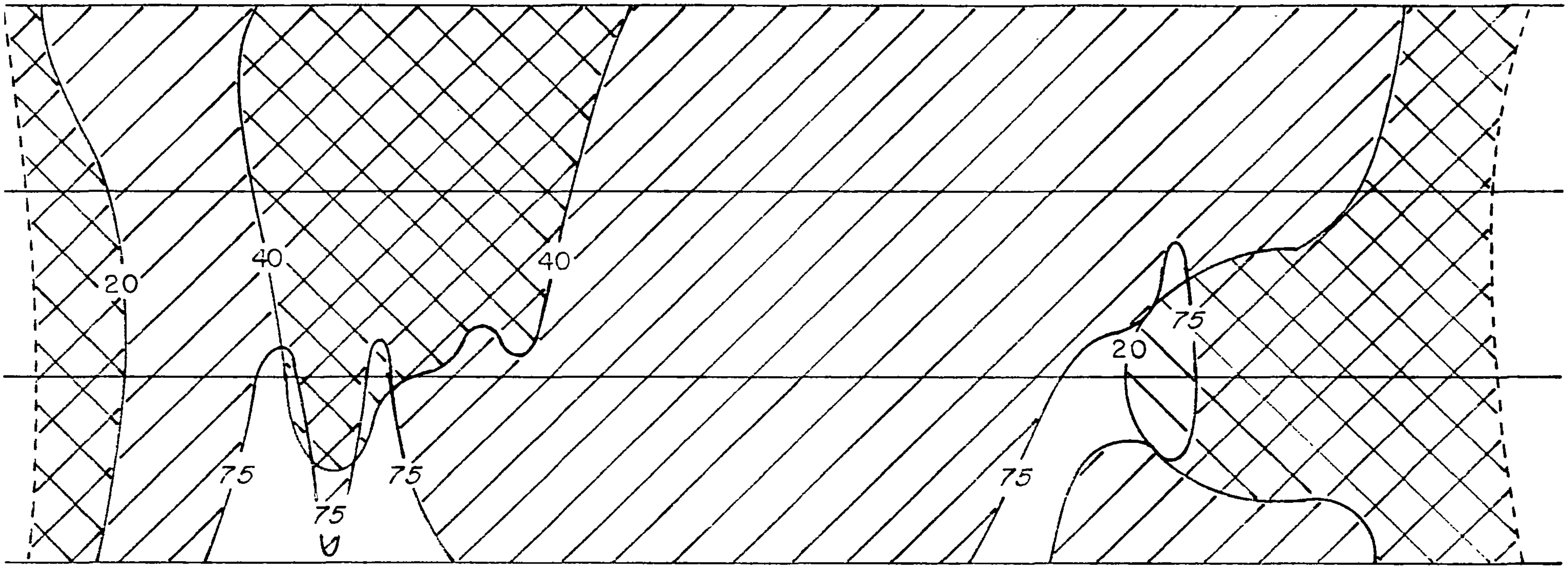

Figure C-10: Composite Map of the Orcutt Mapping Section, Showing Areas Meeting Flow Criteria, Using Rhithrogena hageni as the Indicator Species.

Discharge: 7.58 cms.

Area Meeting Criteria: 72 m^2

5 Meters

Area not meeting depth criteria

Area not meeting velocity criteria

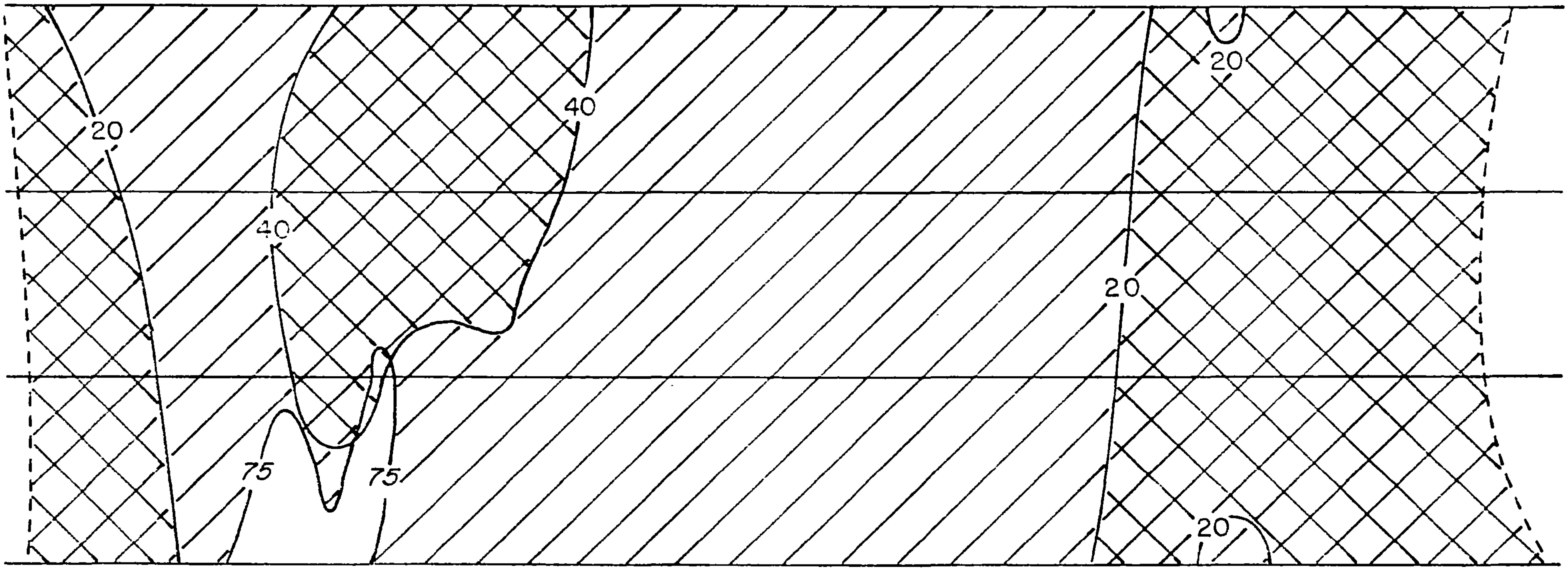

Figure C-11: Composite Map of the Orcutt Mapping Section, Showing Areas Meeting Flow Criteria, Using *Rhithrogena hageni* as the Indicator Species.

Discharge: 5.43 cms.

Area Meeting Criteria: 20 cms.

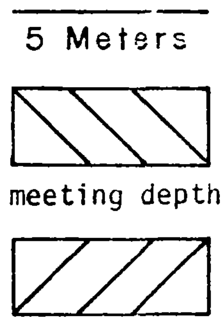

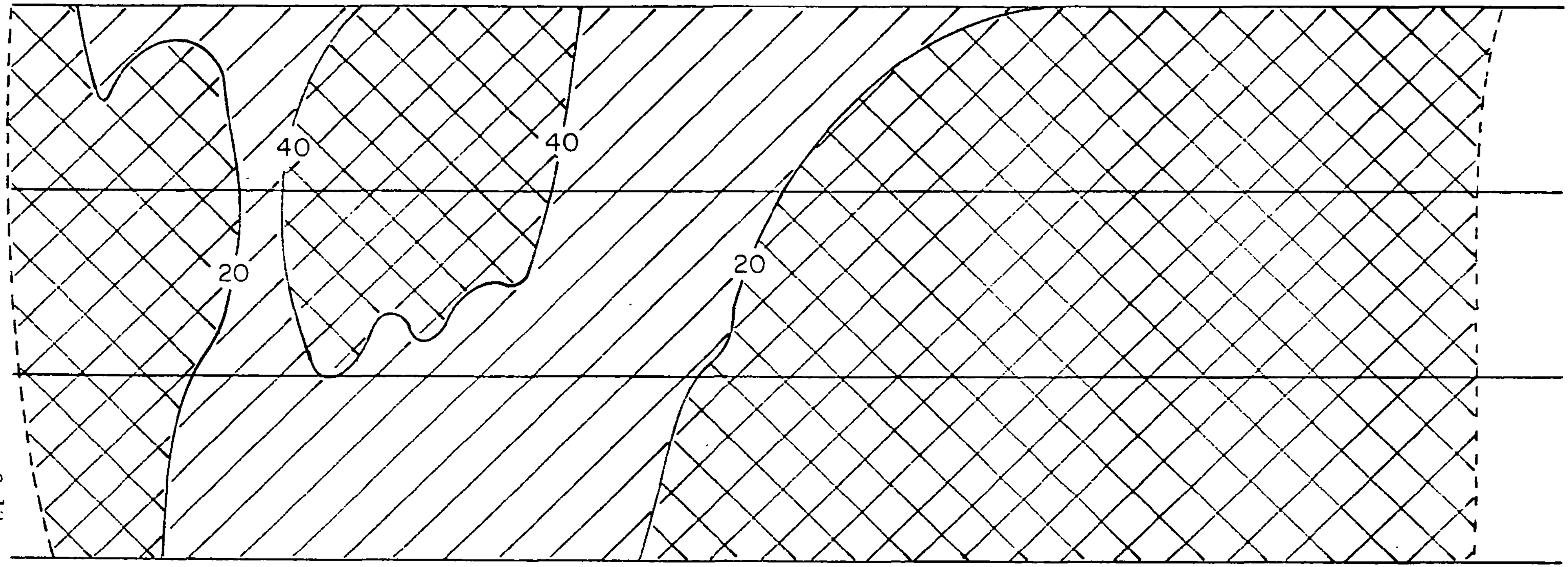

Figure C-12: Composite Map of the Urcutt Mapping Section, Showing Areas Meeting Flow Criteria, Using <u>Rhithrogena hageni</u> as the Indicator Species.

Discharge: 3.85 cms.

Area Meeting Criteria: 0 m^2

5 Meters

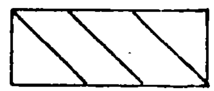

Area not meeting depth criteria

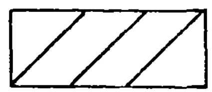

Area not meeting velocity criteria

APPENDIX D

MACROINVERTEBRATE ECOLOGY

APPENDIX D: MACROINVERTEBRATE ECOLOGY

Microprofile Measuring Device

Measurement of the exact composition of the substrate would be an extremely long and time consuming process for each of 175 samples collected in this study. However, the nature of the substrate material determines the profile of the substrate, and it is this profile to which the invertebrates must adapt in order to obtain habitable conditions of current velocity. The index of the profile can provide, with proper interpretation, information on the roughness of the substrate and surface area availability. The method used allows the investigator to measure the substrate profile, before sampling benthic organisms, without having to map the position of the substrate particles or physically remove portions of the substrate for measurement. In this manner, a given piece of substrate can be rapidly recolonized so that samples on the same substrate can be taken again, if necessary.

The prototypic device is designed to fit within a Hess Bottom sampler. The micro-profile sampler is constructed using a circular sheet of plexiglass (about 1 cm. thick) with a diameter of 35.68 cm., to give a tenth-square-meter surface area (see Figure D1). The sheet is prepared by drilling holes in a grid pattern such that 21 holes are placed at 5 cm. intervals in the grid pattern. The holes are drilled large enough to accept 21 threaded steel rods of about 8 mm. diameter (rods of smaller diameter cause too much free play on the plexiglass sheet to be effective). Three of the steel rods are fixed to the sheet at a standard distance of 17.5 cm. from the bottom surface of the sheet with a system of washers, lock washer, and nuts to fit the threaded rods. These three supportive legs are placed to form a uniform triangle in three outer grid holes.

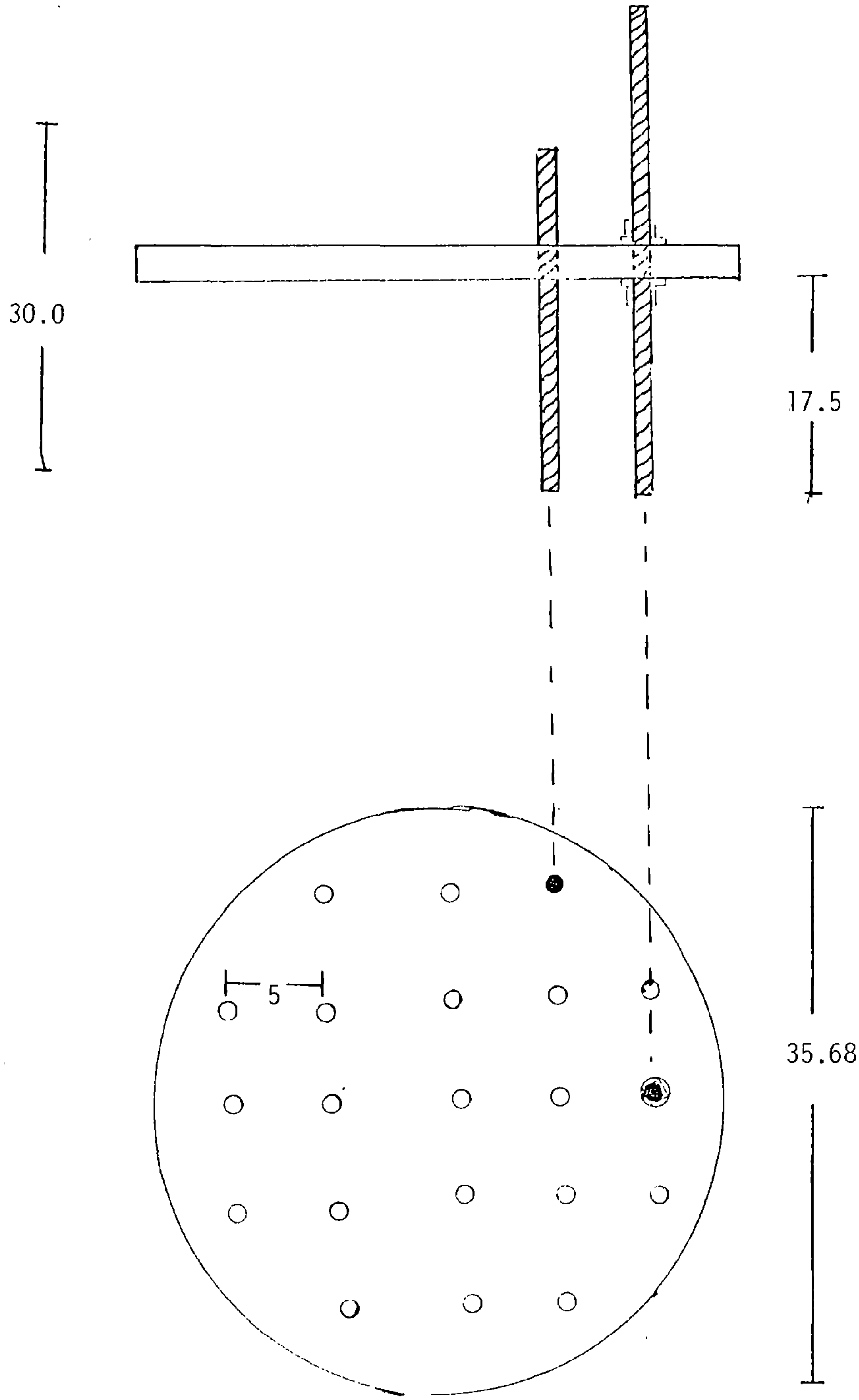

Figure D1. Schematic of Microprofile Measuring Device.
All measurements are in cm.

This device is then placed within the Hess sampler, which has been previously placed in the water upon the substrate area to be sampled. The fixed legs, which provide a "zero" reference point, should be maneuvered to be as close to the base substrate as possible; that is, not upon any large objects protruding from the substrate surface. The remaining 18 rods, each 30 cm. long, are allowed to fall vertically within their respective grid holes. As the rods make contact with various objects on the substrate the rods are clamped (a standard barrel-type pinch clamp is suitable) at the upper surfaces of the plexigless sheet to prevent further movement.

When all rods have been placed, the device can be removed from the Hess sampler (using the fixed legs as handles) and invertebrate sampling can continue by normal procedure. Once the device is removed, the length of the 18 "free" rods are measured from the plexiglass surface to the tip of the rod. If the grid is numbered and the rods are measured and recorded, a three-dimensional schematic drawing of the substrate can be made. The distances to be schematically represented are the lengths of the 18 "free" rods minus the length of a "standard" rod which has been allowed to fall to a flat surface upon which the device is also sitting. The standard deviation of the mean length of the 21 rods (where the three fixed rods are "standard" length) provides a single descriptive index (I) which is useful in habitat description. The index numbers are defined below:

I	PROFILE TYPE
0 - 0.5	Smooth
0.5 - 1.0	Moderately smooth (gravel)
1.0 - 1.5	Small cobbled
1.5 - 2.0	Smooth, medium cobbled
2.0 - 2.5	Rough, medium cobbled
2.5 - 3.0	Large cobbled
3.0 - 4.0	Bouldered
4.0	Critical (angular boulders)

Velocity, depth, micro-profile, and turbulence (by Froude number, F), where:

$$F = \frac{V}{\sqrt{g\,D}} \qquad \text{(Eq. D-1)}$$

and; V = current velocity in cm./sec.

D = depth in centimeters

g = acceleration due to gravity (980 cm./sec^2.)

were compared with diversity of insects in the sample and number of individuals of a given species per sample, in order to determine optimum flow related conditions.

Flow Related Requirements For Macroinvertebrates

The following figures and tables illustrate the optimum conditions of depth, velocity, turbulence, and microprofile for the invertebrates examined. The large square on the velocity and depth Figures (D1 - D31) is the area representing conditions of maximum diversity (also Table D-1). The calculations for this area, the COCD, and the optimum centroids for the individual macroinvertebrates, are described in Chapter 5 of the report. In addition, the area where at least 80% of the macroinvertebrates occurred is also shown on each of the figures (D2 - D31). The centroids, like the COCD, describe the optimum point on the surface for either velocity, depth, and number of individuals, or turbulence, microprofile, and number of individuals. A definite area of maximum diversity was not defined in the relation between microprofile and turbulence (Table D-2). It can be assumed that the maximum diversity area will be generally located in close proximity to the COCD for microprofile and turbulence.

V \ D	0 - 10	10 - 20	20 - 30	30 - 40	40 - 50
0 - 15	.667	1.112	1.405	1.530	1.371
16 - 30	1.348	1.218	1.957	1.054	1.505
31 - 45	1.628	1.893	1.977	1.933	1.845
46 - 60	1.440	1.721	1.605	1.958	1.812
61 - 75	1.523	1.703	1.728	2.034	1.612
76 - 90	1.652	1.809	2.319	2.190	2.156
91 - 105	1.203	1.983	2.211	1.844	2.072
105-120	1.386	1.661	2.612	2.027	1.724
>120	.541	1.802	2.131	2.301	1.817

Table D1. Average Diversities for Depth and Velocity. Average diversity for all samples that occured within the block represented by the increments of depth and current velocity. Current velocity in cm./sec. Depth in cm.

F \ I	.5 - 1.0	1 - 1.5	1.5 - 2.0	2 - 2.5	2.5 - 3	3 - 4
0 - .1		1.399	1.327	1.744		
.1 - .2	1.609		1.356	1.400	1.995	
.2 - .3		2.119	2.099	2.000	1.657	
.3 - .4	1.310	1.871	1.589	1.978	2.064	
.4 - .5	1.946	2.080	1.745	2.017	1.959	2.366
.5 - .6		2.763	2.040	1.560	1.072	
.6 - .7			2.111	1.875		2.6000
>.7	1.476			2.025	1.750	

Table D2. Average Diversities for Microprofile and Turbulence. Average diversity for all samples that occured within the blocks represented by the increments of microprofile anc turbulence.

Table D-3: Centroids of optimum velocity (C_v), depth (C_d), microprofile index (C_i), and Froude Number (C_f) for 38 species of macroinvertebrates in the Tongue River. Depths and velocities have been rounded to the nearest cm. and cm./sec., respectively.

Species	C_v	C_d	C_i	C_f
DIVERSITY	76.	28.	2.01	.401
Ephoron album	97.	30.	2.03	.557
Baitis tricaudatus	74.	28.	2.01	.411
Baetis alexanderi	55.	23.	1.80	.392
Ephemerella margarita	84.	25.	1.99	.502
Ephemerella hystrix	82.	29.	2.05	.526
Tricorythodes minutus	68.	33.	2.00	.356
Choroterpes albiannulata	62.	27.	2.07	.425
Traverella albertana	80.	32.	2.14	.499
Stenonema reesi	60.	27.	1.73	.336
Rhithrogena hageni	82.	32.	2.07	.454
Strophopteryx fasciata	73.	19.	1.97	.478
Paraleuctra sara	74.	15.	2.10	.500
Capnia limata	56.	23.	2.19	.348
Isogenoides frontalis	71.	36.	2.24	.402
Acroneuria abnormis	81.	27.	1.99	.505
Ophiogomphus morrisoni	73.	28.	2.24	.376
Hydroptila sp.	63.	30.	2.09	.343
Cheumatopsyche sp.	74.	33.	2.16	.396
Hydropsyche bifida	76.	33.	2.10	.450
Hydropsyche occidentalis	66.	26.	1.95	.417

Table D-3 (Con't)

Species	C_v	C_d	C_i	C_f
Hydropsyche sp. a	83.	34.	2.07	.462
Hydropsyche sp. b	83.	35.	1.87	.390
Hydropsyche sp. c	61.	31.	2.03	.321
Brachycentrus americanus	68.	28.	1.94	.357
Leptocella sp.	52.	29.	1.74	.274
Athripsodes sp.	79.	27.	1.97	.404
Rhagovelia sp.	22.	31.	2.21	.155
Stenelmis sp. a (1)	72.	30.	2.05	.405
Stenelmis sp. a (a)	73.	29.	2.26	.403
Stenelmis sp. b (1)	62.	25.	1.89	.385
Stenelmis sp. b (a)	70.	33.	1.96	.358
Dubiraphia sp.	57.	28.	1.55	.347
Simulium sp.	78.	27.	2.23	.495
Metriocnemus sp.	78.	31.	1.83	.443
Sphaerium simile	92.	34.	2.00	.500
Physa gyrina	93.	39.	1.82	.421
Dugesia tigrina	48.	23.	1.80	.309

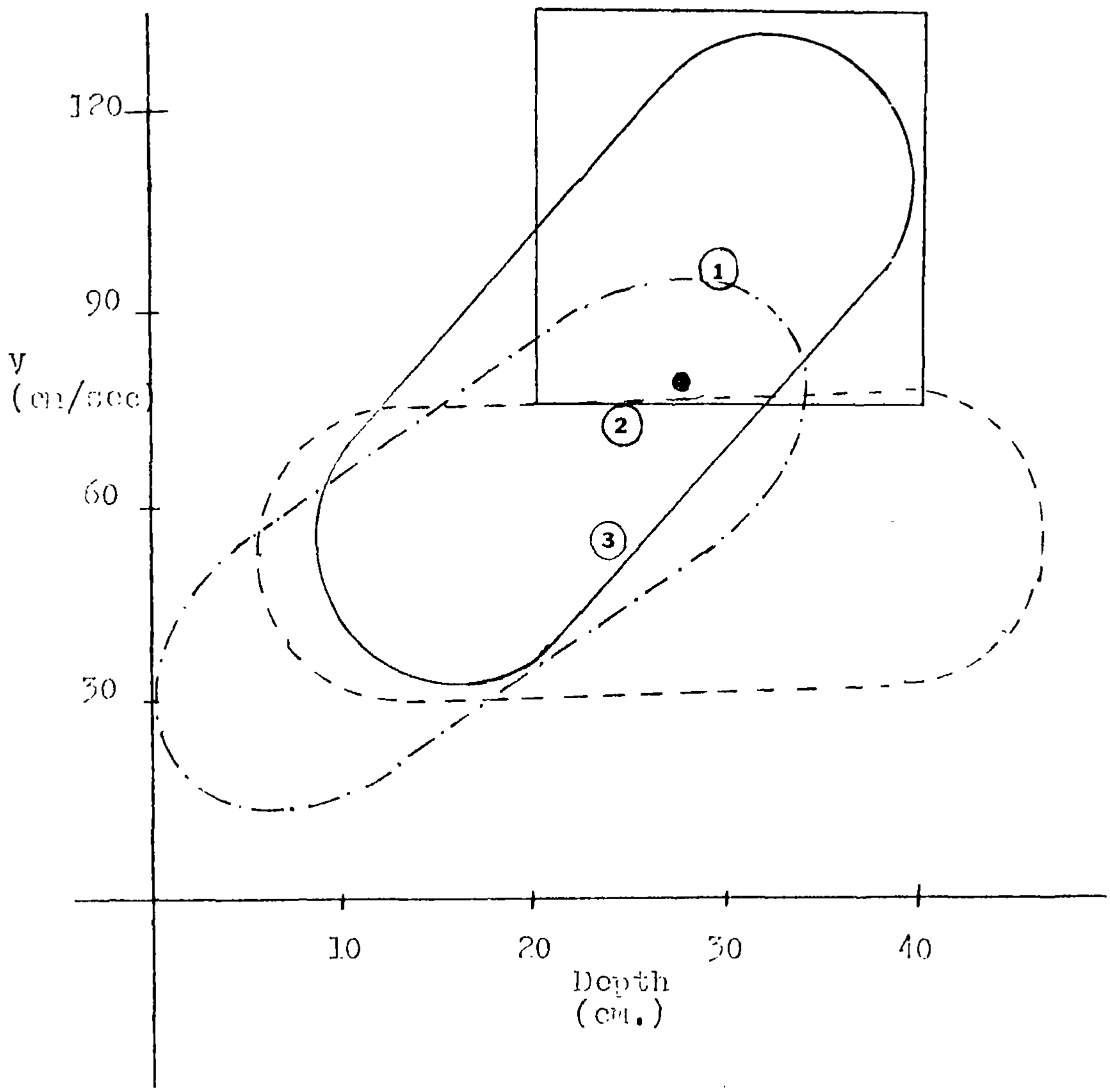

Figure D2. Optimum Depth and Current Velocities. Ephemeroptera. Ephoron album (1 and solid line), Baetis tricaudatus (2 and dashed line), and Baetis alexanderi (3 and alternating dashed and dotted line).

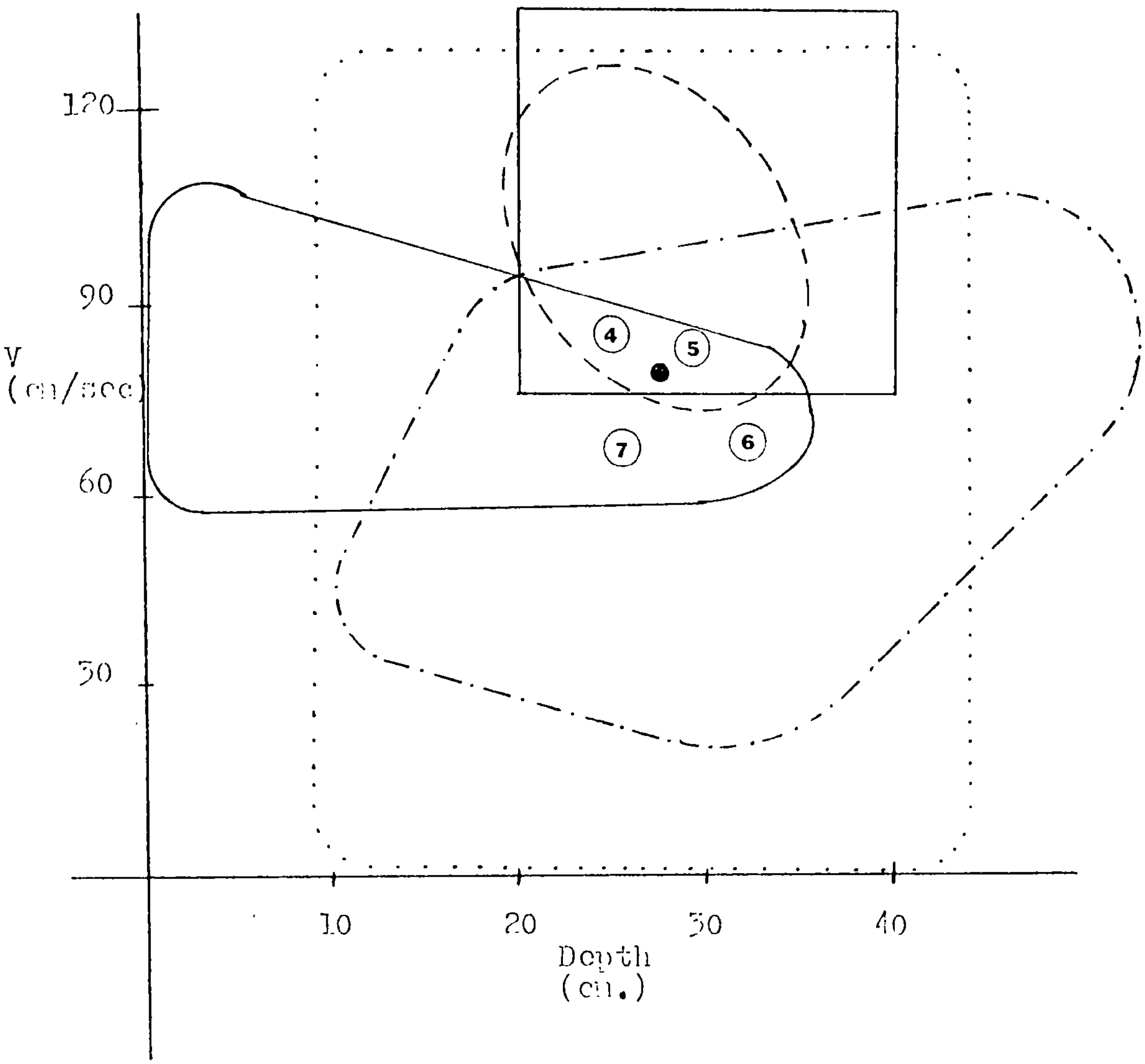

Figure D3. Optimum Depth and Current Velocities. Ephemeroptera. Ephemerella margarita (4 and solid line), Ephemerella hystrix (5 and dashed line), Tricorythodes minutus (6 and alternating dashed and dotted line), and Choroterpes albiannulata (7 and dotted line).

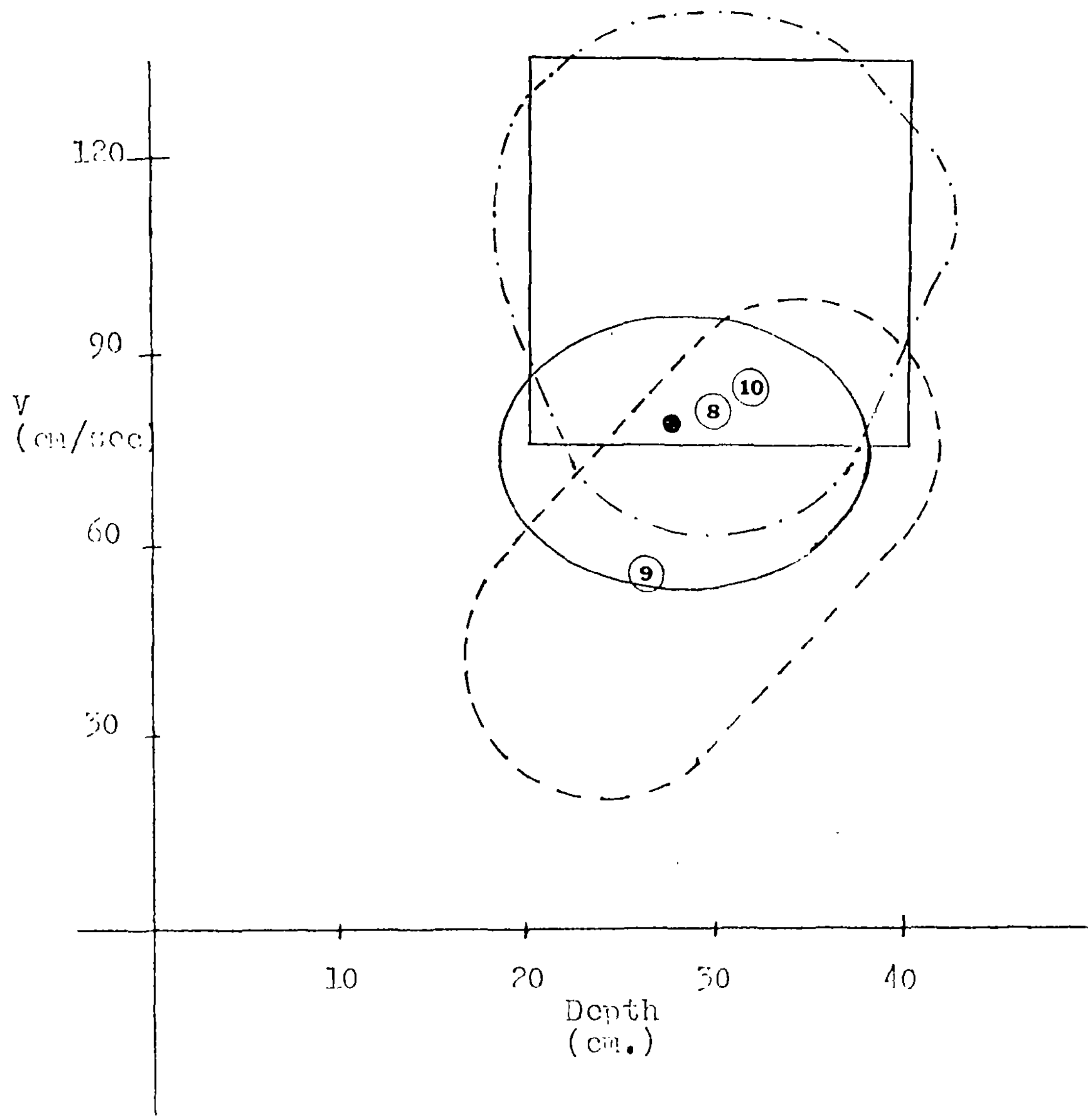

Figure D4. Optimum Depth and Current Velocities. Ephemeroptera. Traverella albertana (8 and solid line), Stenonema reesi (9 and dashed line), and Rhithrogena hageni (10 and alternating dashed and dotted line).

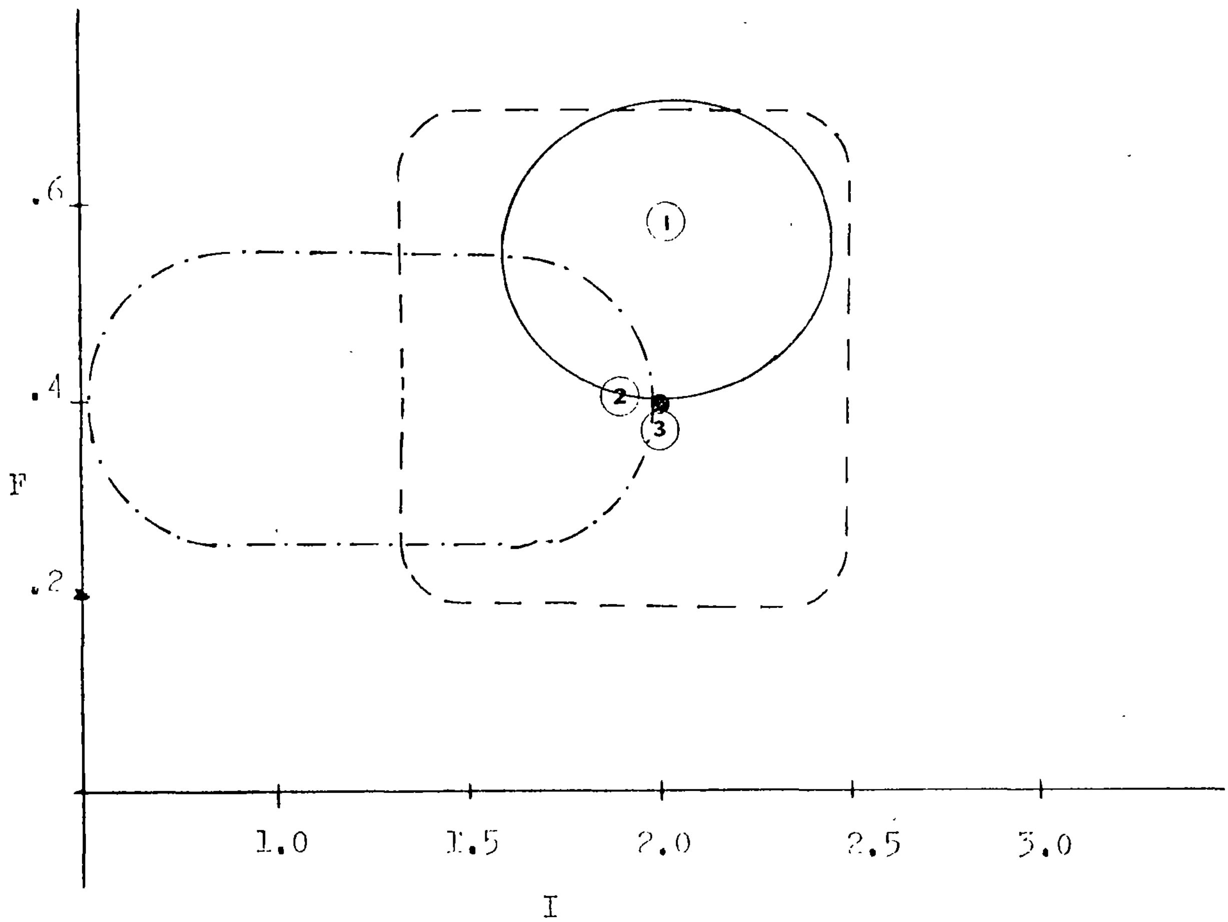

Figure D5. Optimum Turbulence and Microprofile. Ephemeroptera. Ephoron album (1 and solid line), Baetis tricaudatus (2 and dashed line), and Baetis alexanderi (3 and alternating dashed and dotted line).

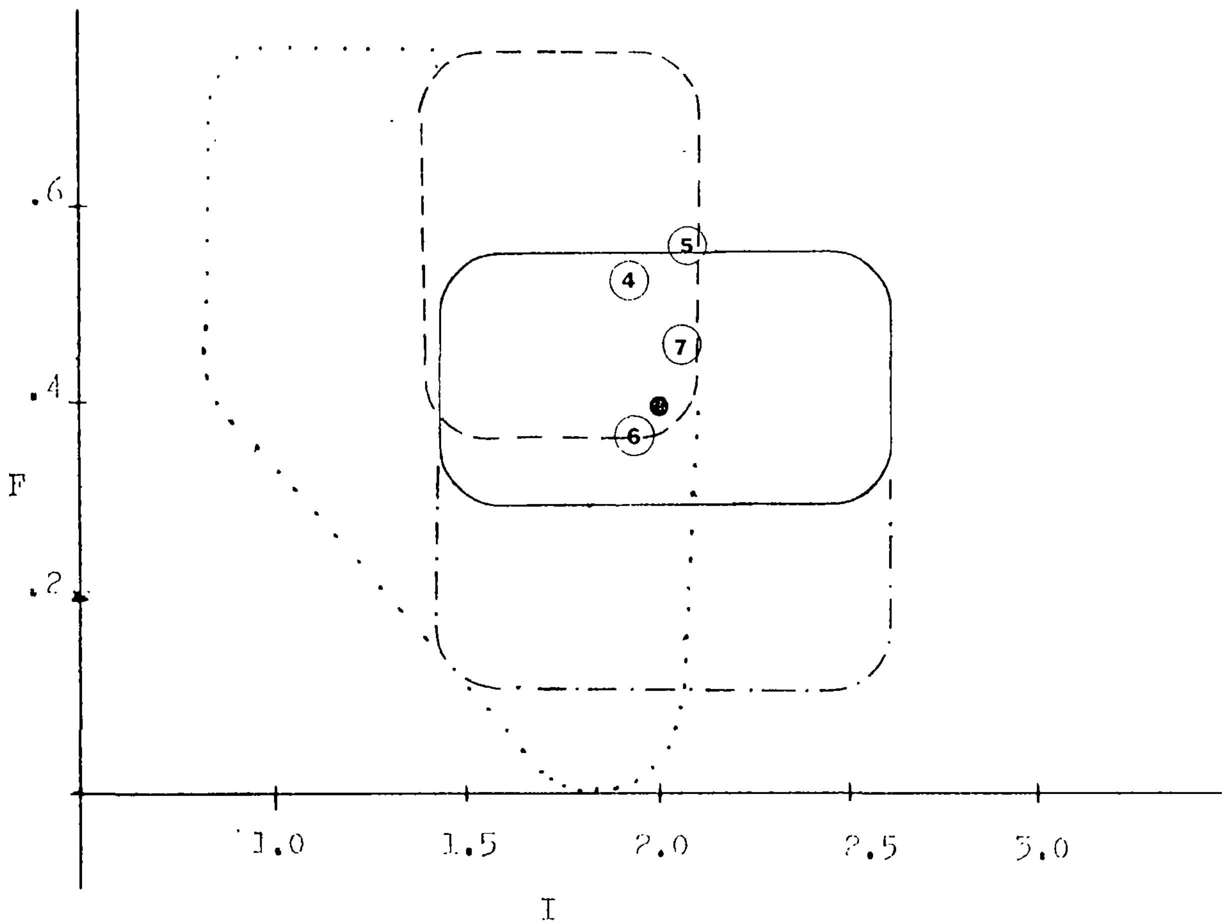

Figure D6. Optimum Turbulence and Microprofile. Ephemeroptera. Ephemerella margarita (4 and solid line), Ephemerella hystrix (5 and dashed line), Tricorythodes minutus (6 and alternating dashed and dotted line), and Choroterpes albiannulata (7 and dotted line).

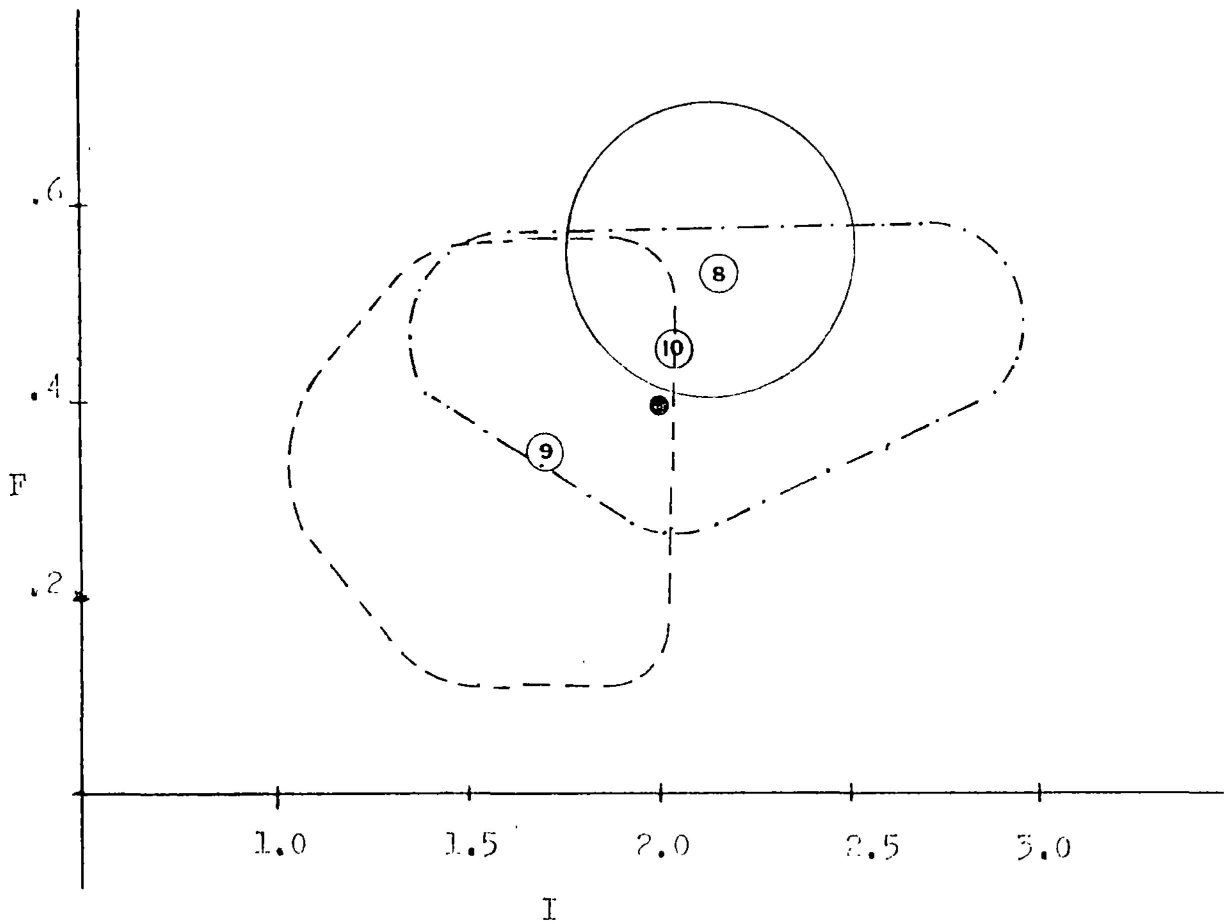

Figure D7. Optimum Turbulence and Microprofile. Ephemeroptera. Traverella albertana (8 and solid line), Stenonema reesi (9 and dashed line), and Rhithrogena hageni (10 and alternating dashed and dotted line).

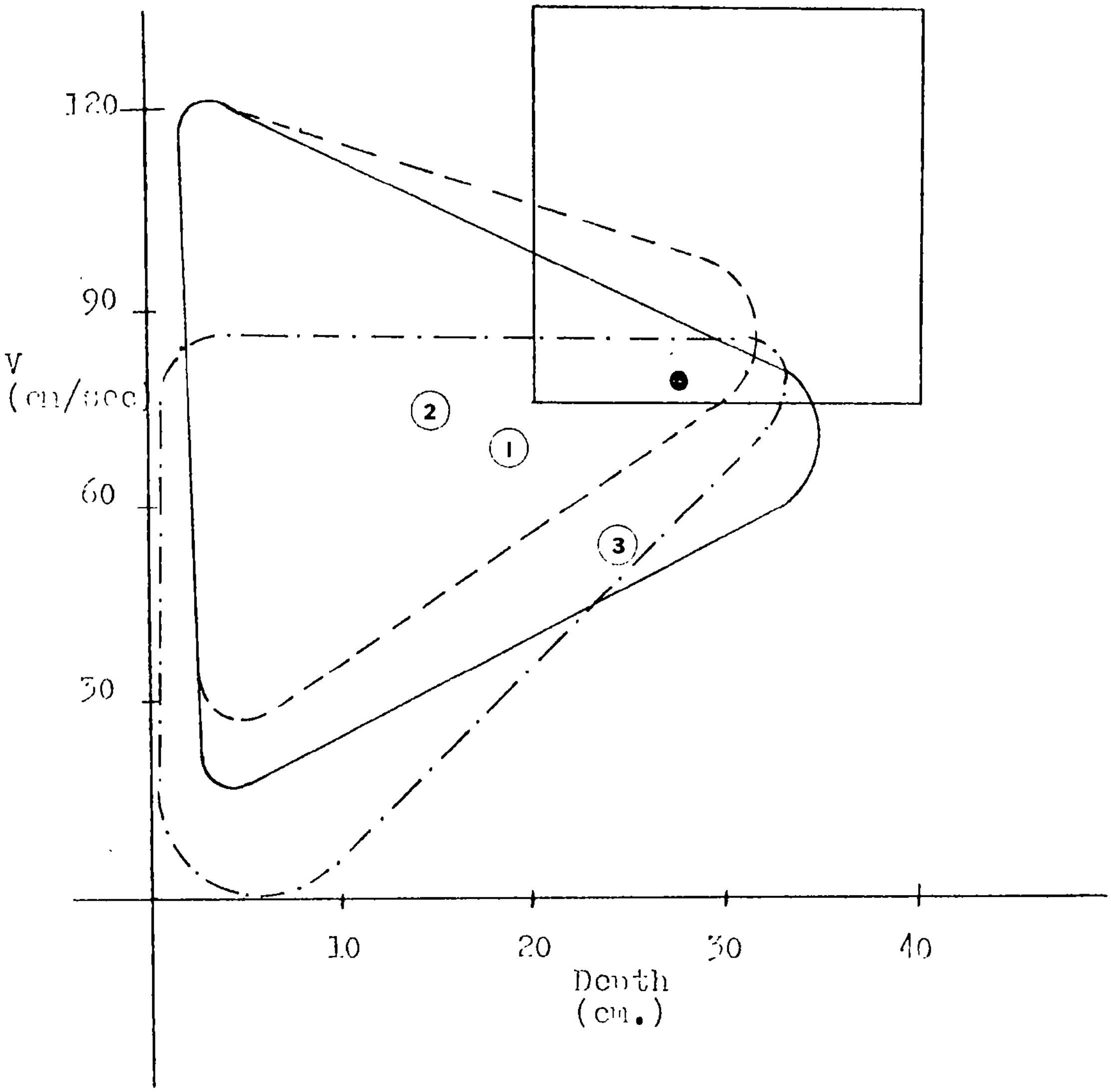

Figure D8. Optimum Depths and Current Velocities. Plecoptera. Strophopteryx fasciata (1 and solid line), Paraleuctra sara (2 and dashed line), and Capnia limata (3 and alternating dashed and dotted line).

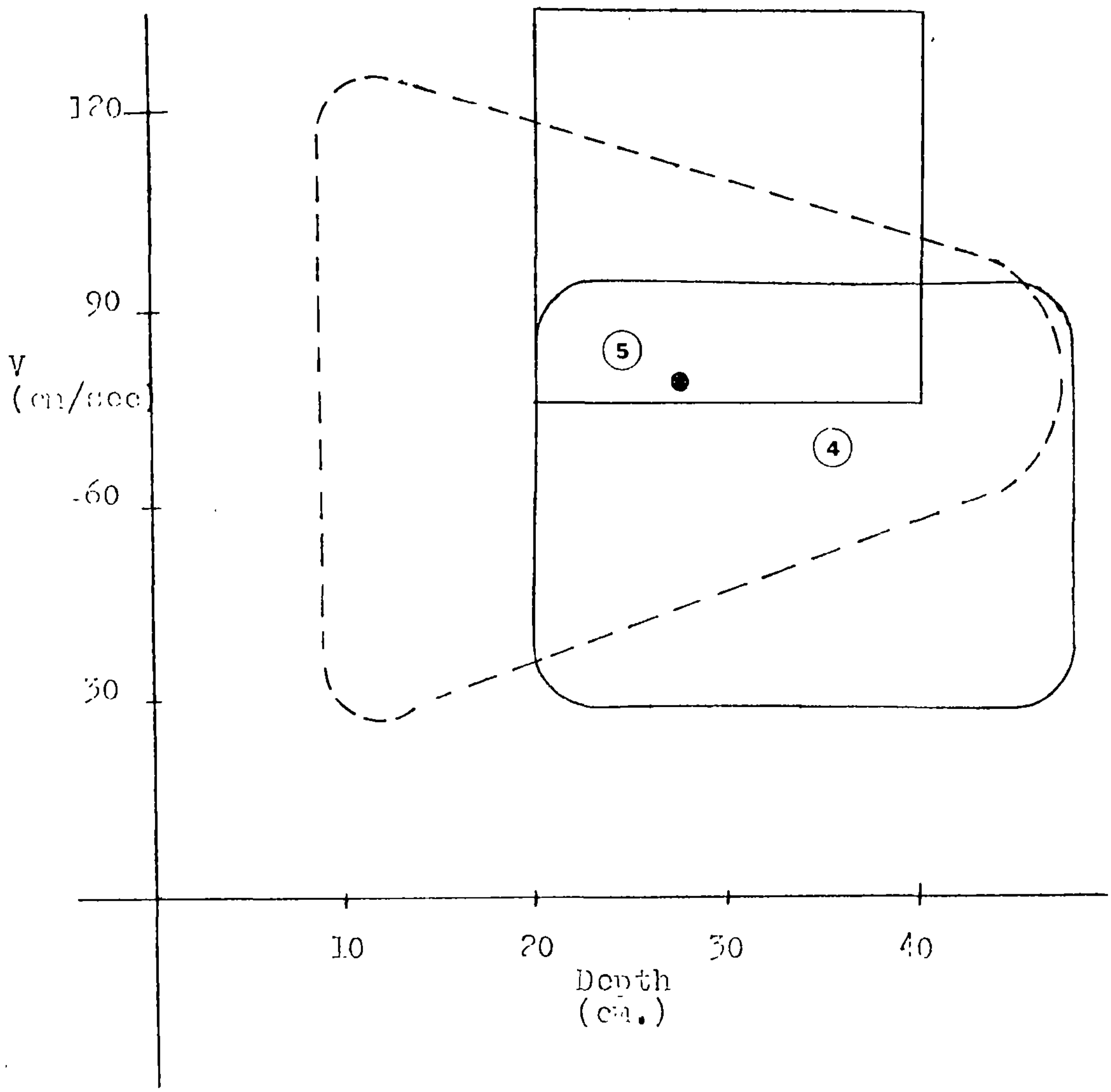

Figure D9. Optimum Depths and Current Velocities. P ecoptera.
Isogenoides frontalis (4 and solid line) and Acroneuria abnormis (5 and dashed line).

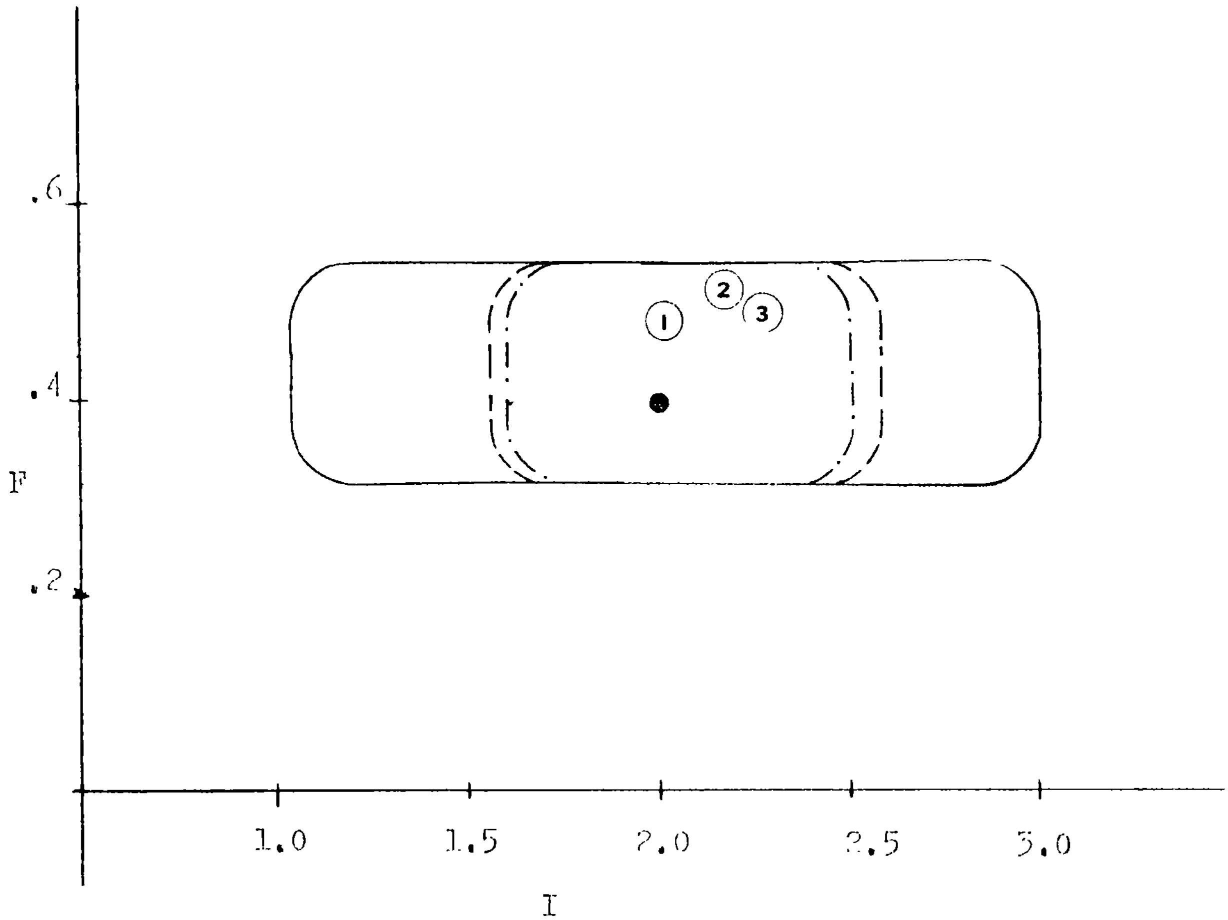

Figure D10. Optimum Turbulence and Microprofile. Plecoptera. Strophopteryx fasciata (1 and solid lines), Paraleuctra sara (2 and dashed line), and Capnia limata (3 and alternating dashed and dotted line).

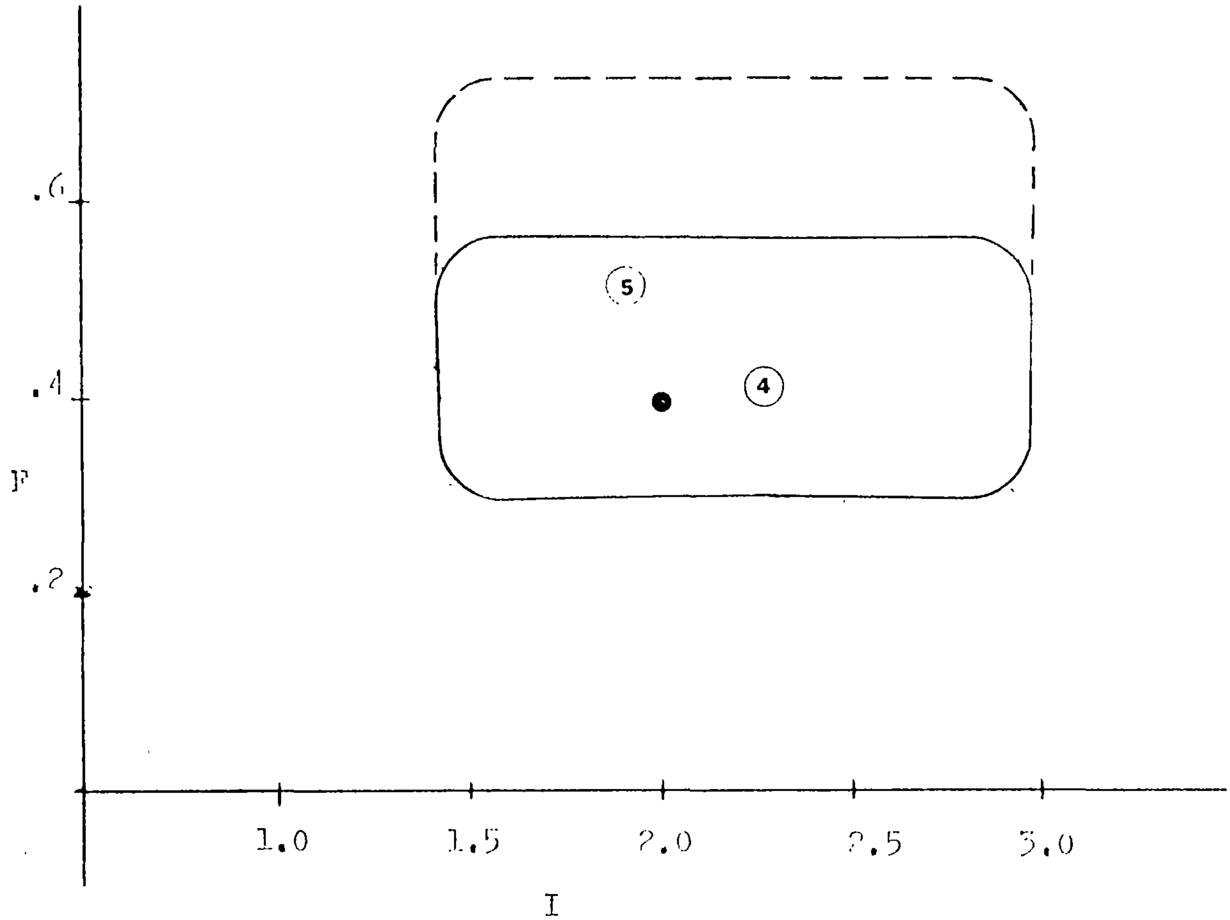

Figure D11. Optimum Turbulence and Microprofile. Plecoptera. Isogenoides frontalis (4 and solid line) and Acroneuria abnormis (5 and dashed line).

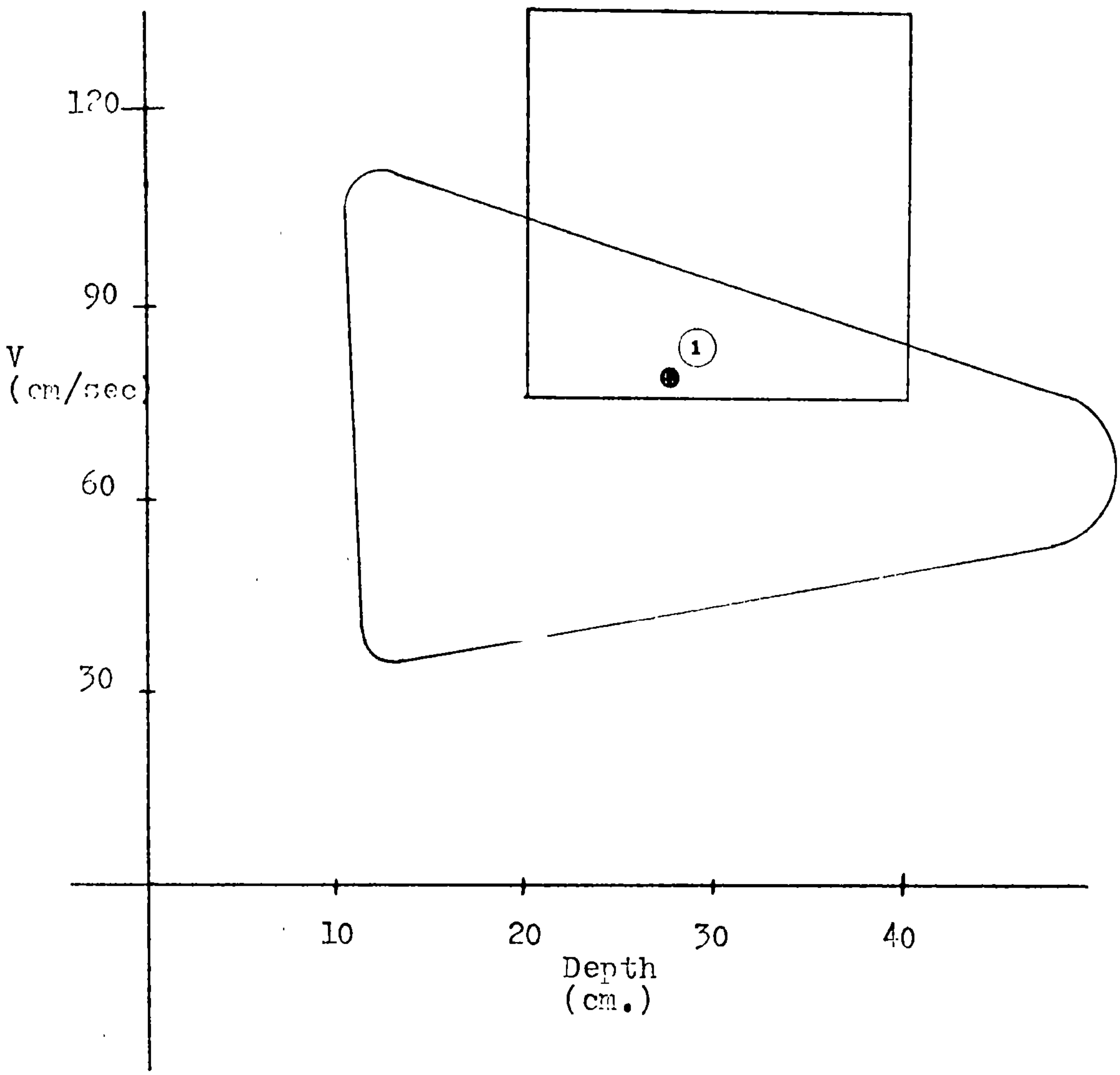

Figure D12. Optimum Depth and Current Velocity. Odonata.
Ophiogomphus morrisoni (1 and solid line).

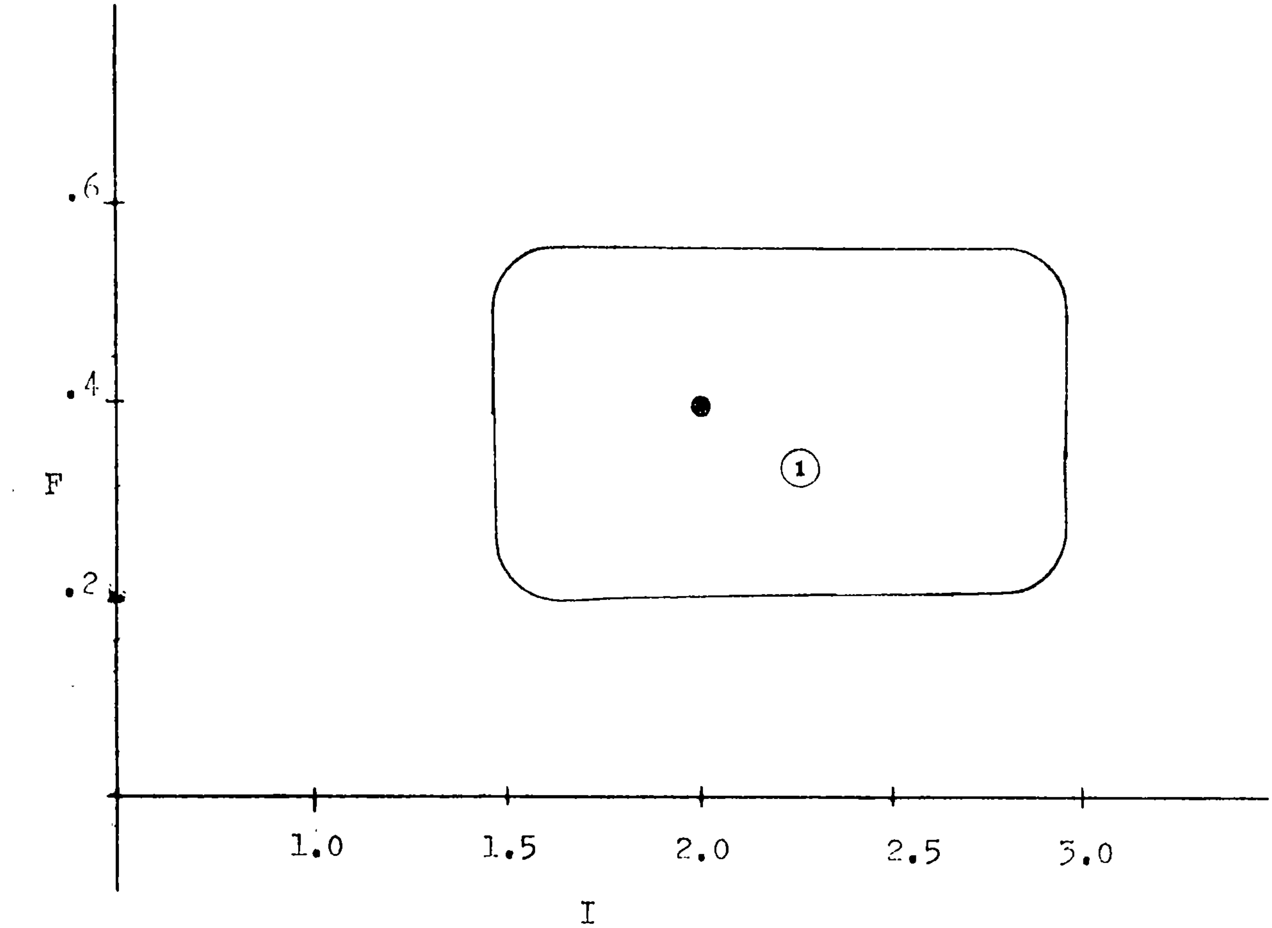

Figure D13. Optimum Turbulence and Microprofile. Odonata. Ophiogomphus morrisoni. (1 and solid line).

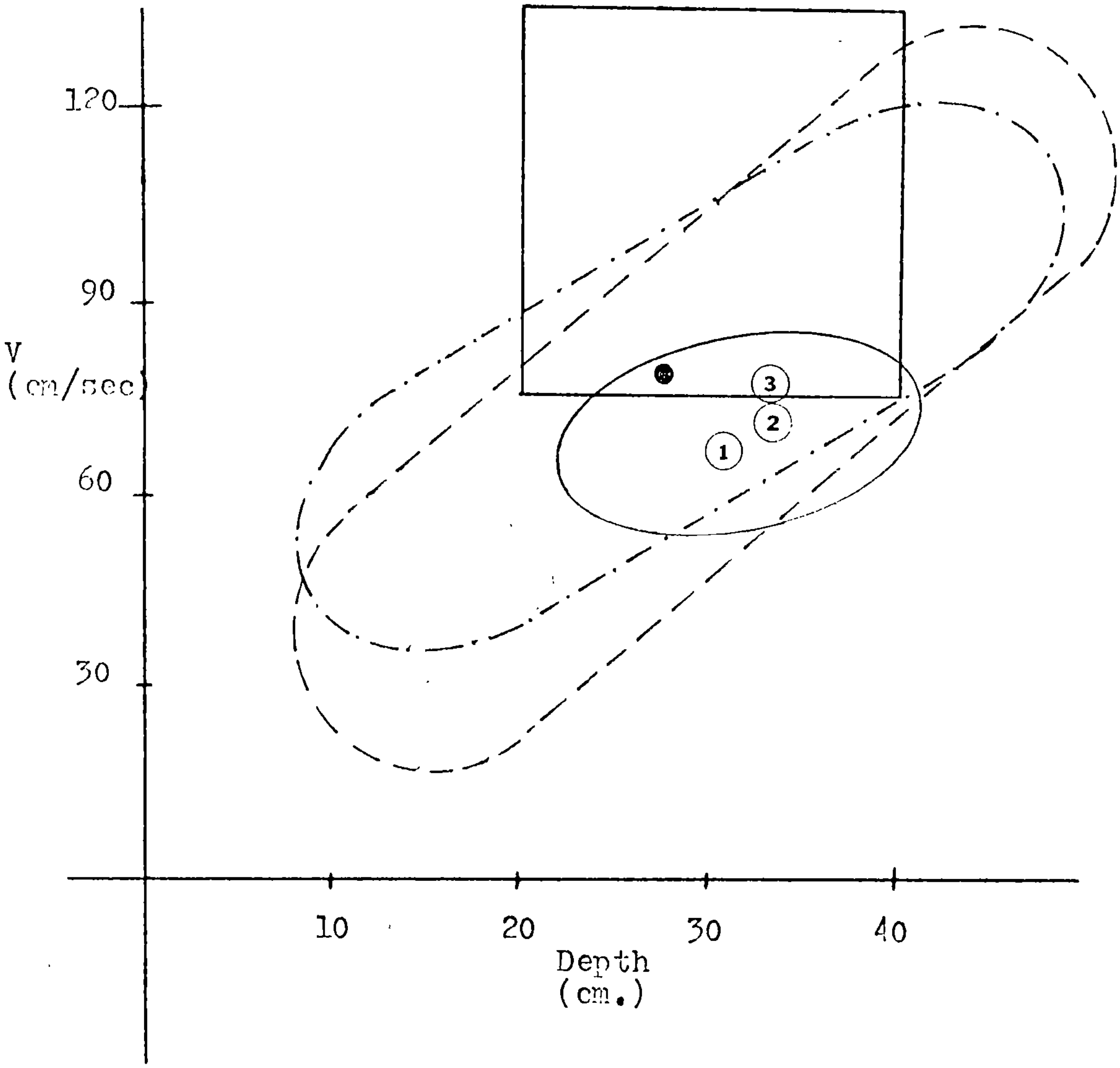

Figure D14. Optimum Depth and Current Velocity. Trichoptera. Hydroptila sp. (1 and solid line), Cheumatopsyche spp. (2 and dashed line), and Hydropsyche bifida (3 and alternating dashed and dotted line).

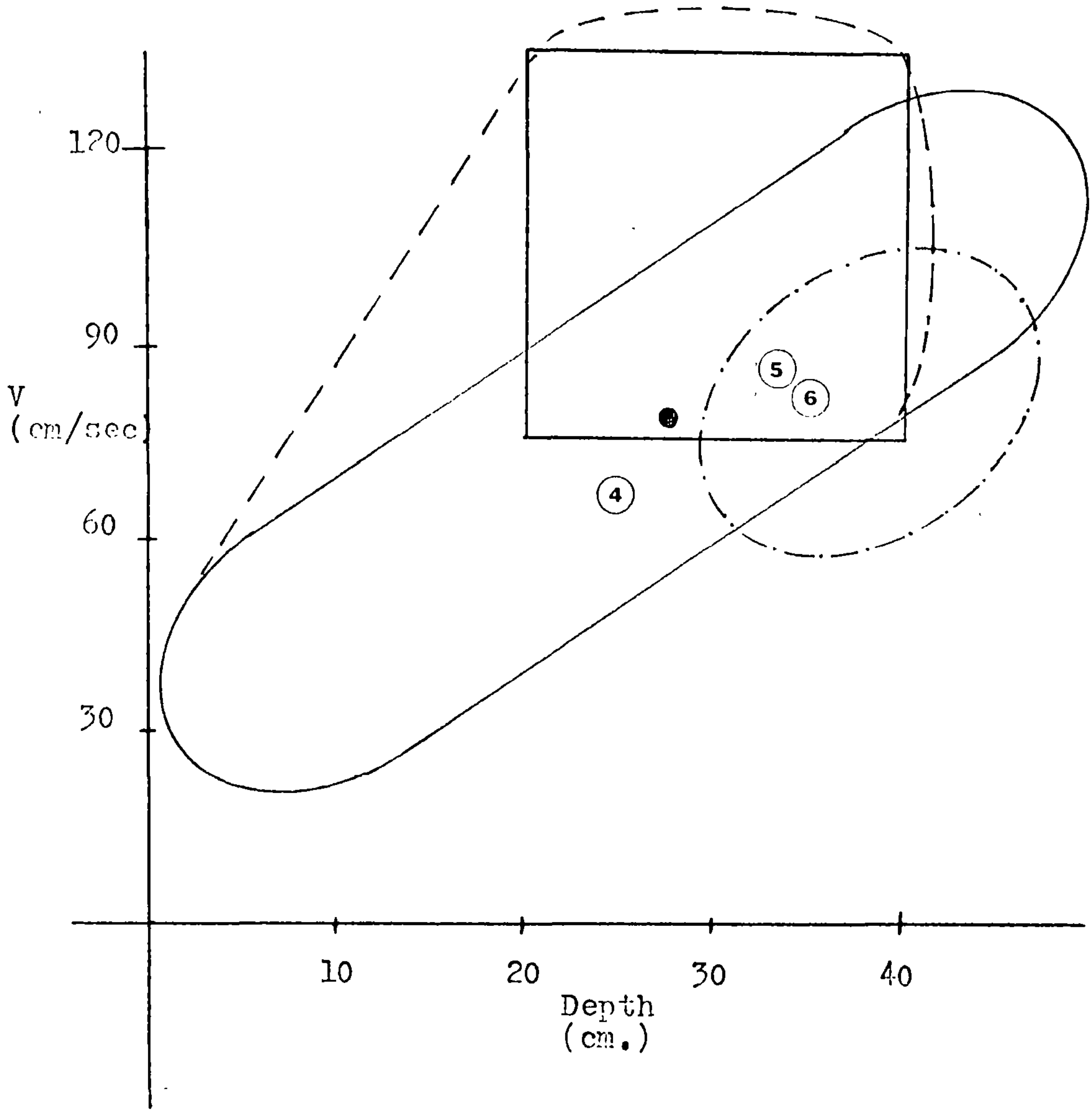

Figure D15. Optimum Depth and Current Velocity. Trichoptera. Hydropsyche occidentalis (4 and solid line), Hydropsyche sp.a (5 and dashed line), and Hydropsyche sp. b (6 and alternating dashed and dotted line).

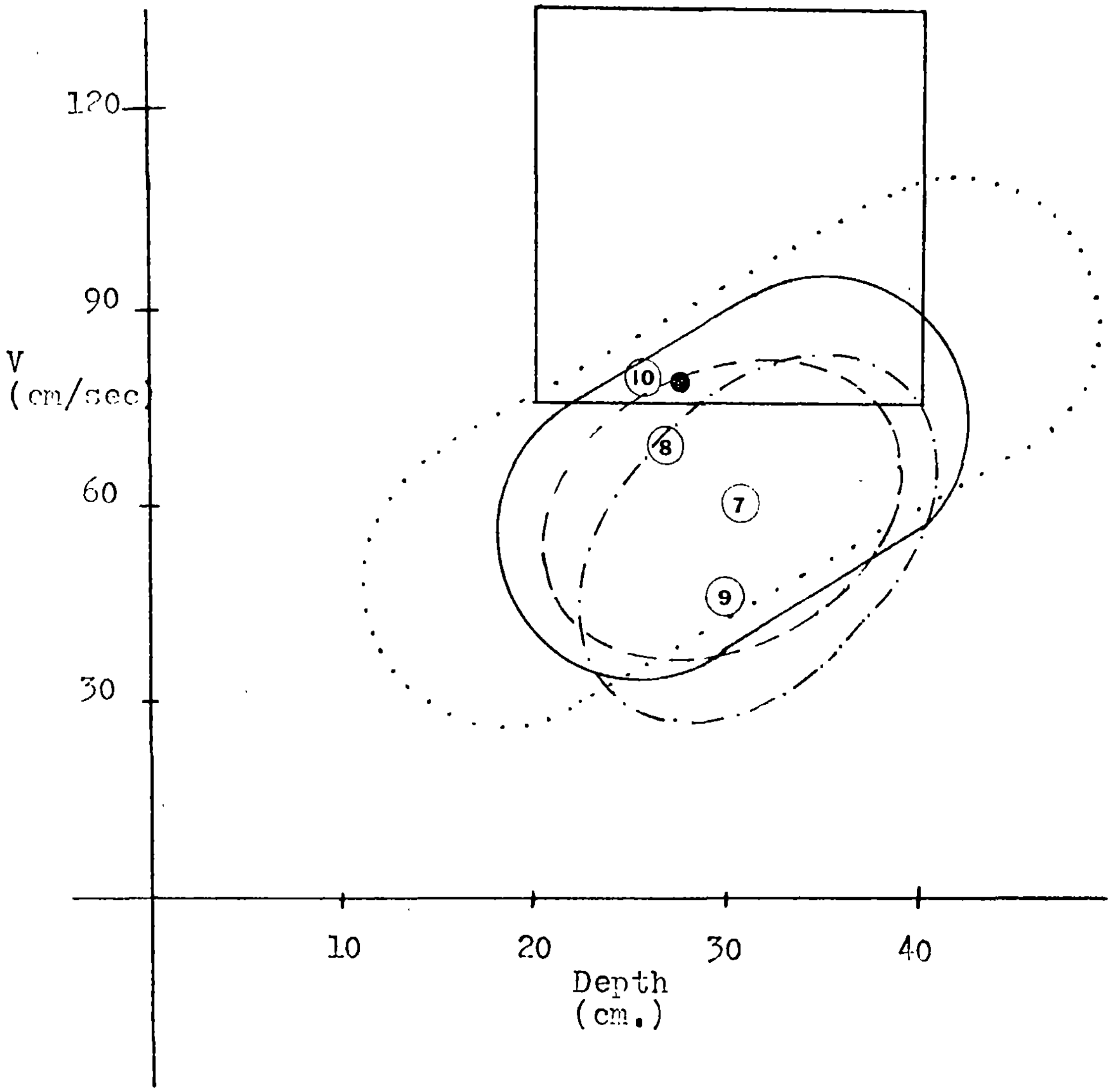

Figure D16. Optimum Depth and Current Velocity. Trichoptera. Hydropsyche sp. c (7 and solid line), Brachycentrus americanus (8 and dashed line), Leptocella sp. (9 and alternating dashed and dotted line), and Athripsodes sp. (10 and dotted line).

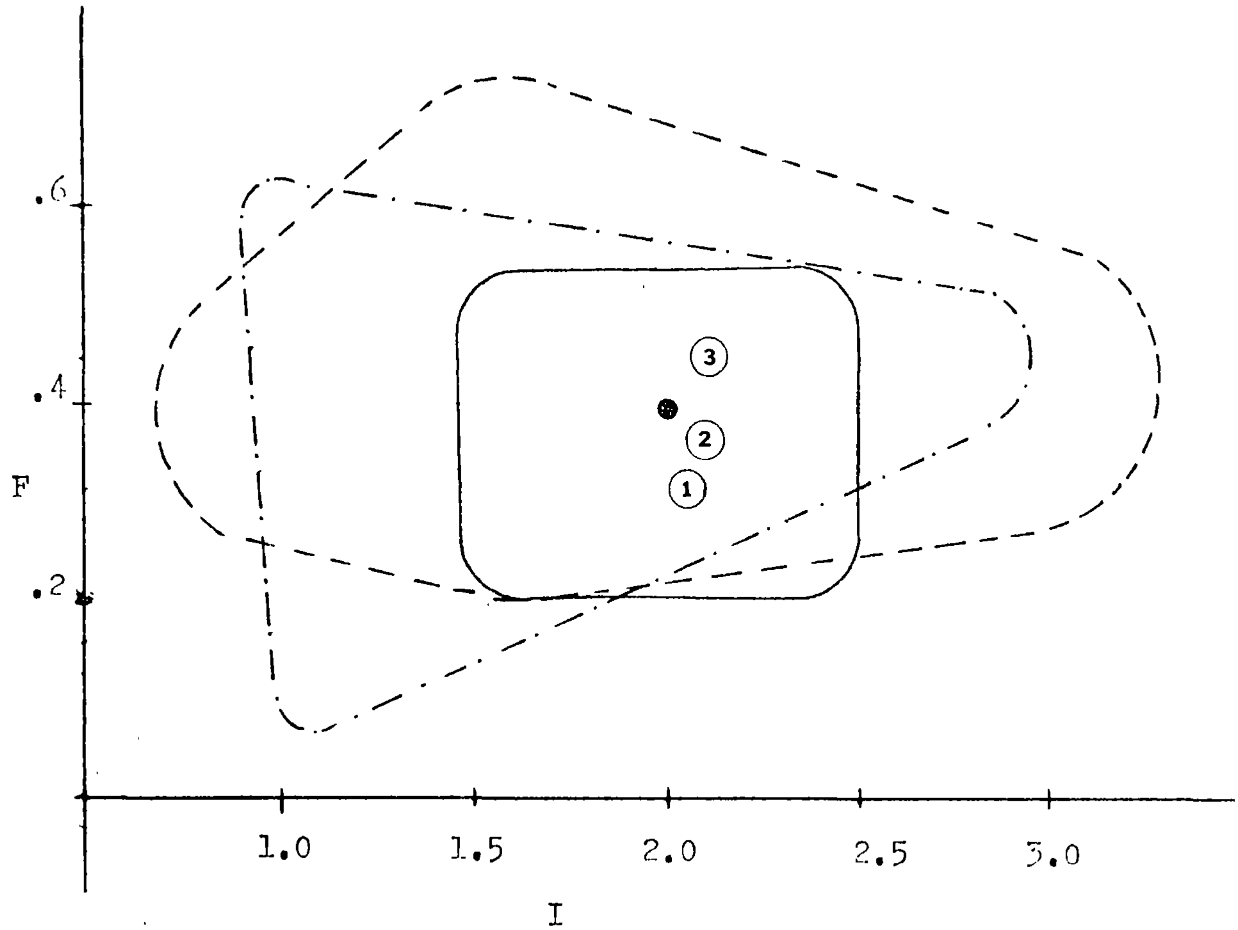

Figure D17. Optimum Turbulence and Microprofile. Trichoptera. Hydroptila sp. (1 and solid line), Cheumatopsyche spp. (2 and dashed line), and Hydropsyche bifida (3 and alternating dashed and dotted line).

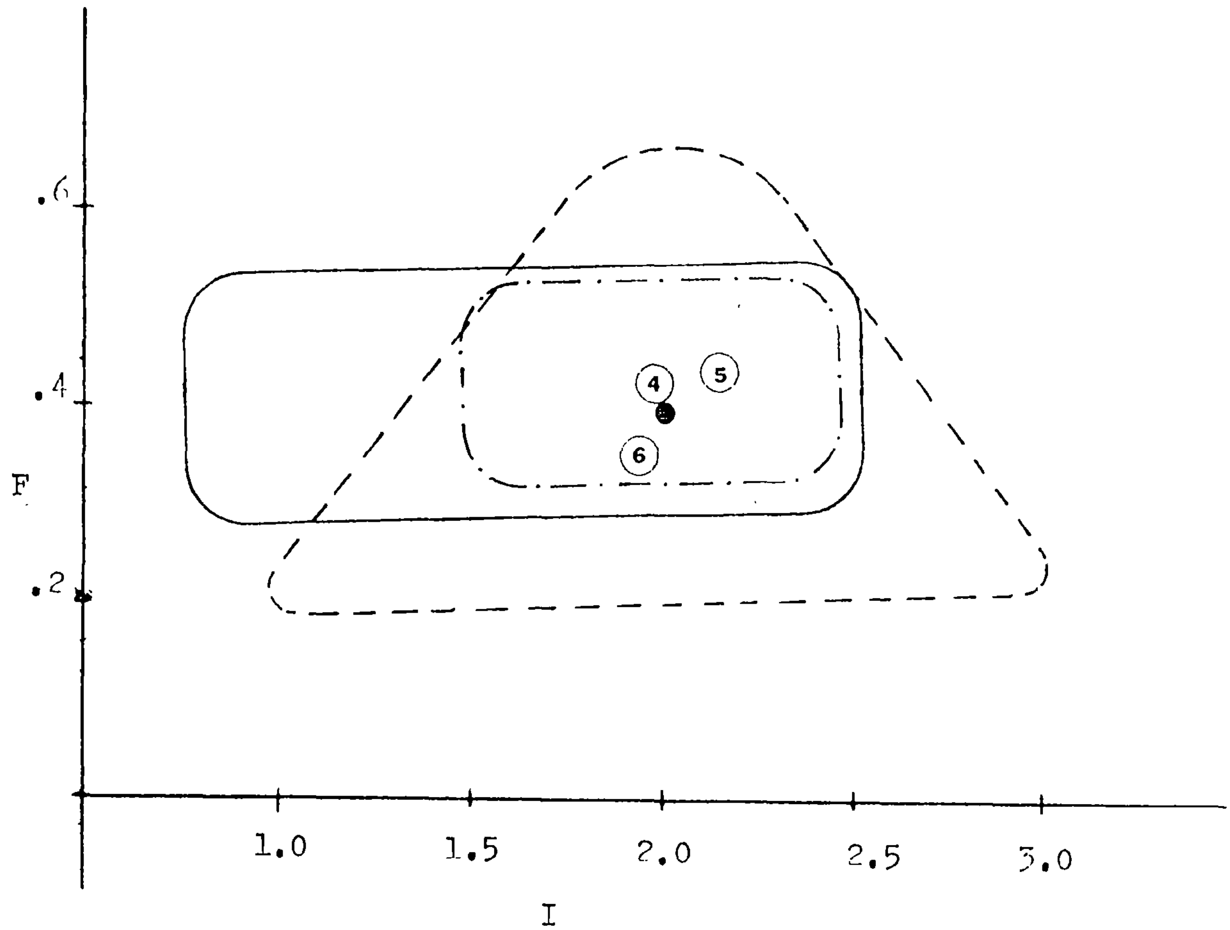

Figure D18. Optimum Turbulence and Microprofile. Trichoptera. Hydropsyche occidentalis (4 and solid line), Hydropsyche sp. a (5 and dashed line), and Hydropsyche sp. b (6 and alternating dashed and dotted line).

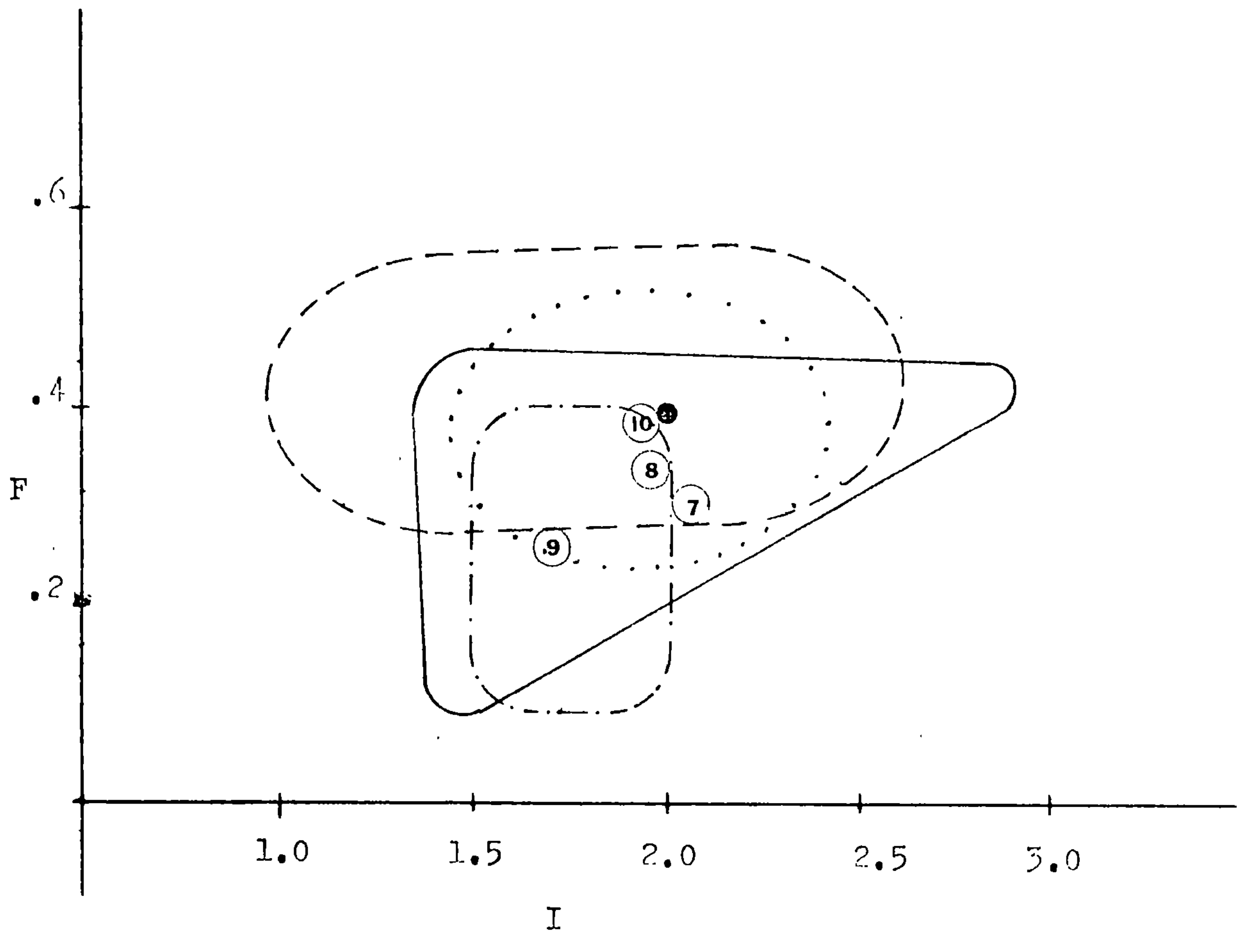

Figure D19. Optimum Turbulence and Microprofile. Trichoptera. Hydropsyche sp. c (7 and solid line), Brachycentrus americanus (8 and dashed line), Leptocella sp. (9 and alternating dashed and dotted line), and Athripsodes sp. (10 and dotted line).

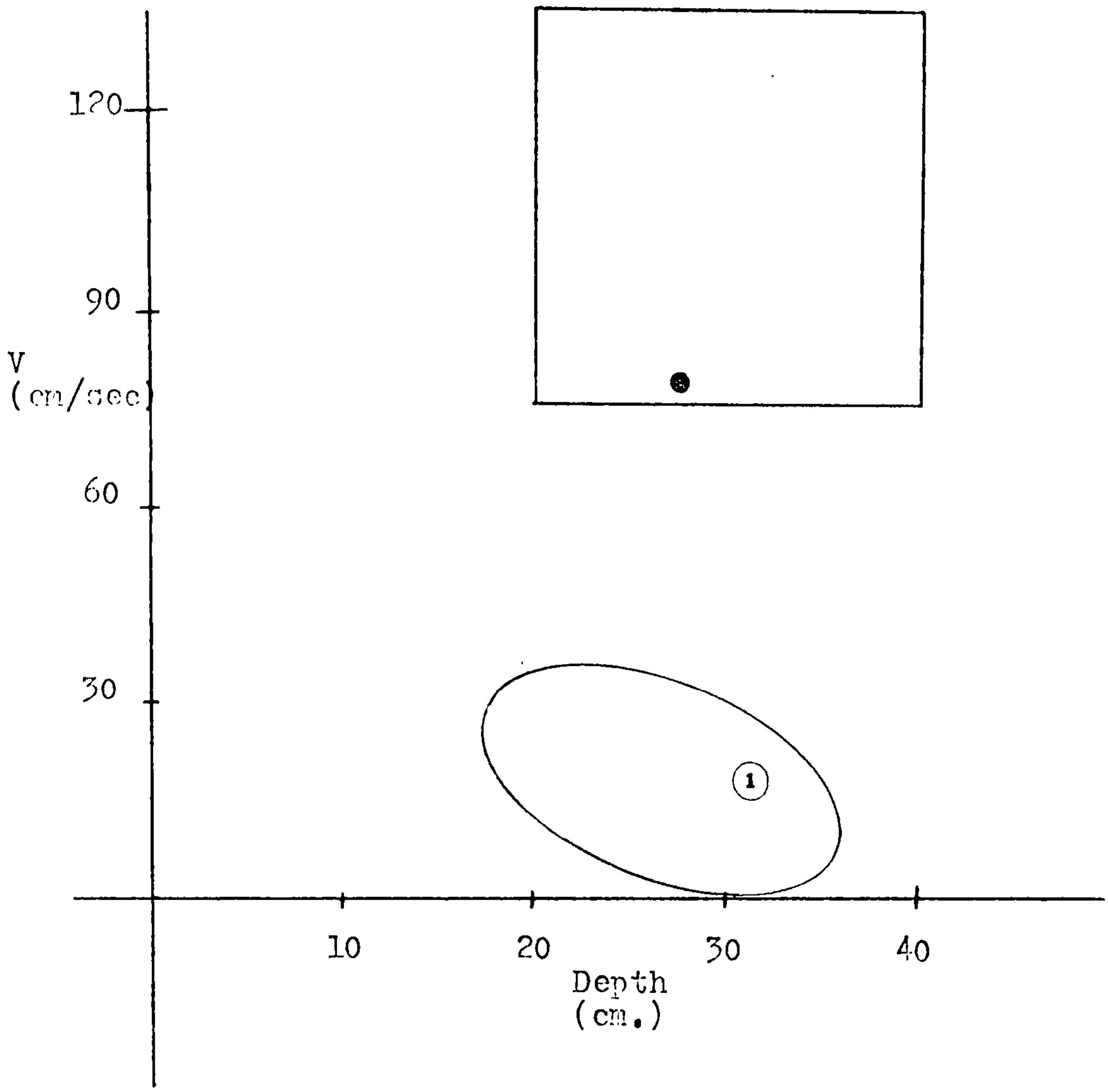

Figure D20. Optimum Depth and Current Velocity. Hemiptera.
Rhagovelia sp. (1 and solid line).

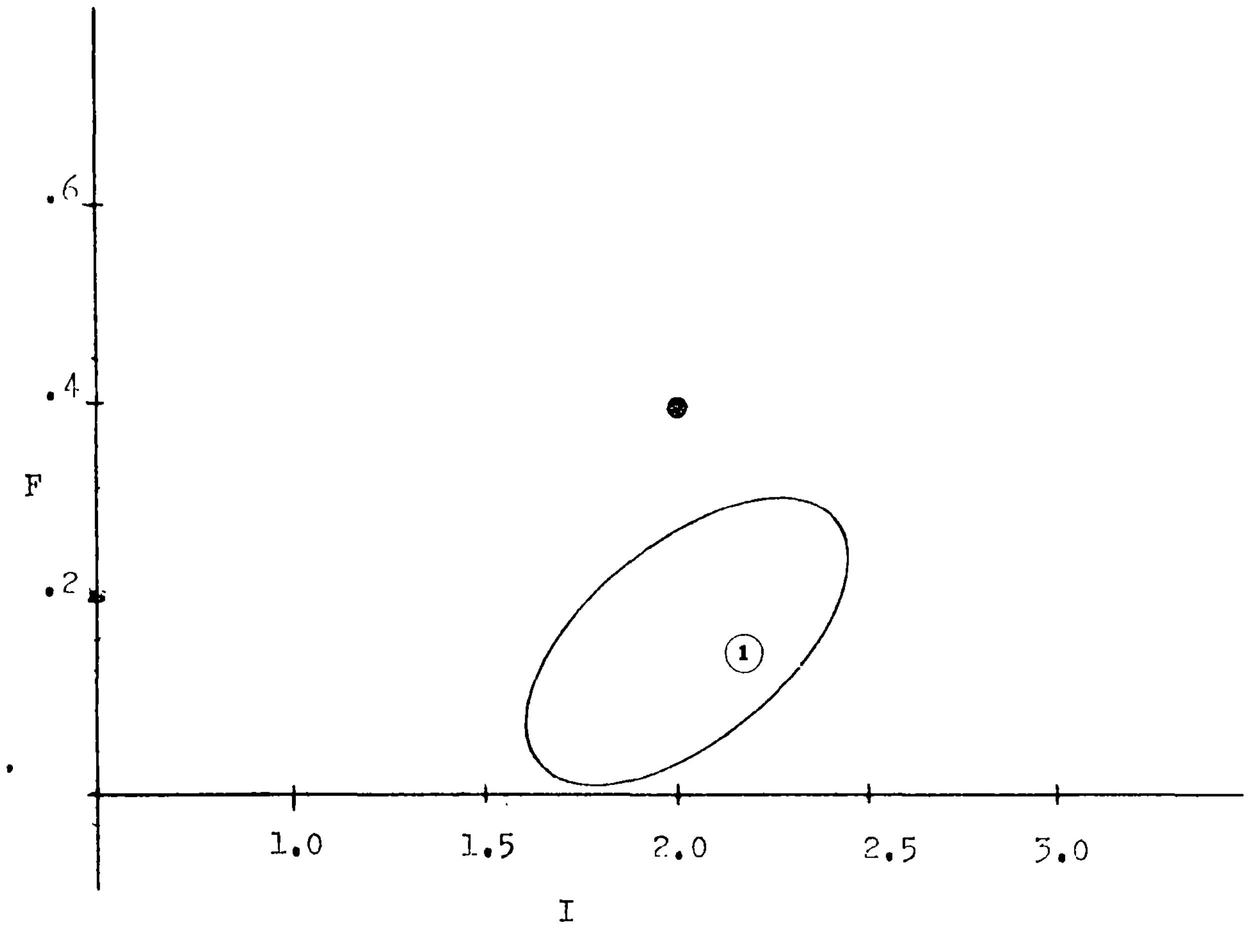

Figure D21. Optimum Turbulence and Microprofile. Hemiptera. Rhagovelia sp. (1 and solid line).

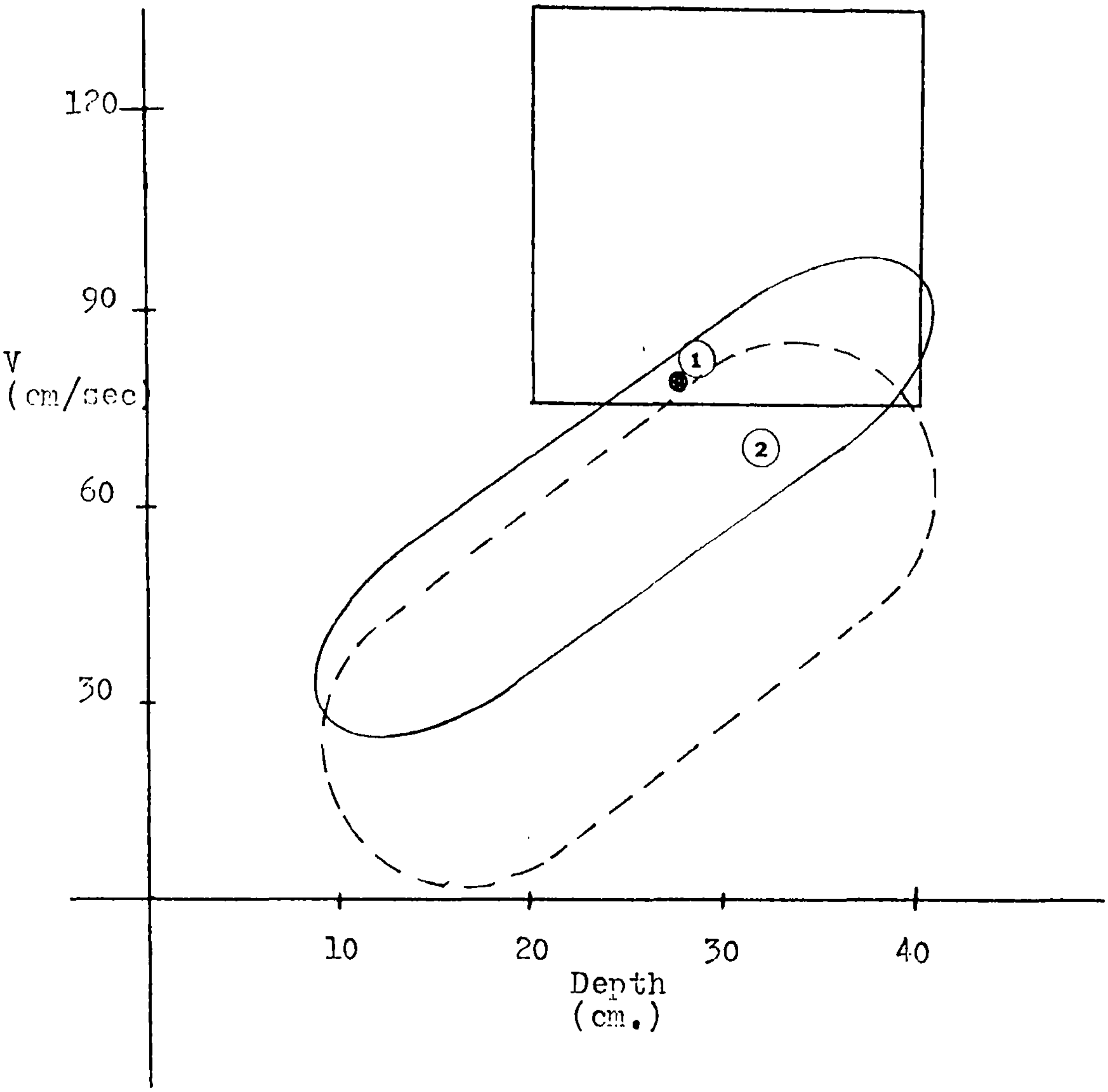

Figure D22. Optimum Depth and Current Velocity. Coleoptera. Stenelmis sp. a (adult) (1 and solid line) and Stenelmis sp. b (adult) (2 and dashed line).

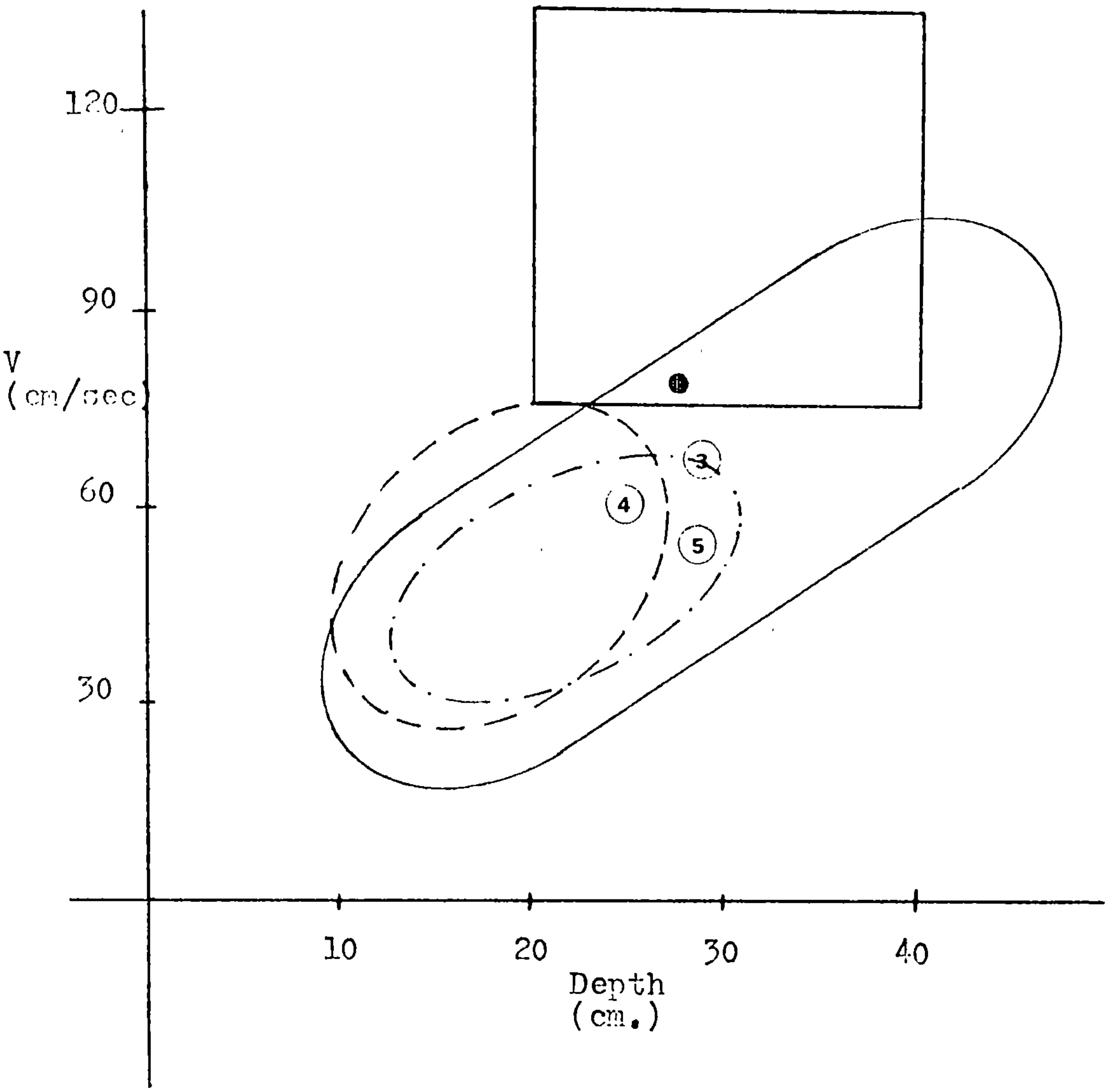

Figure D23. Optimum Depth and Current Velocity. Coleoptera. Stenelmis sp. a (larvae) (1 and solid line), Stenelmis sp. b (larvae) (2 and dashed line), and Dubiraphia sp. (3 and alternating dashed and dotted line).

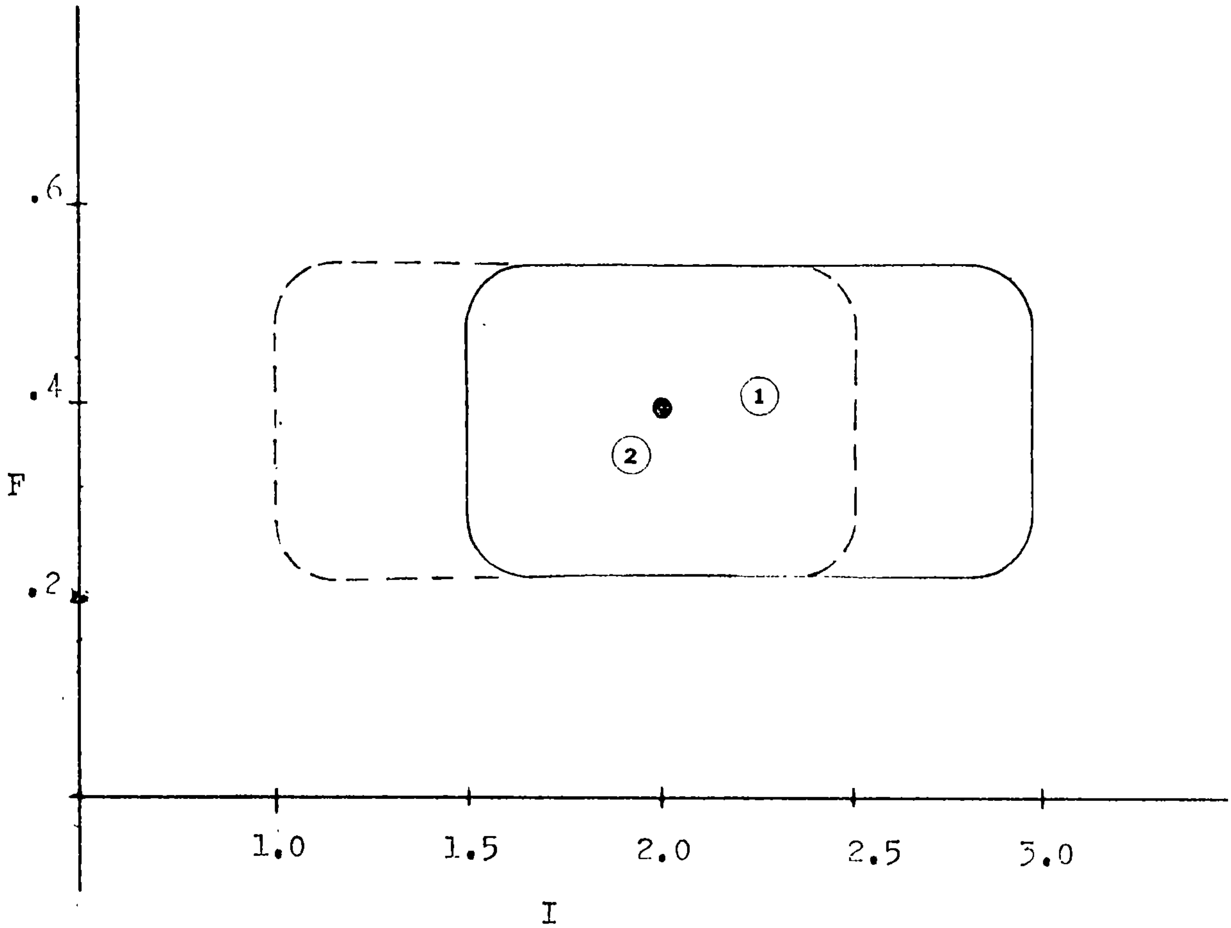

Figure D24. Optimum Turbulence and Microprofile. Coleoptera. Stenelmis sp. a (adult) (1 and solid line) and Stenelmis sp. b (adult) (2 and dashed line).

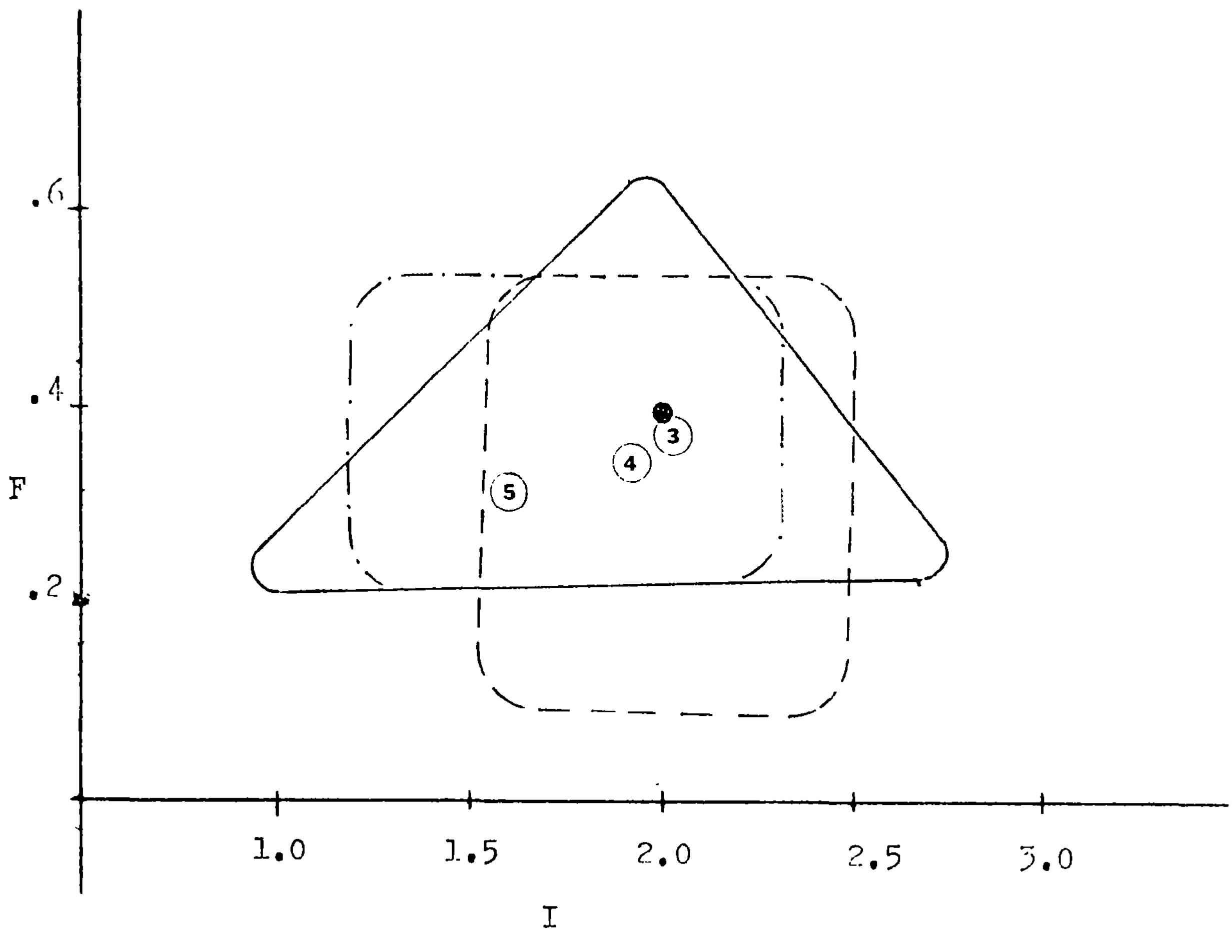

Figure D25. Optimum Turbulence and Microprofile. Coleoptera. Stenelmis sp. a (larvae)(1 and solid line), Stenelmis sp. b (larvae)(2 and dashed line), and Dubiraphia sp. (3 and alternating dashed and dotted line).

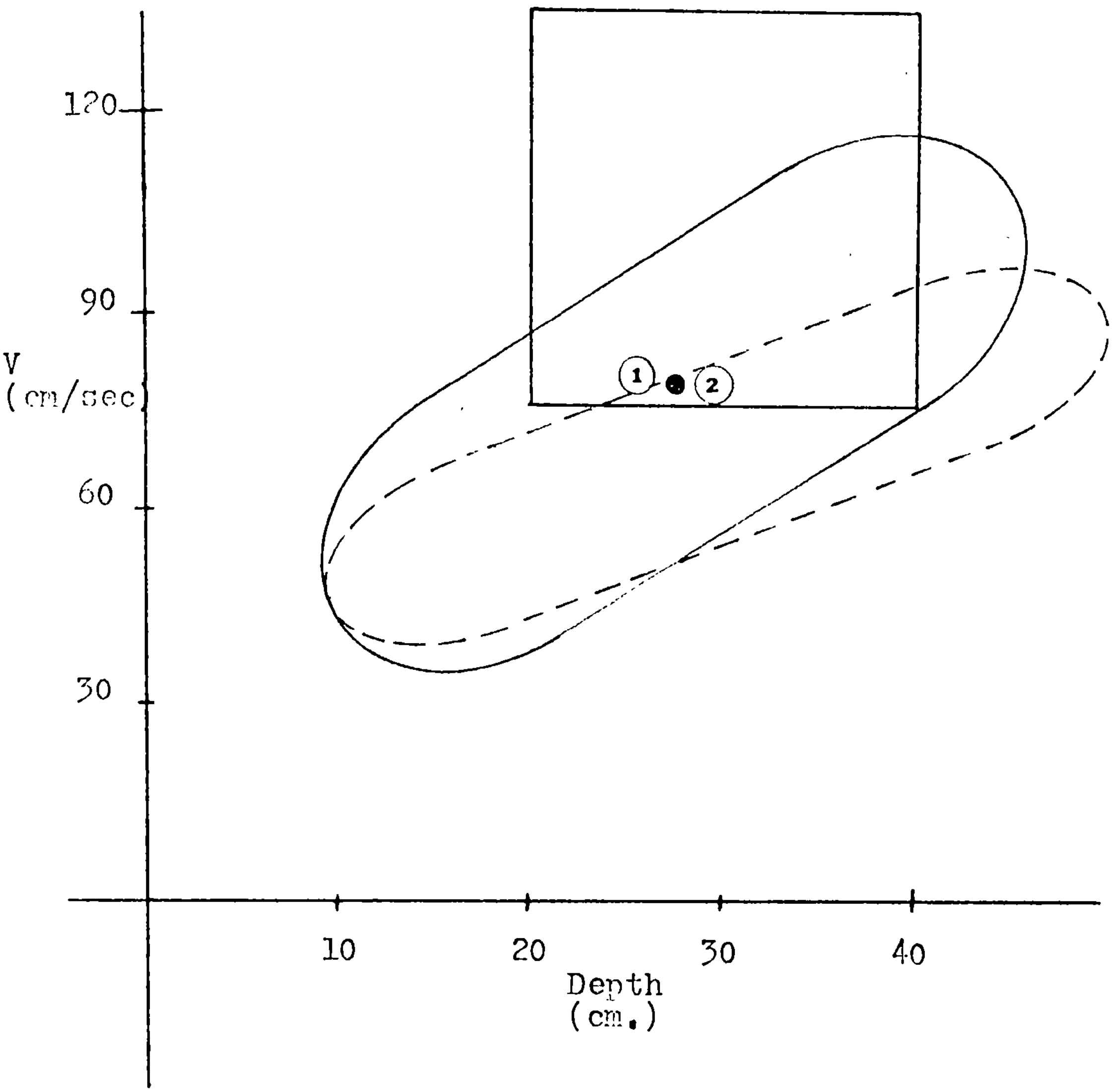

Figure D26, Optimum Depth and Current Velocity. Diptera. Simulium spp. (1 and solid line) and Metriocnemus sp. (2 and dashed line).

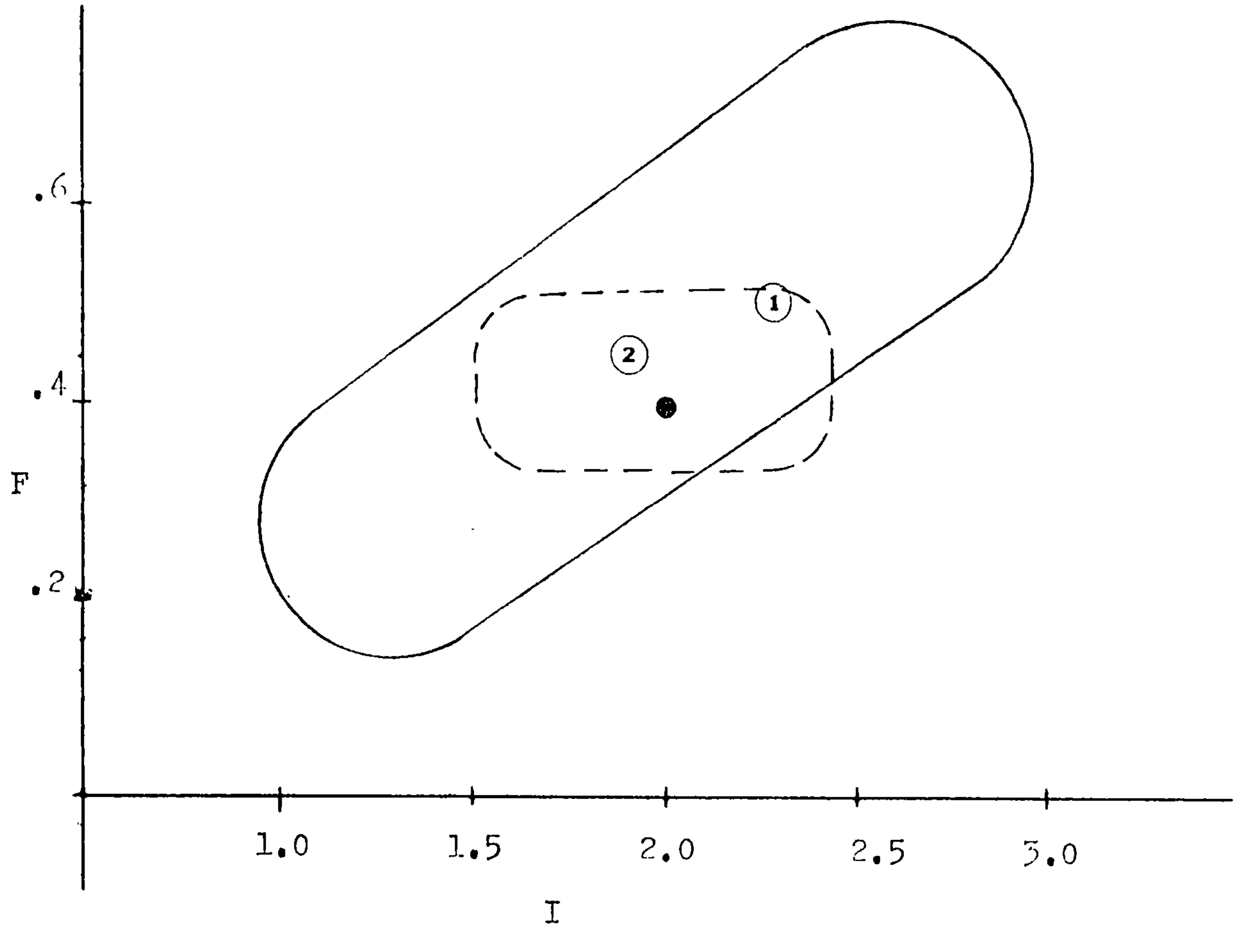

Figure D27. Optimum Turbulence and Microprofile. Diptera. Simulium spp. (1 and solid line) and Metriocnemus sp. (2 and dashed line).

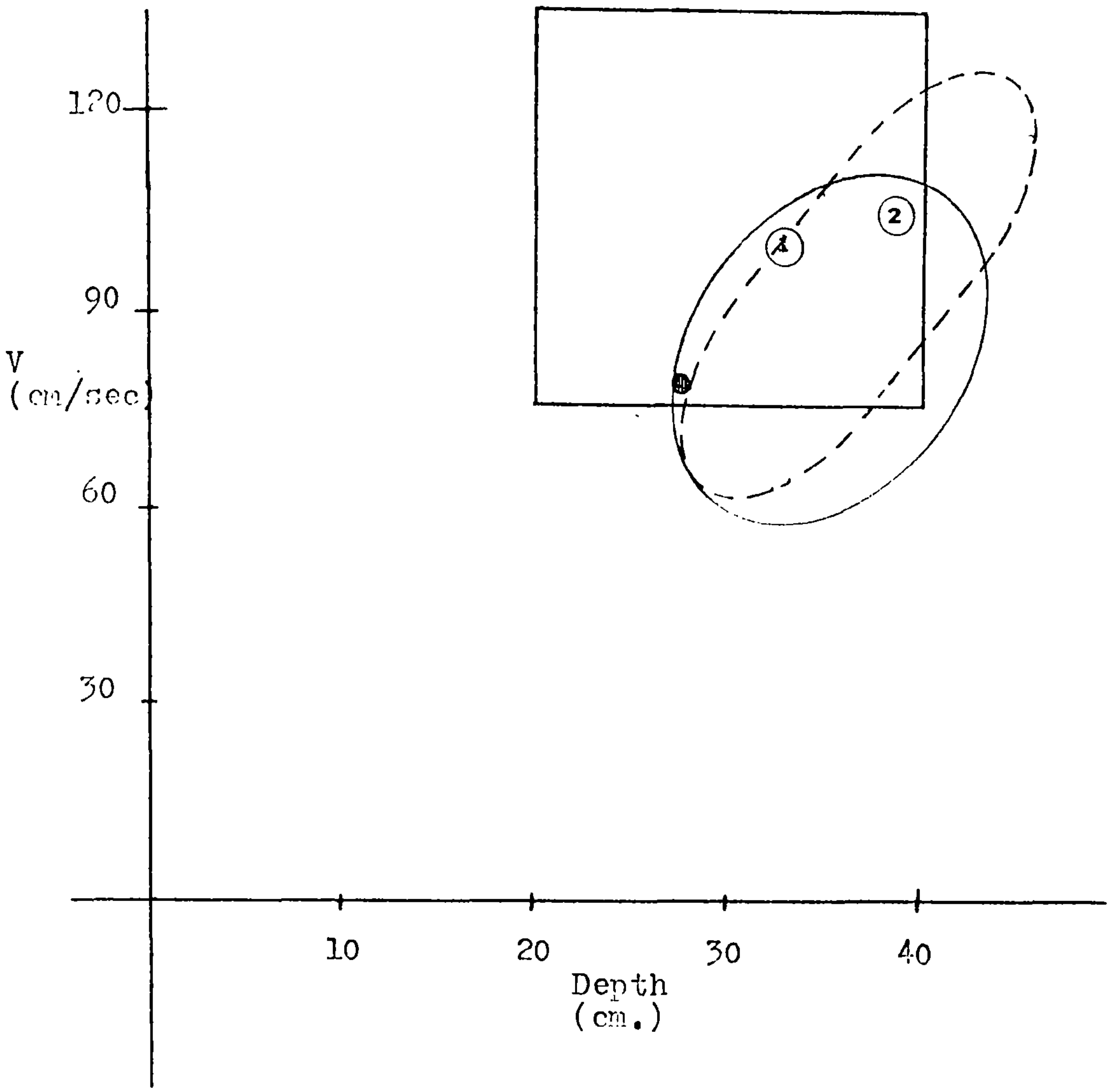

Figure D28. Optimum Depth and Current Velocity. Mollusca. Sphaerium simile (1 and solid line) and Physa gyrina (2 and dashed line).

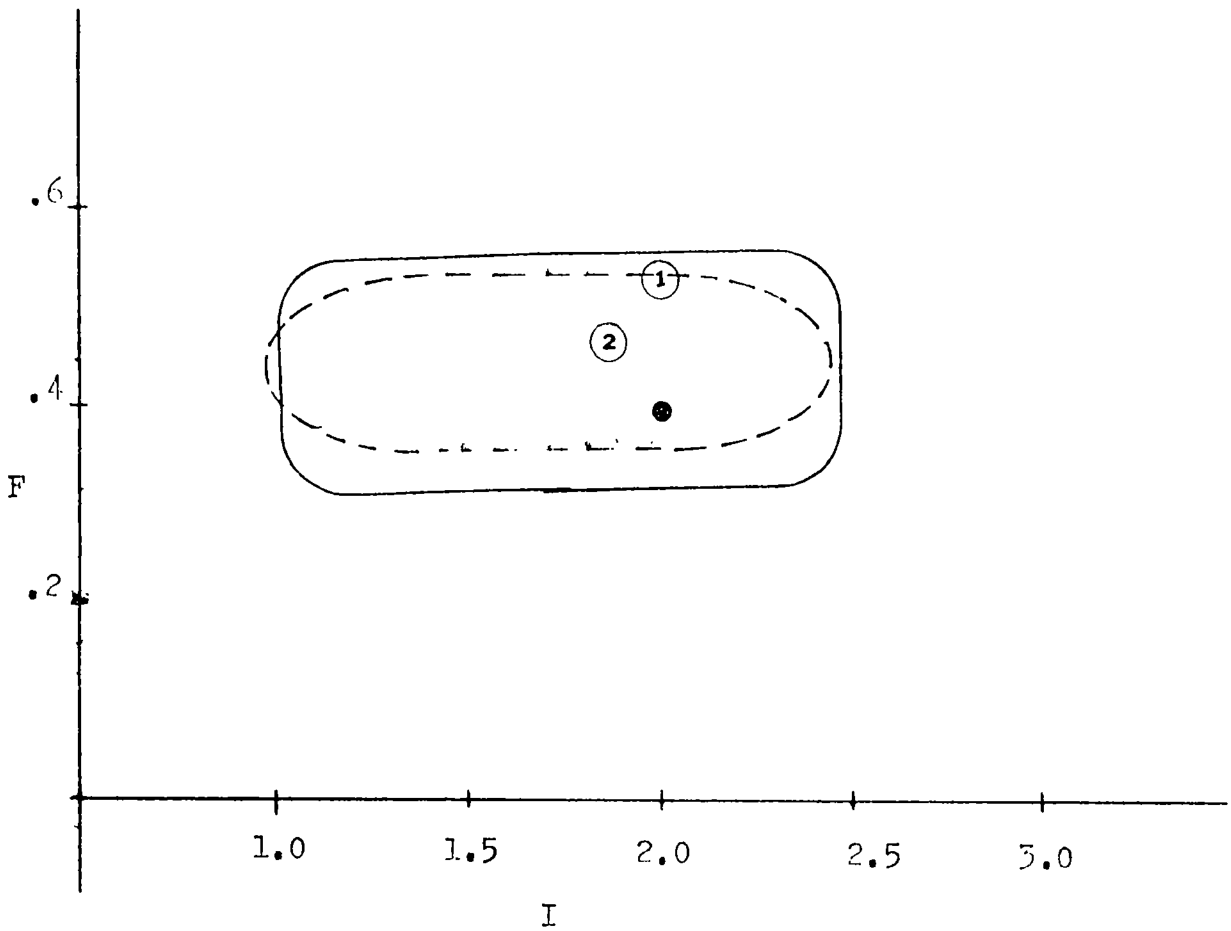

Figure D29. Optimum Turbulence and Microprofile. Mollusca. Sphaerium simile (1 and solid line) and Physa gyrina (2 and dashed line).

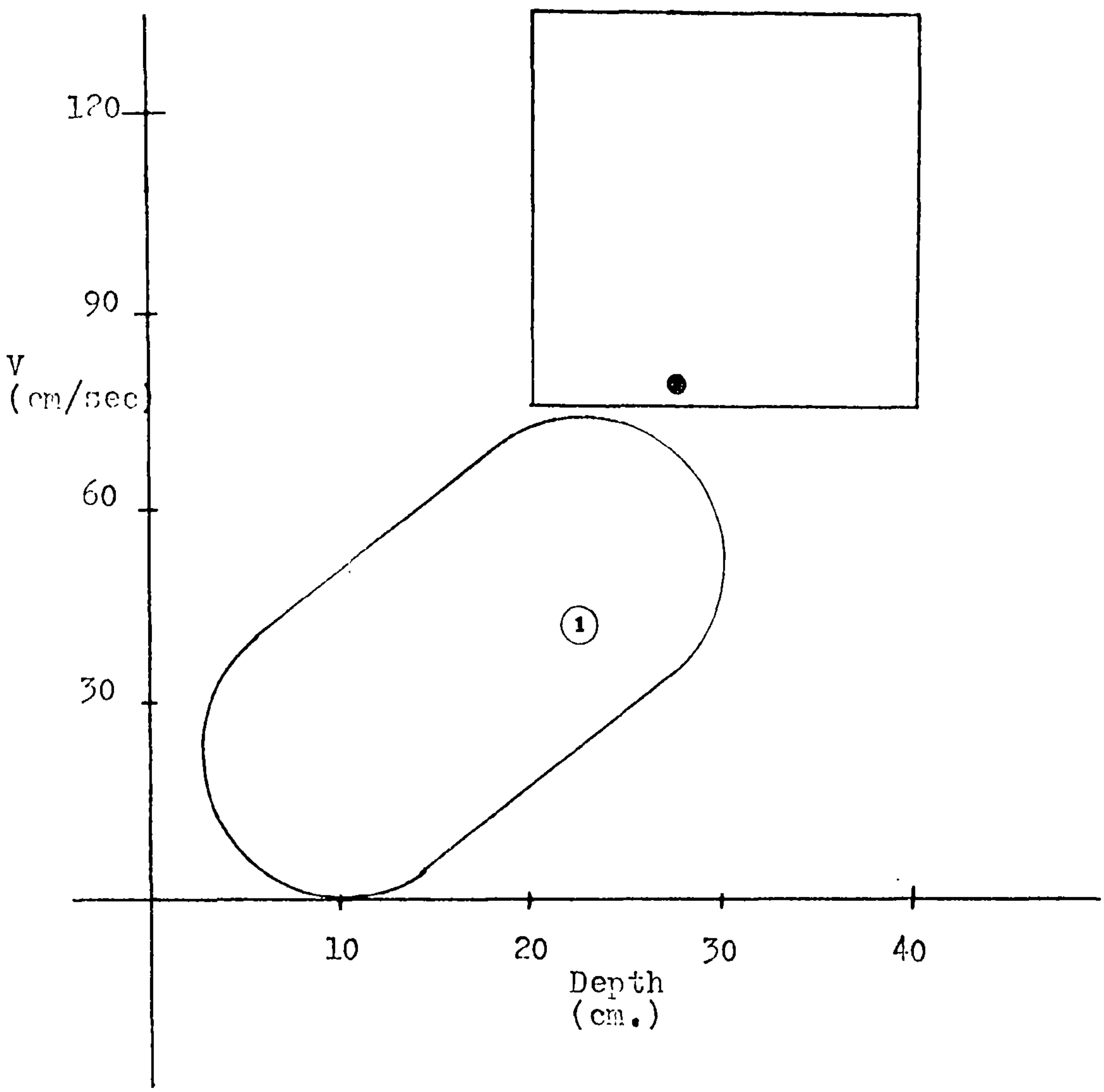

Figure D30. Optimum Depth and Current Velocity. Turbellaria. Dugesia tigrina (1 and solid line).

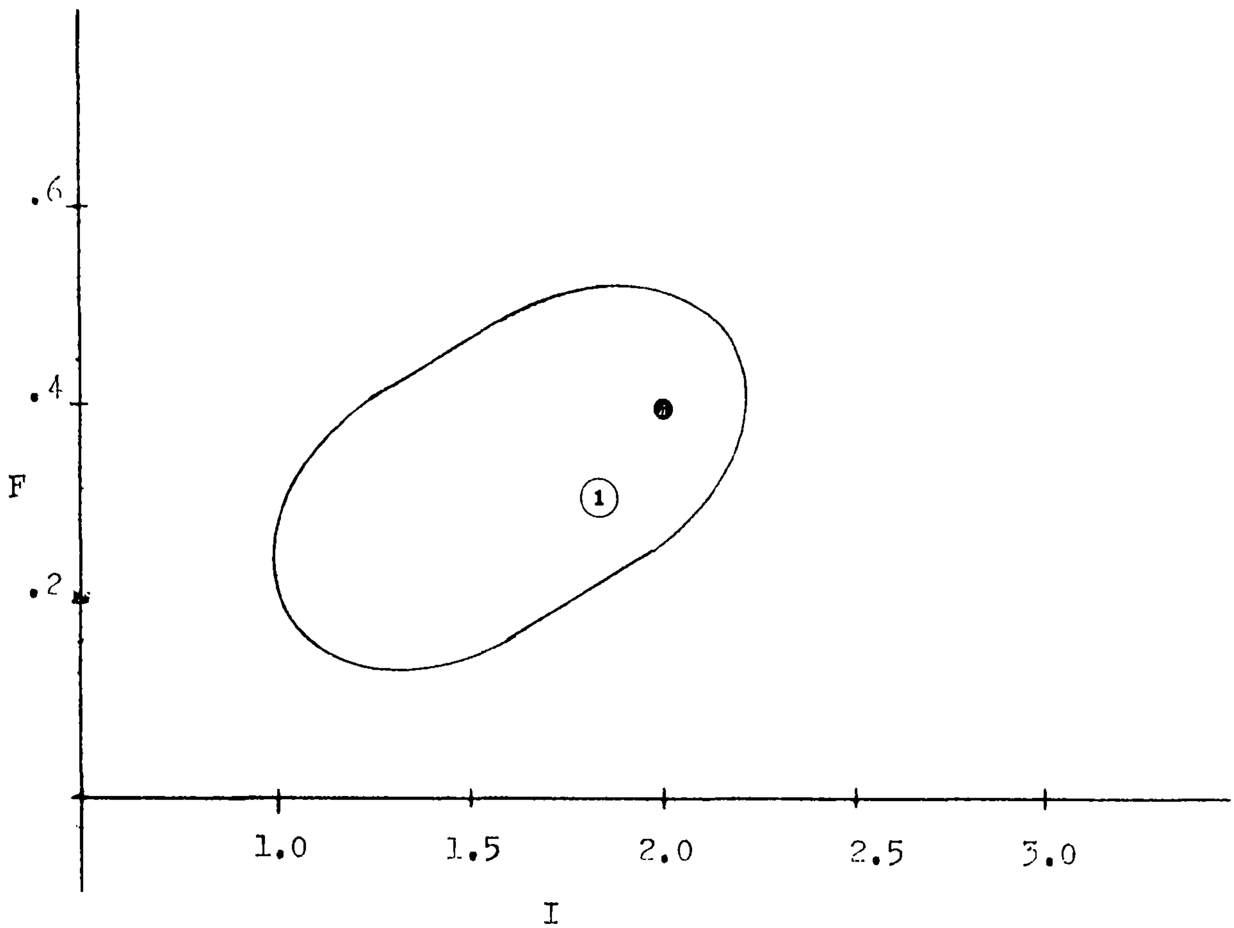

Figure D31. Optimum Turbulence and Microprofile. Turbellaria. Dugesia tigrina (1 and solid line).

Distribution and Abundance

Kite-diagrams (Figures D34 and D35) are presented showing relative abundance and longitudinal distribution along the Tongue River (Figure D32, Table D4). Dashed lines indicate the presence of the organism in that section of the river, as determined by kick samples, for which relative abundances have not been determined.

Analysis of the kite-diagrams to determine community associations can be accomplished through the use of clustering techniques. A modified Jaccard association coefficient (Church, 1976) is used to compare community structures, as determined by Hess samples for distributional information. An association matrix is constructed where the association values are determined as follows:

$$J_{ij} = P_i \times P_j \qquad \text{(Eq. D2)}$$

where $$P_i = (a + b)/(a + b + c) \qquad \text{(Eq. D3)}$$

and $$P_j = (a + c)/(a + b + c) \qquad \text{(Eq. D4)}$$

when a is the sum of the relative abundances of those species which occur in both samples i and j, b is the sum of the relative abundances of those species which occur only in sample i, and c is the sum of the relative abundances of species which occur only in sample j.

Dendrograms (Figures D33) are constructed by using the WPGMA (weighted pair-group using mathematical averages) clustering method (Sneath and Sokal, 1974). The dendrogram indicates those samples which are most closely related (that is, most similar) by connecting them together at the highest possible association coefficient. Coefficients range from 0 to 1, where 1 is identity. Thus, for example, in the fall-winter distribution, samples III' and III are virtually identical with an association coefficient of .974. It is for this reason that sample site III' was eliminated from further consideration in subsequent logitudinal sampling. The high degree of similarity of community structure indicates that the effects of the sewage effluent in the town of Birney is small enough so that samples taken at site III would be representative of the aquatic community of the general area.

From the dendrogram of the fall-winter distribution (Figure D33), it can be seen that three distinct communities exist along the length of the Tongue River. Sites I and II are in the cold water section and association with communities in the warm water section is very small (.475). In the upper warm water area a distinct community exists, as shown by samples III' and III, and IV. Sample V seems transitional between the upper and lower warm water communities, and as such, is not closely associated with either. It does, however, seem to be most closely associated with the upper warm water community. The lower river shows a third distinct community. In this area, the close association between sites VI and VII, with such different substrates (Table D4) indicates the preference of the insects in these areas for a distinct profile (tending to be smooth) rather than a substrate material type. Turbidity and algal cover seem to be variables which may also cause close association of these two communities.

It can be seen that the transition zone between cold water and warm water habitats (as delineated in Figures D33 and D34, and by sample III') serves as the border for the upstream distribution of many organisms. Only a few insect genera (Baetis, Strophopteryx, Hydropsyche, Simulium, and Metriocnemus) extend the entire length of the river, through both cold and warm water environments.

The Effect of Hypolimnial Discharge:

Neel (1963) states that if a reservoir is deep enough to become thermally stratified and has a hypolimnial drain, the discharge of cold water has a stabilizing effect on the thermal regime of the river below the dam, such that temperatures are considerably colder in the summer and warmer in the winter. Hubbs (1972) has found that the reduction of 24-hour temperature fluctuations

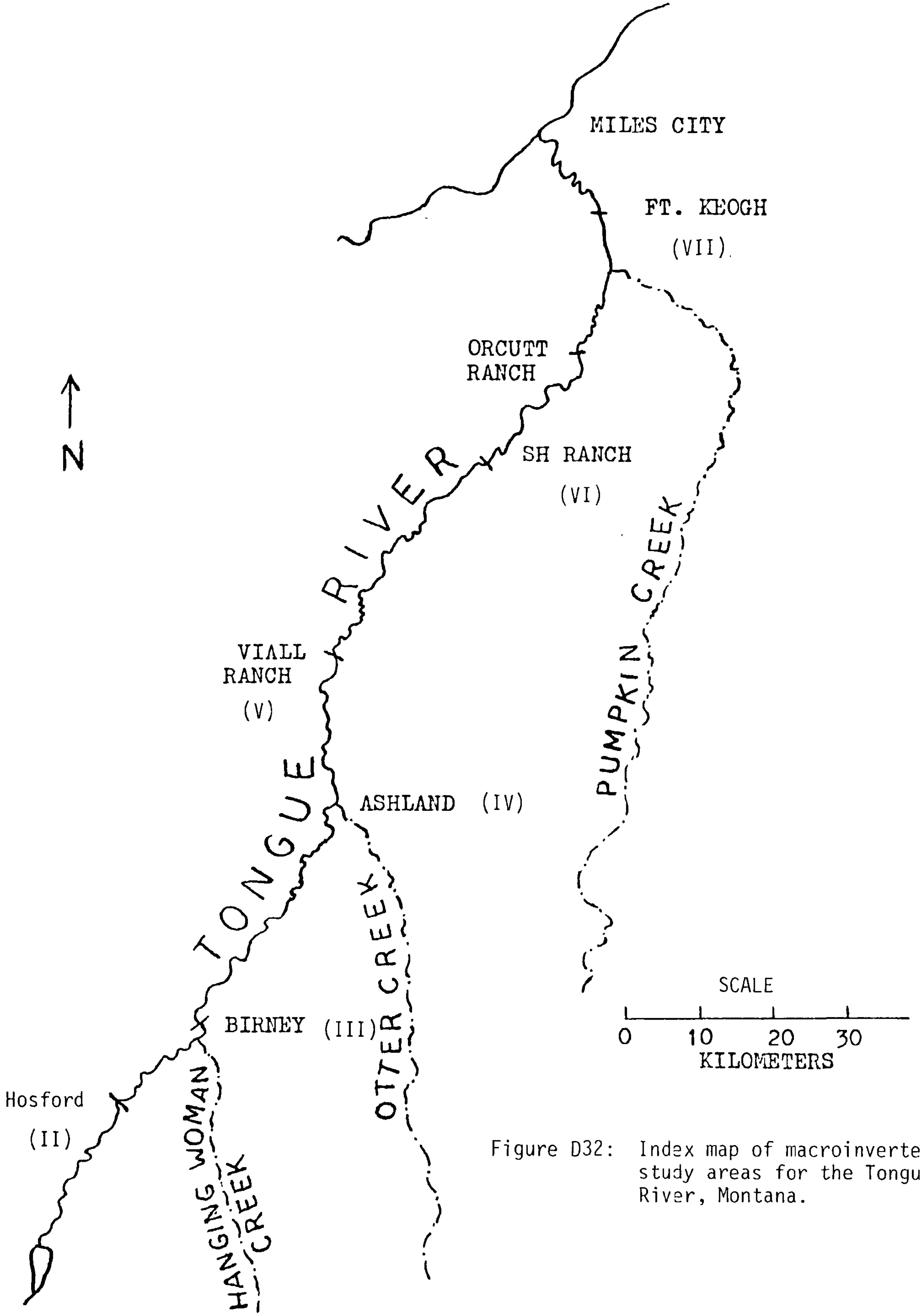

Figure D32: Index map of macroinvertebrate study areas for the Tongue River, Montana.

TABLE D4

Collection Area Characteristics

AREA	TURBIDITY	SUBSTRATE	PERIPHYTON
I II	Low	Medium to large cobble	Cladophora, Spirogyra, dense mats
III' III	Low to moderate	Medium to large cobble	Cladophora, Spirogyra, sparse mats
IV	Low	Medium to small cobble	Mostoc, sparse Cladophora
V	Moderate	Medium cobble	Mostoc, sparse Cladophora
VI	Moderate to Heavy	Bedrock with medium cobble	Heavy Nostoc
VII	Heavy	Medium cobble and sand	Heavy Nostoc

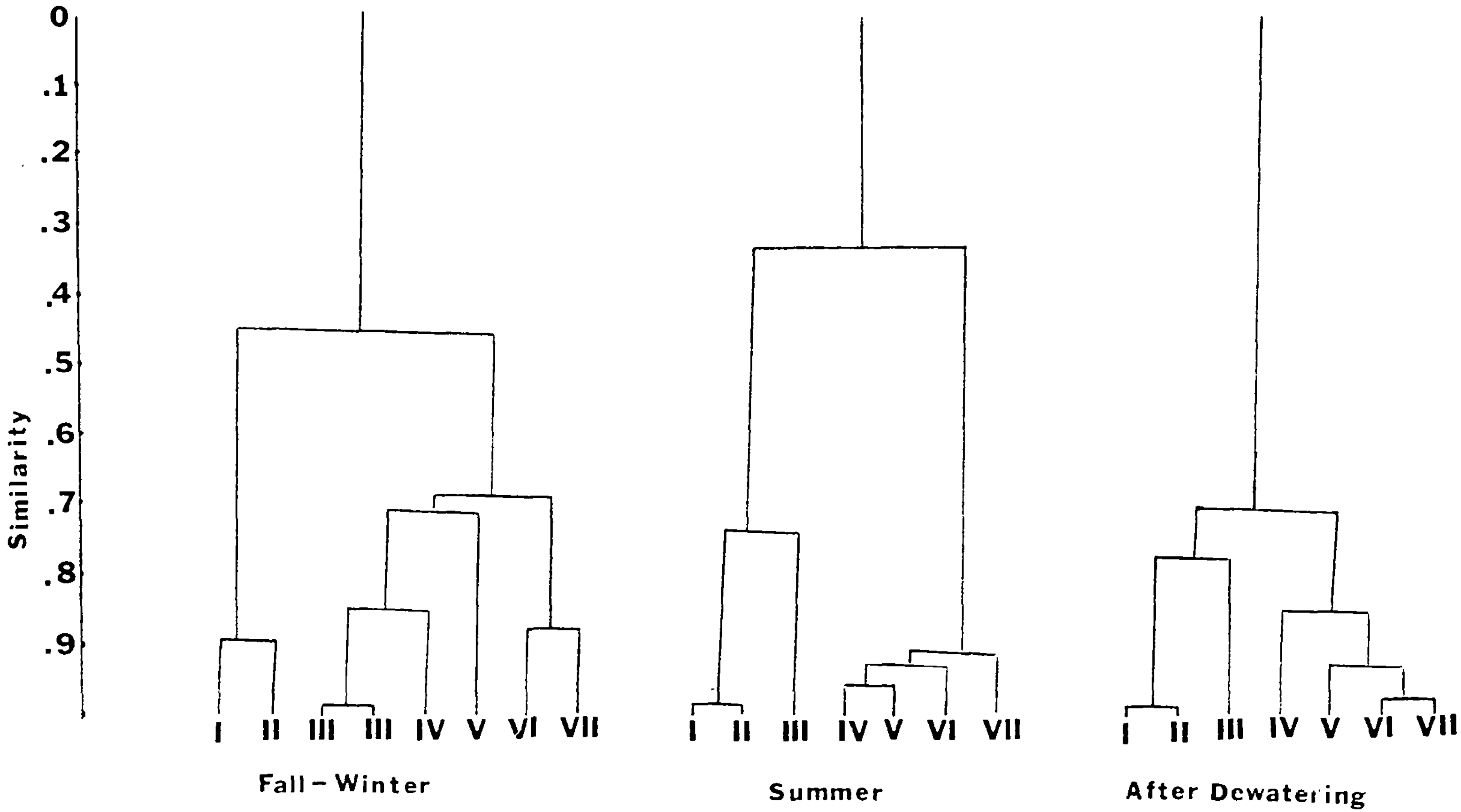

Figure D33. Association Dendrograms. See text for details.

Figure D34. Fall-Winter Benthic Macroinvertebrate Abundances.

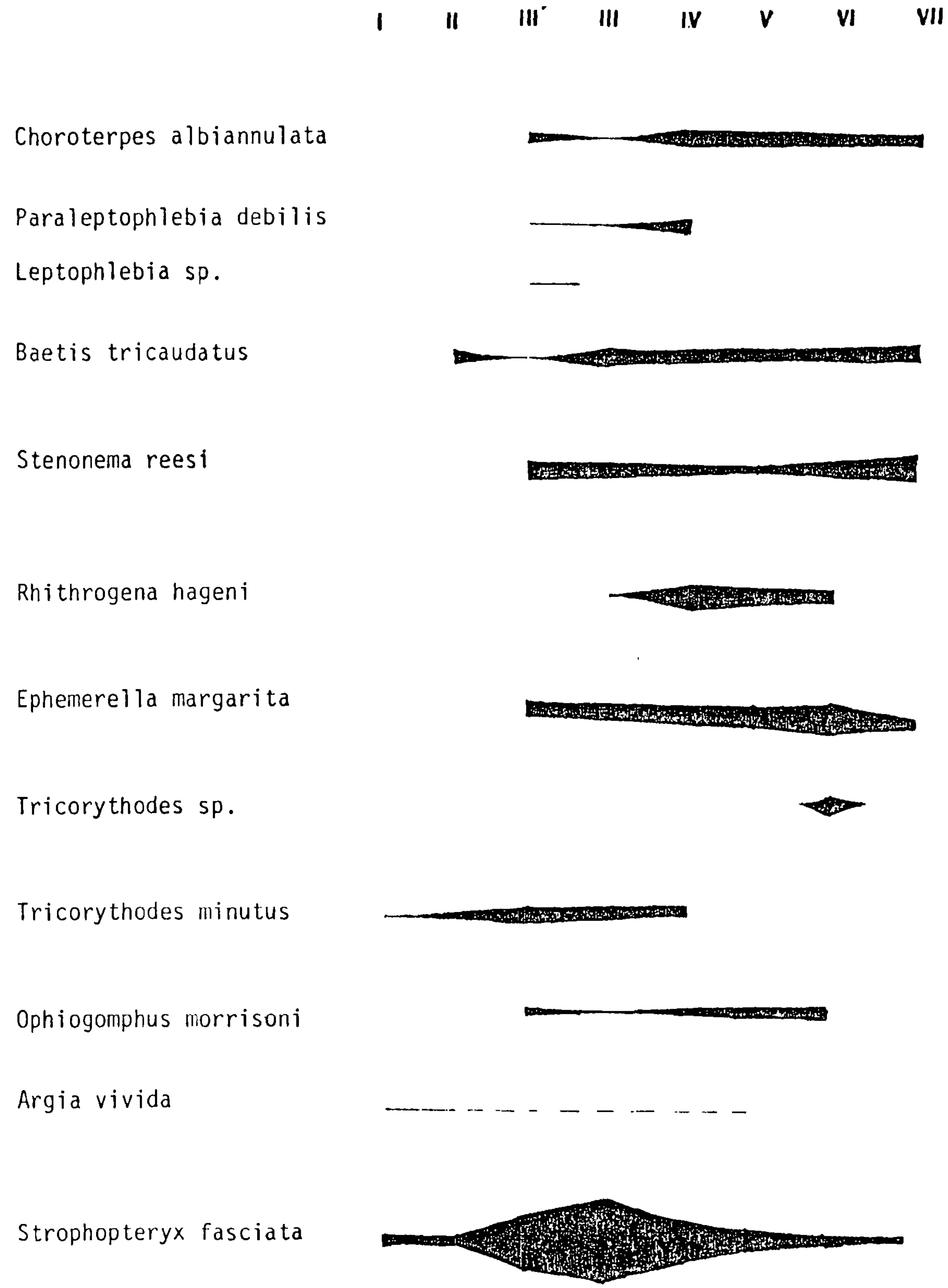

Figure D34 (cont.)

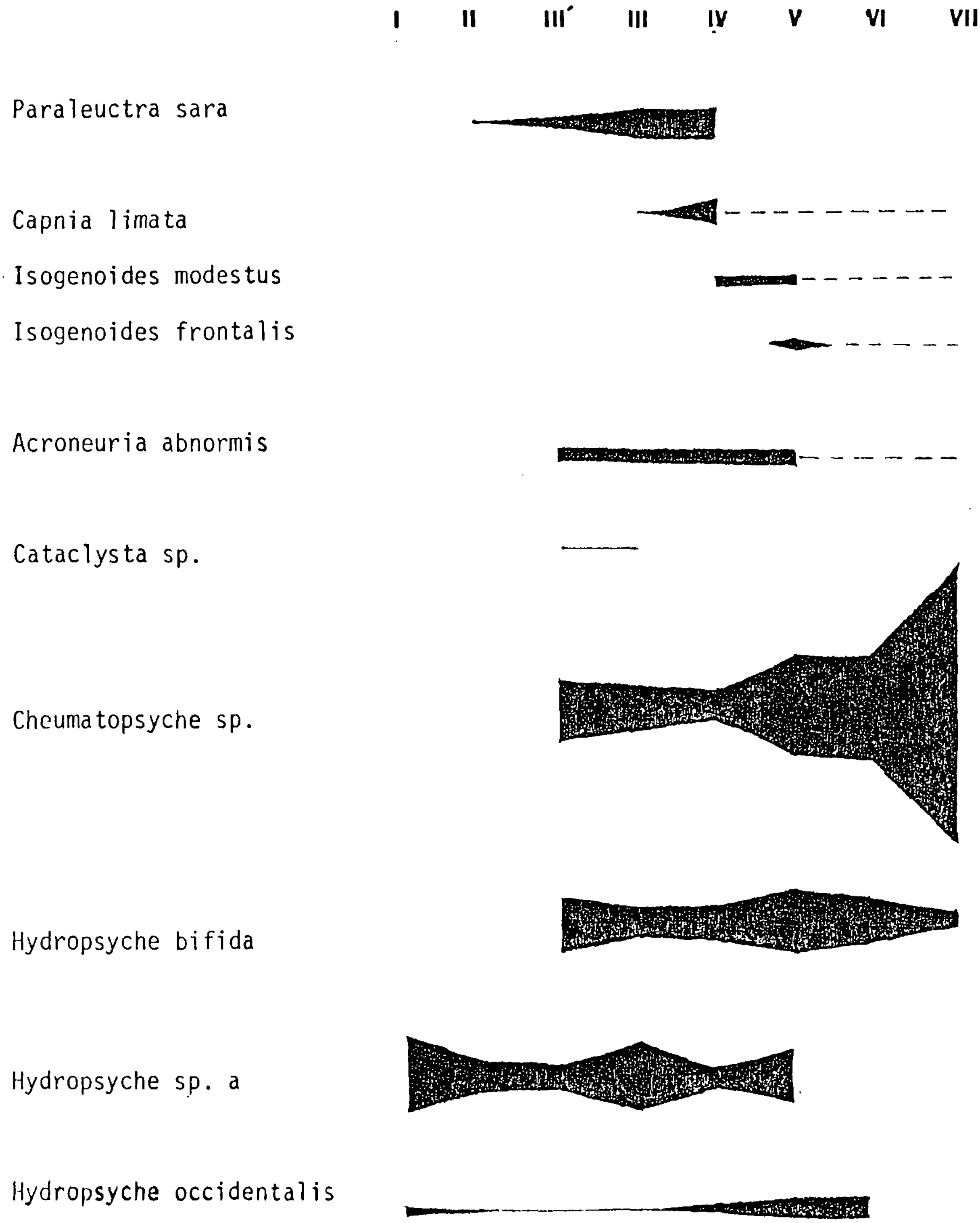

Figure D34 (cont.)

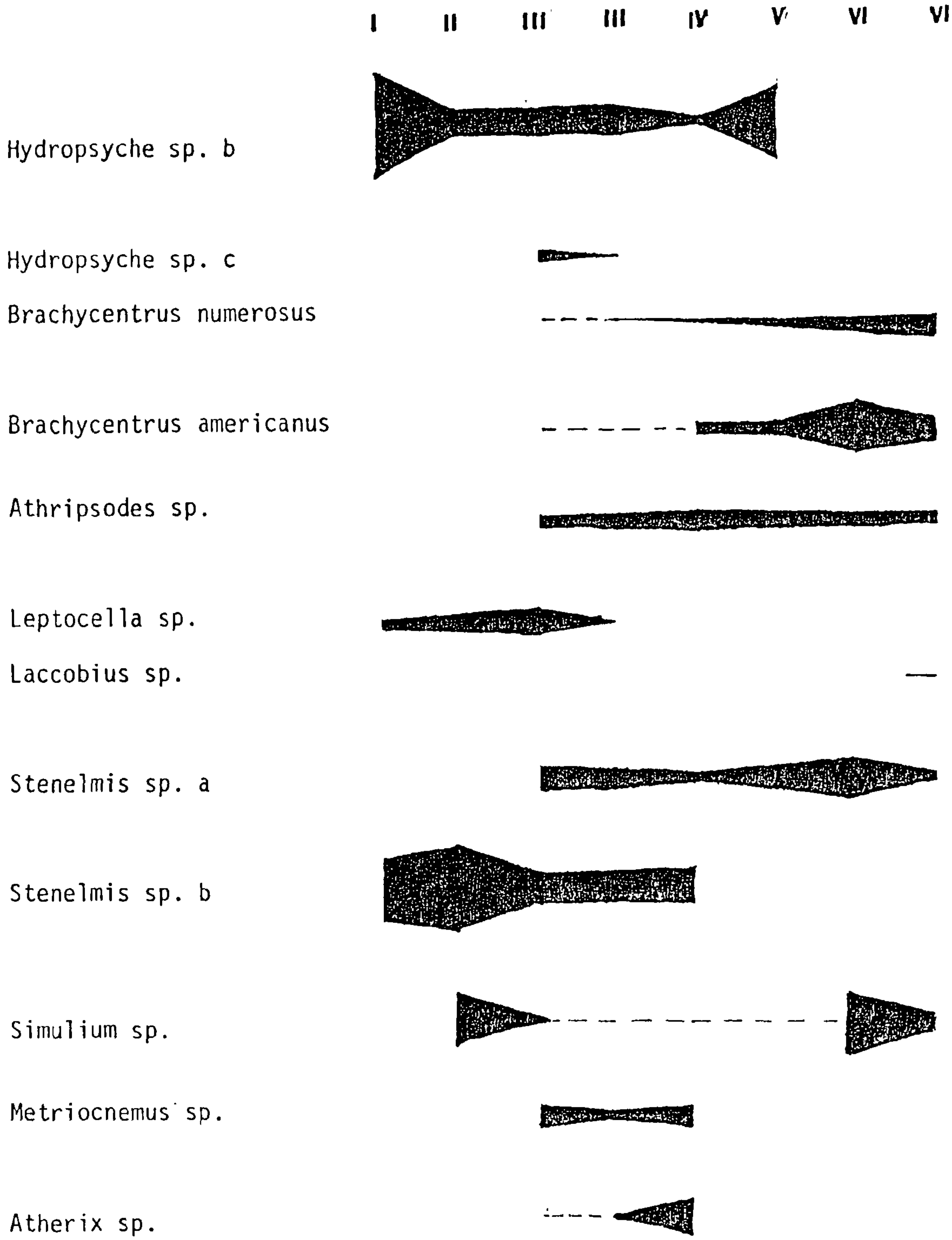

Figure D34 (cont.)

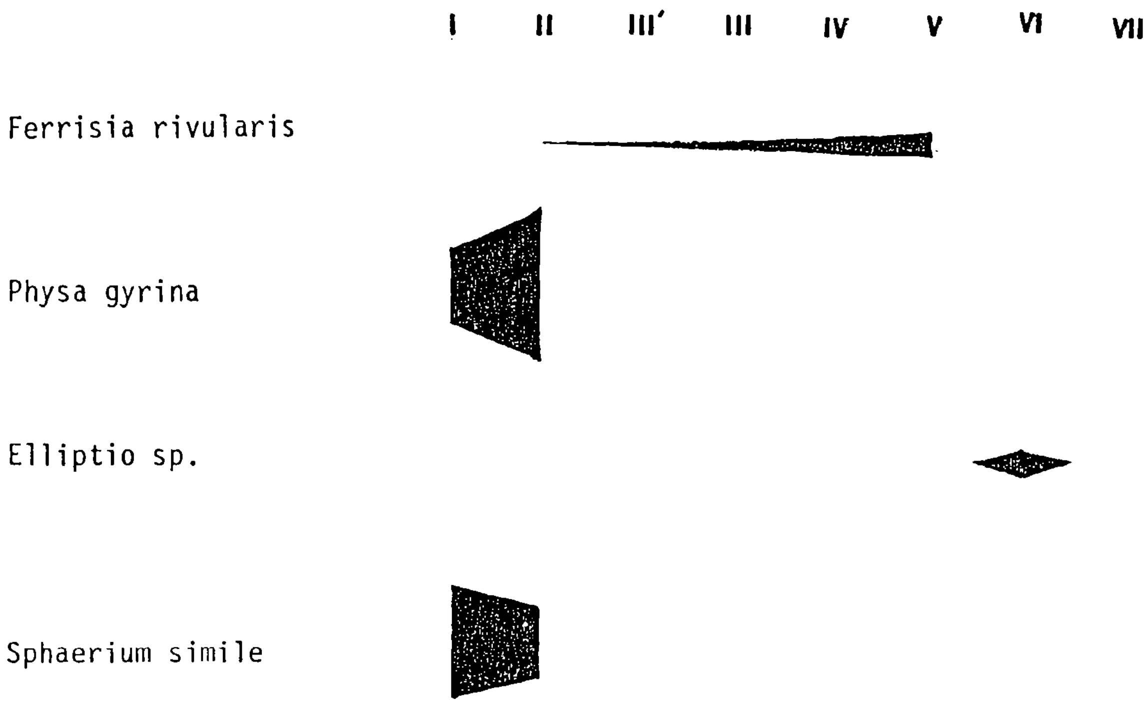

Figure D35. Summer Benthic Macroinvertebrate Abundances.

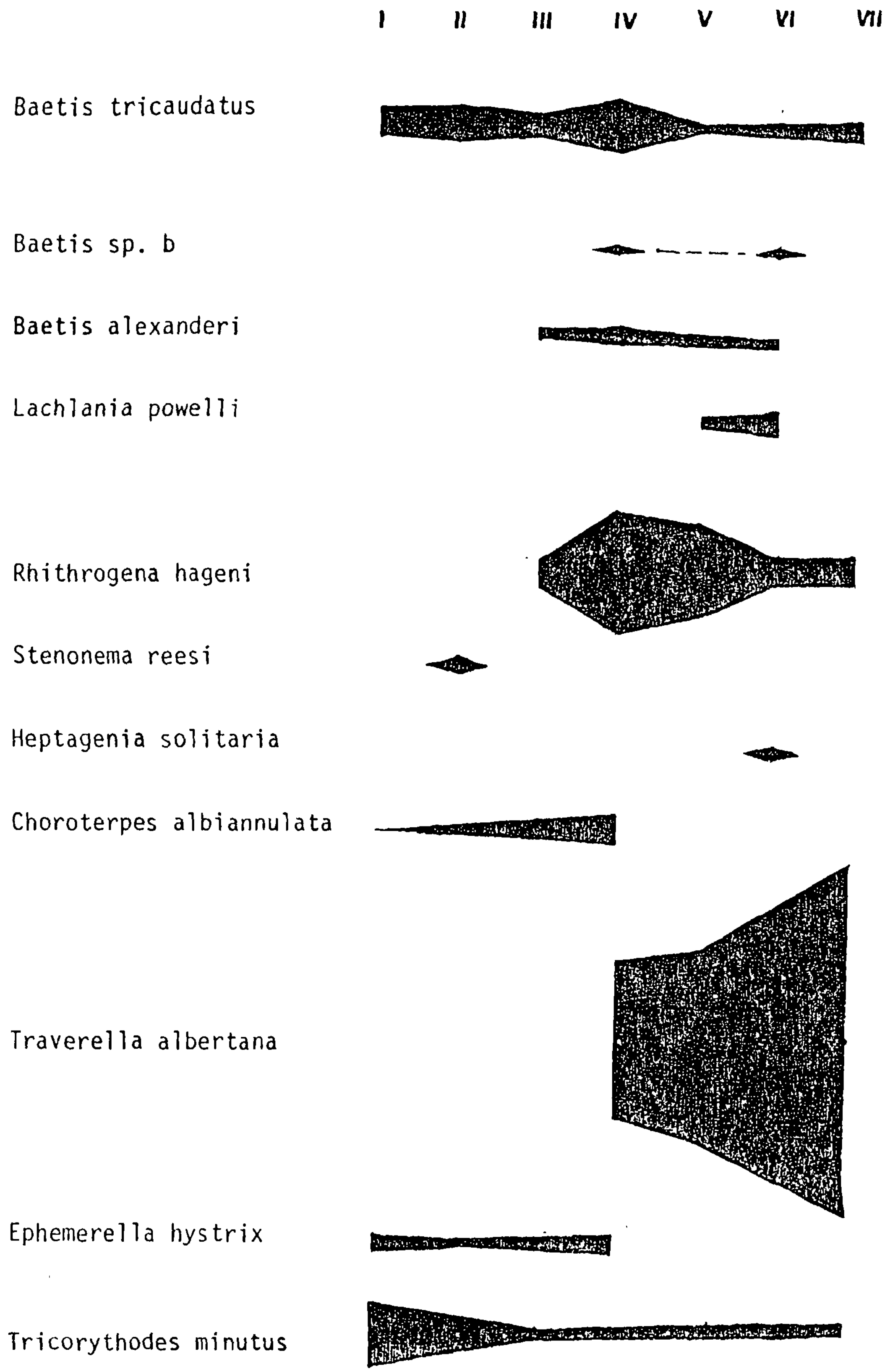

Figure D35 (cont.)

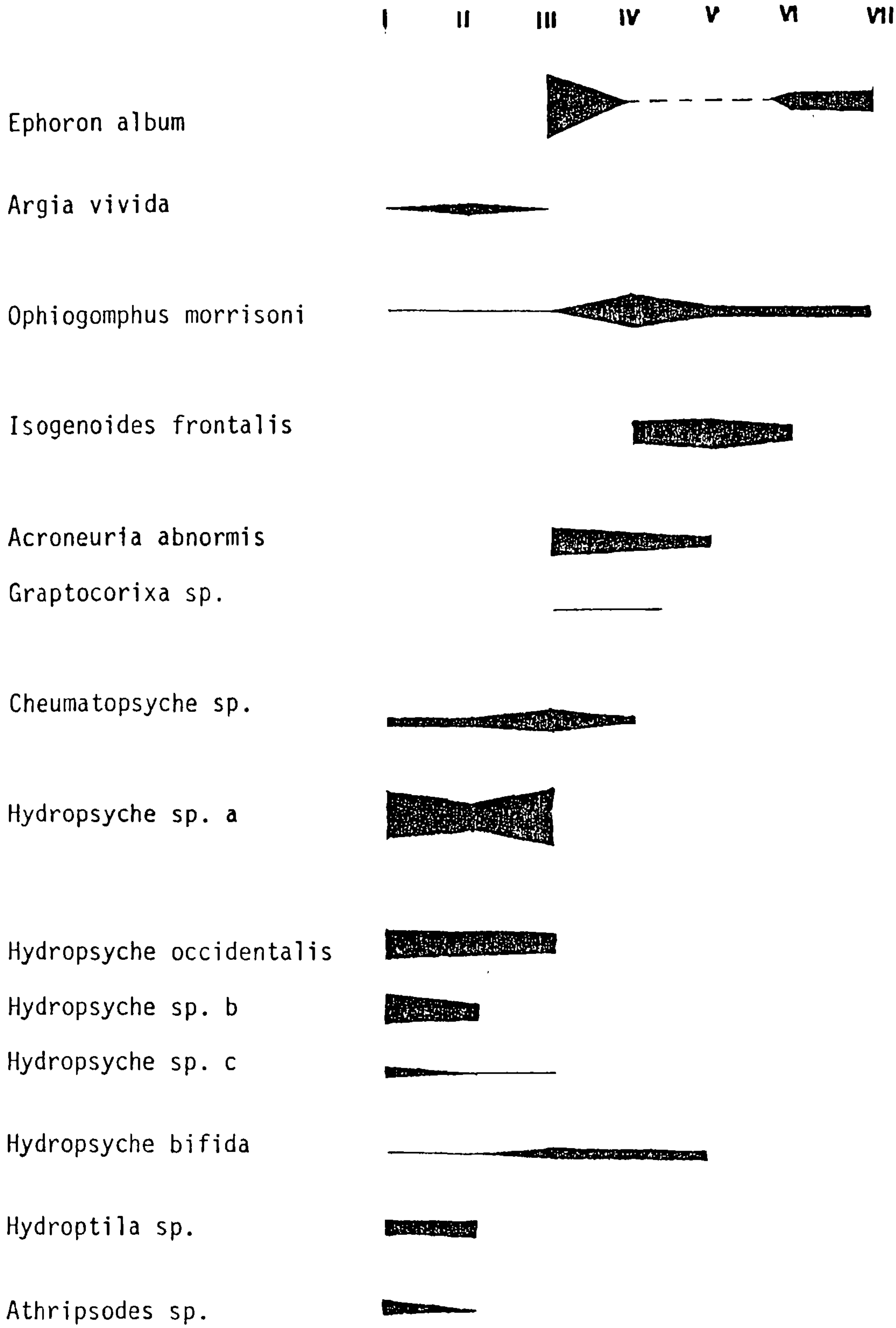

Figure D35 (cont.)

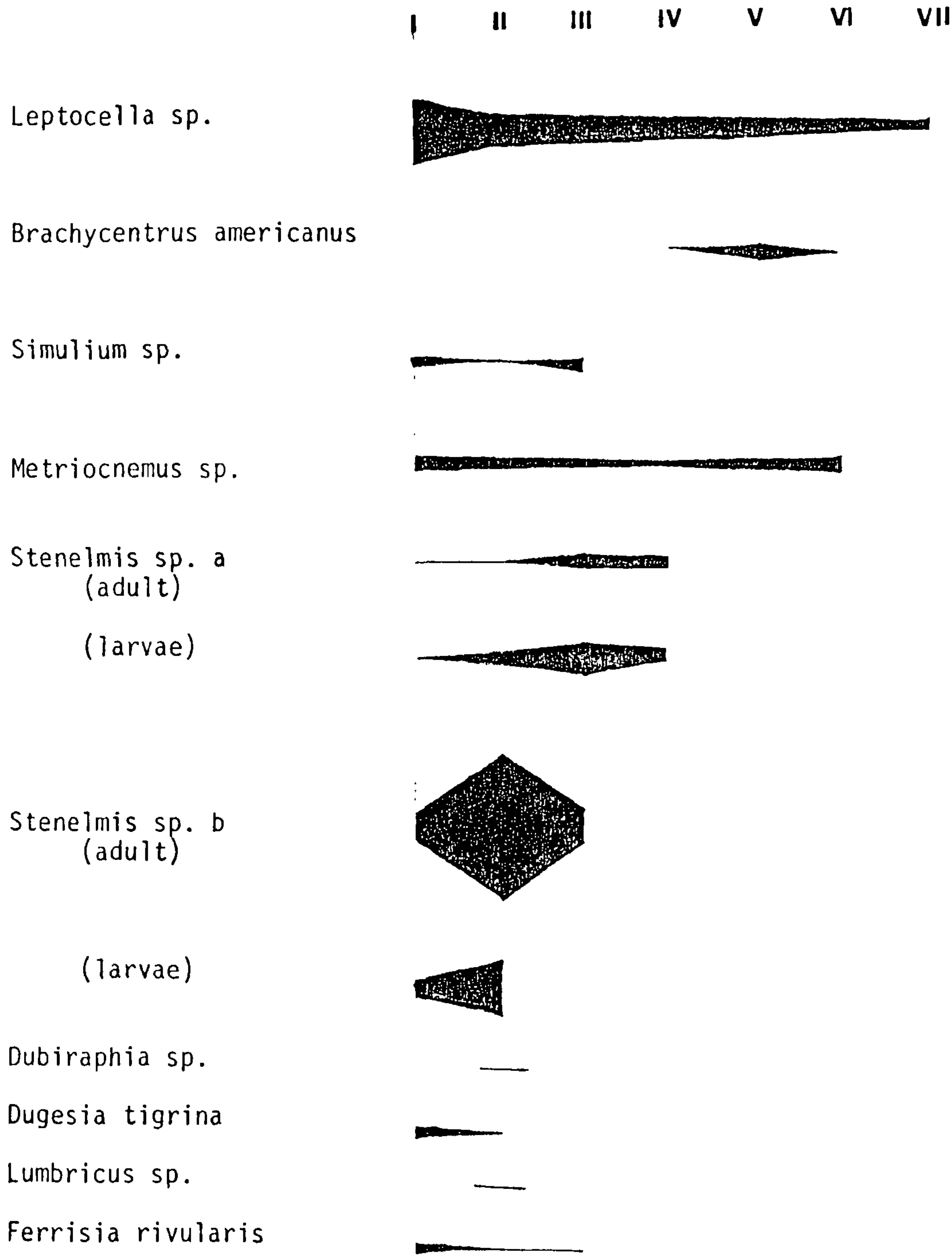

Figure D35 (cont.)

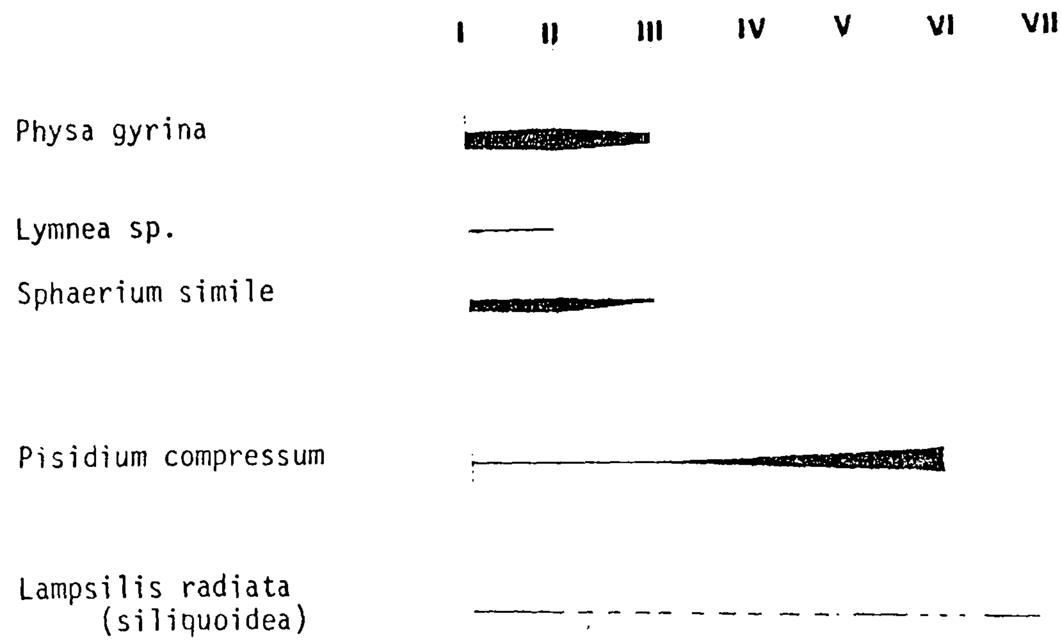

causes a marked decrease in the number of invertebrate species. Most organisms live best in a situation of thermal flux which synchronizes the life cycle and stimulates growth of insect instars. This information is supported by work on the mayflies by Ide (1935) and more recently by Trottier (1971) on the effects of temperature on the life-cycle of dragonflies.

Ward (1974) found that the South Platte River, in Colorado, was typical in its responses to hypolimnion srain from the Cheesman Dam. Benthic algae increased in the cold water section through a combination of decreased turbidity, increased nutrients, increased flow constancy, and decreased bank and bed erosion. Filamentous chlorophytes were especially enhanced. Although densities of some invertebrates may increase below a reservoir, diversity is markedly decreased and increases slowly downstream. Ward also predicted that those species able to survive and mate under low temperature condition, and adjusted to depend on photoperiod and endogenous rhythms to avoid winter emergence, are those species most likely to be dominant in this area. In addition, Ward suggests that these are unstable communities within which a relatively minor biotic or abiotic change would produce great changes in community structure.

Lemkuhl (1972), in studies of the Saskatchewan River, has found that diapause eggs, which require temperature fluctuations to hatch, will hot hatch in areas influenced by hypolimnial release. Fifteen species of mayflies were found above the reservoir, and none in the thermally altered area below the hypolimnial release. Due to constant temperature, four criteria were not met: 1.) the necessity of freezing temperatures to break egg diapause; 2.) a rapid fluctuation from freezing to higher temperatures to induce hatching in some species; 3.) the requirement of a minimum termperature over a given period of time to stimulate nymph maturation; and 4.) a certain number of degree days at high temperatures for emergence to take place. The inference is made that non-mayfly aquatic insects, which often have similar requirements, are eliminated from these areas for the same reasons. Spence and Hynes (1971) have also found that lowered temperatures cause the increase in growth and abundance of periphyton (by reduing the number of grazers), which leads to a radical alteration of the substrate. This eliminates many substrate specific organisms and increases the number of available microhabitats for those species which would be less abundant under normal conditions. Spence and Hynes argue that the effects of a hypolimnial release changes the benthos in the same way as mild organic pollution.

Pearson, Kramer, and Franklin (1968) and Ward (1974) found that with increasing distance from the dam, atmospheric conditions and tributary waters combine to return the river to its pre-impoundment state and the numbers of invertebrate species increase. Depending on the discharge rate, the depth of the hypolimnion, and the hydraulic geometry of the river, the hypolimnial effects can extend to a distance of 150 km. below the reservoir.

Radford and Hartland-Rowe (1971), from their work on the Kananaskis River in Alberta, found that areas affected by hypolimnial release show low diversity and densities of invertebrates. This situation continues into the uneffected portions of the river where densities and diversity of invertebrates increases, but is still substantially lower than in similar unimpounded rivers.

Hilsenhoff (1971), working on Mill Creek in Wisconsin, has found that preimpoundment surveys showed diverse fauna of Ephemeroptera, Trivhoptera, Diptera, and Coleoptera. After impoundment the community was almost completely eliminated and replaced with Simuliidae and Chironomidae. Increases in total phosphorus and nitrogen, as well as altered thermal regime, were the implied causes for the change in community structure.

Isom (1969) and Bates (1962), in separate investigations on influences of mainstream impoundments in the Tennessee Valley, have found a decline in mollusc diversity as a result of hypolimnial releases. Although the unionicean clams were greatly reduced, the Lampsilinae and other smaller clams persist and often make up the entire community in the area directly below a hypolimnial drain reservoir. Trotzky and Gregory (1974) found the same effects of hypolimnial discharge dams on woodland streams in Maine.

The Tongue River Reservoir dam has a hypolimnial discharge and the biological situations described above are distinctly exhibited on the Tongue River. In the area of the river affected by the hypolimnial discharge the insect fauna is diminished and the dominant forms are the molluscs Physa gyrina and Sphaerium simile, along with the riffle beetle Stenelmis sp. b. Based on the collection point data (Table D4), the cold water area is also an area of low turbidity and increased periphyton, as exemplified by the dense mats of Cladophora. Stolier (1963) observed similar relationships between a hypolimnial dam release and Cladophora on the Marias River in Montana. These dense mats of Cladophora apparently provide a tremendous increase in the availability of suitable habitats for the riffle beetles, as large numbers (up to 2250 individuals/m^2) have been found inhabiting the dense mats of filamentous algae. Open areas of small and medium cobble are, likewise, inhabited by large numbers of Sphaerium and Physa (400 individuals/m^2).

Elliott (1967) and Hynes (1970) have shown that there is a definite trend for adults of the Ephemeroptera, Plecoptera, and Trichoptera to fly upstream for the purposes of oviposition. Although this event has not been investigated on the Tongue River, it is a likely occurence. However, assuming that Lemkuhl's hypotheses for the temperature requirements of diapause eggs is correct, the eggs deposited in the cold water section of the river do not undergo sufficient temperature fluctuations to break diapause. Thus, the insect larvae and nymphs, except in the few cases mentioned previously, do not occur in the cold water section and the insect eggs in this area probably remain in diapause until their death. Where the original temperature regime is re-established (at III' and downstream) the increase of the insect species is quite pronounced.

Van der Schalie (1973) has determined the temperature tolerances of many pulmonate snails, in particular Physa gyrina. The animals fail to feed and grow in areas where the mean water temperature is less than 4° C. In addition, although growth is faster at temperatures above 24° C., this advantage is offset by greater survival and reproductive abilities at lower temperatures. Although growth is possible at temperatures above 30° C., the organism will not reproduce. Thus, the physid snails seem to thrive best in waters where cool temperatures exist in the winter. These river conditions are reproduced in the area of the Tongue River influenced by the hypolimnial discharge. Because the higher summer temperatures of the middle river are not conducive to molluscan growth and reproduction and these greater temperature fluctuations are conducive to proper insect development as well, Physa and Sphaerium are diminished or eliminated and the dominant invertebrates are the hydropsychids and Strophopteryx fasciata. In addition, the algal cover of Cladophora is reduced (through increased grazing and chemical changes) and Nostoc is present.

Even though diversity has increased, due to a return to warm water conditions of thermal flux and increased suspended and organic matter in the water from tributary and irrigation flow, the communtiy may still be considered impoverished. Compared to invertebrate communities in a similar unimpounded river, the Middle and Lower Yellowstone (Newell, 1975), the number of species of invertebrates at any station on the Tongue River is considerably lower. Although the environments are similar, the influence of the hypolimnion discharge is dominant.

Finally, as the river nears its junction with the Yellowstone River, a third community is present. Increased turbidity causes the amount of available light to be reduced, and the abrasive action of suspended particles fouls many insect gills or causes alteration of the substrate to other than optimum conditions (Hynes, 1970). Thus, in the area of the lower river, where turbidity is high, the benthic fauna is dominated by Cheumatopsyche, which can take advantage of the suspended matter in its feeding habits. The dominant algal form in this area is Nostoc.

The Effect of Flow Reduction:

In order to reduce pressure on the Tongue River dam during a six week period, the control gates were left open during the greater part of the spring and summer of 1975 to drain the reservoir as much as possible. This continual release of water from the reservoir did not allow complete formation of a hypolimnion layer. Water released during this period was observed to have temperatures only 1° or 2° C. cooler than at the mouth of the river at Miles City (Figure D36). The release of water at these elevated temperatures eliminated the cold water environment associated with the stretch of river below the dam.

The alteration of community structures can be seen in the dendrogram (Figure D33) and kite-diagram (Figure D37). Warming of this section of the river has apparently made it habitable to most of the insect species which are commonly found in the upper warm water section. The dendrogram shows that site III has become more closely associated with sites I and II. No clear dominant can be discerned in the "cold" water area; however, the hydropsychids and Stenelmis sp. b are most abundant and the formerly dominant Physa and Sphaerium are considerably reduced.

There are two possible explanations for the new community composition in the area. If the ideas of Lemkuhl (1972) are accepted and one assumes that adults fly upstream to lay eggs, the change in thermal regime to that of greater temperature fluctuations has probably allowed the hatching of diapause eggs, and nymphal and larval development of many insects, which the formerly cooler waters would not have allowed. The presence of individuals (in some samples)

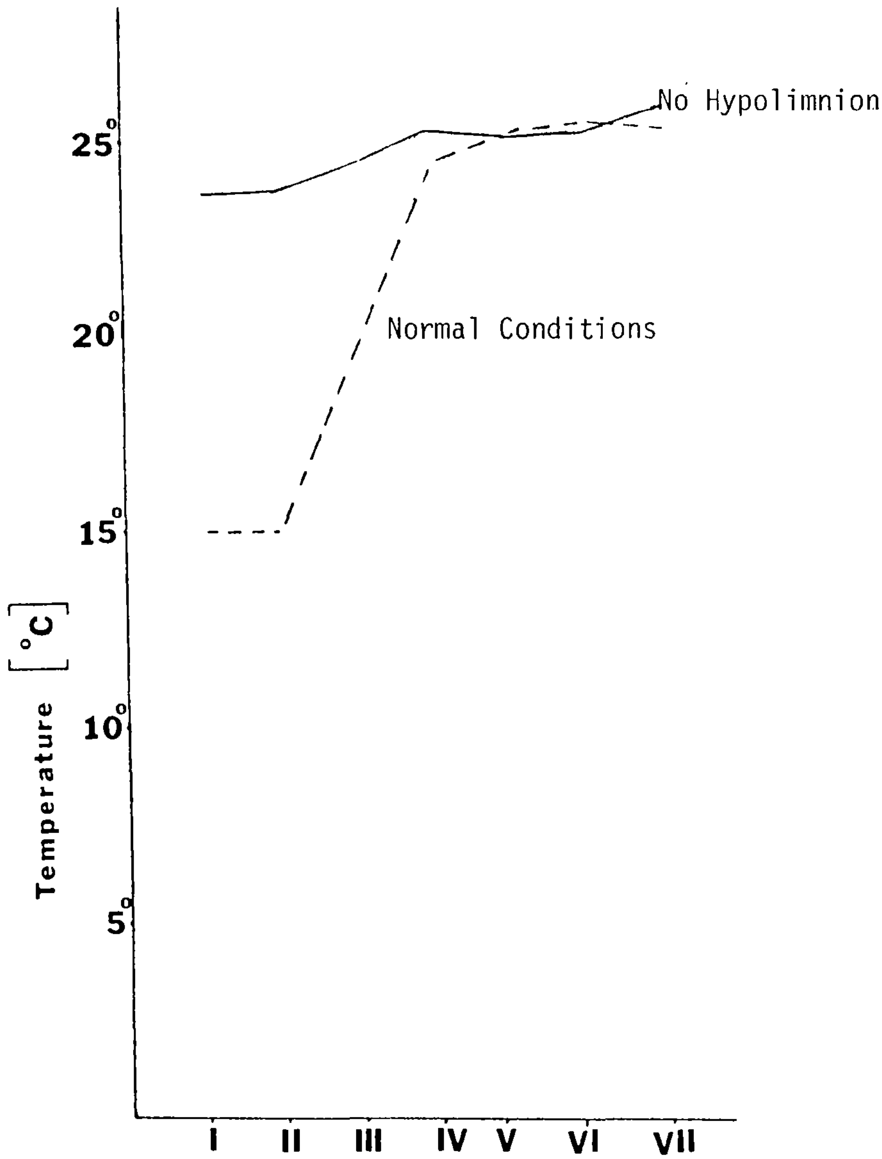

Figure D36. Summer Temperatures. Tongue River.

which are obviously not first or second instar (that is, some individuals close to emergence) precludes this idea as being the sole explanation.

Madsen, Bengtson, and Butz (1973) and Bishop and Hynes (1969) have shown the evidence of positive rheotaxis in aquatic insects, through the upstream migration of virtually all larval and nymphal stages of all the major groups of aquatic insects. Upstream migration is quite pronounced in the Ephemeroptera (particularly Baetis), the Trichoptera, the Coleoptera, and Diptera. Thus, the presence of many aquatic insects in this community seems to be due to the hatching of diapause eggs, influenced by thermal changes in the section, and the upstream migration of larval and nymphal forms to an area which had been formerly uninhabitable, and acted as an apparent barrier to upstream migration.

The lower part of the river, as shown by dendrogram (Figure D33), is no longer divided into two distinct communities. The dominance and great abundance of the two mayflies, Traverella albertana and Rhithrogena hageni, from sample point IV downstream dampens the effect of changes in number or occurence of the rarer species of aquatic insects. It should be noted as well, that the lower part of the river is dominated almost exclusively by short-lived summer species of mayflies which do not occur in the fall and winter samples.

Figure D37. Distribution and Relative Abundance. Macroinvertebrates. After Massive Flow Reduction.

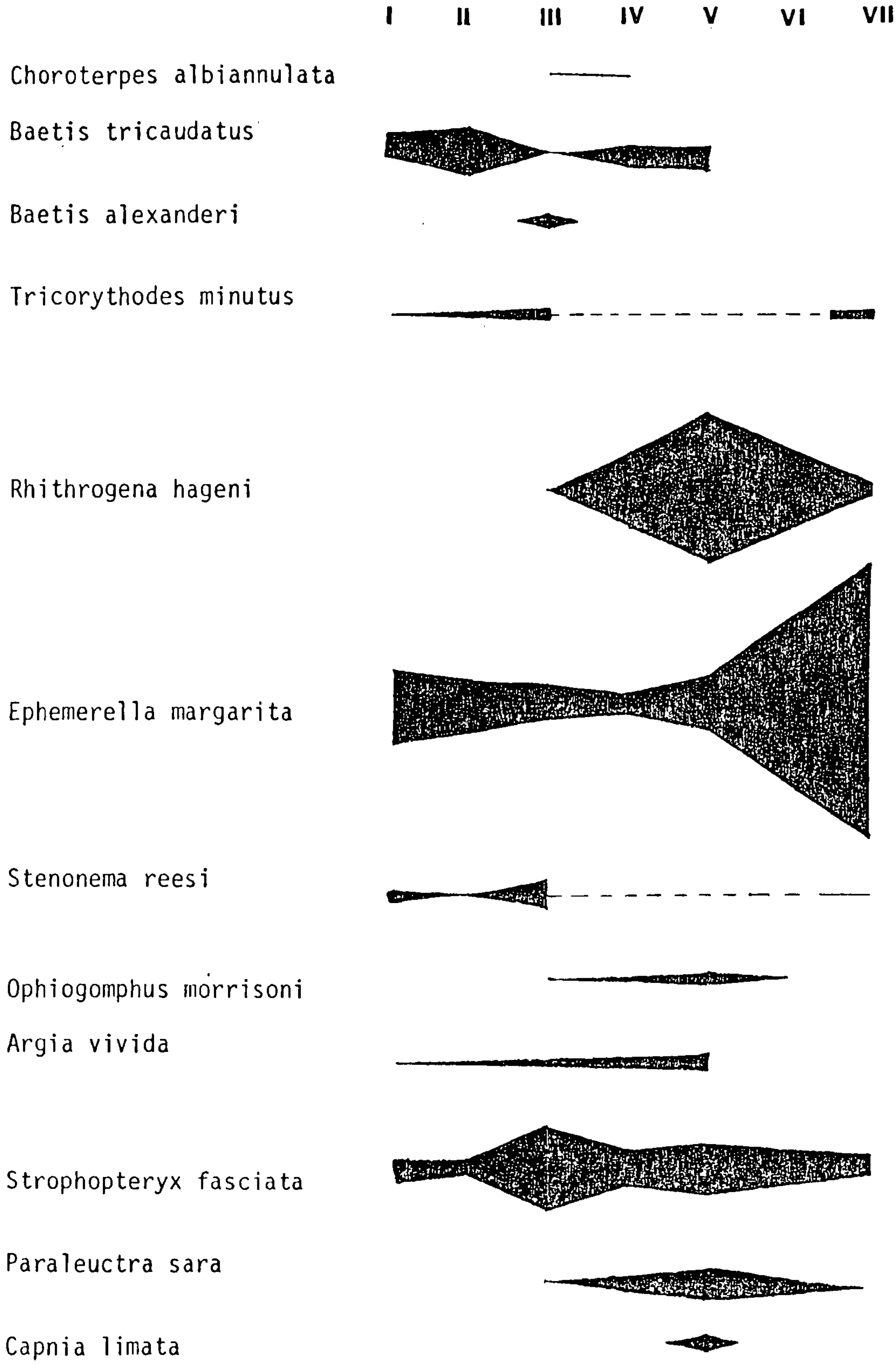

Figure D37 (cont.)

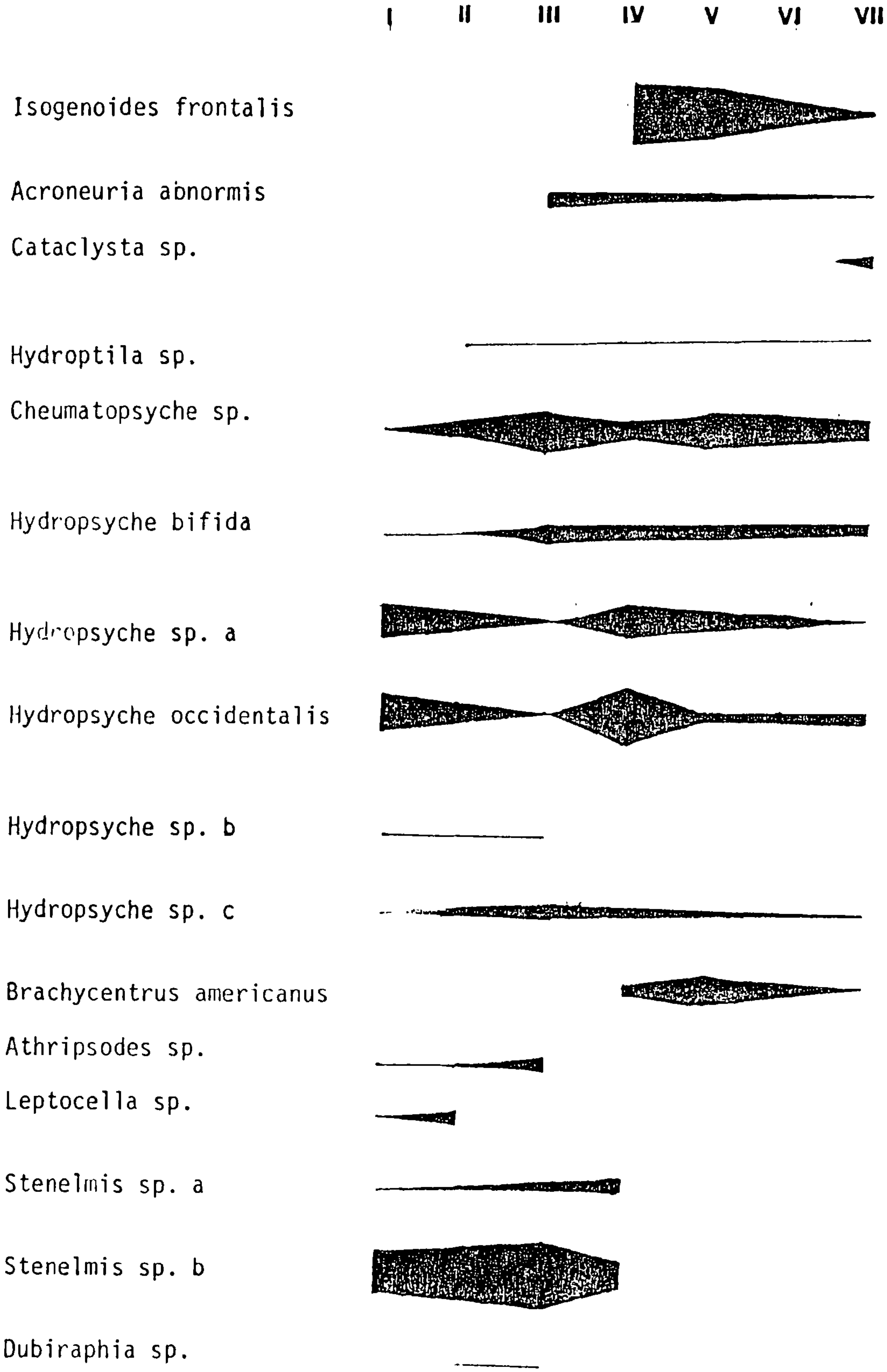

Figure D37 (cont.)

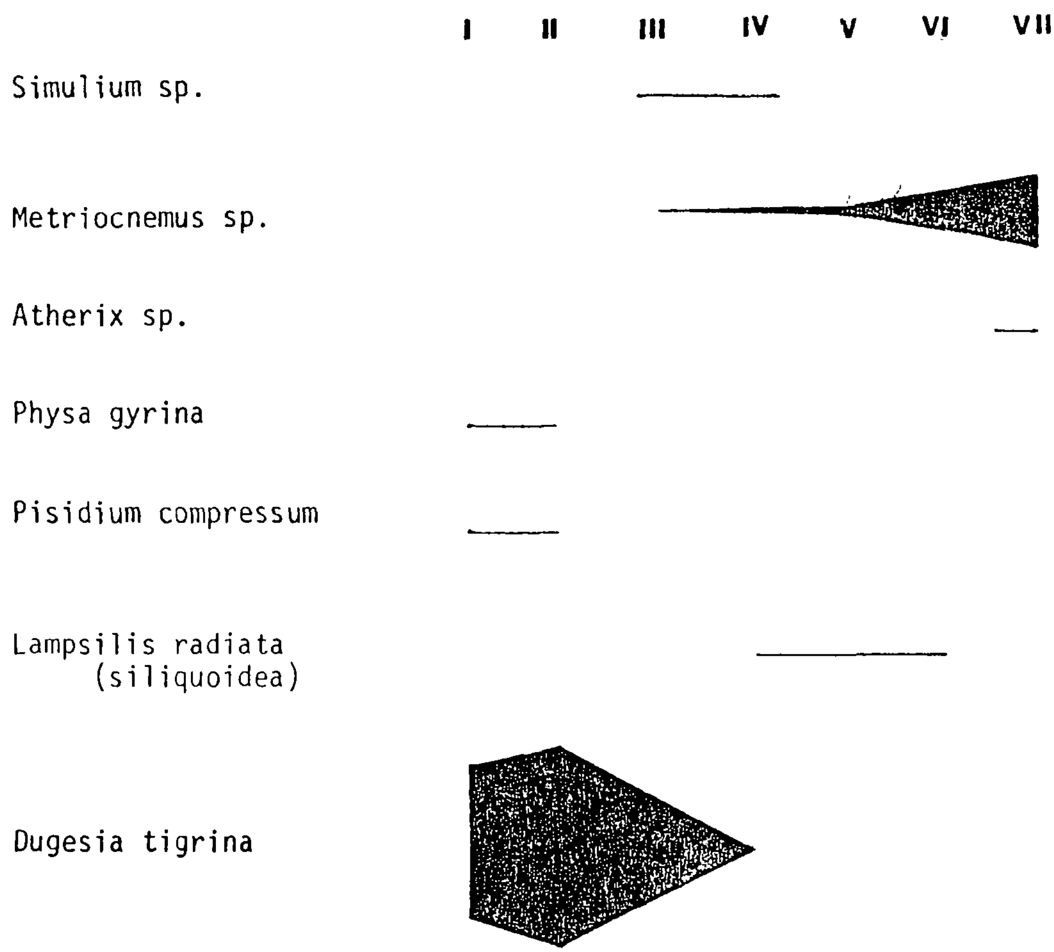

References

Anderson, N.H., 1966, Depressent effect of moonlight on activity of aquatic insect. Nature, Lond. 209(5020): 319-320.

Bates, J.M. 1962, The impact of impoundment on the mussel fauna of Kentucky Reservoir, Tennessee River. American Midland Naturalist. 68(1): 232-236.

Bishop, J.E. and H.B.N. Hynes. 1969a, Downstream drift of the invertebrate fauna in a stream ecosystem. Archiv fur Hydrobiologie. 66(1): 56-90.

__________. 1969b, Upstream movements of the benthic invertebrates in the Speed River, Ontario. J. Fish. Res. Bd. Canada 26(2): 279-298.

Bovee, K.D. 1975a, The determination, assessment, and design of "in-stream value" studies for the Northern Great Plains region. Report of the Northern Great Plains Resources Program, Denver, Colorado.

__________. 1975b, Assessment and implementation of "in-stream value" studies for the Northern Great Plains. Mont. Acad. of Sci. Proc. Ft. Union Coal Field Symposium. 2: 112-123.

Briggs, C.B. 1948, The quantitative effects of a dam upon the bottom fauna of a small California stream. Tran. Am. Fish. Soc. 78: 70-81.

Britt, N.W. 1962, Biology of two species of Lake Erie mayflies, Ephoron album (Say) and Ephemera simulans (Walker). Ohio Biological Survey Bulletin. 1(5): 1-70.

Cheatum, E.P. 1934, Limnological investigations on respiration, annual migratory cycle, and other related phenomena in fresh-water pulmonate snails. Trans. Am. Micros. Soc. 53(4): 348-406.

Church, J.O. 1976, Cluster analysis in biological studies. Presented paper at 24th Annual Meeting of the North American Benthological Society.

Clampitt, P.T. 1970, Comparative ecology of the smails Physa gyrina and Physa integra(Basommatophora: Physidae). Malacologia. 10(1): 113-151.

__________. 1974. Seasonal migratory cycle and related movements of the fresh-water pulmonate smail, Physa gyrina. Am. Mid. Nat. 92(2): 275-300.

Cummins, K.W. 1964, A review of stream ecology with special emphasis on organism-substrate relationships. Pymatuning Symposia in Ecology, Spec. Pub. No. 4: 2-51.

Dewitt, R.M. 1955, The ecology and life history of the pond snail, Physa gyrina. Ecology 36(1): 40-44.

Dodds, G.S. and F.L. Hisaw. 1924, Ecological studies of aquatic insect. I. Adaptations of mayfly to swift streams. Ecology 5(2): 137-148.

_______. 1925, Ecological studies of qquatic insects. III. Adaptations of caddisfly larvae to swift streams. Ecology 6(2): 123-137.

Edington, J.M. 1968, Habitat preferences in net-spinning caddis larvae with special reference to the influence of water velocity. J. Anim. Ecol. 37(3): 675-692.

Egglishaw, H.J. 1969, The distribution of benthic invertebrates on substrata in fast flowing streams. J. Anim. Ecol. 38(1): 19-32.

Elliott, J.M. 1967, The life histories and drifting of the Plecoptera and Ephemeroptera in a Dartmoor stream. J. Anim. Ecol. 36(2): 343-362.

Ellis, M.M. 1941, Fresh-water impoundments. Trans. Am. Fish. Soc. 71: 80-93.

Elser, A.A. 1975, Fish distribution and diversity of a Montana prairie stream. Mont. Acad. of Sci. Proc. Ft. Union Coal Field Symposium. 2: 124-137.

Emlen, J.M. 1973, Ecology: An Evolutionary Approach,Addison Wesly, Reading, Mass.

Eriksen, C.H. 1964, Benthic invertebrates and some substrate-current-oxygen interrelationships. Pymatuning Symposia in Ecology, Spec. Pub. No. 4, 98-114.

Gordon, A.E. and J.B. Wallace. 1975, Distribution of the family Hydropsyche (Trichoptera) in the Savannah River Basin of North Carolina and Georgia. Hydrobiologia. 46: 405-423.

Harrod, J.J. 1965, Effect of current speed on the cephalic fans of the larva of Simulium ornatum var. nitidifrons Edwards (Diptera: Simuliidae). 26(1): 8-12.

Heiman, D.R. and A.W. Knight. 1975, The influence of temperature on the bioenergetics of the carniverous stonefly nymph, Acroneuria californica Banks (Plecoptera: Perlidae). Ecology. 56(1): 105-116.

Hilsenhoff, W.L. 1971, Changes in the downstream insect and amphipod fauna caused by an impoundment with a hypolimnion drain. Ann. Ent. Soc. Am. 64(3): 743-746.

Hubbs, C. 1972, Some thermal consequences of environmental manipulations of water. Biol. Conserv. 4(3): 185-188.

Hughes, D.A. 1966a, On the dorsal light response in a mayfly nymph. Anim. Behav. 14: 13-16.

_______. 1966b, The role of responses to light in the selection and maintenance of microhabitat by the nymphs of two species of mayfly. Anim. Behav. 14: 17-33.

Hynes, H.B.N. 1970, The Ecology of Running Waters. University of Toronto Press, Toronto, Ontario, Canada.

_______. 1976, The Biology of Plecoptera. Ann. Rev. Ent. 21: 135-153.

Isom, B.G. 1969, Effects of storage and mainstream reservoirs on benthic macroinvertebrates in the Tennessee Valley. From G.E. Hall (ed.) Fisheries Biology and Limnology. Spec. Publ. No. 8, Am. Fish. Soc. Washington, D.C.

Lemkuhl, D.M. 1972, Changes in thermal regime as a cause of reduction of benthic fauna downstream of a reservoir. J. Fish. Res. Bd. Canada. 29: 1329-1332.

__________, and N.H. Anderson. 1974, Microdistribution and density as factors affecting the downstream drift of mayflies. Ecology. 53(4): 661-667.

Linduska, J.P. 1942, Bottom type as a factor influencing the local distribution of mayfly nymphs. Can. Ent. 74(1): 26-30.

Madsen, B.L. 1969, Reactions of Brachyptera risi (Morton)(Plecoptera) nymphs to water current. Oikos. 20: 95-100.

__________, and J. Bengtson and I. Butz. 1973, Observations on upstream migration by imagines of some Plecoptera and Ephemeroptera. Limnology and Oceanography. 18: 678-681.

McBride, J.R. and A.J. Silverman. 1973, Forty percent of the nation's coal: Development of the Northern Great Plains. Montana Public Affairs Report #16.

Minshall, G.W. and P.V. Winger. 1968, The effect of reduction of stream flow on invertebrate droft. Ecology. 49(3): 380-382.

Montana State Department of Natural Resources and Conservation, Water Resources Division, 1974. Proposed repairs to the Tongue River Dam. Draft environmental impact statement.

Neel, J.K. 1963, Impact of Reservoirs. Limnology in North America. David Frey (ed.). University of Wisconsin Press, Madison, Wisconsin.

Newell, R.L. 1975, Longitudinal changes in the macroinvertebrate fauna of the Yellowstone River. Mont. Acad. of Sci. Proc. Ft. Union Coal Field Symposium. 2: 199-211.

Nielsen, A. 1950, The torrential invertebrate fauna. Oikos. 2: 176-196.

Pearson, W.D. and R. Franklin. 1968, Some factors affecting drift rates of Baetis and Simuliidae in a large river. Ecology. 49: 75-81.

__________, R.H. Kramer, and D.R. Franklin. 1968, Macroinvertebrates in the Green River below Flaming Gorge Dam, 1964-65 and 1967. Proc. Utah Acad. Sci. 28: 148-167.

Percival, E. and H. Whitehead. 1929, A quantitative study of the fauna of some types of stream-bed. J. Ecol. 17: 282-314.

Pfeifer, R.F. and W.F. McDiffett. 1975, Some factors affecting primary productivity of stream riffle communities. Archiv fur Hydrobiologie. 75(3): 306-317.

Philipson, G.N. 1954, The effect of water flow and oxygen concentration on six species of caddis fly (Trichoptera) larvae. Proc. Zool. Soc. London. 124: 547-564.

______________. 1969, Some factors affecting the net-spinning of the caddis fly Hydropsyche instabilis Curtis (Trichoptera; Hydorpsychidae). Hydrobiologia. 34(3/4): 369-377.

Radford, D.S. and R. Hartland-Rowe. 1971, A preliminary investigation of bottom fauna and invertebrate drift in an unregulated and a regulated stream in Alberta. J. App. Ecol. 8(3): 883-903.

Sneath, P.H.A. and R.R. Sokal. 1973, Numerical Taxonomy. W.H. Freeman and Co., San Francisco.

Spence, J.A. and H.B.N. Hynes. 1971, Differences in benthos upstream and downstream of an impoundment. J. Fish. Res. Bd. Canada. 28: 35-43.

Stolier, Q.J. 1963, Some limnological effects of Tiber Reservoir on the Marias River, Montana. Mont. Acad. of Sci. 23: 111-137.

Thorup, J. 1966, Substrate type and its value as a basis for the delimination of the bottom fauna communities in running waters. Pymatuning Lab. Ecol. Spec. Pub., No. 4, 59-74.

Trottier, R. 1971, Effect of temperature on the life cycle of Anax junius (Odonata: Aeshnidae) in Canada. Can. Ent. 103(12): 1671-1683.

Trotzky, H.M. and R.W. Gregory. 1974, The effects of water flow manipulation below a hydroelectric power dam on the bottom fauna of the upper Kennebec River, Maine. Tran. Am. Fish. Soc. 103(2): 318-324.

Ulfstrand, S. 1967, Microdistribution of benthic species (Ephemeroptera, Plecoptera, Diptera: Simuliidae) in Lapland streams. Oikos. 18: 293-310.

___________. 1968, Benthic animal communities in Lapland streams. Oikos Supplementum. 10: 120pp.

Van der Schalie, H. and E.G. Berry. 1973, Effects of temperature on growth and reproduction of aquatic snails. Environmental Protection Agency, Ecological Research Series, EPA-R3-021.

Wallace, J.B. 1975a, The larval retreat and food of Arctopsyche; with phylogenetic notes on feeding adaptations in Hydropsychidae larvae (Trichoptera): Ann. Ent. Soc. Am. 68(1): 167-173.

___________. 1975b, Food partitioning in net-spinning Trichoptera larvae: Hydropsyche venularis, Cheumatopsyche etrona, and Macronema zebratum (Hydropsychidae). Ann. Ent. Soc. Am. 68(3): 463-472.

Ward, J.V. 1974, A temperature-stressed stream ecosystem below a hypolimnial release mountain reservoir. Archiv fur Hydrobiologie. 74(2): 247-275.

Waters, T.F. 1962, A method to estimate the production rate of a stream invertebrate. Tran. Am. Fish Soc. 91(3): 243-250.

__________. 1964, Recolonization of denuded stream bottom areas by drift. Trans. Am. Fish. Soc. 93(3): 311-315.

__________. 1965, Interpretation of invertebrate drift in streams. Ecology. 49(1): 75-81.

__________. 1966, Production rate, population density, and drift of a stream invertebrate. Ecology. 47(4): 595-604.

__________. 1972, The drift of stream insects. Ann. Rev. Ent. 17: 253-272.

__________, and R.J. Knapp. 1961, An improved bottom fauna sampler. Trans. Am. Fish. Soc. 90: 225-238.

Wene, G. and F.I. Wickliff. 1940, Modification of a stream bottom and its effect on the insect fauna. Can. Ent. 72: 131-135.

APPENDIX E

HYDROLOGIC CONTOUR MAPS

SPAWNING CRITICAL AREA

1. Flow direction is from left to right.

2. For easier interpretation, depth contours are indicated by vertical typeface. Velocity contours are indicated by slanting typeface.

3. Hatchered areas on contour maps indicate isolated areas of reduced depth or velocity, depending on the type of map.

4. Dashed lines indicate edge of water, either at stream banks or on exposed bars.

Figure E-1: Substrate Map of the Ft. Keogh Spawning Section.

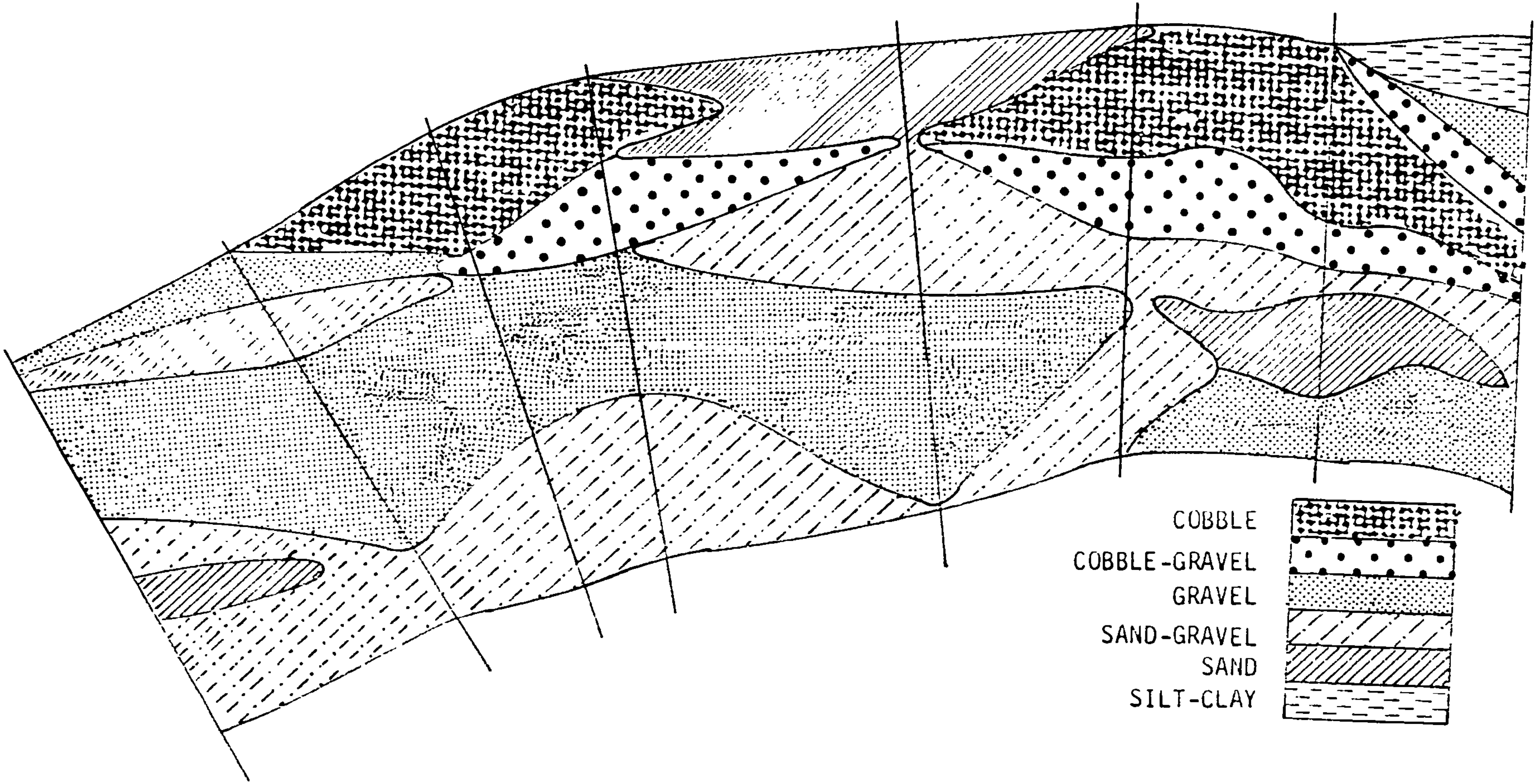

Figure E-2: Velocity Contour Map for the Ft. Keogh Spawning Section, with Velocities in cm./sec.
Discharge: 11.0 cms.

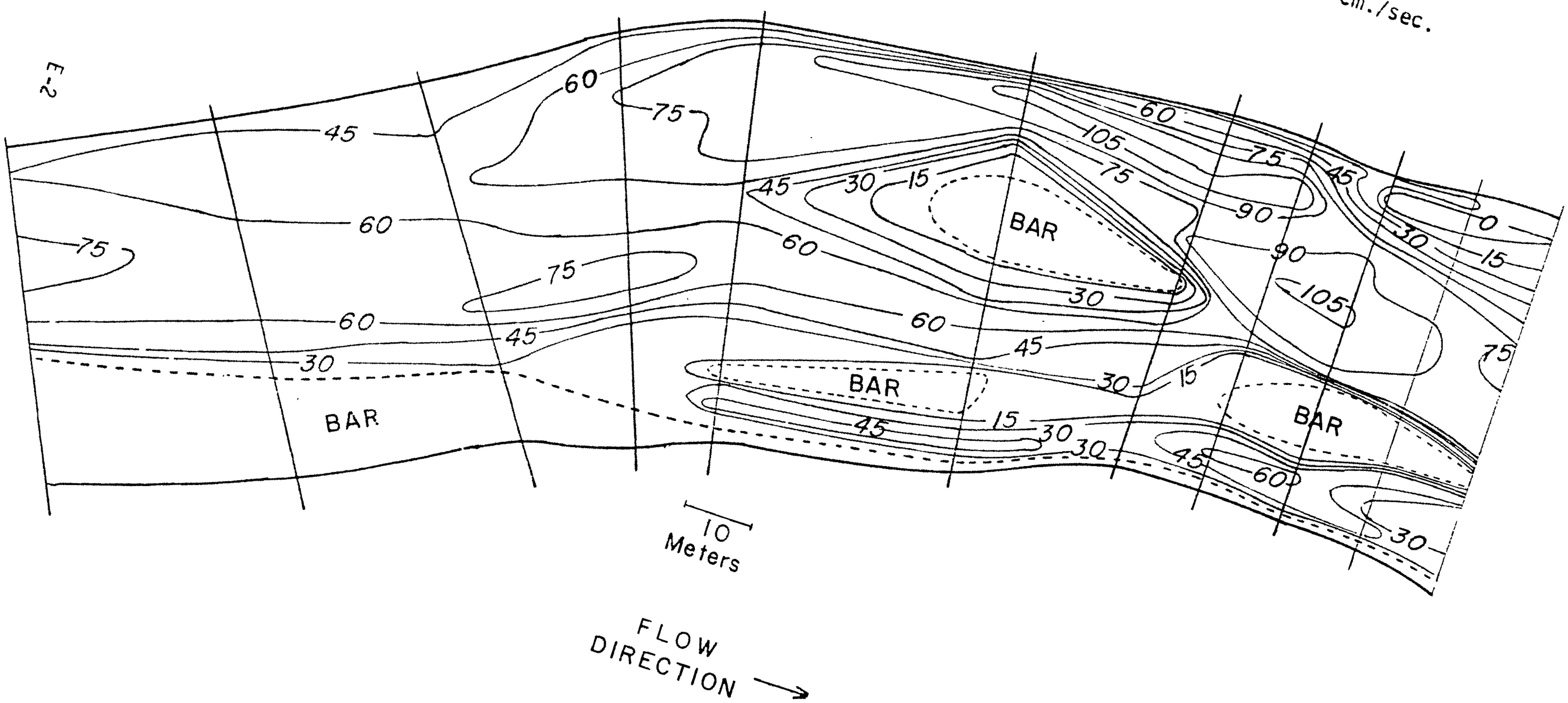

Figure E-3: Depth Contour Map for the Ft. Keogh Spawning Section, with Depths in cm. Discharge: 11.0 cms.

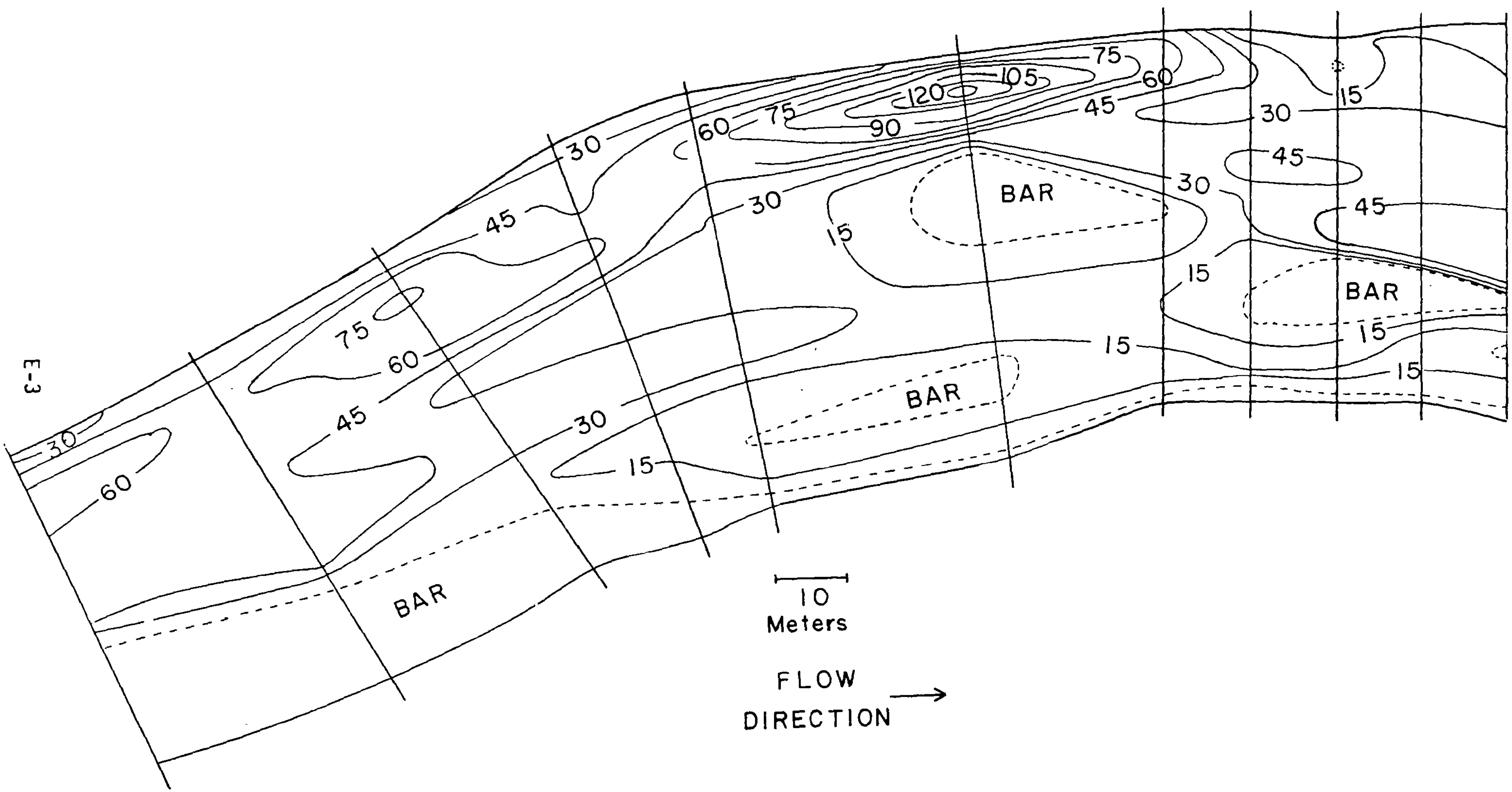

Figure E-4: Velocity Contour Map for the Ft. Keogh Spawning Section, with Velocities in cm./sec.
Discharge: 13.0 cms.

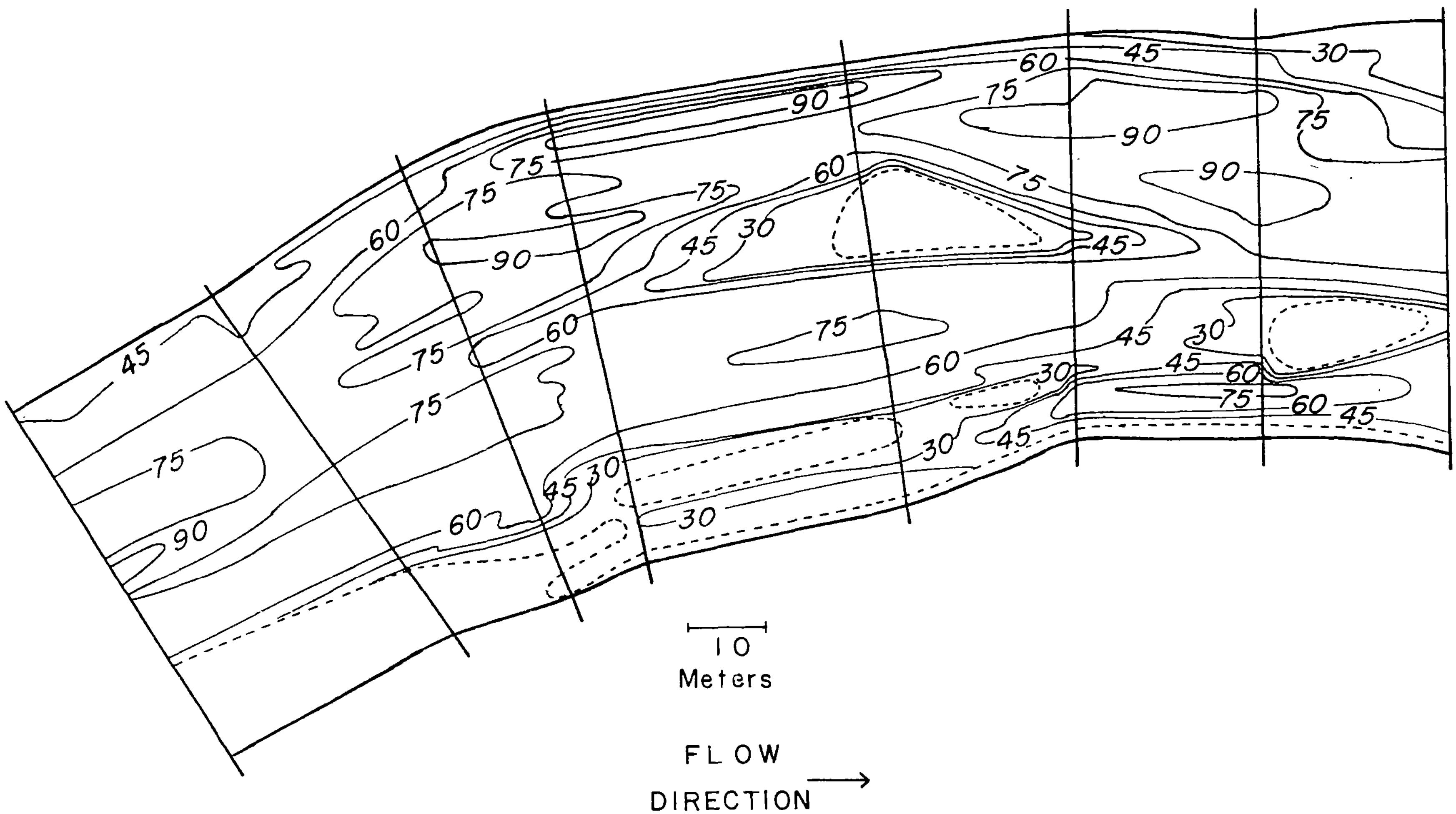

Figure E-5: Depth Contour Map for the Ft. Keogh Spawning Section, with Depths in cm. Discharge: 13.0 cms.

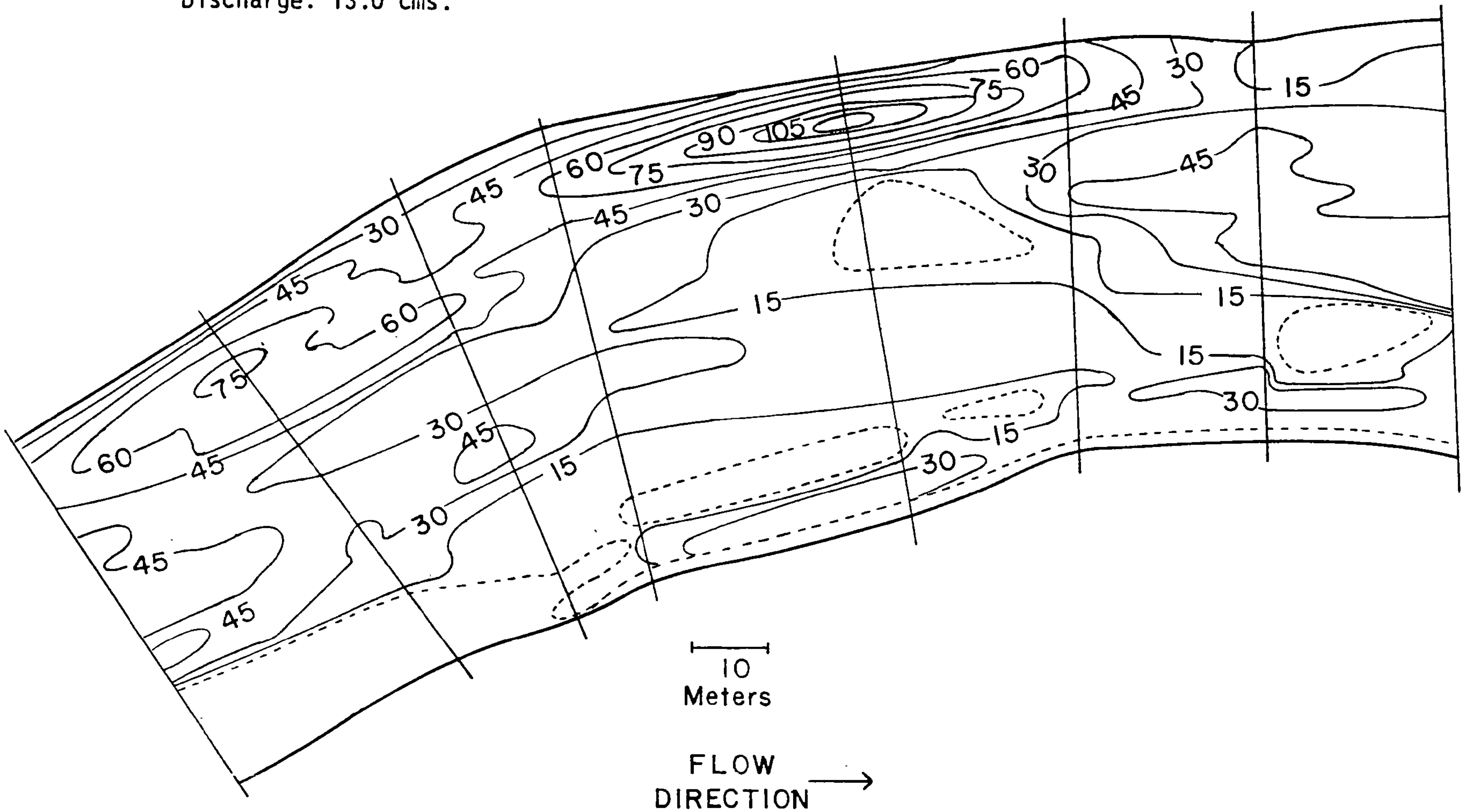

Figure E-6: Velocity Contour Map for the Ft. Keogh Spawning Section, with Velocities in cm./sec.
Discharge: 16.1 cms.

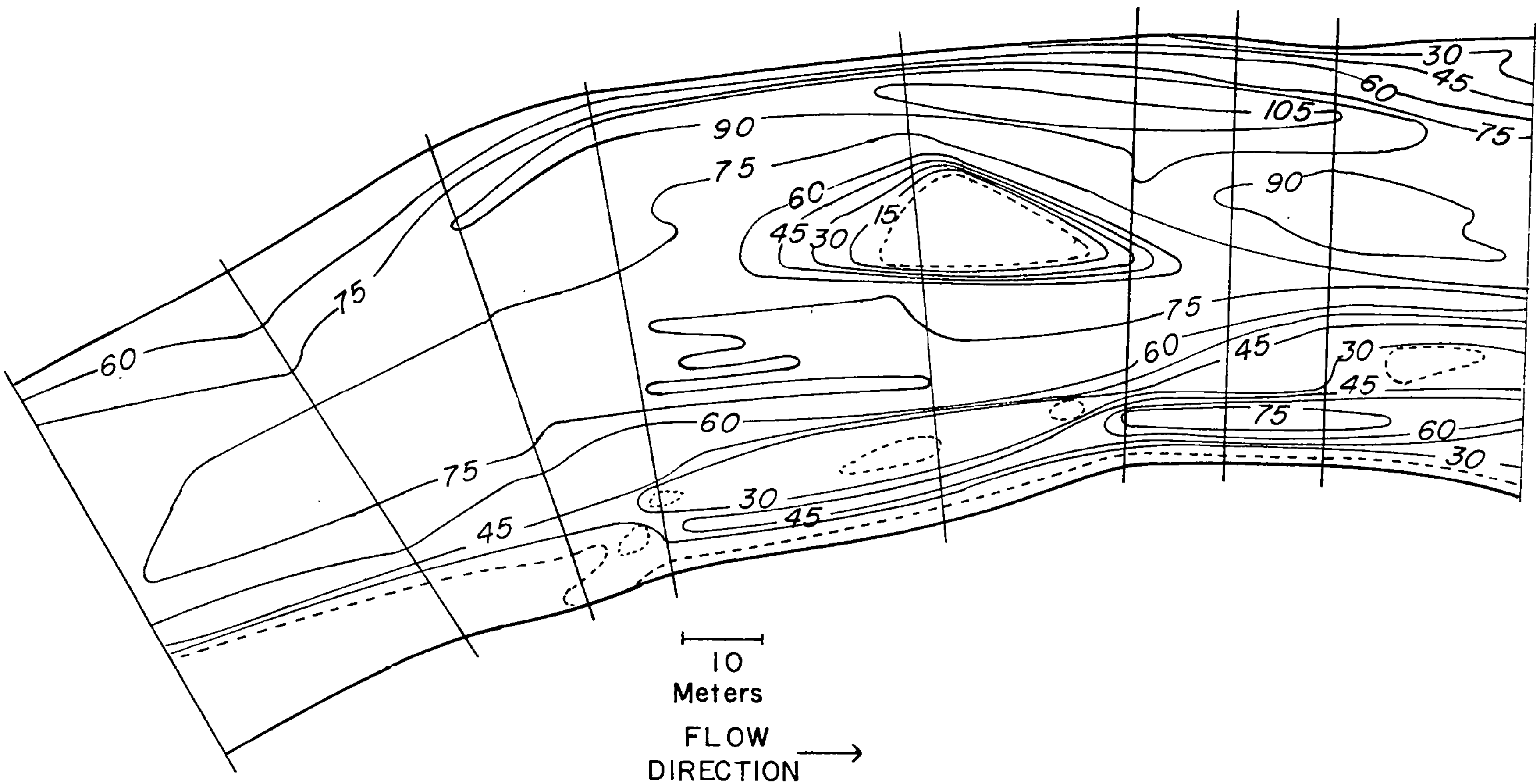

Figure E-7: Depth Contour Map for the Ft. Keogh Spawning Section, with Depths in cm.
Discharge: 16.1 cms.

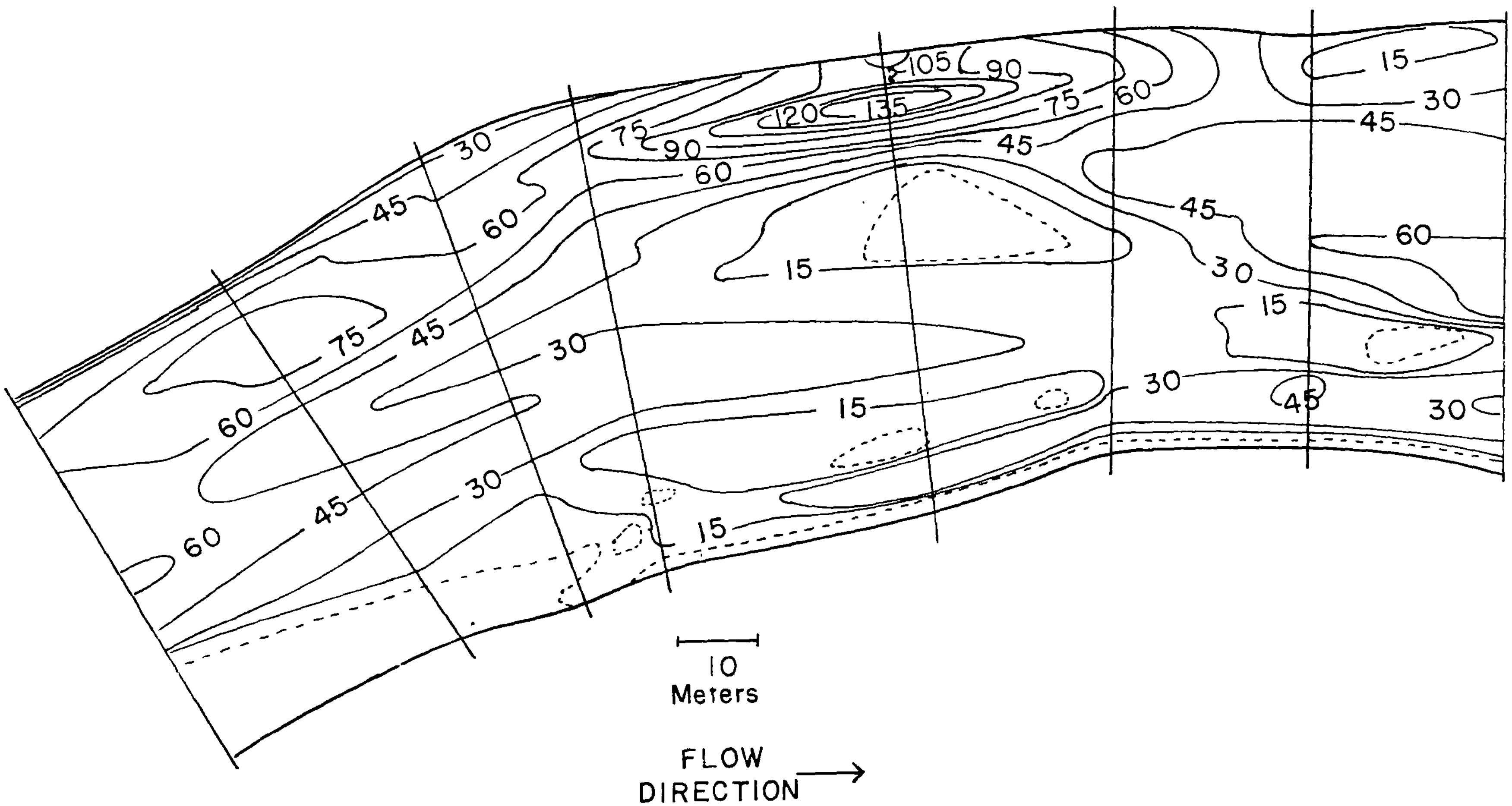

Figure E-8: Velocity Contour Map for the Ft. Keogh Spawning Section, with Velocities in cm./sec.
Discharge: 18.1 cms.

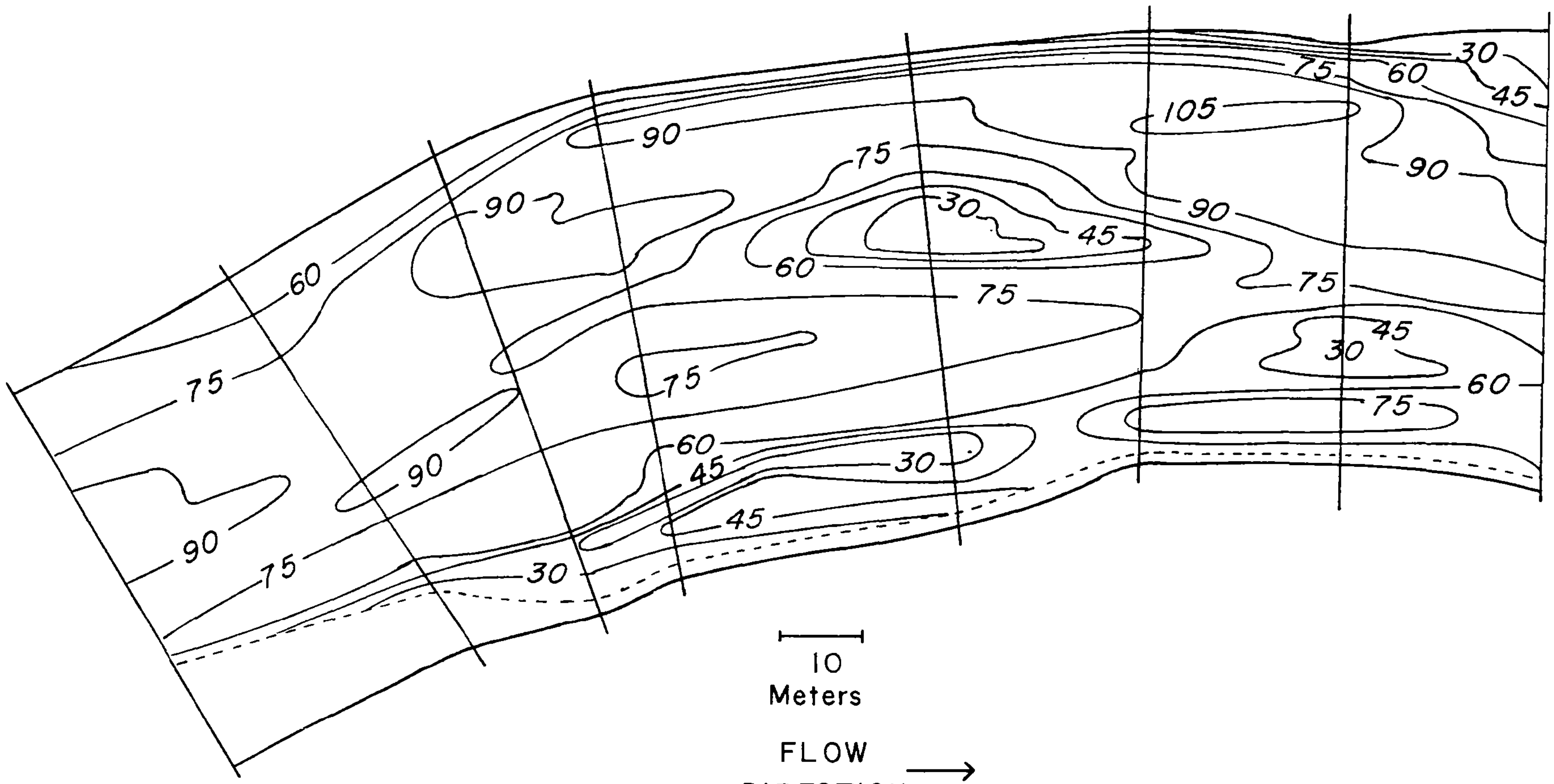

Figure E-9: Depth Contour Map for the Ft. Keogh Spawning Section, with Depths in cm.
Discharge: 18.1 cms.

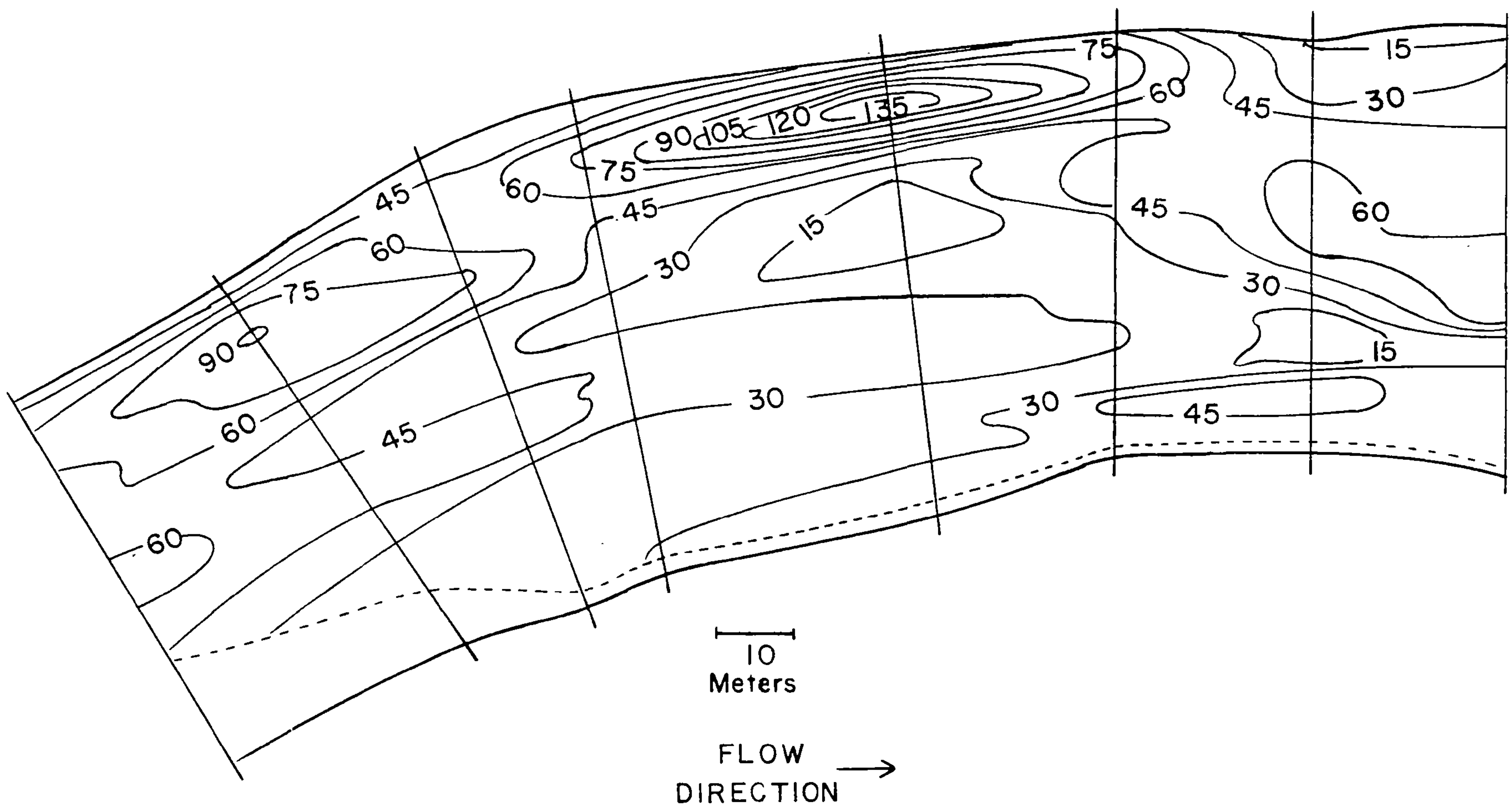

Figure E-10: Velocity Contour Map for the Ft. Keogh Spawning Section, with Velocities in cm./sec. Discharge: 20.2 cms.

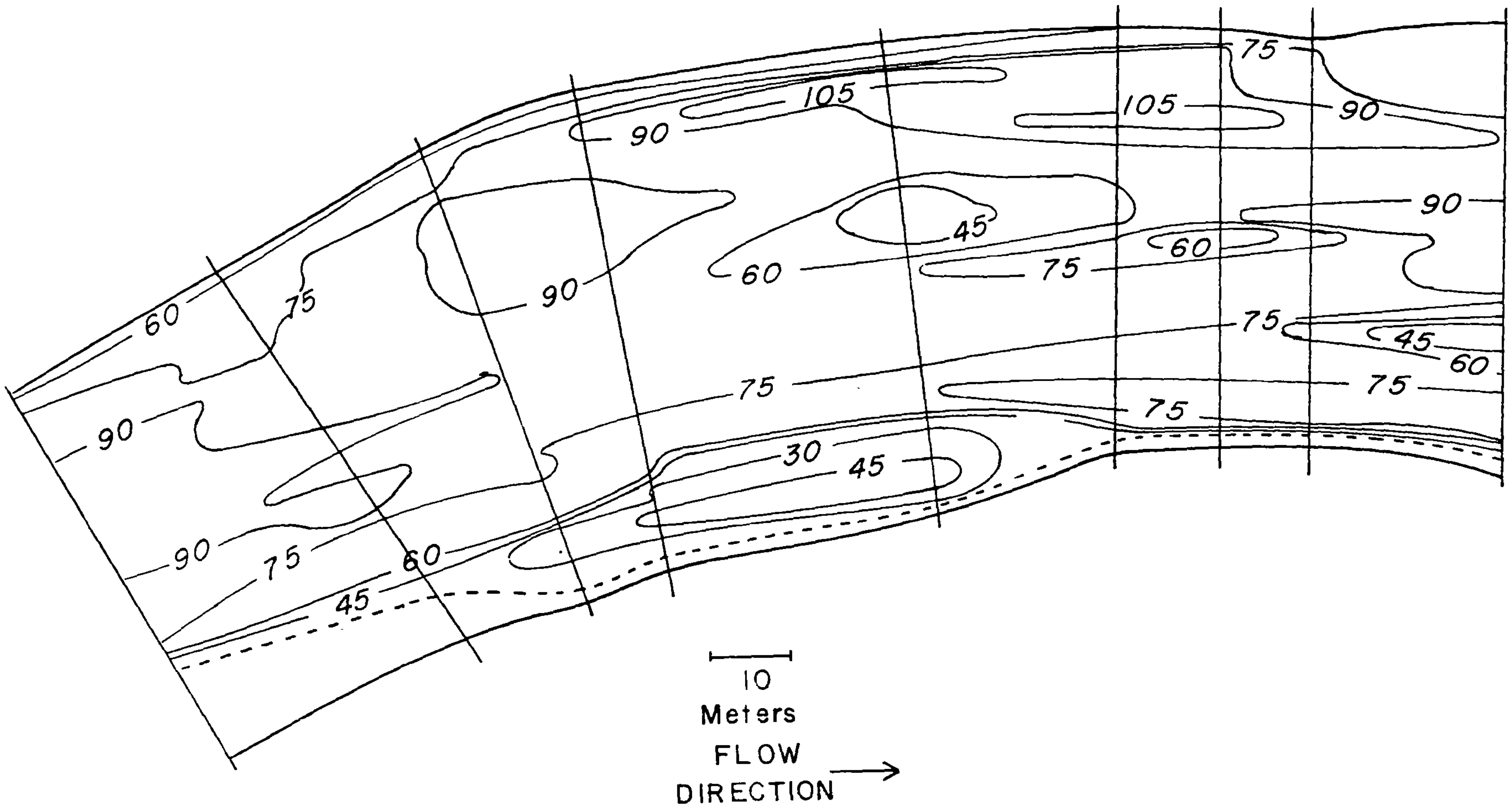

Figure E-11: Depth Contour Map for the Ft. Keogh Spawning Section, with Depths in cm. Discharge: 20.2 cms.

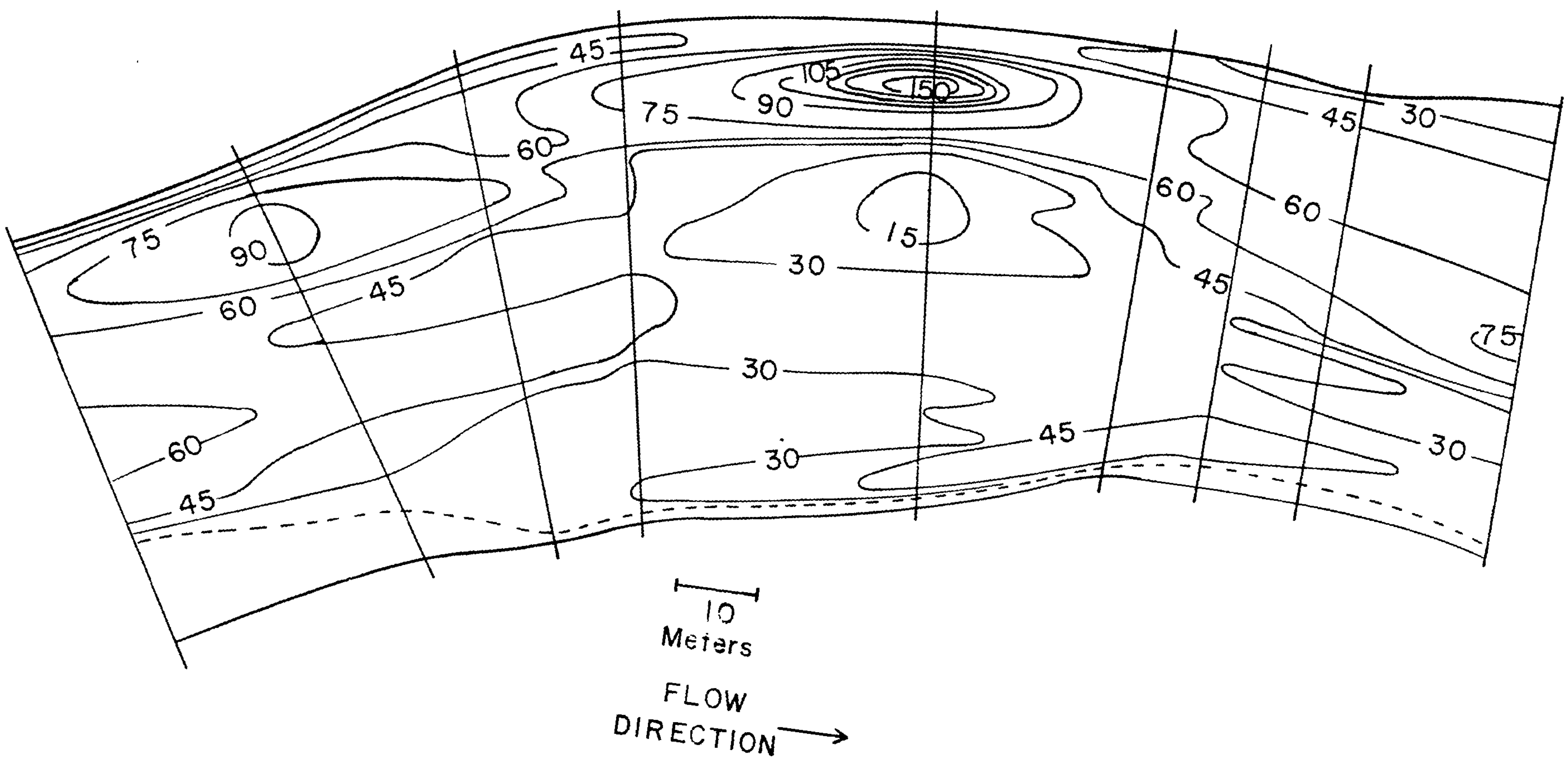

Figure E-12: Velocity Contour Map for the Ft. Keogh Spawning Section, with Velocities in cm./sec. Discharge: 22.5 cms.

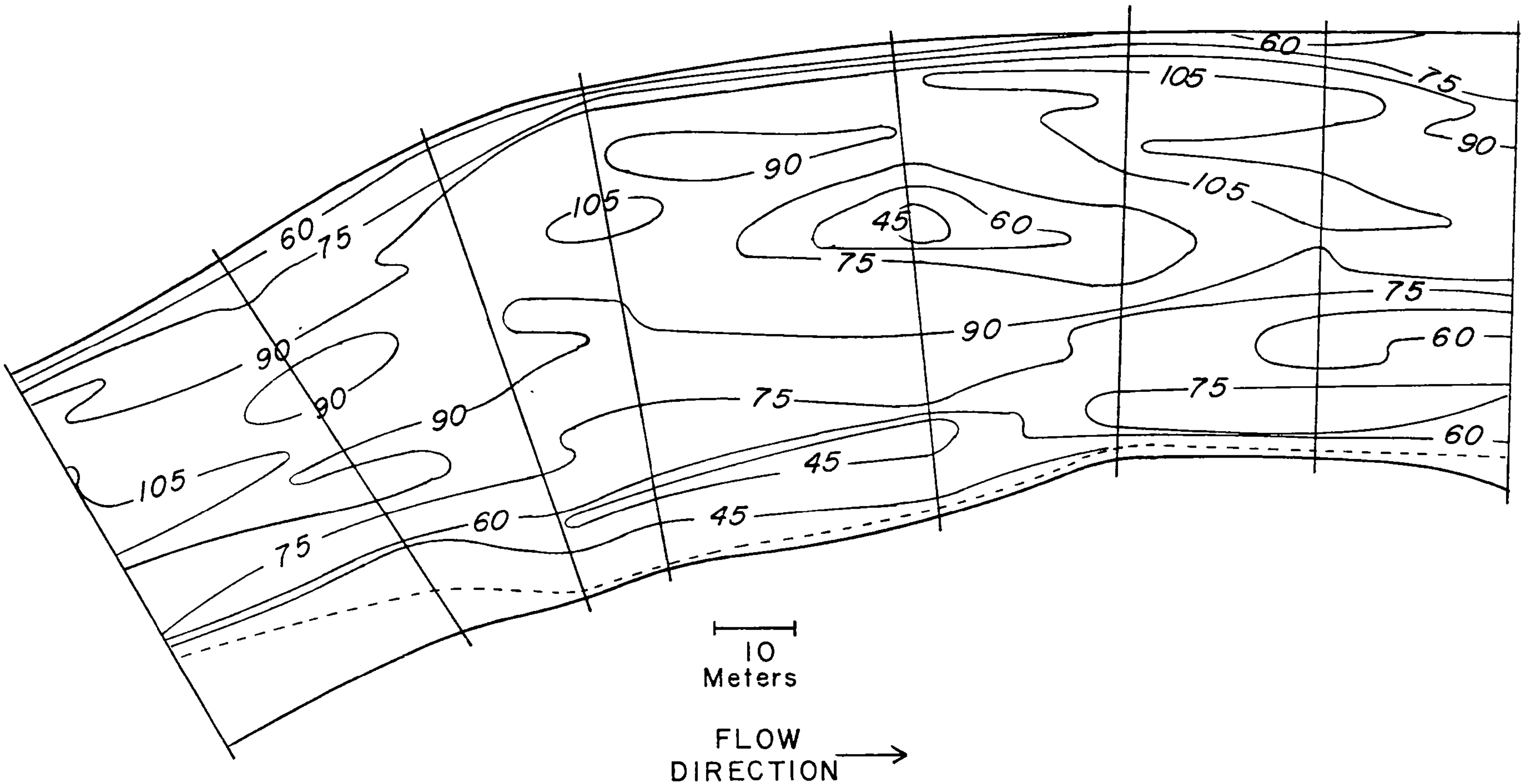

Figure E-13: Depth Contour Map for the Ft. Keogh Spawning Section, with Depths in cm.
Discharge: 22.5 cms.

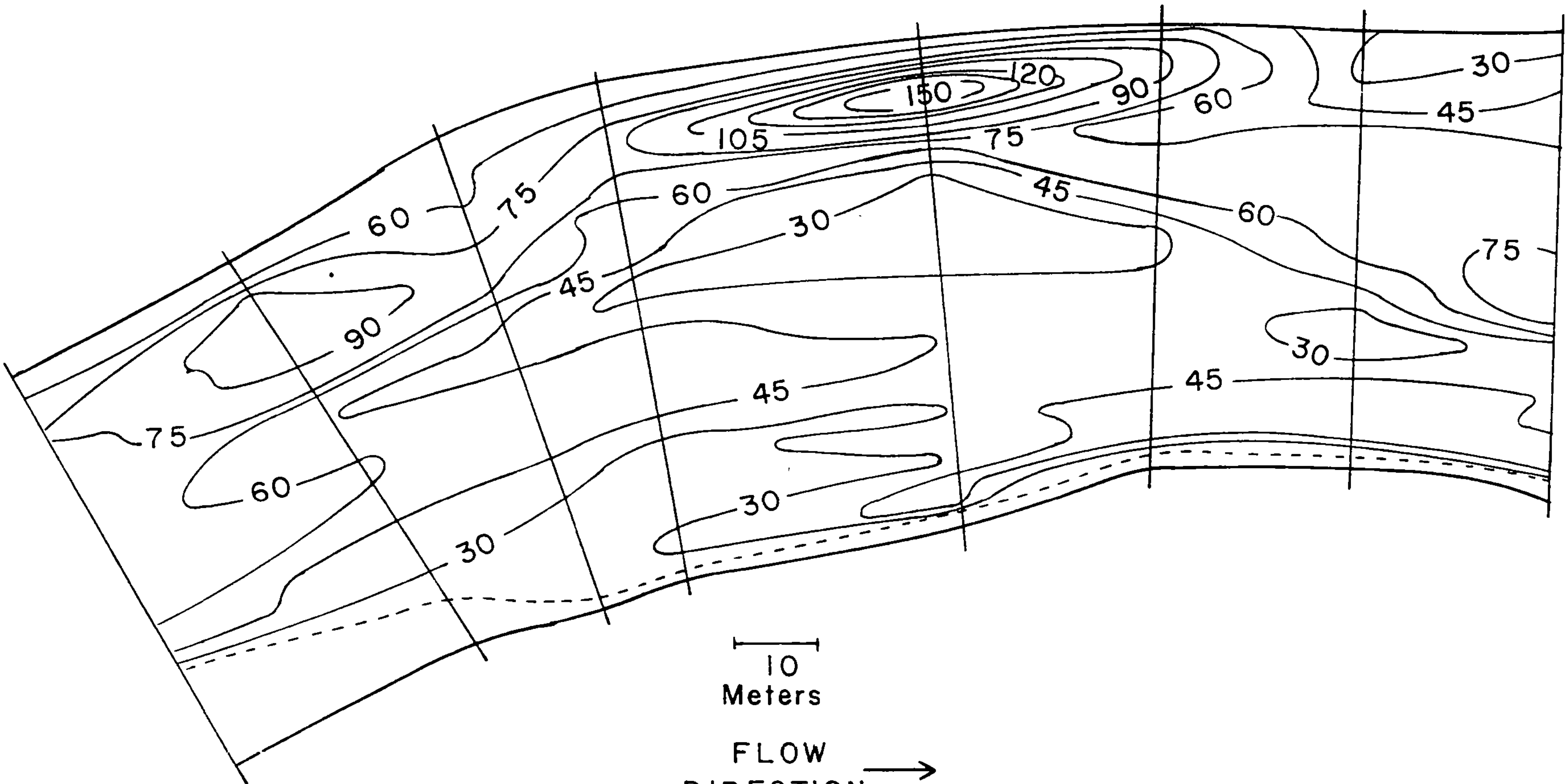

E-14: Velocity Contour Map for the Ft. Keogh Spawning Section, with Velocities in cm./sec.
Discharge: 25.5 cms.

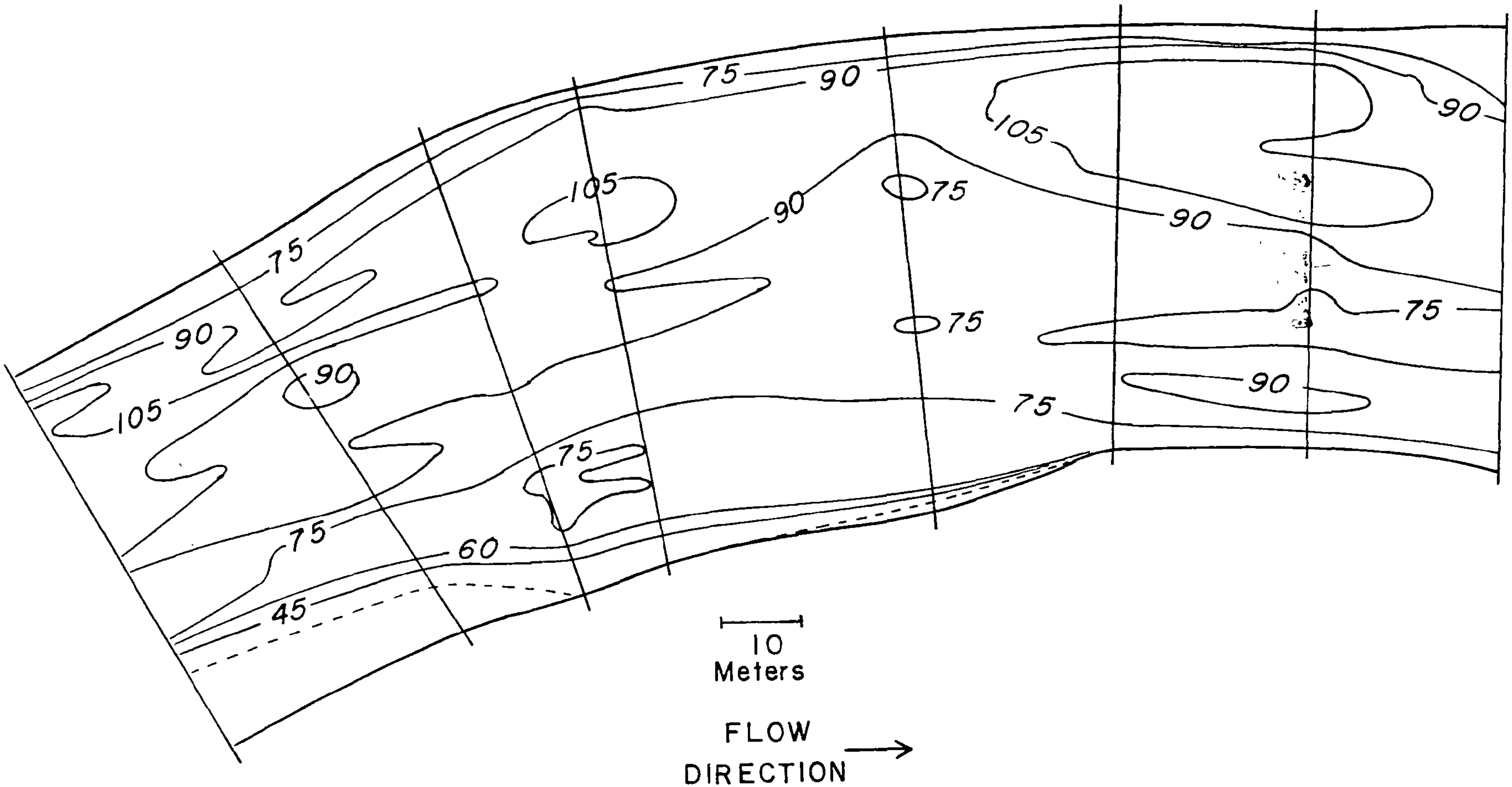

E-14

Figure E-15: Depth Contour Map for the Ft. Keogh Spawning Section, with Depths in cm. Discharge: 25.5 cms.

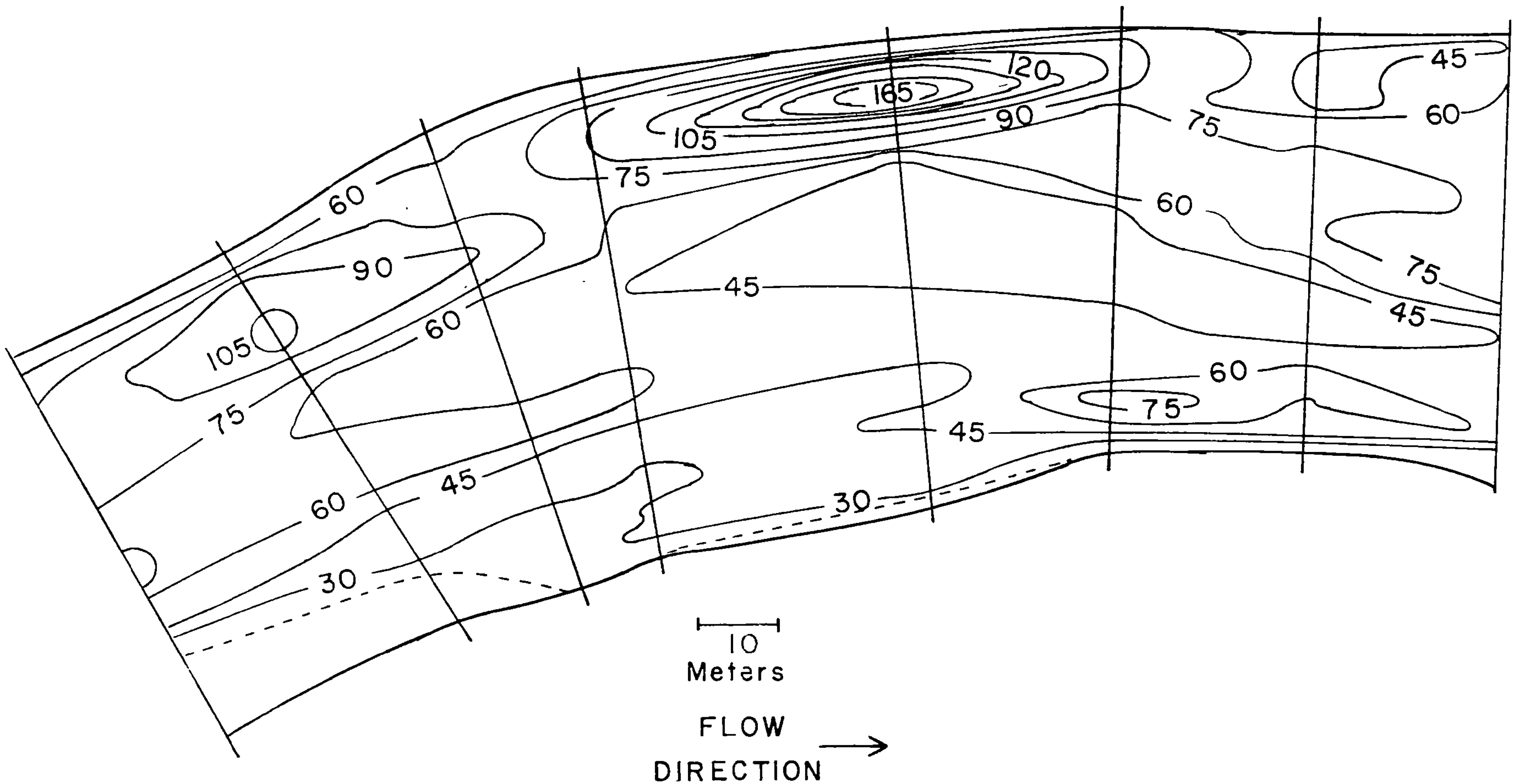

Figure E-16: Velocity Contour Map for the Ft. Keogh Spawning Section, with Velocities in cm./sec.
Discharge: 28.3 cms.

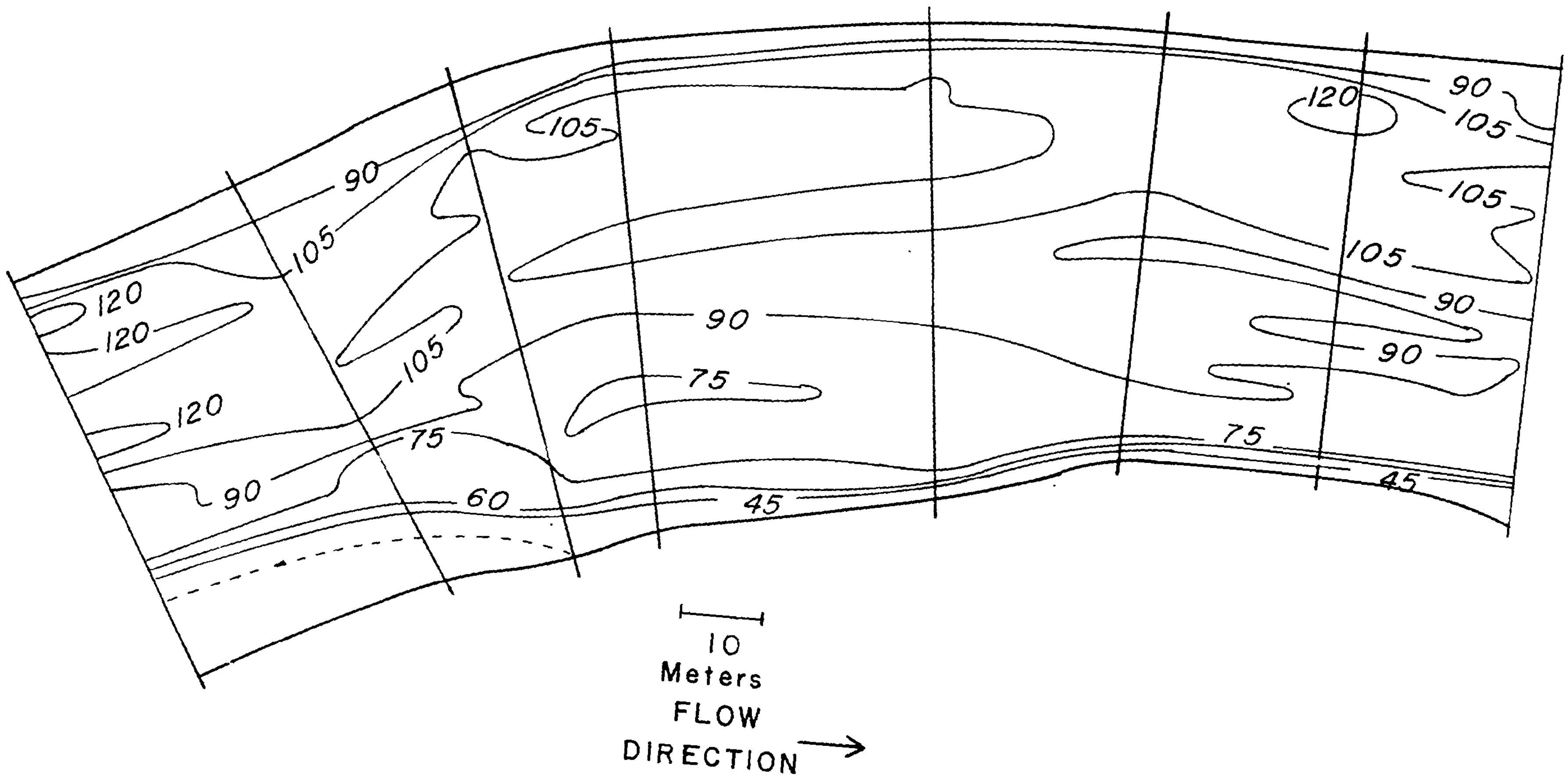

Figure E-17: Depth Contour Map for the Ft. Keogh Spawning Section, with Depths in cm. Discharge: 28.3 cms.

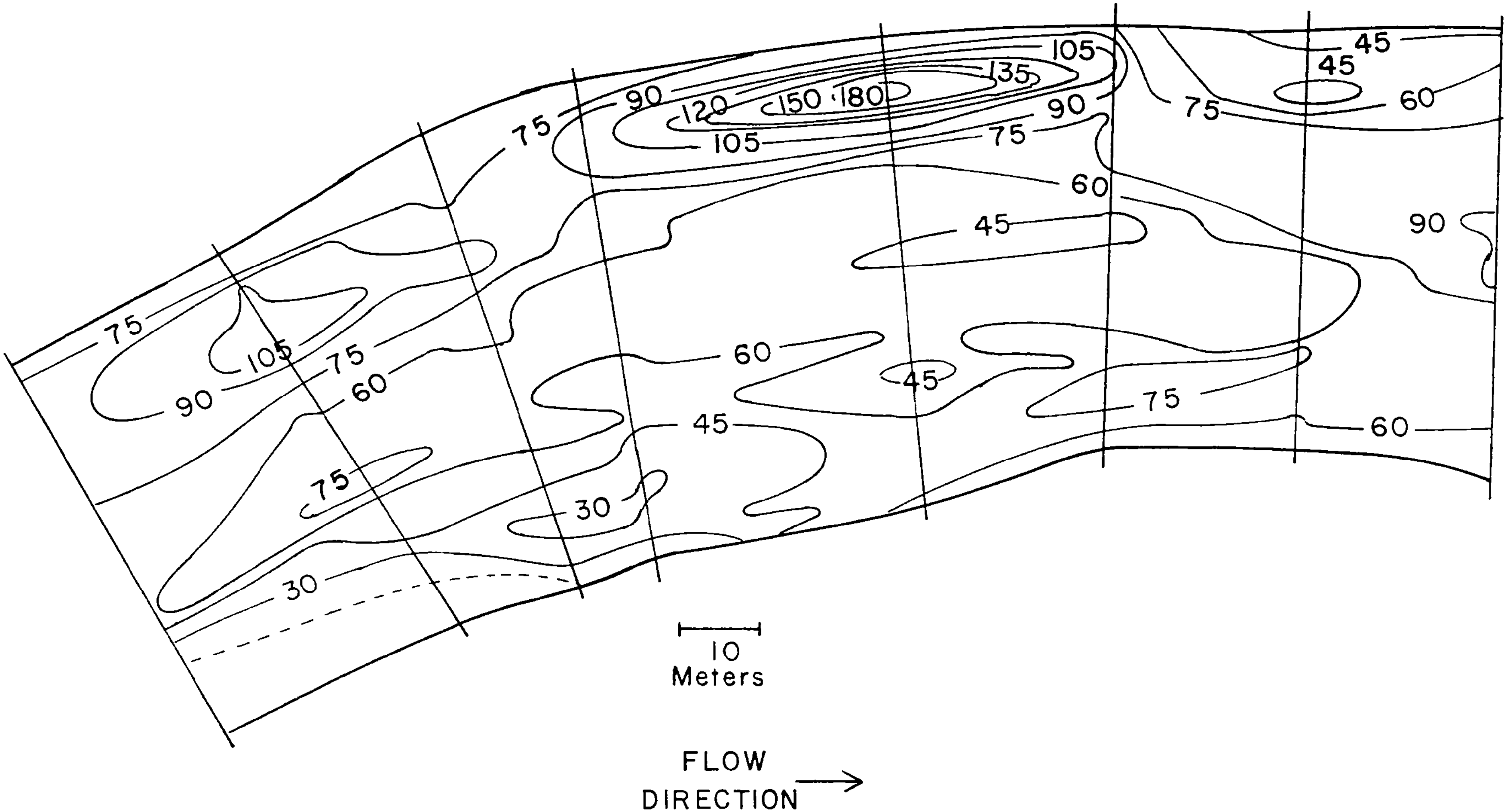

APPENDIX F

COMPOSITE MAPS

SPAWNING CRITICAL AREA

1. Flow direction is from left to right.

2. These maps indicate areas meeting preferred conditions of depth, velocity, and substrate, for spawning shovelnose sturgeon.

3. For easier interpretation, depth contours are indicated by vertical typeface. Velocity contours are indicated by slanting typeface.

4. Cross-hatched areas on composite maps indicate areas which do not meet flow criteria for spawning shovelnose sturgeon. Only those stream areas without cross-hatching meet flow criteria.

5. Dashed lines indicate water's edge, either at stream banks or on exposed bars.

Figure F-1: Composite Map of the Ft. Keogh Spawning Section, Showing Areas Meeting Flow Criteria for Spawning Shovelnose Sturgeon.

Discharge: 11.0 cms.

Area Meeting Criteria: 290 m^2

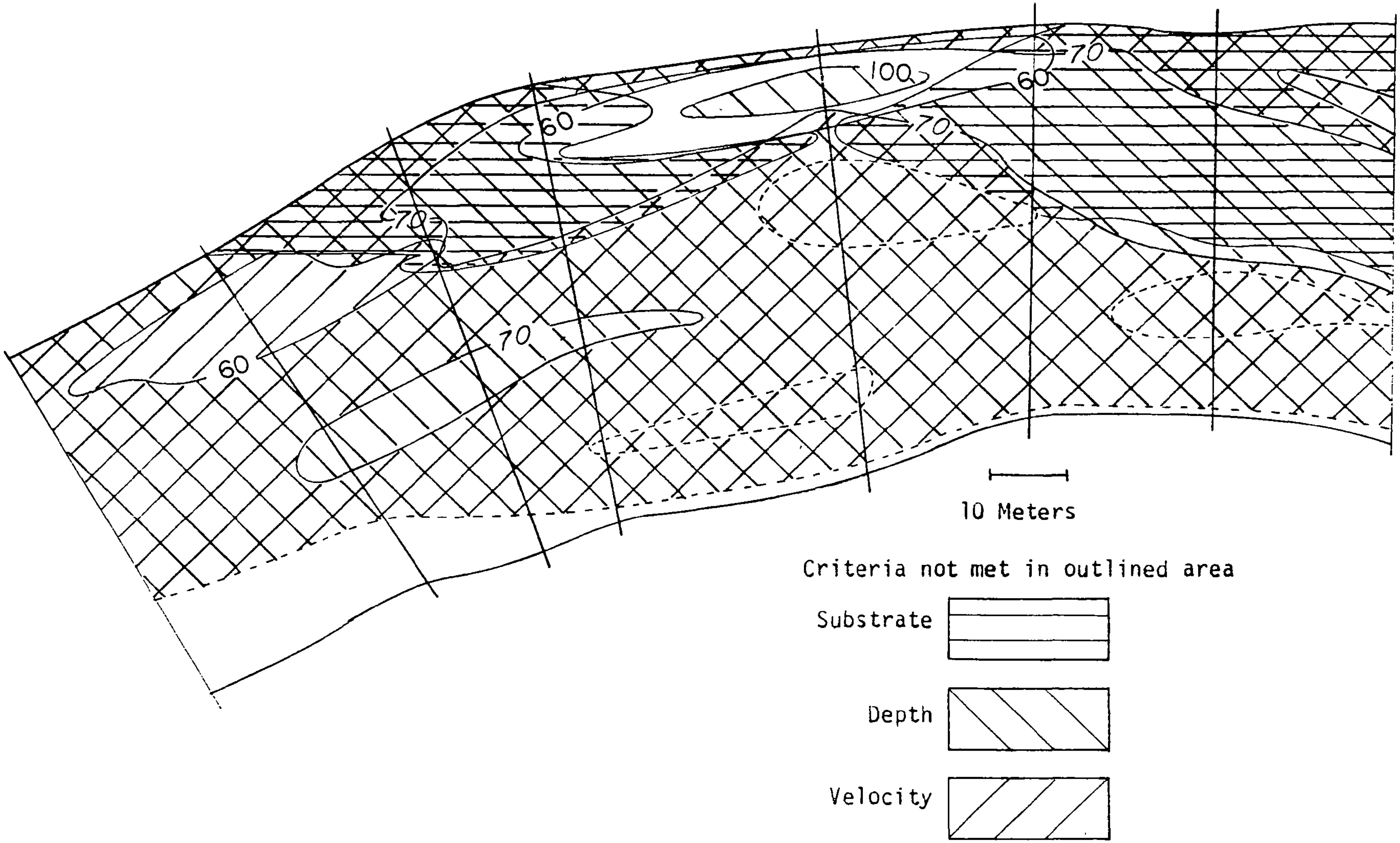

Figure F-2: Composite Map of the Ft. Keogh Spawning Section, Showing Areas Meeting Flow Criteria for Spawning Shovelnose Sturgeon.

Discharge: 13.0 cms.

Area Meeting Criteria: 330 m^2

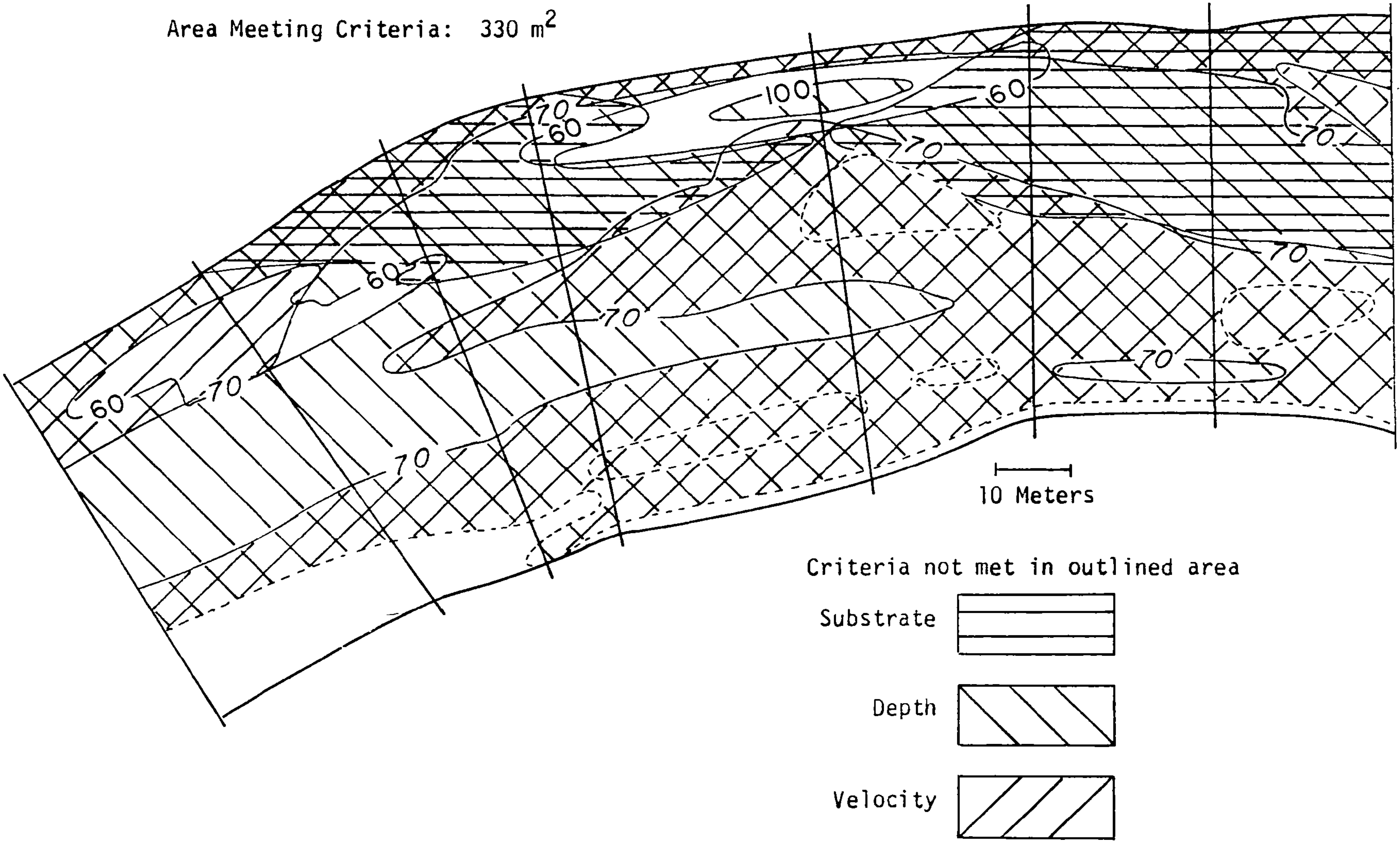

Figure F-3: Composite Map of the Ft. Keogh Spawning Section, Showing Areas Meeting Flow Criteria for Spawning Shovelnose Sturgeon.

Discharge: 16.1 cms.

Area Meeting Criteria: 570 m^2.

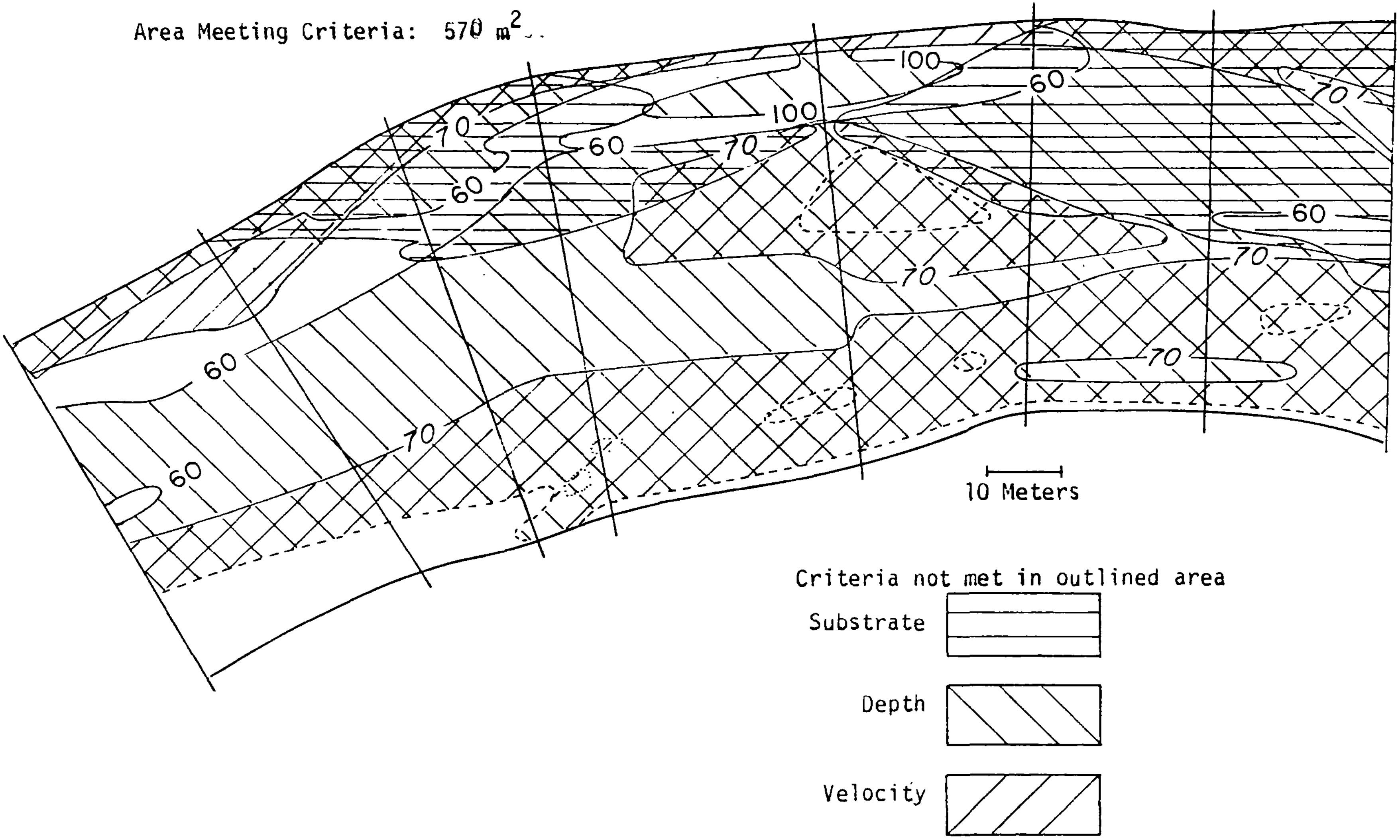

Figure F-4: Composite Map of the Ft. Keogh Spawning Section, Showing Areas Meeting Flow Criteria for Spawning Shovelnose Sturgeon.

Discharge: 18.1 cms.

Area Meeting Criteria: 710 m^2

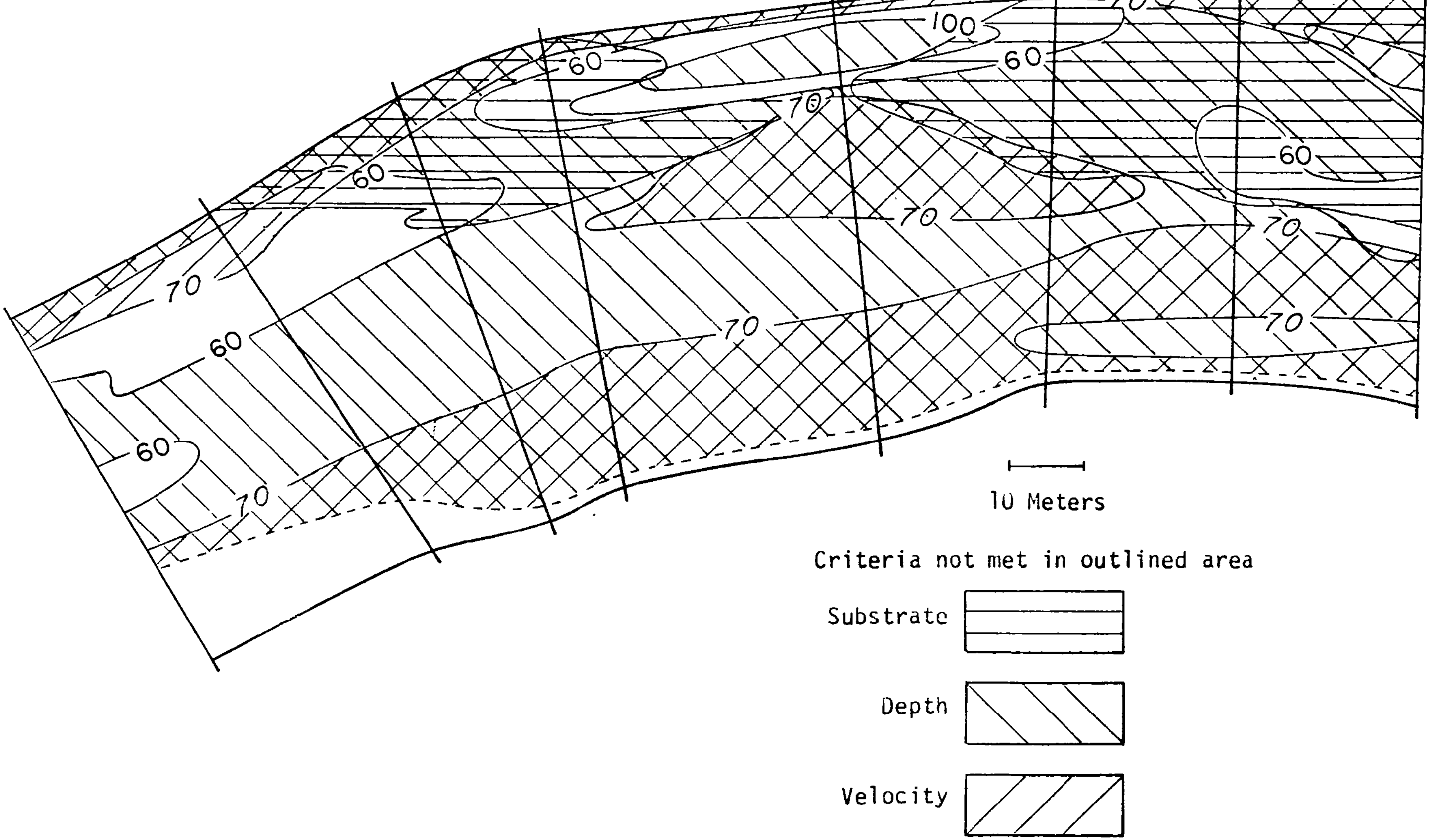

Figure F-5: Composite Map of the Ft. Keogh Spawning Section, Showing Areas Meeting Flow Criteria for Spawning Shovelnose Sturgeon.

Discharge: 20.2 cms

Area Meeting Criteria: 870 m^2

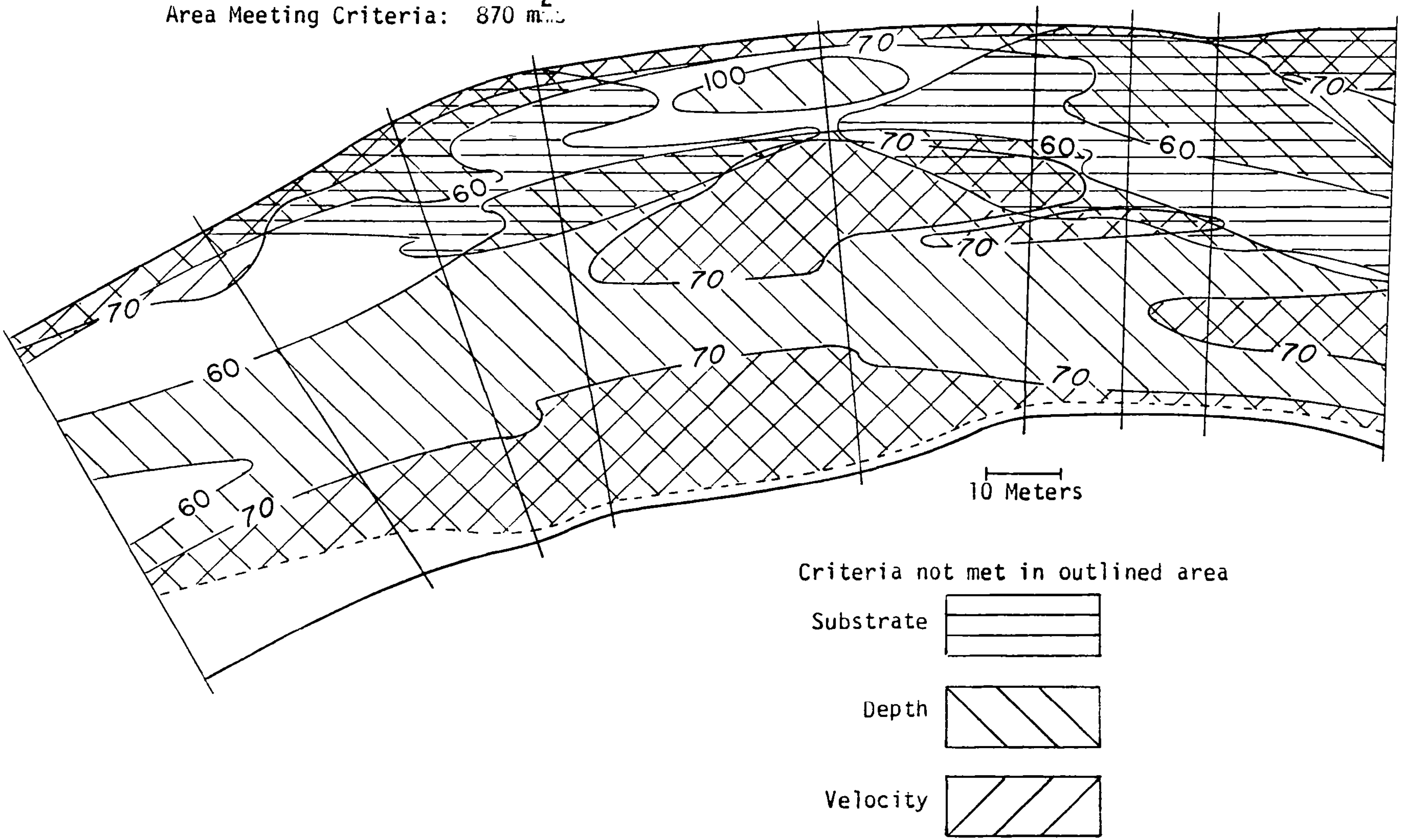

Figure F-6: Composite Map of the Ft. Keogh Spawning Section, Showing Areas Meeting Flow Criteria for Spawning Shovelnose Sturgeon.

Discharge: 22.5 cms.

Area Meeting Criteria: 1320 m^2

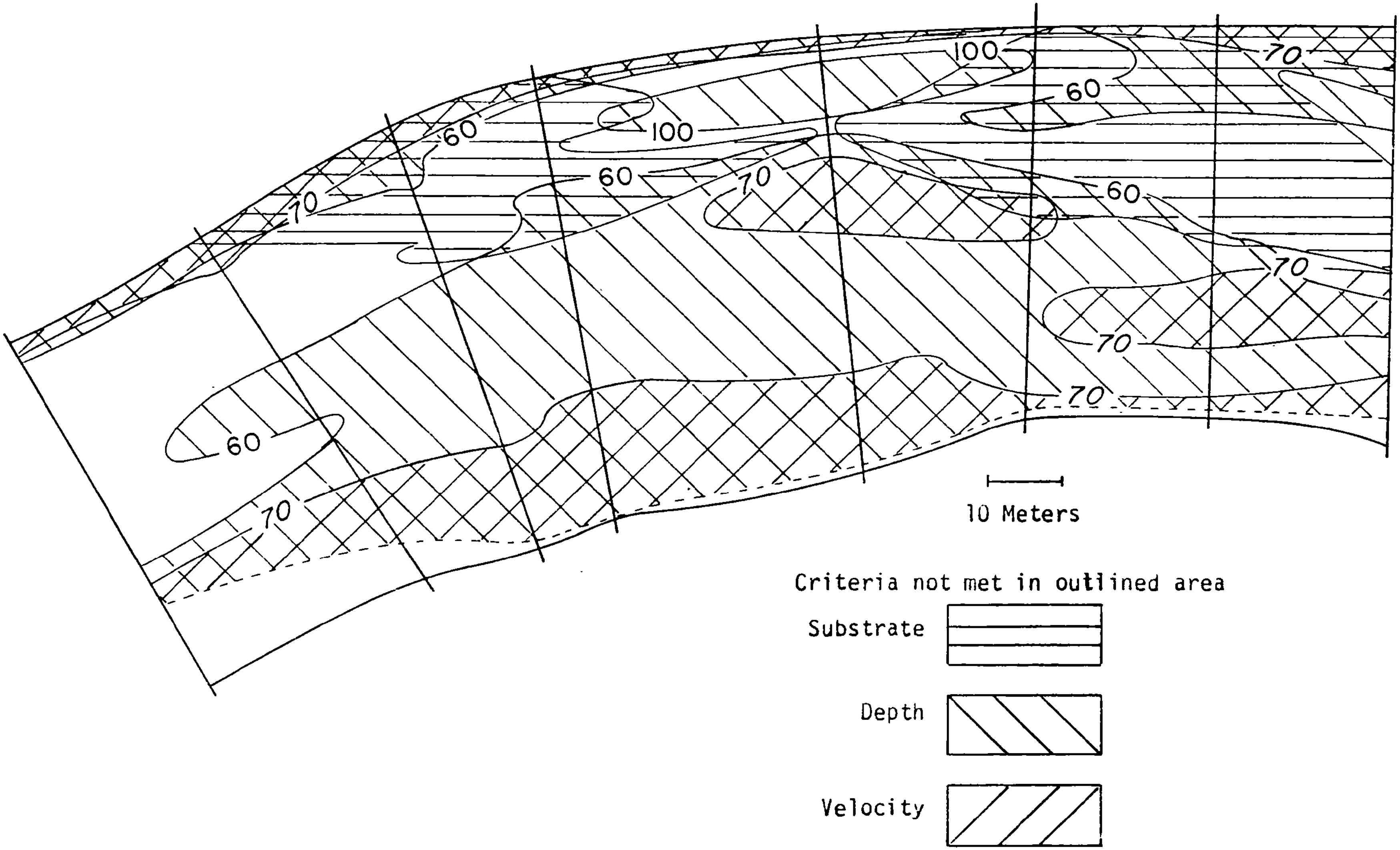

Figure F-7: Composite Map of the Ft. Keogh Spawning Section, Showing Areas Meeting Flow Criteria for Spawning Shovelnose Sturgeon.

Discharge: 25.5 cms.

Area Meeting Criteria: 1940 m^2

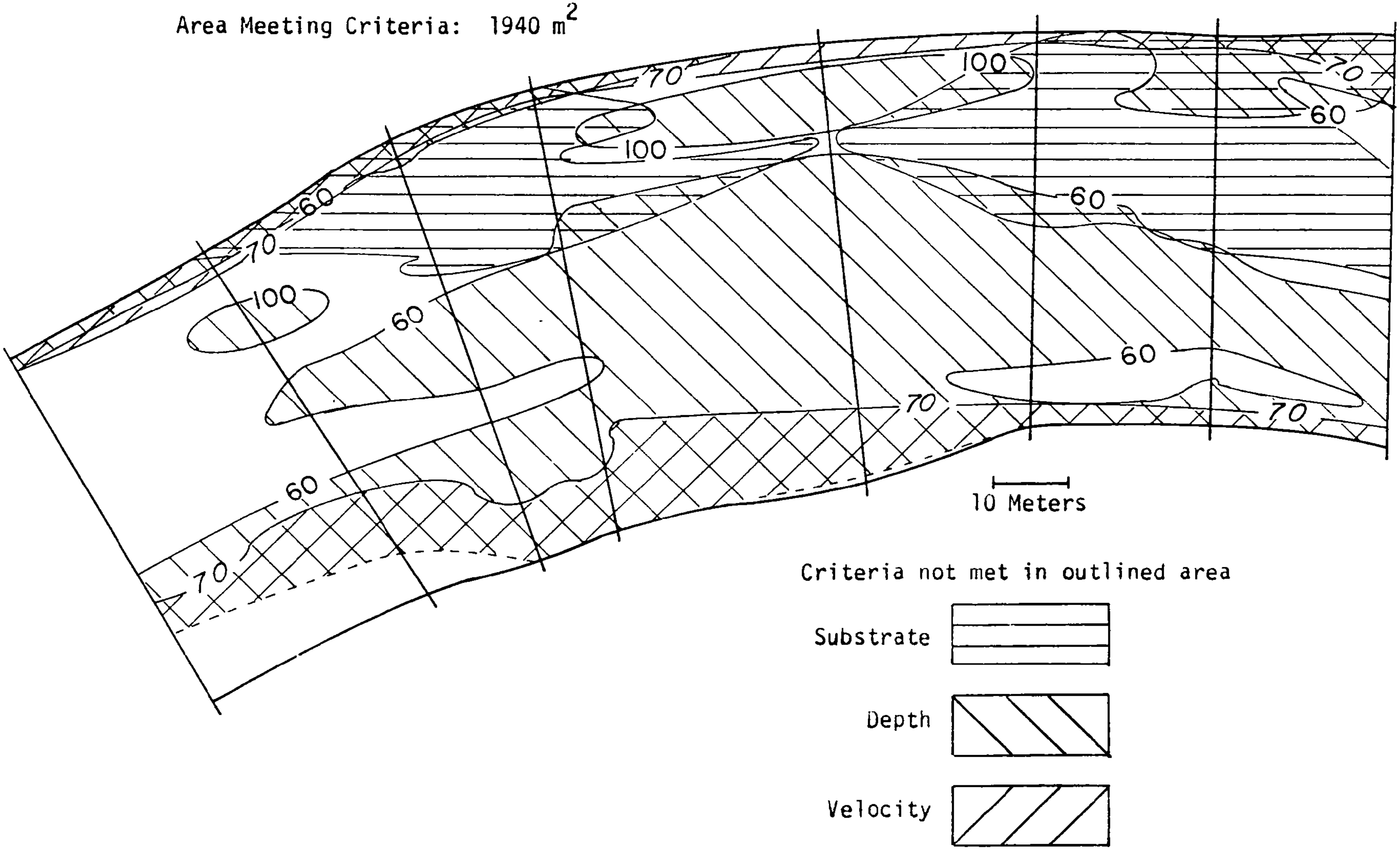

Figure F-8: Composite Map of the Ft. Keogh Spawning Section, Showing Areas Meeting Flow Criteria for Spawning Shovelnose Sturgeon.

Discharge: 28.3 cms.

Area Meeting Criteria: 2470 m^2

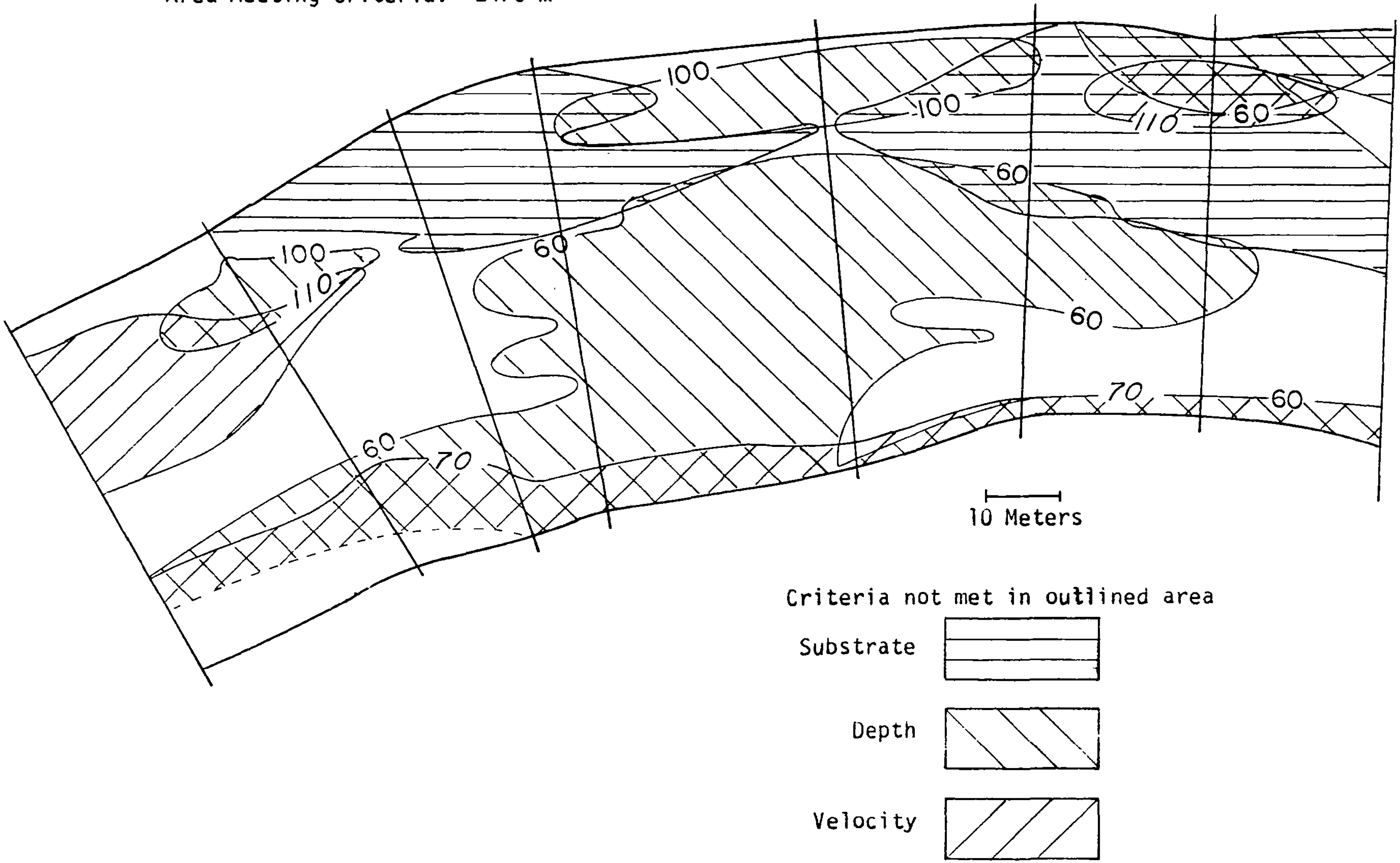

APPENDIX G

HYDROLOGIC CONTOUR MAPS

EXPERIMENTAL CHANNEL SECTION

1. This experimental channel was located in a side channel around a large island in the Viall Ranch section. Flow was manipulated by a diversion structure at the head of the island.

2. Direction of flow is from top of page to bottom.

3. For easier interpretation, depth contours are indicated by vertical typeface. Velocity contours are indicated by slanting typeface.

4. Hatchered areas on contour maps indicate isolated areas of reduced depth of velocity, depending on the type of map.

5. Dashed lines indicate edge of water, either at stream banks or on exposed bars.

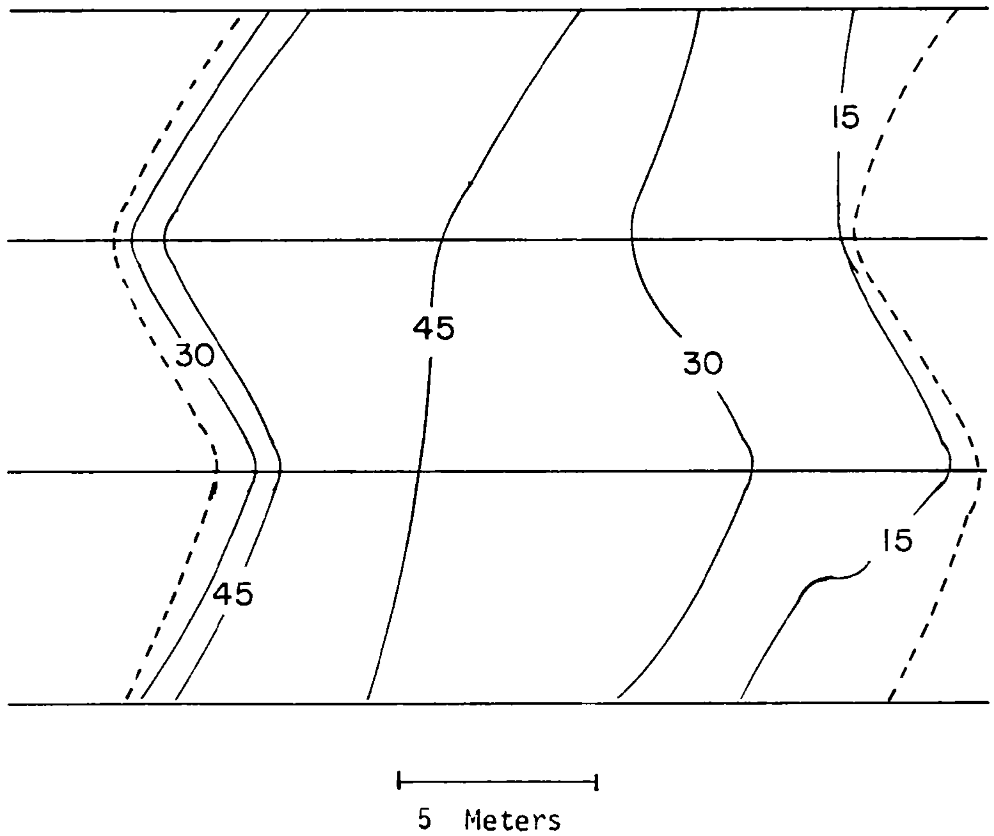

Figure G-1: Depth Contour Map for Riffle #1 of the Experimental Channel Section. Depths in cm.
Experimental Discharge: 4.70 cms.

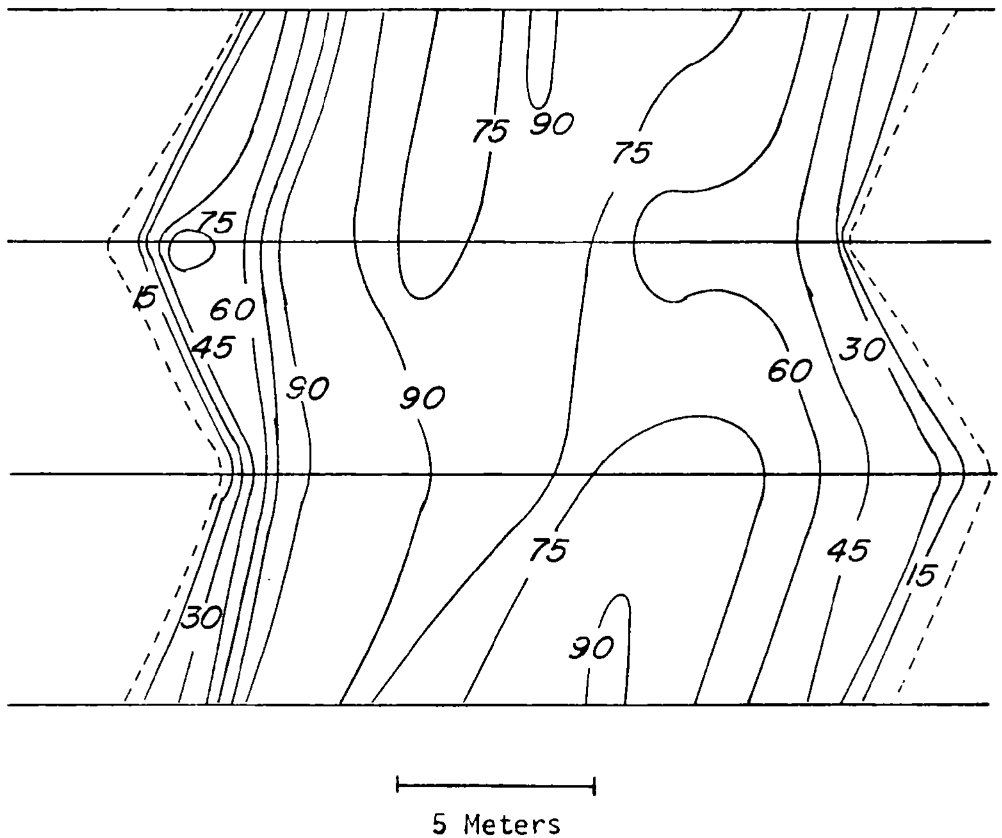

Figure G-2: Velocity Contour Map for Riffle #1 of the Experimental Channel Section. Velocities in cm./sec. Experimental Discharge: 4.70 cms.

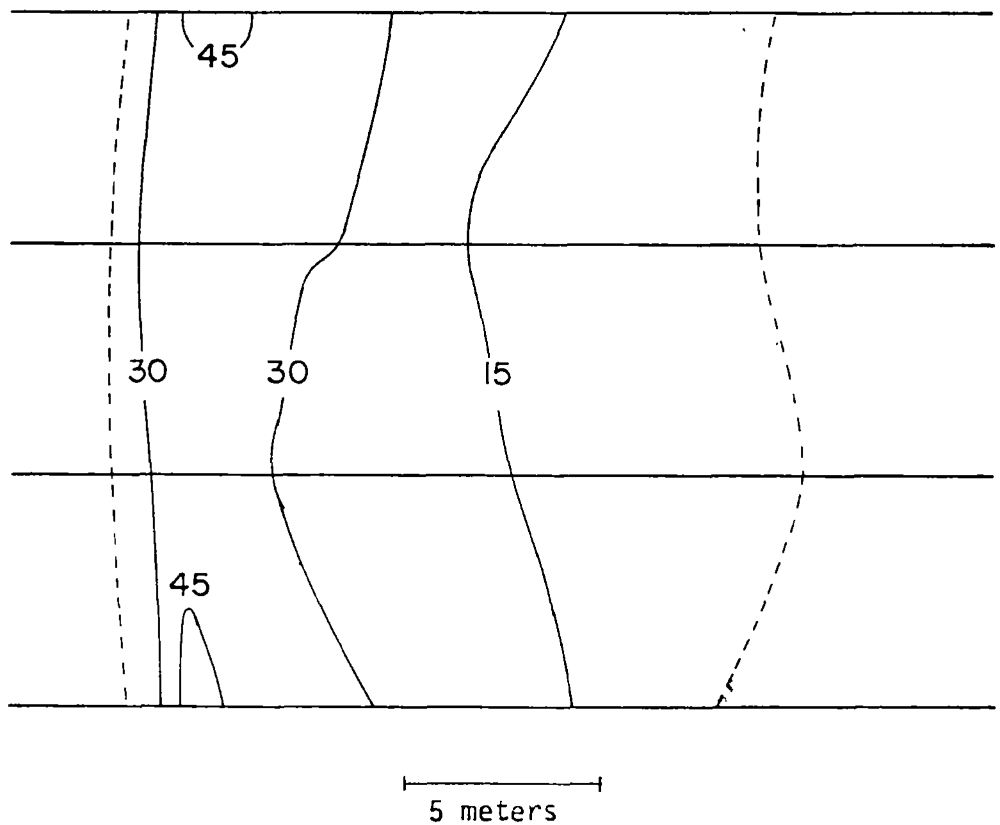

Figure G-3: Depth Contour Map for Riffle #1 of the Experimental Channel Section. Depths in cm. Experimental Discharge: 2.12 cms.

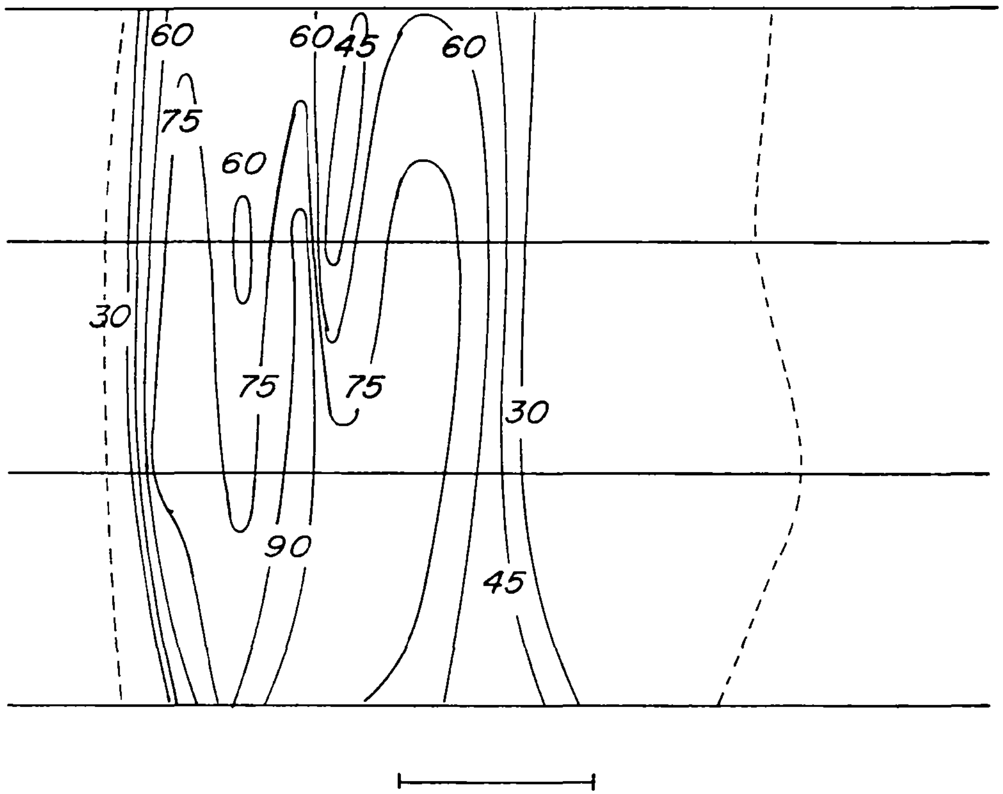

Figure G-4: Velocity Contour Map for Riffle #1 of the Experimental Channel Section. Velocities in cm./sec. Experimental Discharge: 2.12 cms.

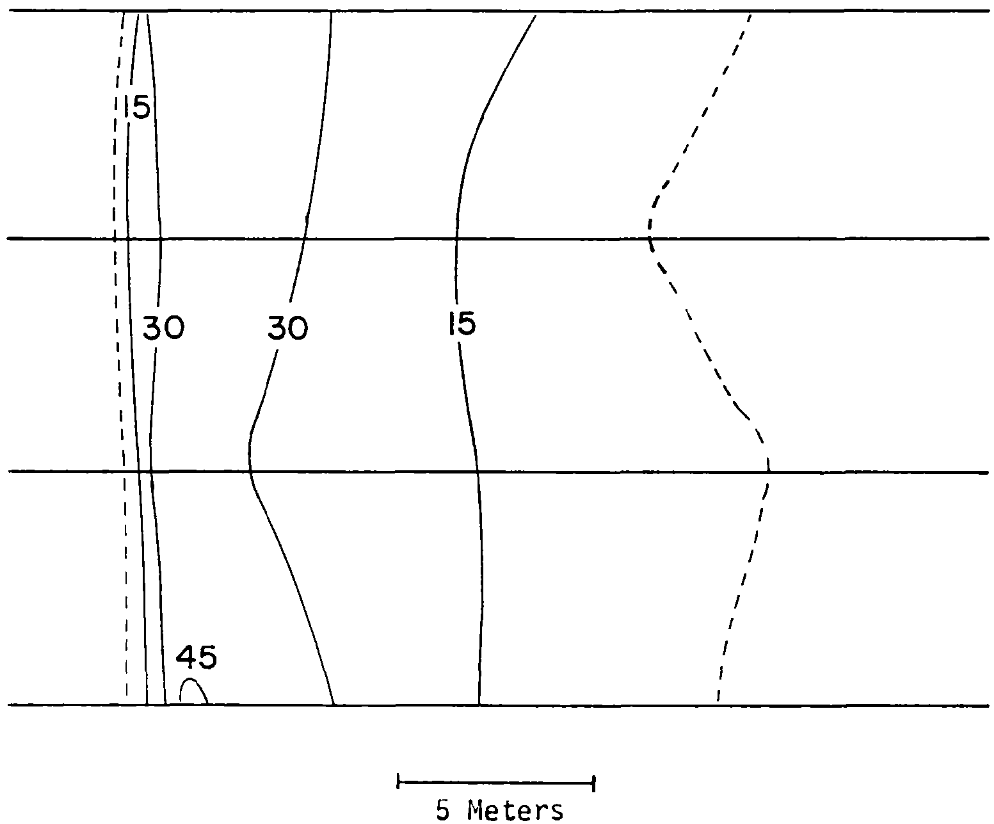

Figure G-5: Depth Contour Map for Riffle #1 of the Experimental Channel Section. Depths in cm. Experimental Discharge: 1.58 cms.

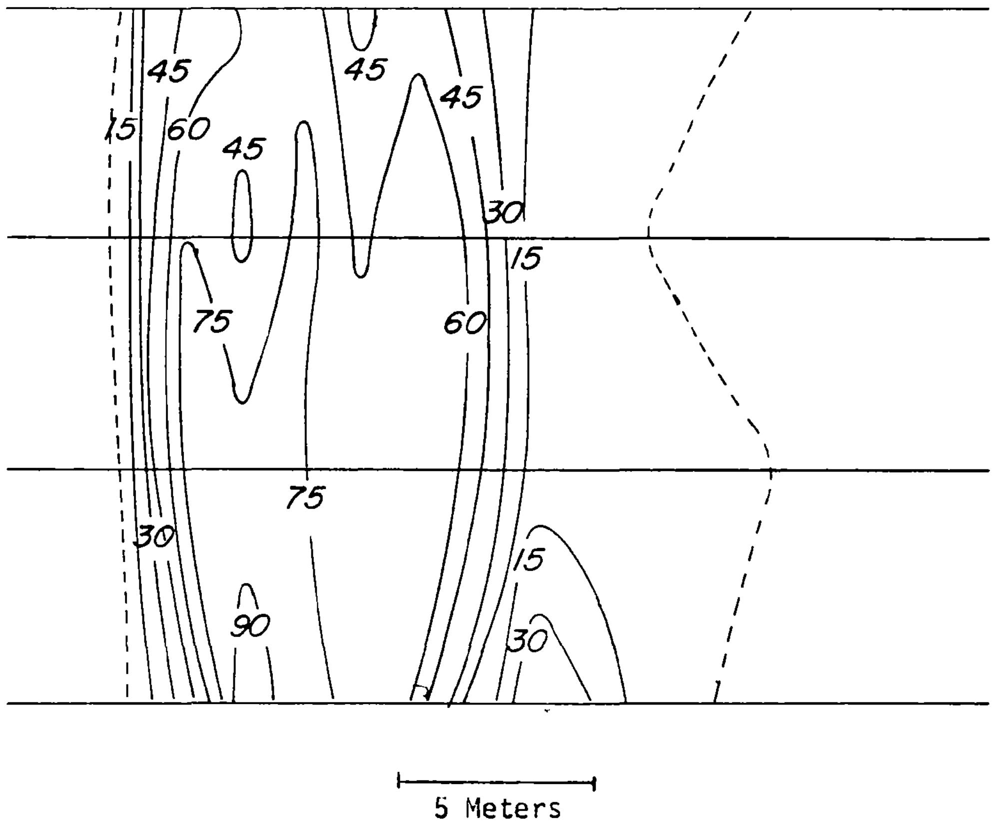

Figure G-6: Velocity Contour Map for Riffle #1 of the Experimental Channel Section. Velocities in cm./sec. Experimental Discharge: 1.58 cms.

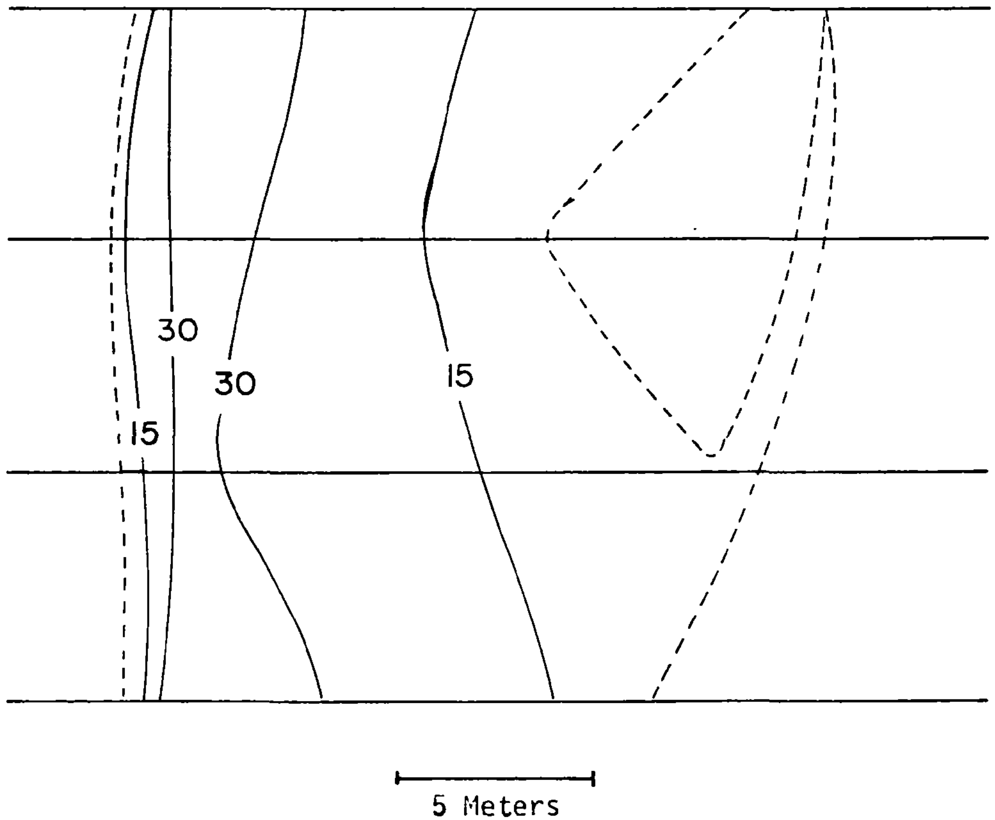

Figure G-7: Depth Contour Map for Riffle #1 of the Experimental Channel Section. Depths in cm. Experimental Discharge: 1.27 cms.

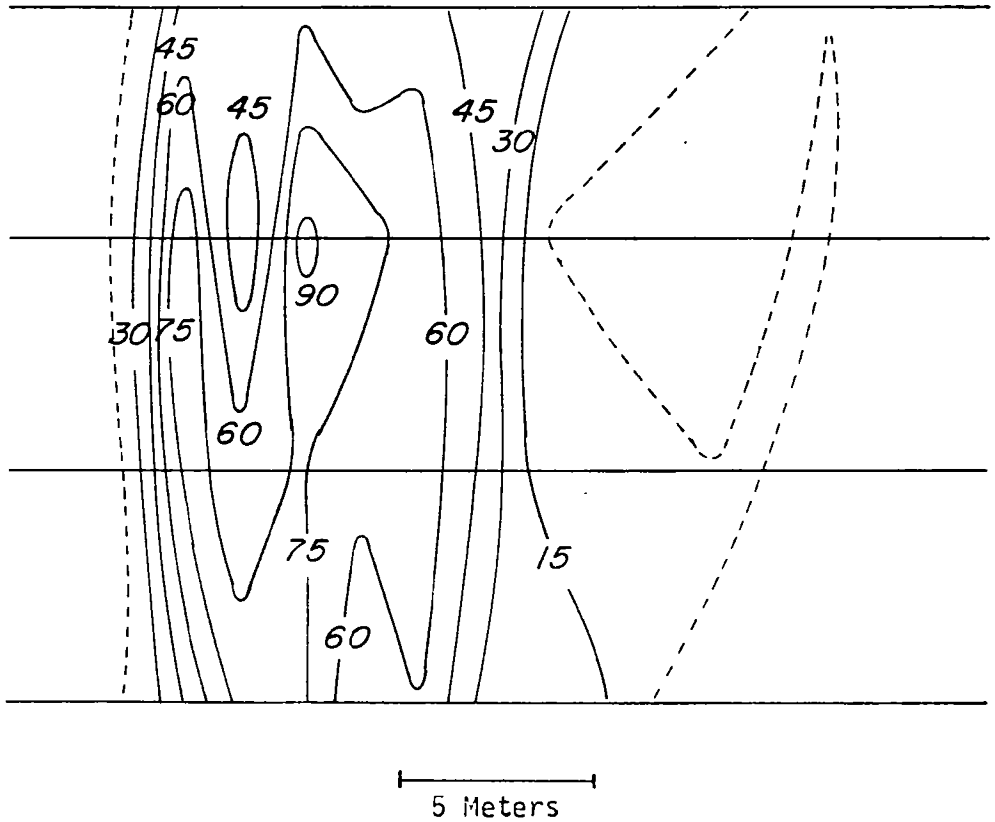

Figure G-8: Velocity Contour Map for Riffle #1 of the Experimental Channel Section. Velocities in cm./sec. Experimental Discharge: 1.27 cms.

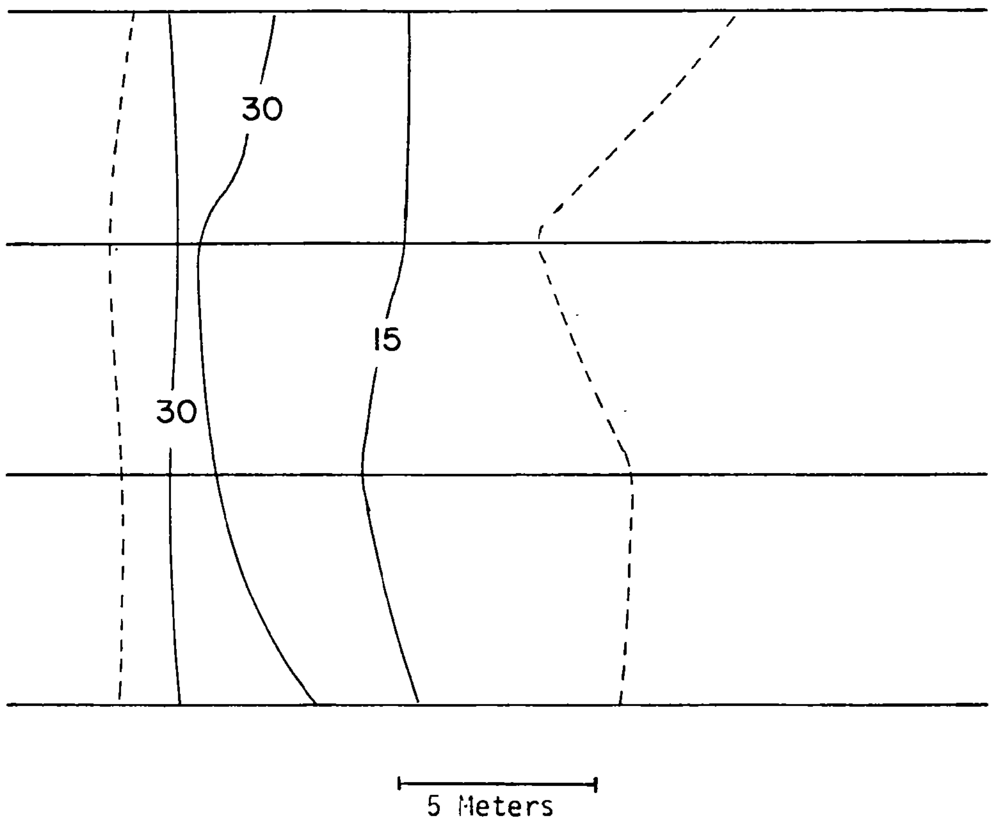

Figure G-9: Depth Contour Map for Riffle #1 of the Experimental Channel Section. Depths in cm. Experimental Discharge: 1.07 cms.

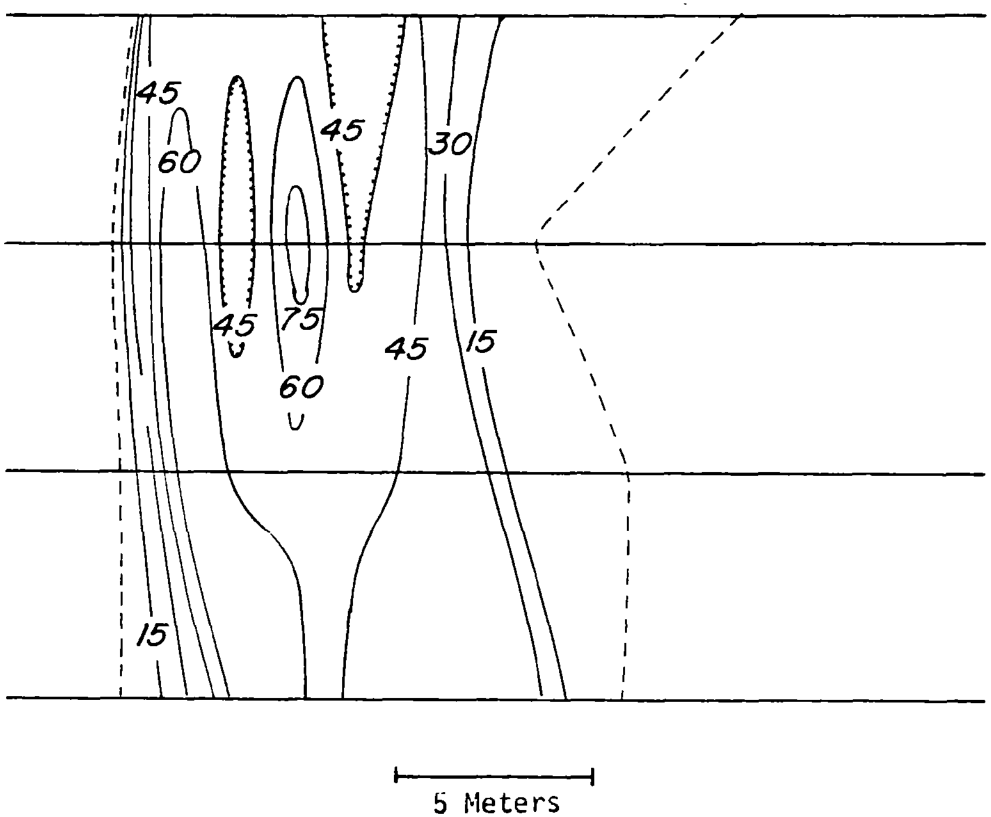

Figure G-10: Velocity Contour Map for Riffle #1 of the Experimental Channel Section. Velocities in cm./sec. Experimental Discharge: 1.07 cms.

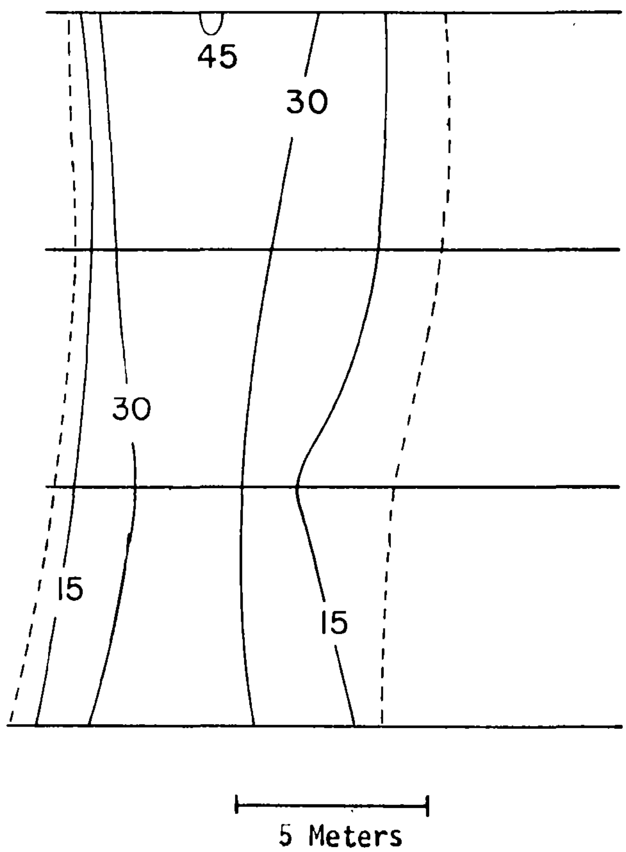

Figure G-11: Depth Contour Map for Riffle #2 of the Experimental Channel Section. Depths in cm. Experimental Discharge: 2.12 cms.

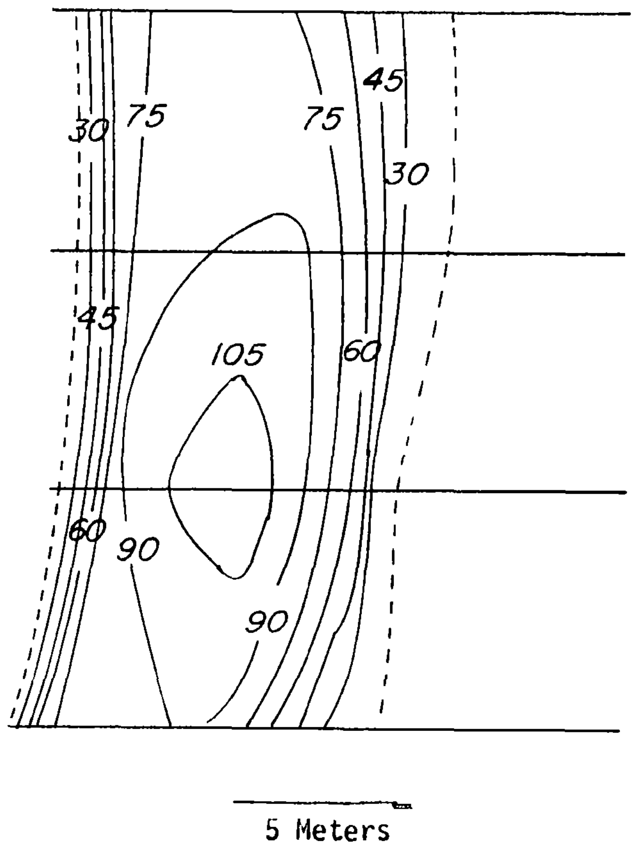

Figure G-12: Velocity Contour Map for Riffle #2 of the Experimental Channel Section. Velocities in cm./sec. Experimental Discharge: 2.12 cms.

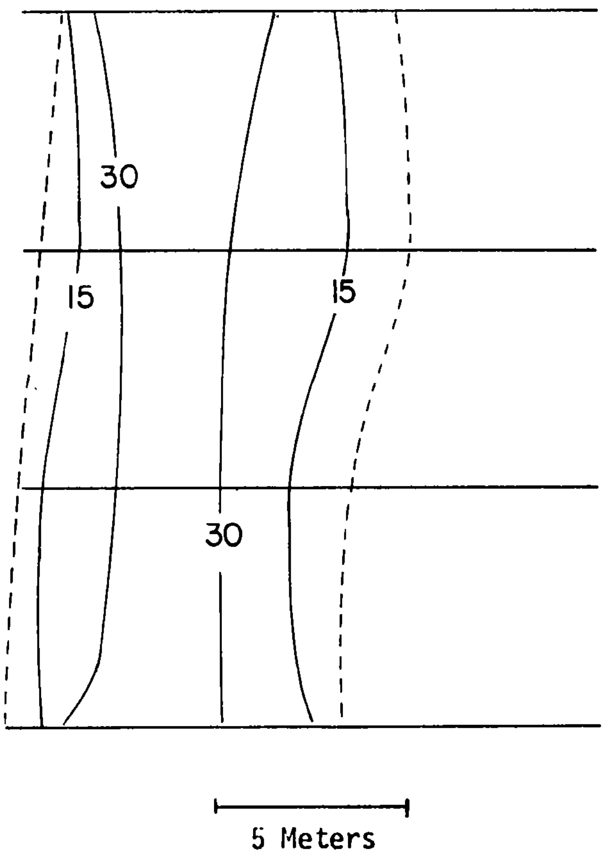

Figure G-13: Depth Contour Map for Riffle #2 of the Experimental Channel Section. Depths in cm. Experimental Discharge: 1.47 cms.

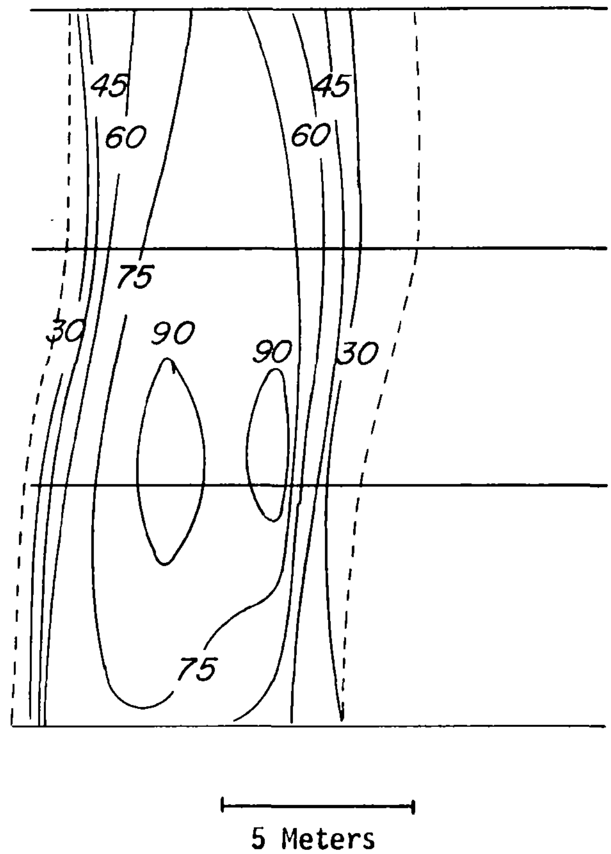

Figure G-14: Velocity Contour Map for Riffle #2 of the Experimental Channel Section. Velocities in cm./sec. Experimental Discharge: 1.47 cms.

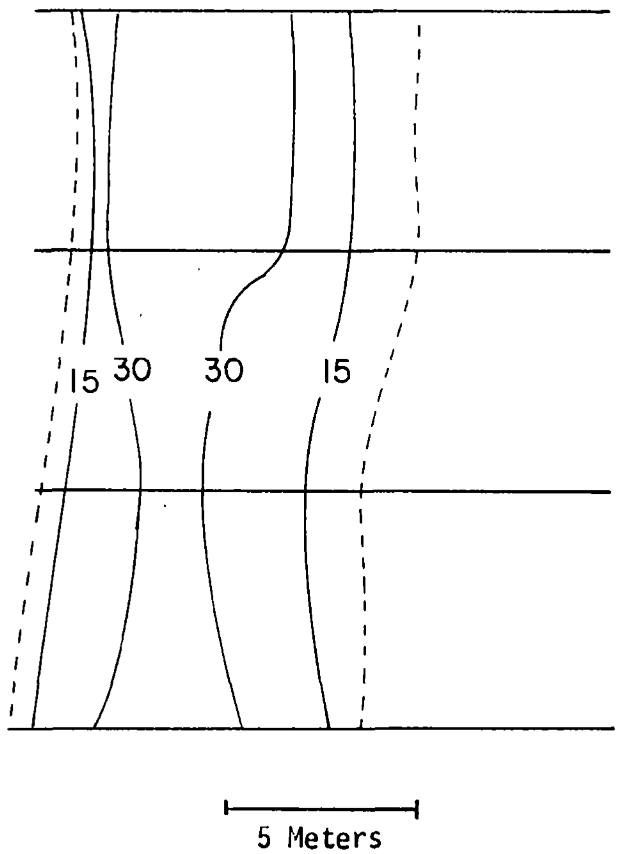

Figure G-15: Depth Contour Map for Riffle #2 of the Experimental Channel Section. Depths in cm. Experimental Discharge: 1.33 cms.

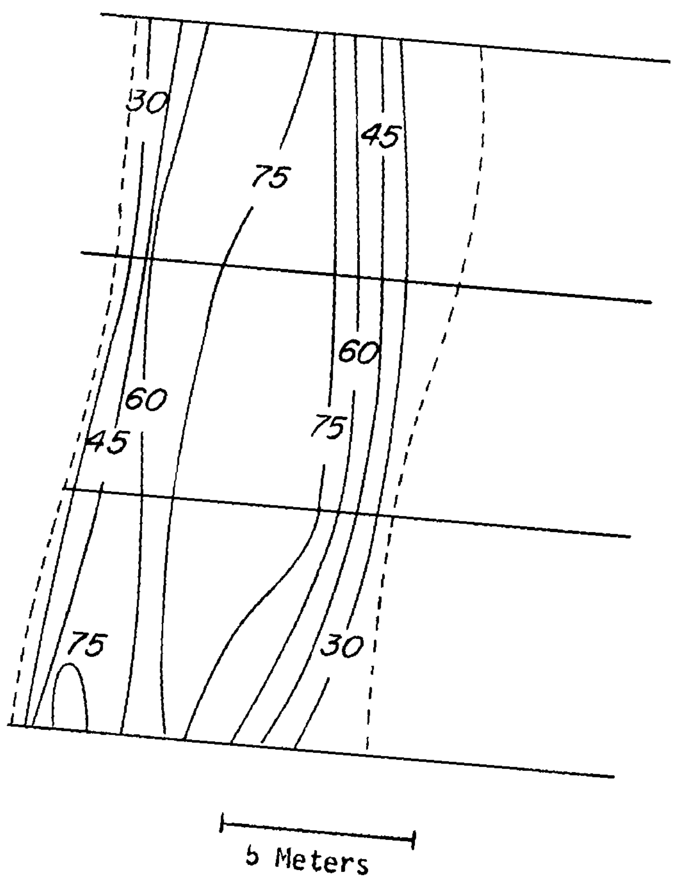

Figure G-16: Velocity Contour Map for Riffle #2 of the Experimental Channel Section. Velocities in cm./sec. Experimental Discharge: 1.33 cms.

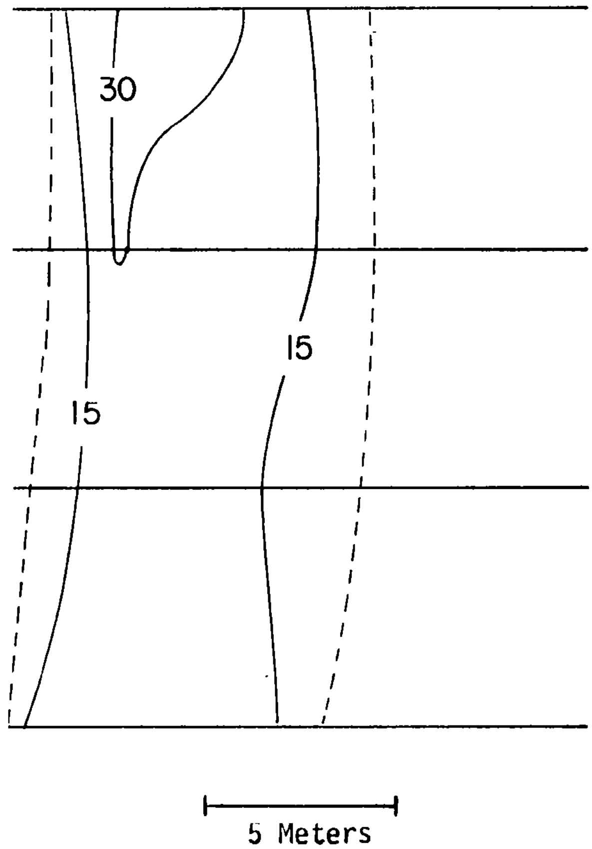

Figure G-17: Depth Contour Map for Riffle #2 of the Experimental Channel Section. Depths in cm. Experimental Discharge: 1.08 cms.

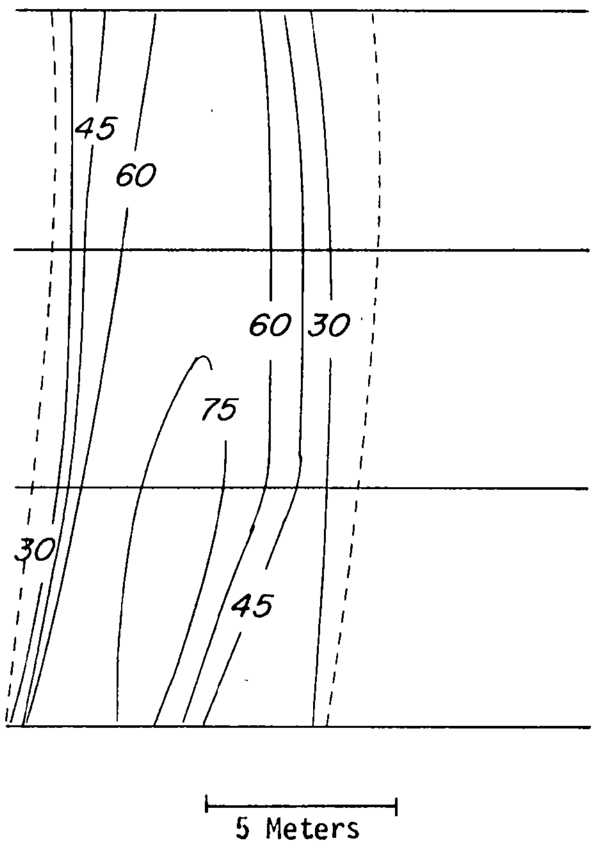

Figure G-18: Velocity Contour Map for Riffle #2 of the Experimental Channel Section. Velocities in cm./sec. Experimental Discharge: 1.08 cms.

APPENDIX H

COMPOSITE MAPS

EXPERIMENTAL CHANNEL SECTION

1. This experimental channel was located in a side channel around a large island in the Viall Ranch section. Flow was minipulated by a diversion structure at the head of the island.

2. Direction of flow is from top of page to bottom.

3. For easier interpretation, depth contours are indicated by vertical typeface. Velocity contours are indicated by slanting typeface.

4. Cross-hatched areas on composite maps indicate areas which do not meet flow criteria for the stonecat. Only those stream areas without cross-hatching meet flow criteria.

5. Dashed lines indicate water's edge, either at banks or on exposed bars.

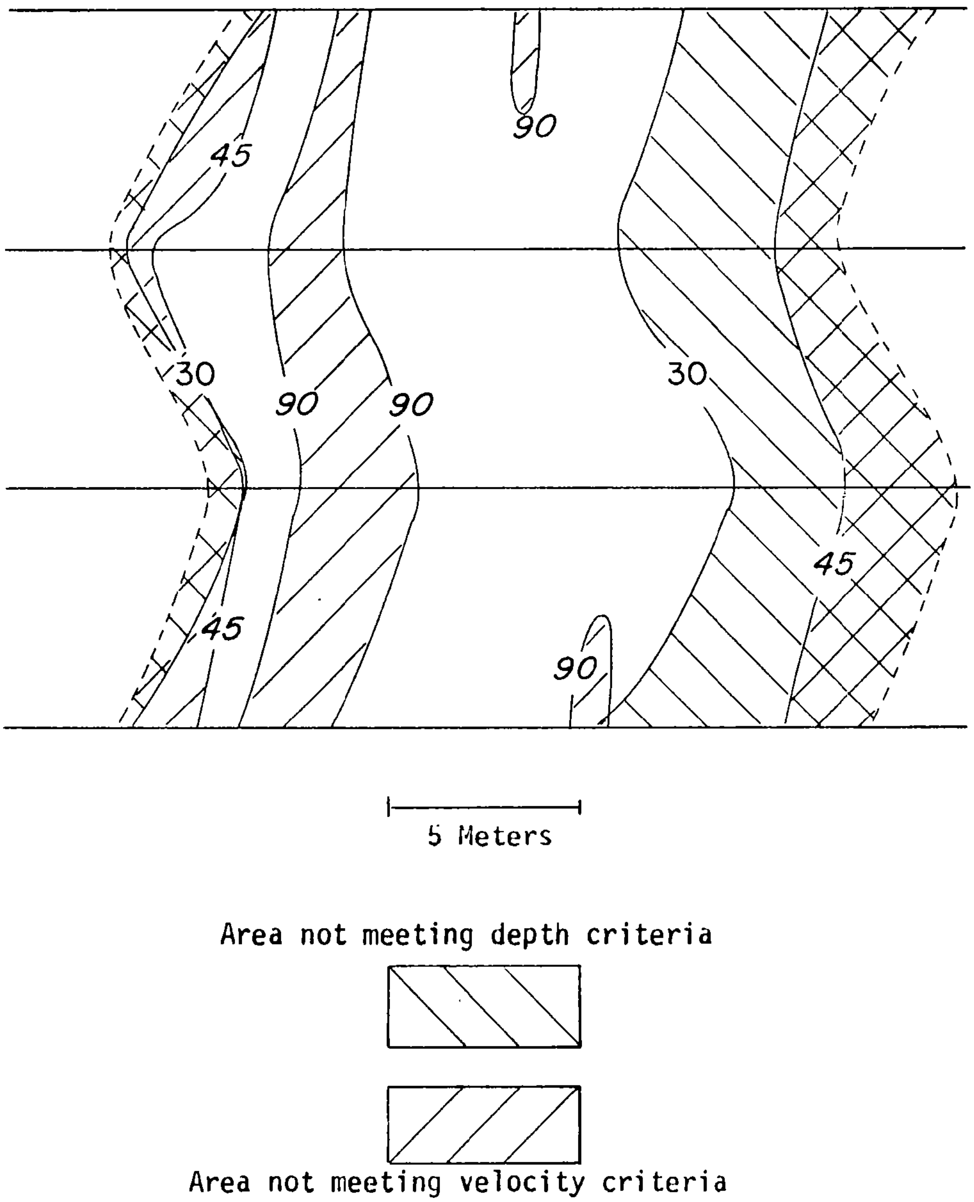

Figure H-1: Composite Map for Riffle #1 of the Experimental Channel Section, Showing Areas Meeting Flow Criteria for the Stonecat. Experimental Discharge: 4.70 cms. Area Meeting Criteria: 163 square meters.

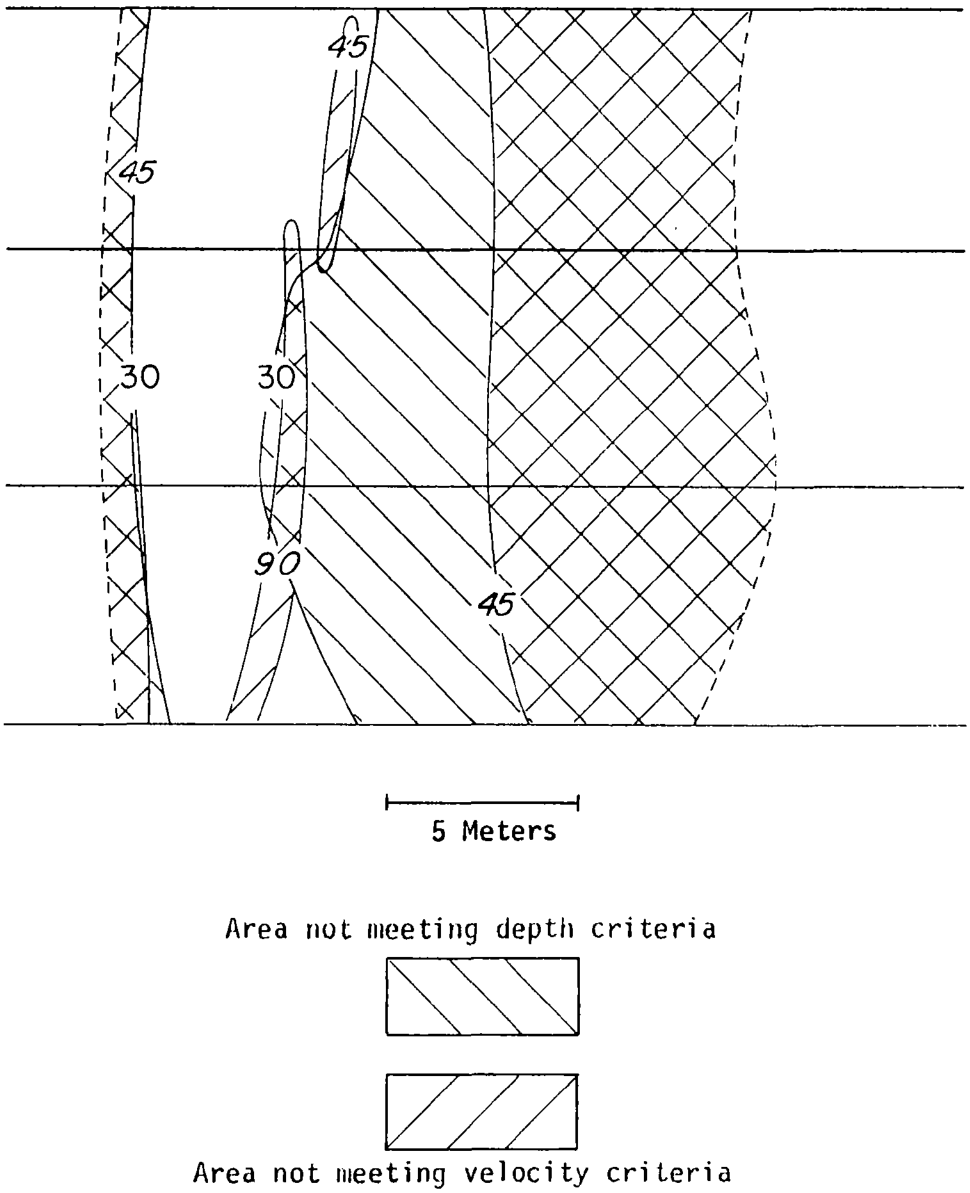

Figure H-2: Composite Map for Riffle #1 of the Experimental Channel Section, Showing Areas Meeting Flow Criteria for the Stonecat. Experimental Discharge: 2.12 cms. Area Meeting Criteria: 72 square meters.

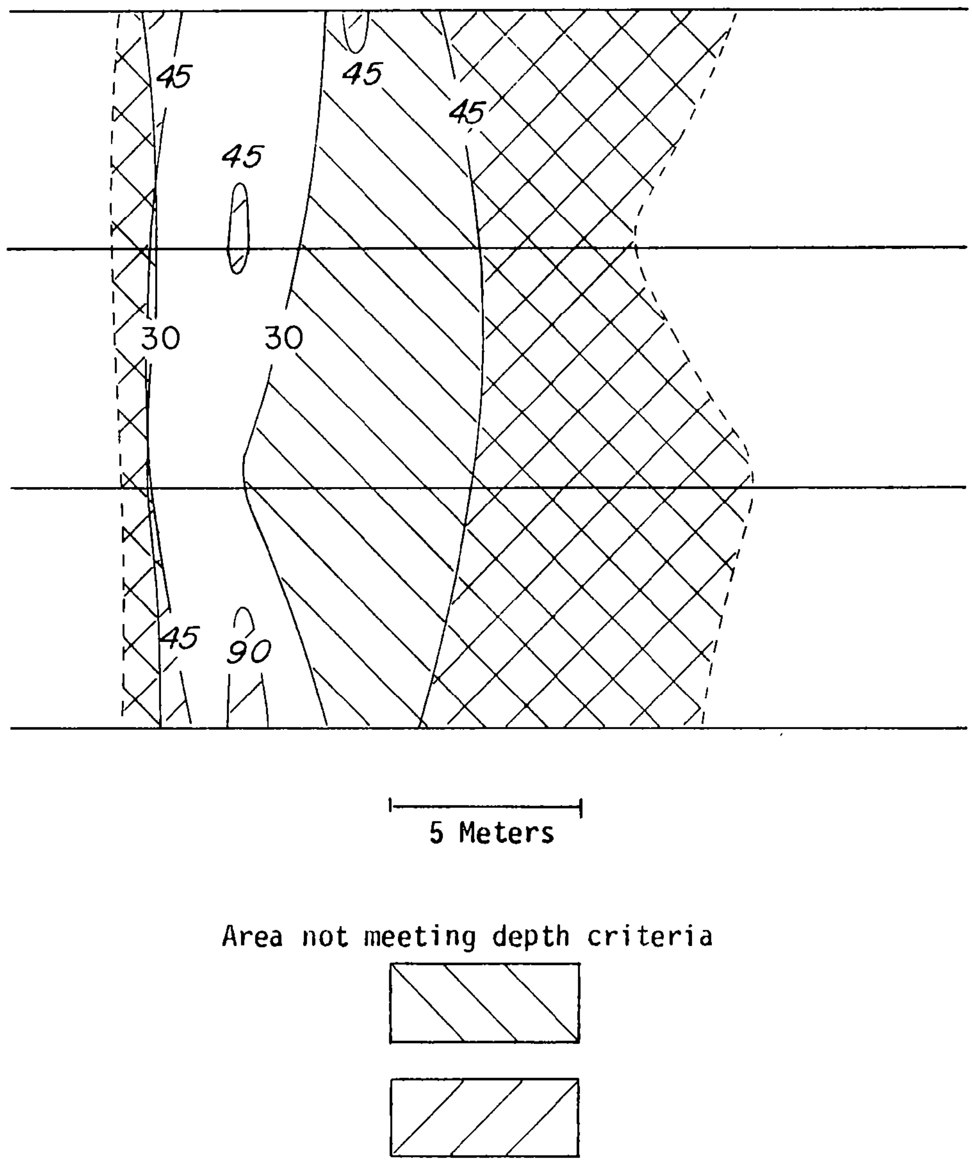

Figure H-3: Composite Map for Riffle #1 of the Experimental Channel Section, Showing Areas Meeting Flow Criteria for the Stonecat. Experimental Discharge: 1.58 cms. Area Meeting Criteria: 59 square meters.

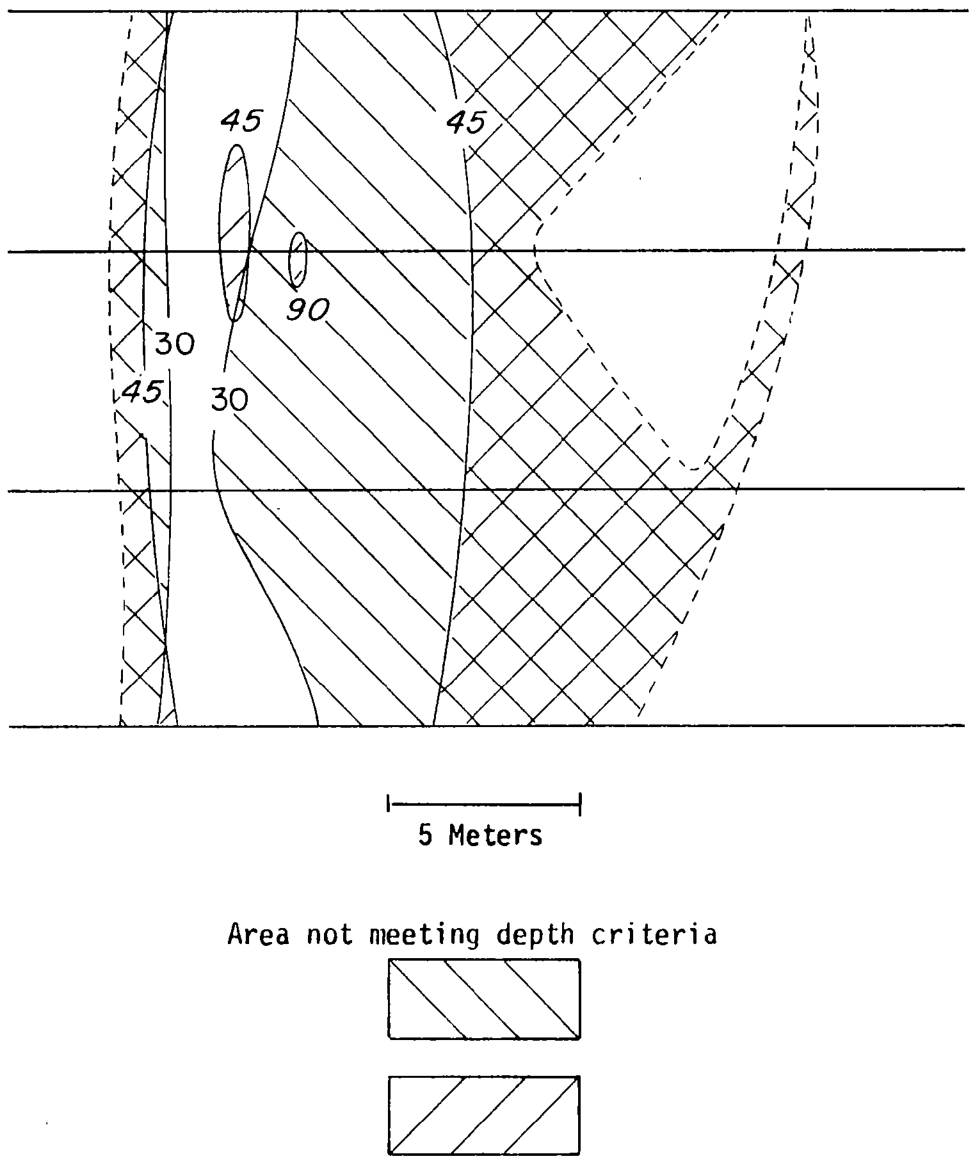

Figure H-4: Composite Map for Riffle #1 of the Experimental Channel Section, Showing Areas Meeting Flow Criteria for the Stonecat. Experimental Discharge: 1.27 cms. Area Meeting Criteria: 39 square meters.

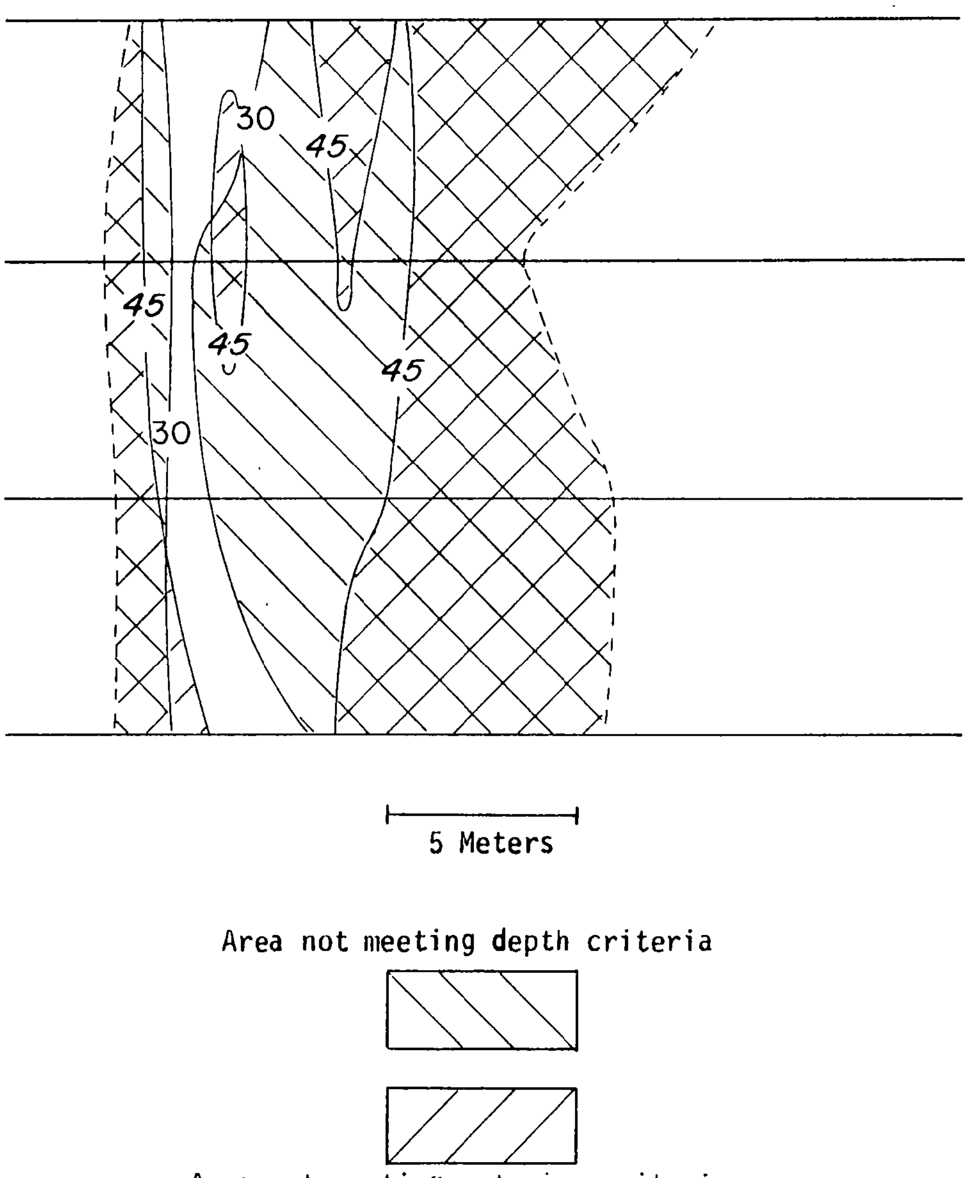

Figure H-5: Composite Map for Riffle #1 of the Experimental Channel Section, Showing Areas Meeting Flow Criteria for the Stonecat. Experimental Discharge: 1.07 cms. Area Meeting Criteria: 27 square meters.

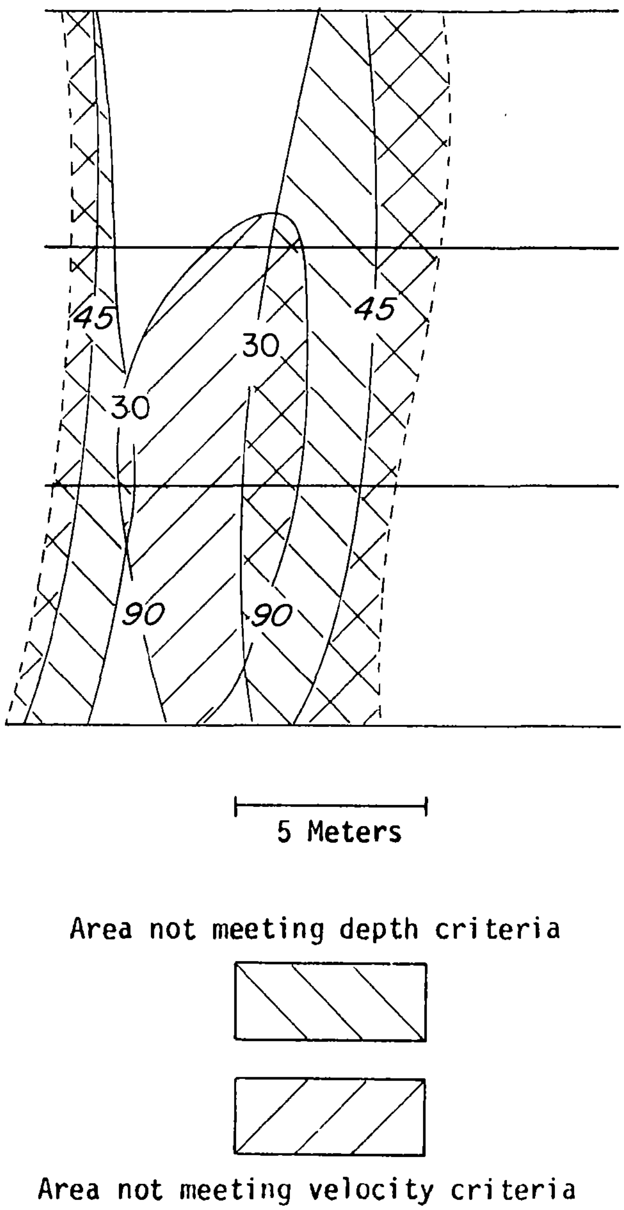

Figure H-6: Composite Map for Riffle #2 of the Experimental Channel Section, Showing Areas meeting Flow Criteria for the Stonecat. Experimental Discharge: 2.12 cms. Area Meeting Criteria: 36 square meters.

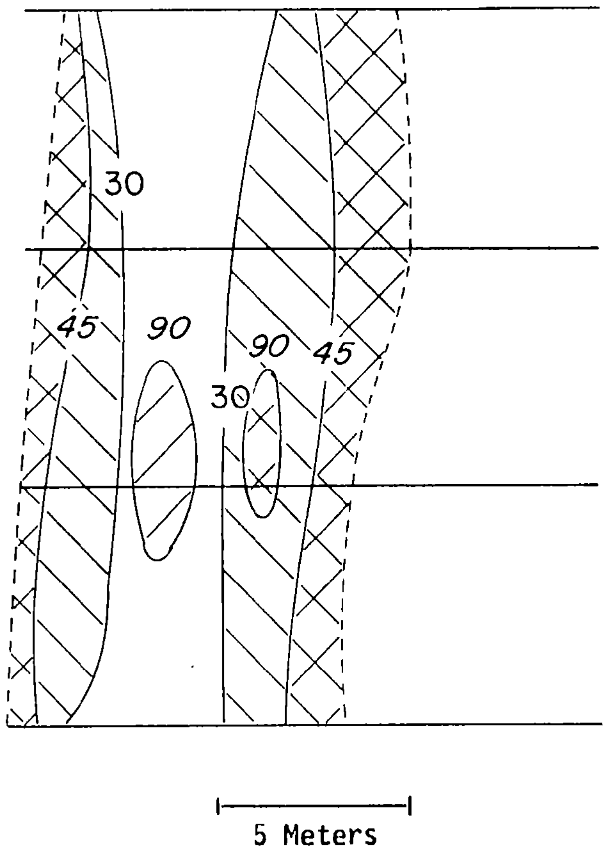

Area not meeting depth criteria

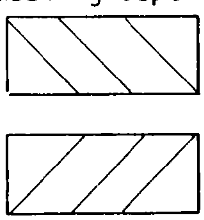

Area not meeting velocity criteria

Figure H-7: Composite Map for Riffle #2 of the Experimental Channel Section, Showing Areas Meeting Flow Criteria for the Stonecat. Experimental Discharge: 1.58 cms. Area Meeting Criteria: 53 square meters.

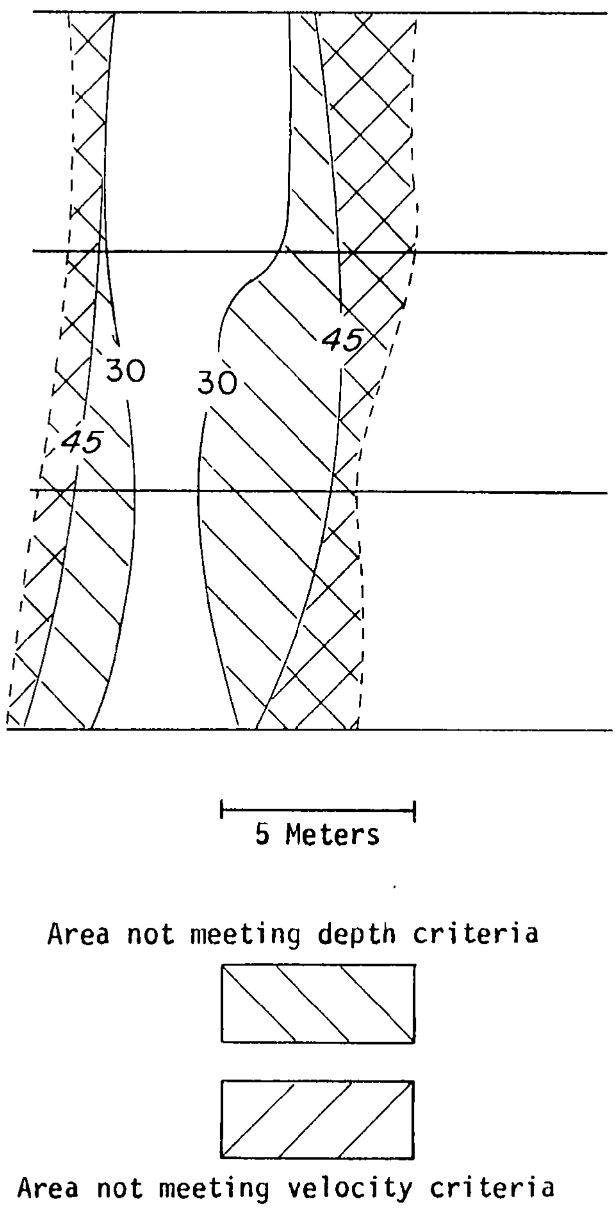

Figure H-8: Composite Map for Riffle #2 of the Experimental Channel Section, Showing Areas Meeting Flow Criteria for the Stonecat. Experimental Discharge: 1.33 cms. Area Meeting Criteria: 60 square meters.

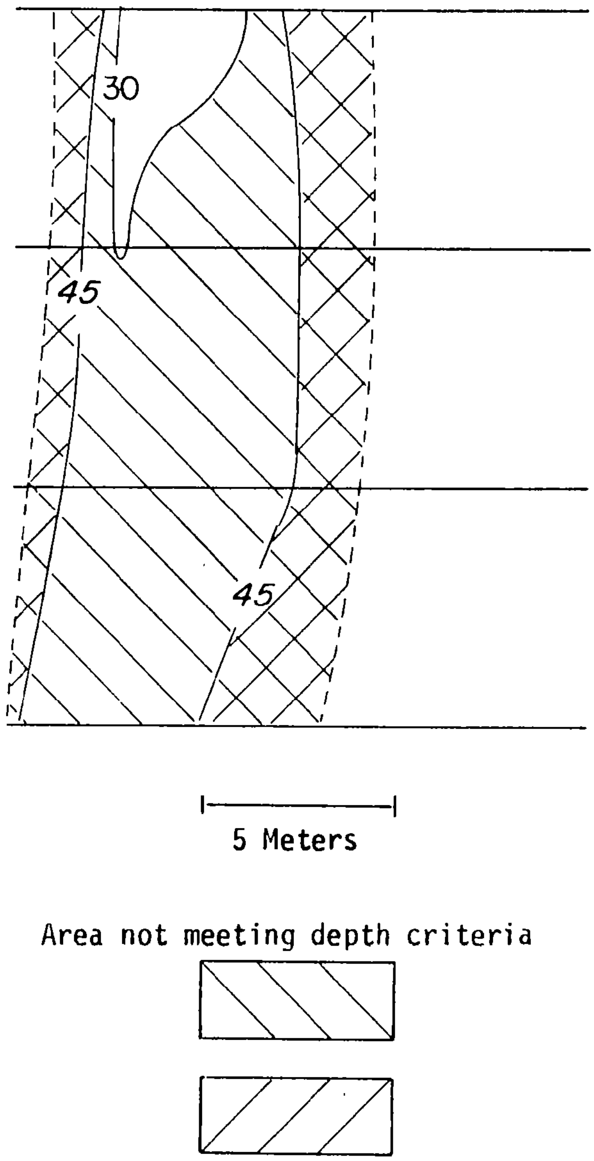

Figure H-9: Composite Map for Riffle #2 of the Experimental Channel Section, Showing Areas Meeting Flow Criteria for the Stonecat. Experimental Discharge: 1.07 cms. Area Meeting Criteria: 11 square meters.

APPENDIX I

ICE FORMATION CROSS SECTIONAL DIAGRAMS

1. Cross hatched areas indicate surface ice sheet

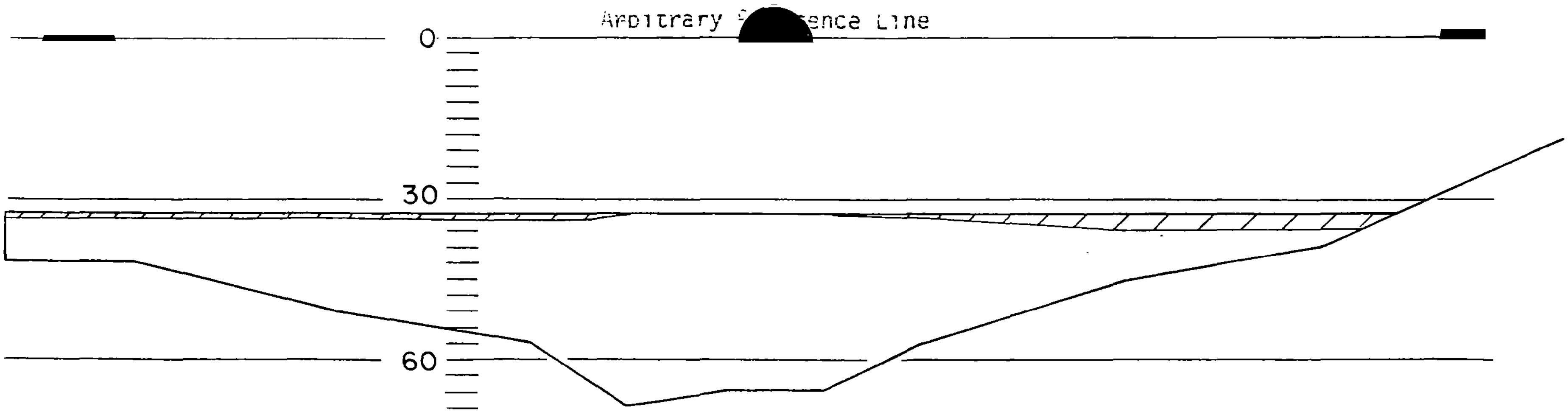

Figure I-1a: Cross-sectional view of channel and surface ice sheet at transect 1, Orcutt Ranch Section, 11/20/75. Vertical scale in cm. below arbitrary datum.

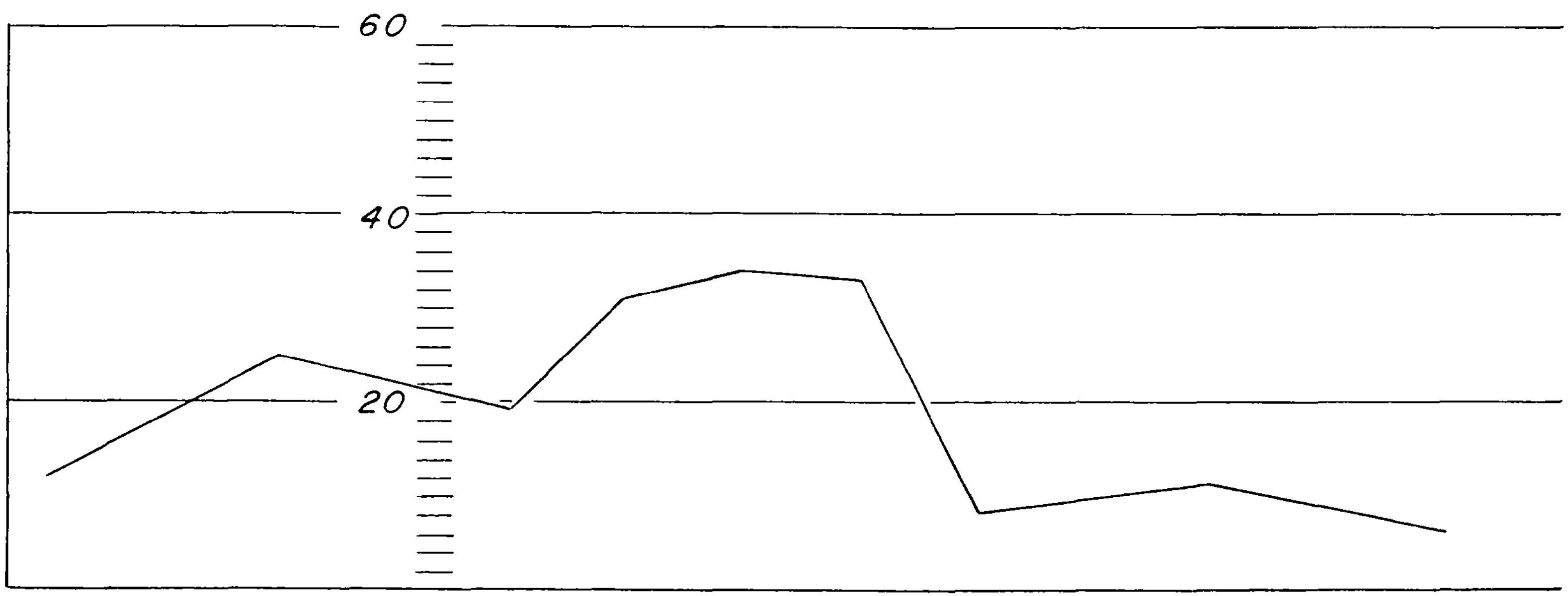

Figure I-1b: Velocities, in cm./sec., at corresponding ice measurement locations on above transect.

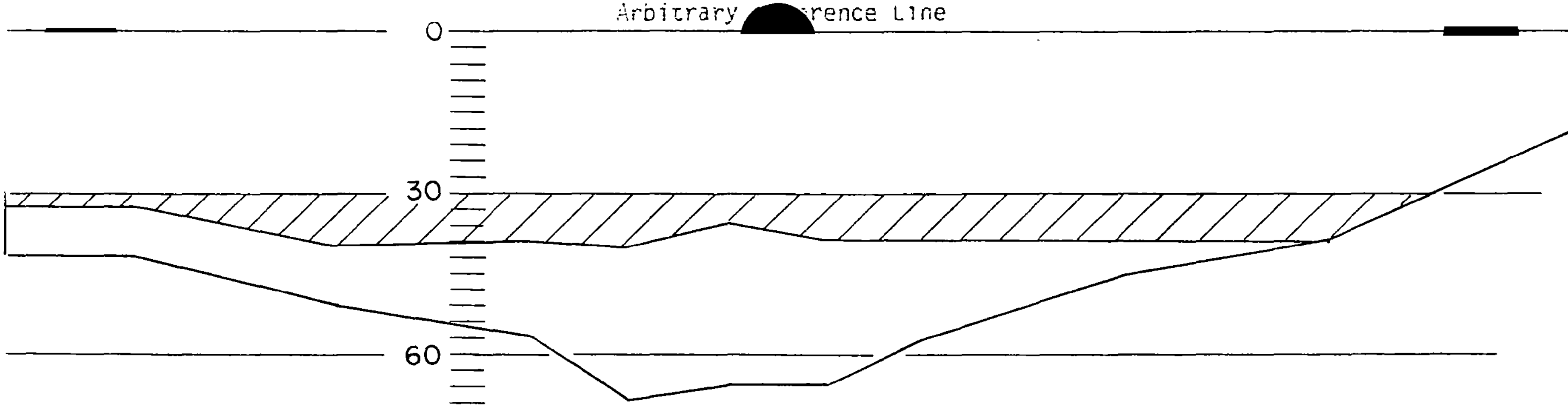

Figure I-2a: Cross-sectional view of channel and surface ice sheet at transect 1, Orcutt Ranch Section, 11/26/75. Vertical scale in cm. below arbitrary datum.

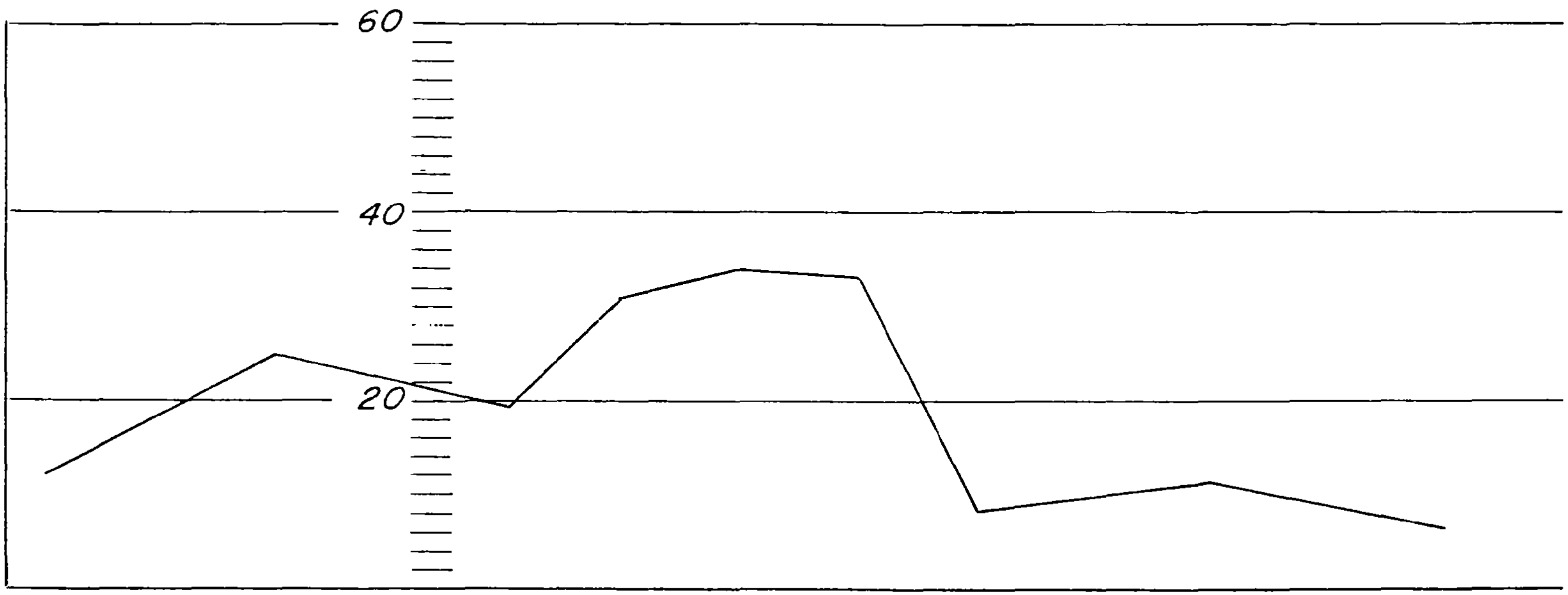

Figure I-2b: Velocities, in cm./sec., at corresponding ice measurement locations on above transect.

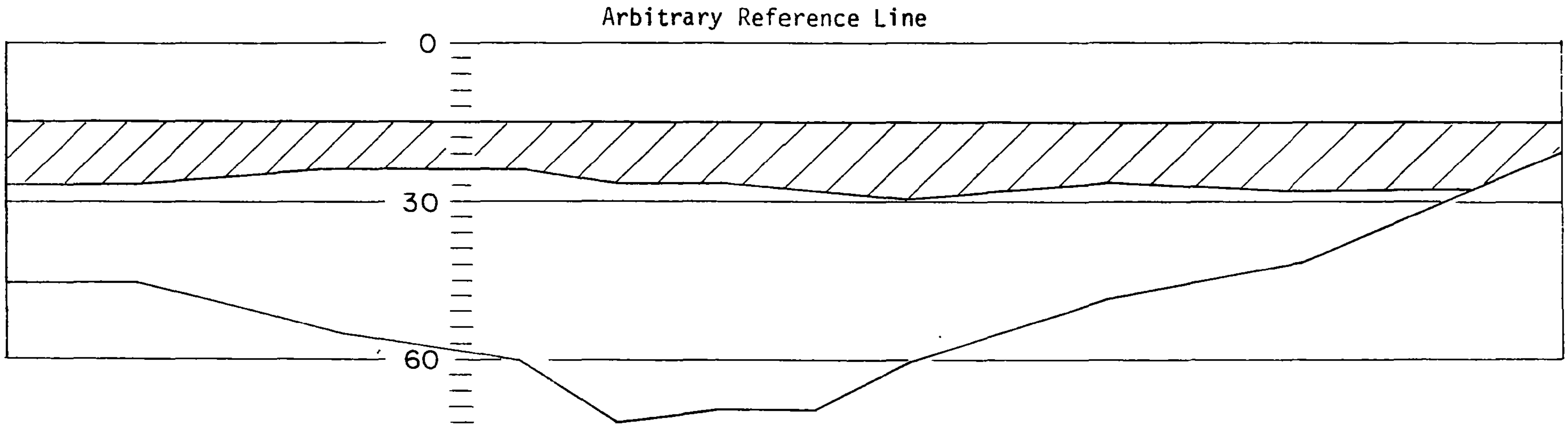

Figure I-3a: Cross-sectional view of channel and surface ice sheet at transect 1, Orcutt Ranch Section, 12/4/75. Vertical scale in cm. below arbitrary datum.

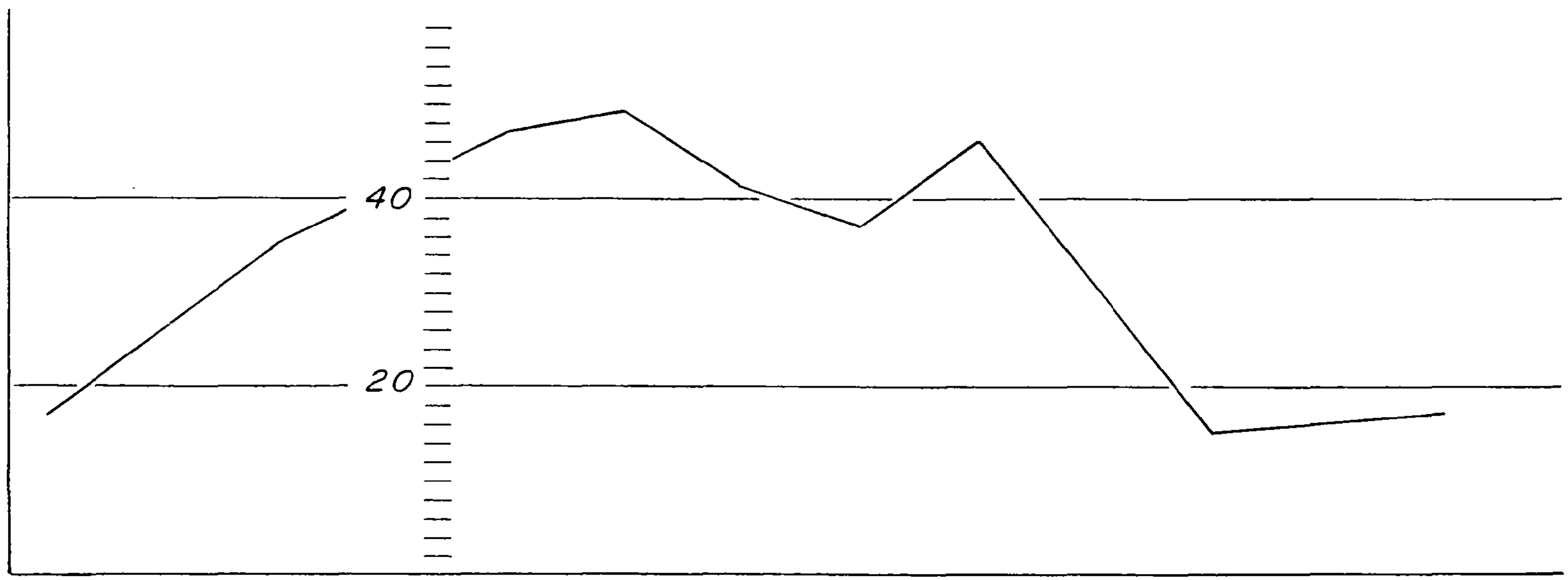

Figure I-3b: Velocities, in cm./sec., at corresponding ice measurement locations on above transect.

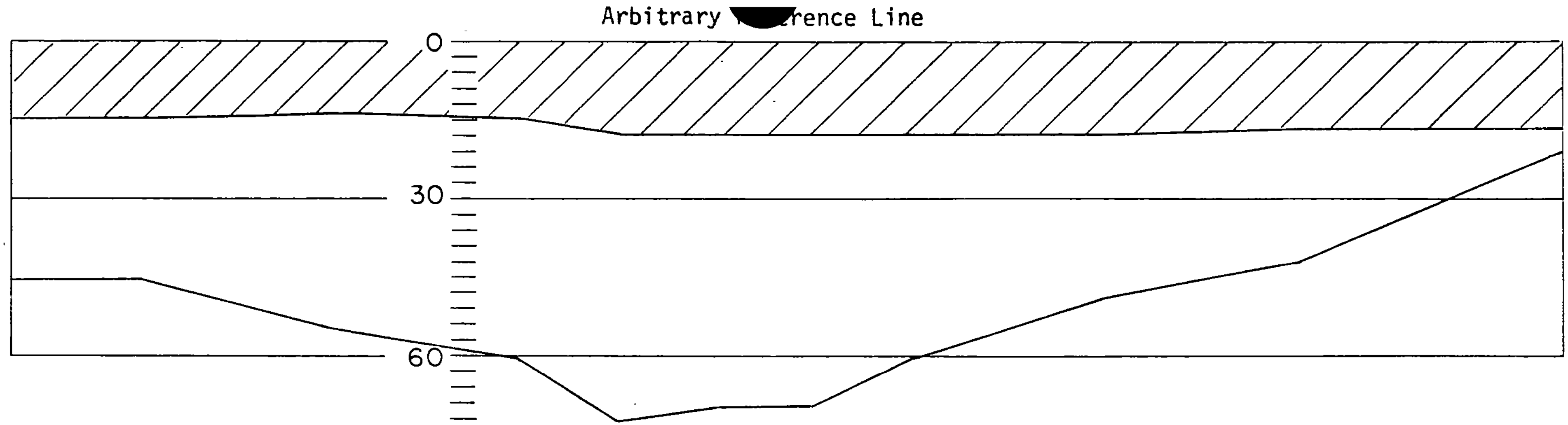

Figure I-4a: Cross-sectional view of channel and surface ice sheet at transect 1, Orcutt Ranch Section, 12/23/75. Vertical scale in cm. below arbitrary datum.

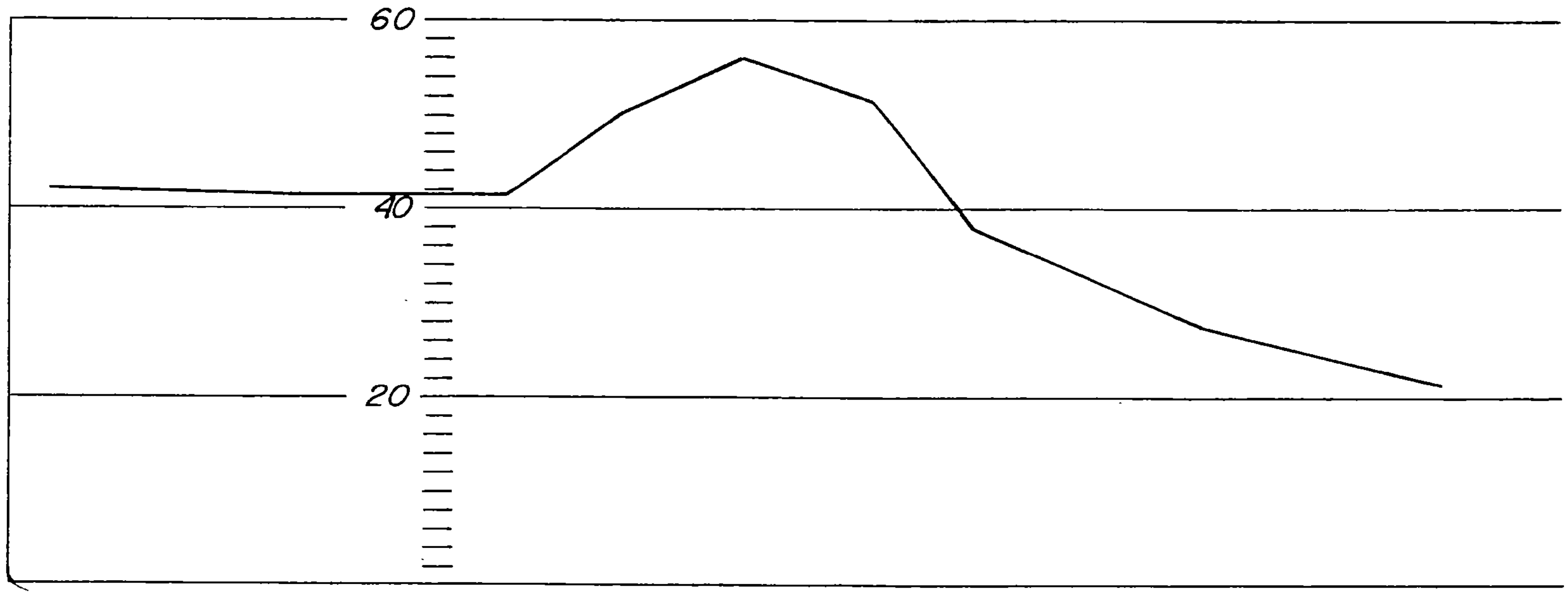

Figure I-4b: Velocities, in cm./sec., at corresponding ice measurement location on above transect.

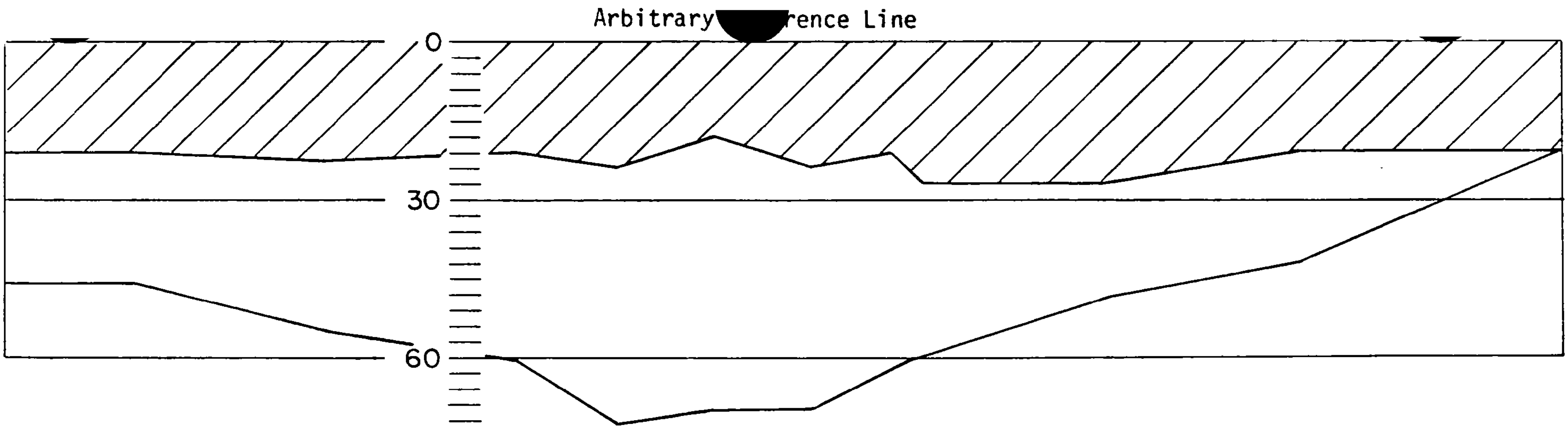

Figure I-5a: Cross-sectional view of channel and surface ice sheet at transect 1, Orcutt Ranch Section, 1/9/76. Vertical scale in cm. below arbitrary datum.

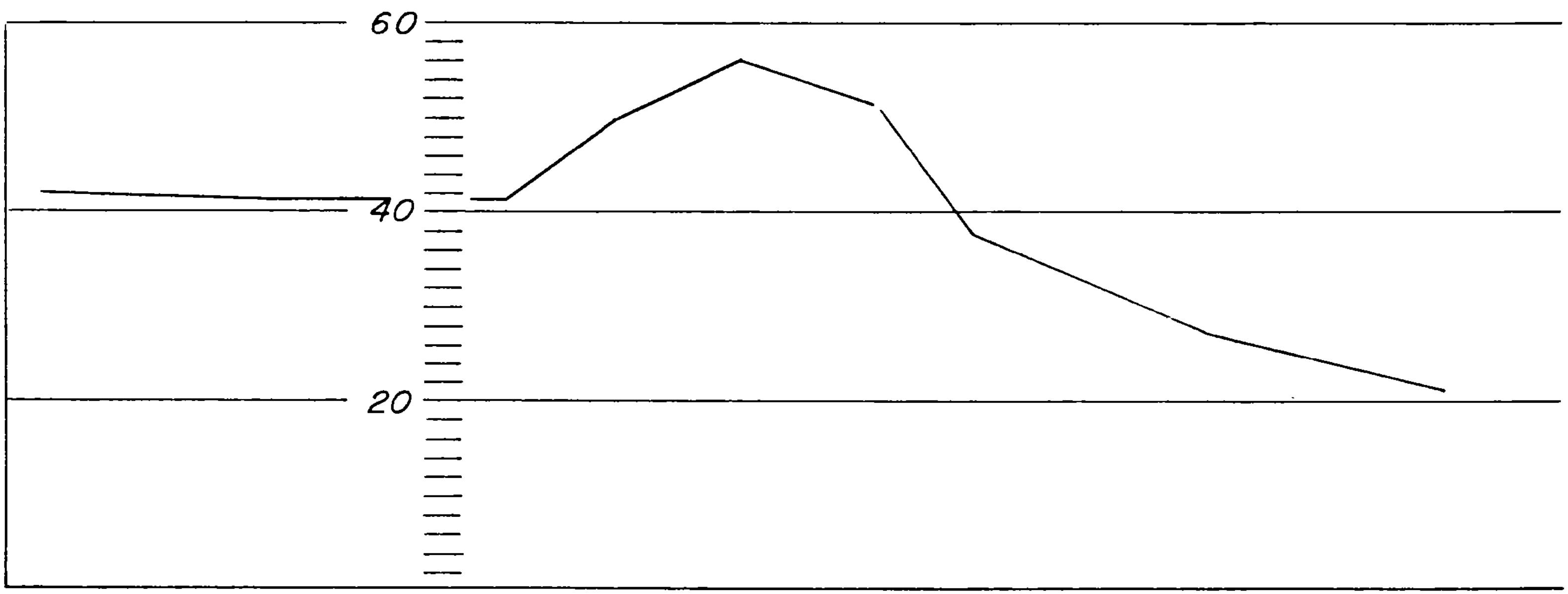

Figure I-5b: Velocities, in cm./sec., at corresponding ice measurement locations on above transect.

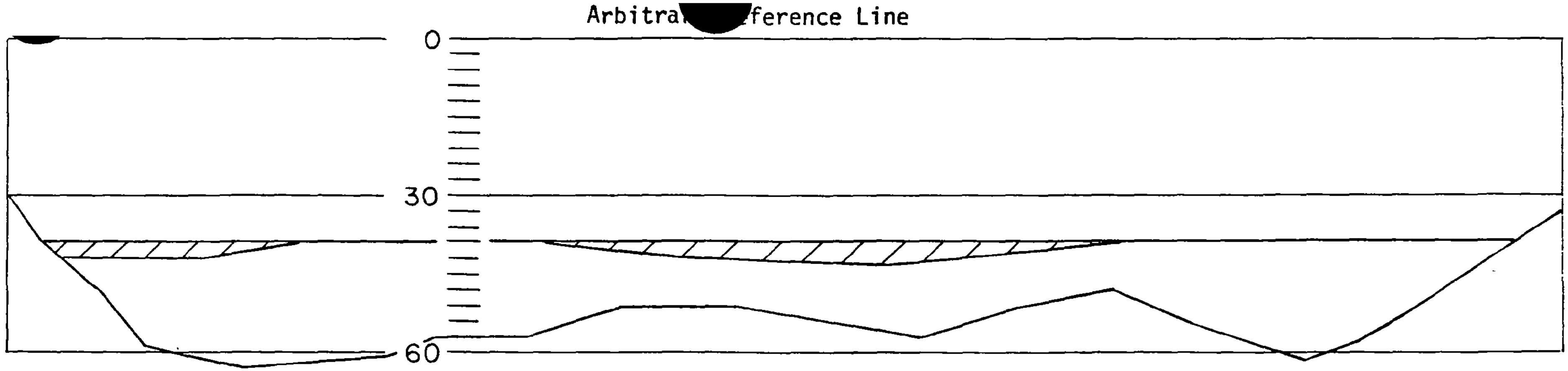

Figure I-6a: Cross-sectional view of channel and surface ice sheet at transect 2, Orcutt Ranch Section, 11/20/75. Vertical scale in cm. below arbitrary datum.

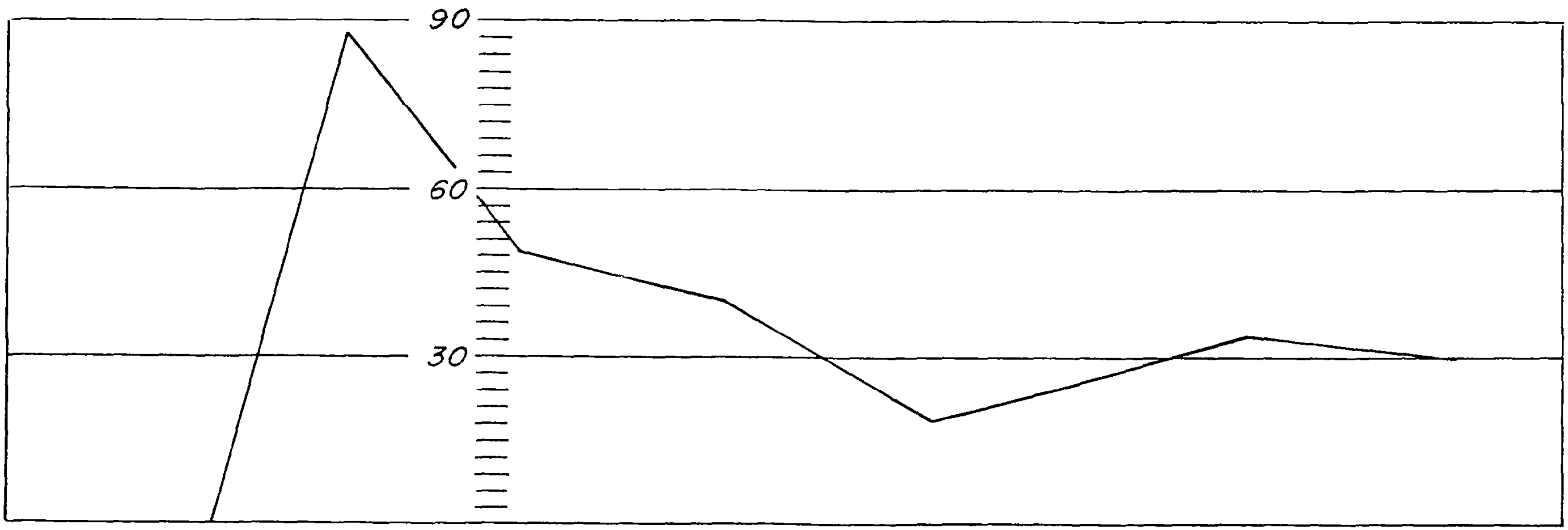

Figure I-6b: Velocities, in cm./sec. at corresponding ice measurement locations on above transect.

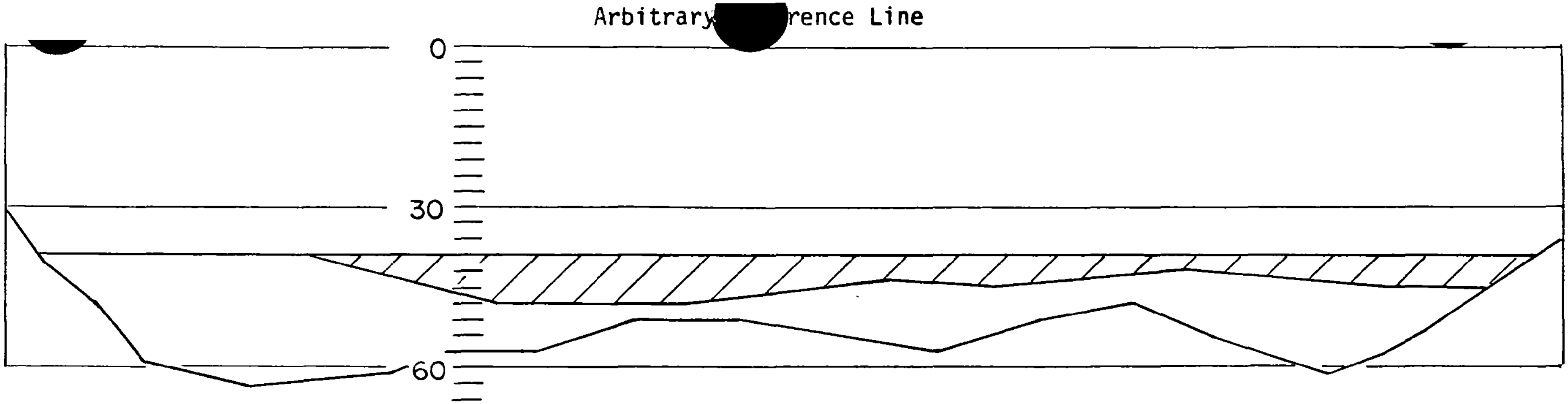

Figure I-7a: Cross-sectional view of channel and surface ice sheet at transect 2, Orcutt Ranch Section, 11/26/75. Vertical scale in cm. below arbitrary datum.

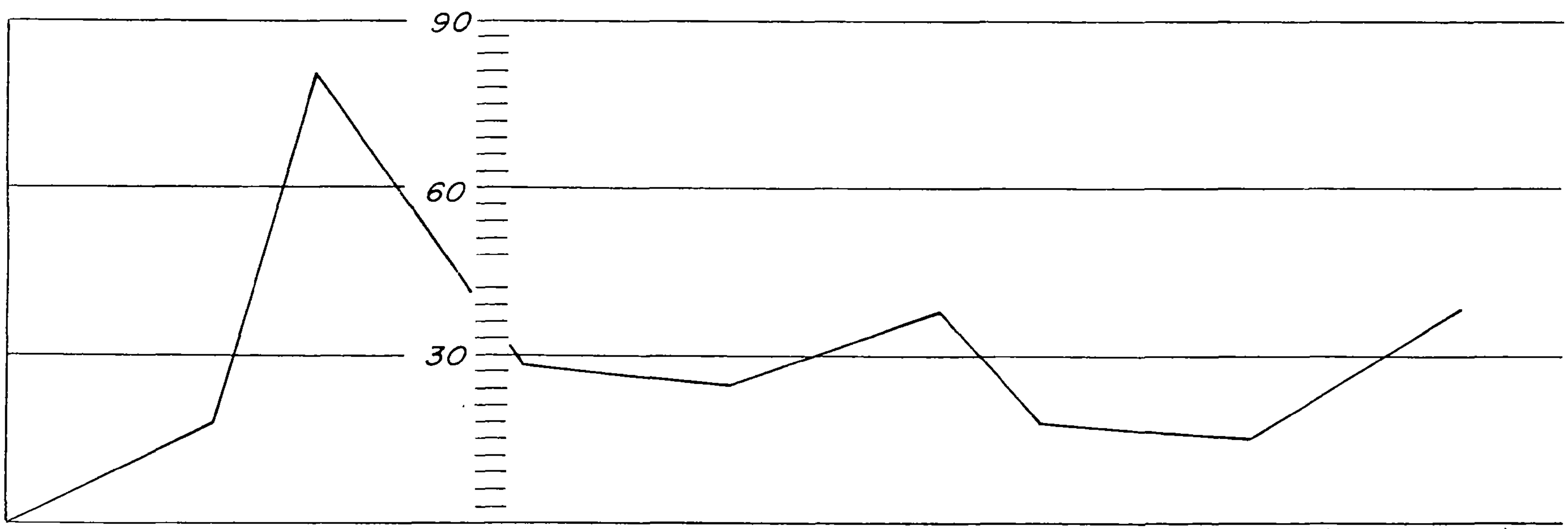

Figure I-7b: Velocities, in cm./sec., at corresponding ice measurement locations on above transect.

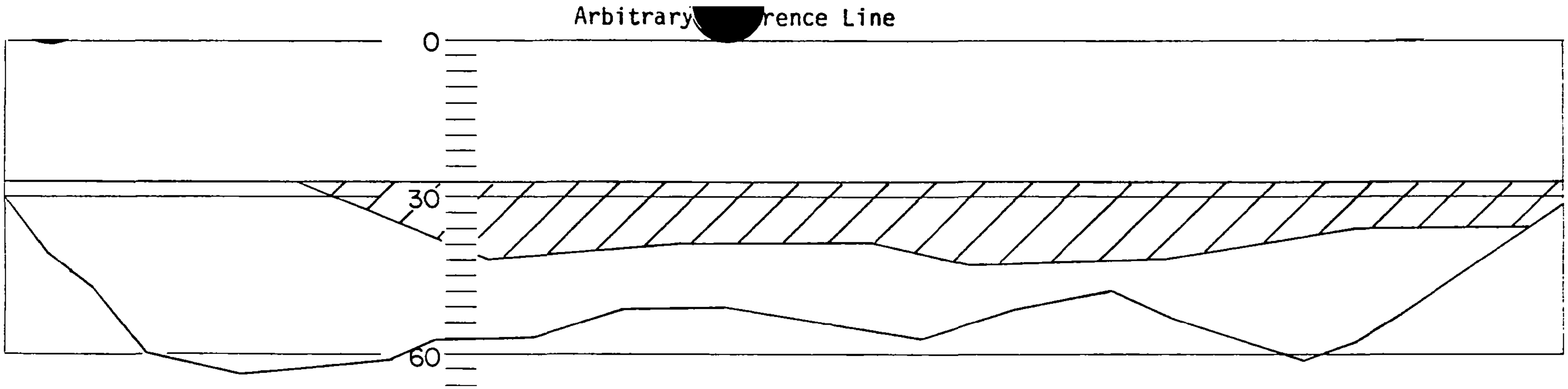

Figure I-8a: Cross-sectional view of channel and surface ice sheet at transect 2, Orcutt Ranch Section, 12/4/75. Vertical scale in cm. below arbitrary datum.

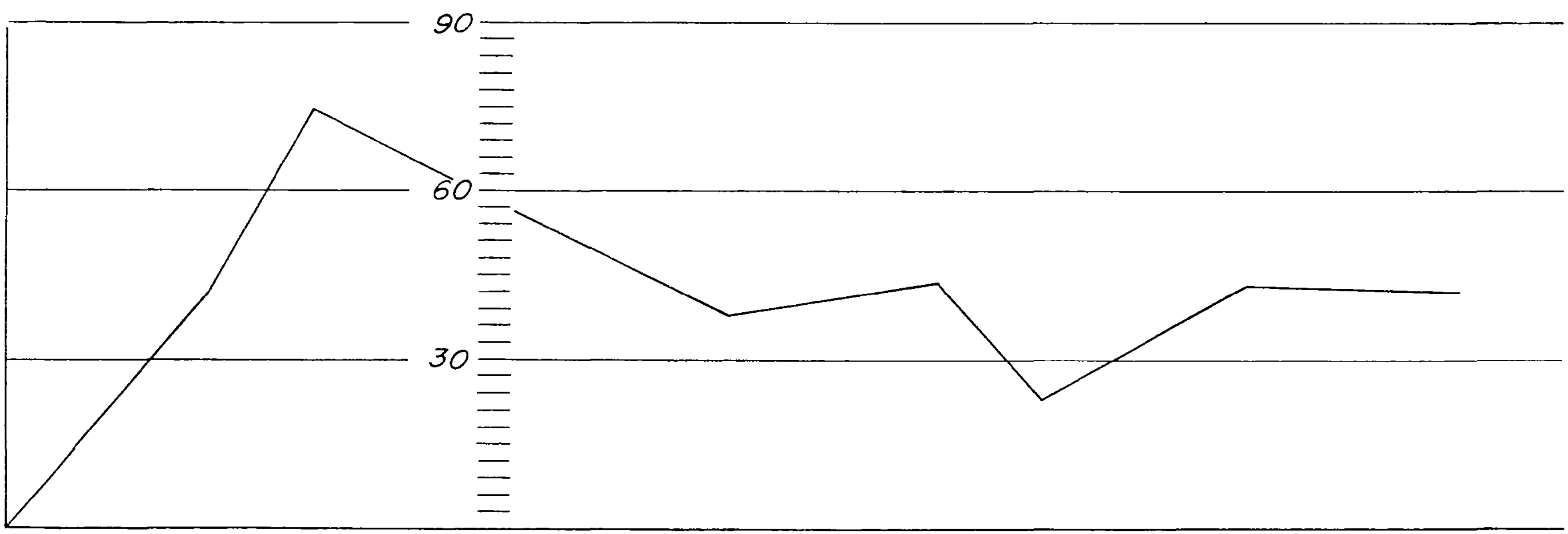

Figure I-8b: Velocities, in cm./sec., at corresponding ice measurement locations on above transect.

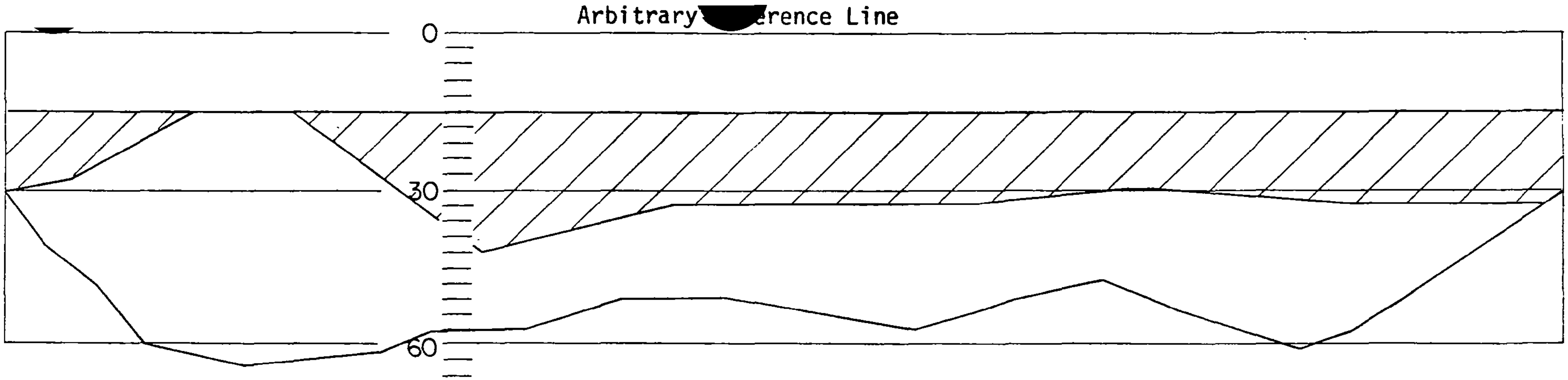

Figure I-9a: Cross-sectional view of channel and surface ice sheet at transect 2, Orcutt Ranch Section, 12/23/75. Vertical scale in cm. below arbitrary datum.

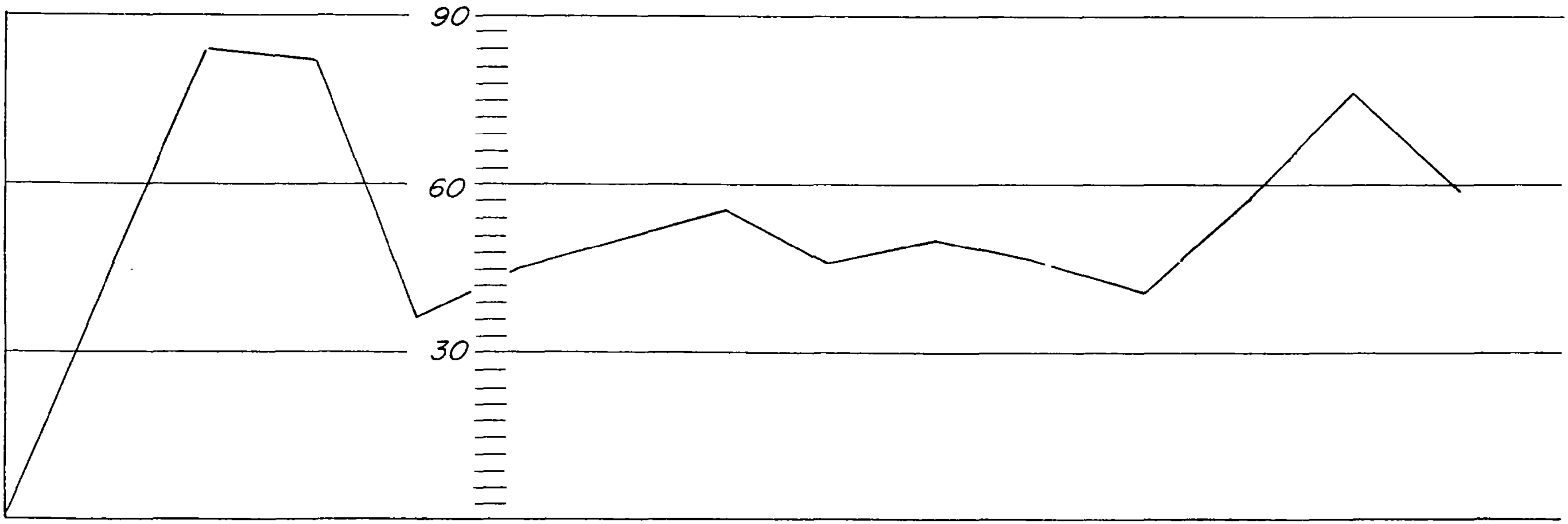

Figure I-9b: Velocities, in cm./sec., at corresponding ice measurement locations on above transect.

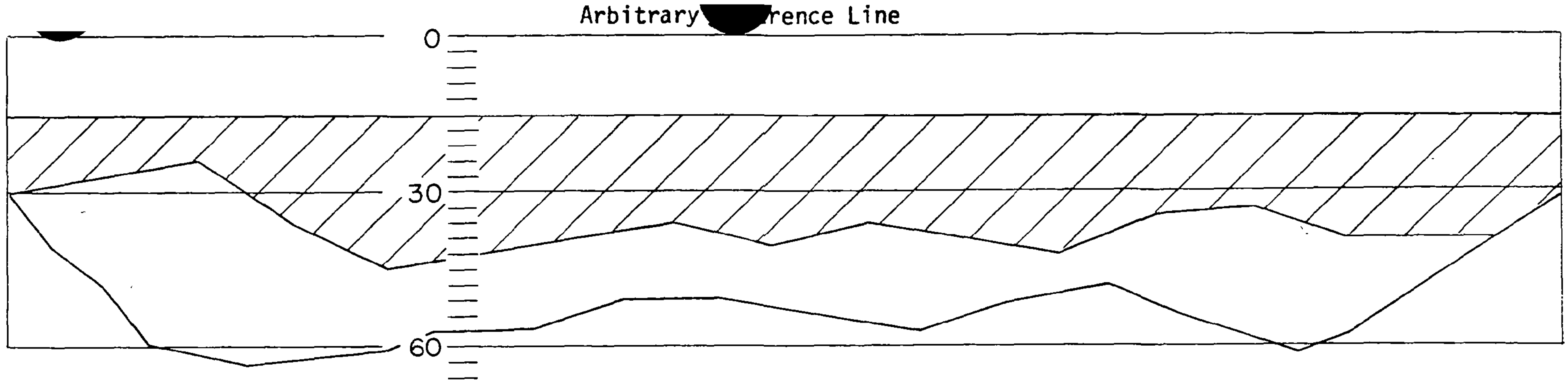

Figure I-10a: Cross-sectional view of channel and surface ice sheet at transect 2, Orcutt Ranch Section, 1/9/76. Vertical scale in cm. below arbitrary datum.

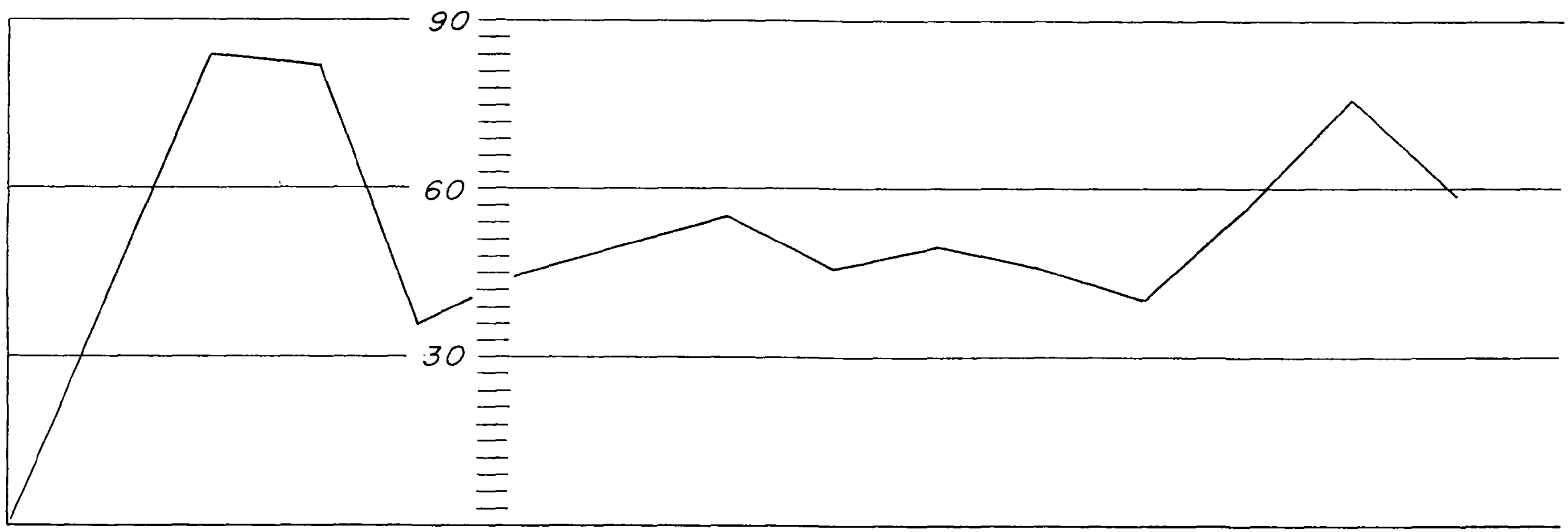

Figure I-10b: Velocities, in cm./sec., at corresponding ice measurement locations on above transect.

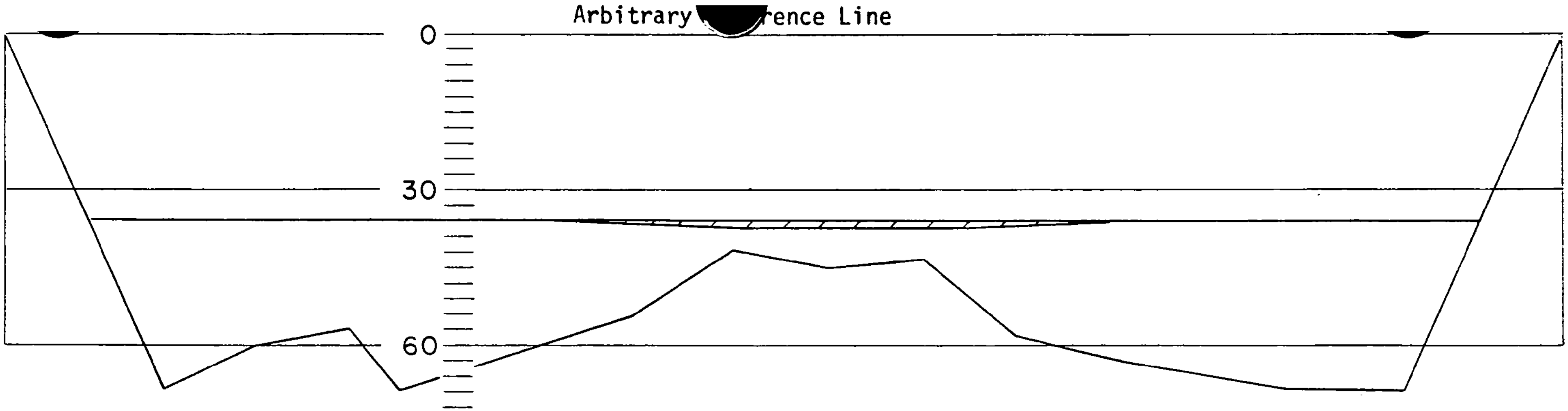

Figure I-11a: Cross-sectional view of channel and surface ice sheet at transect 3, Orcutt Ranch Section, 11/20/75. Vertical scale in cm. below arbitrary datum.

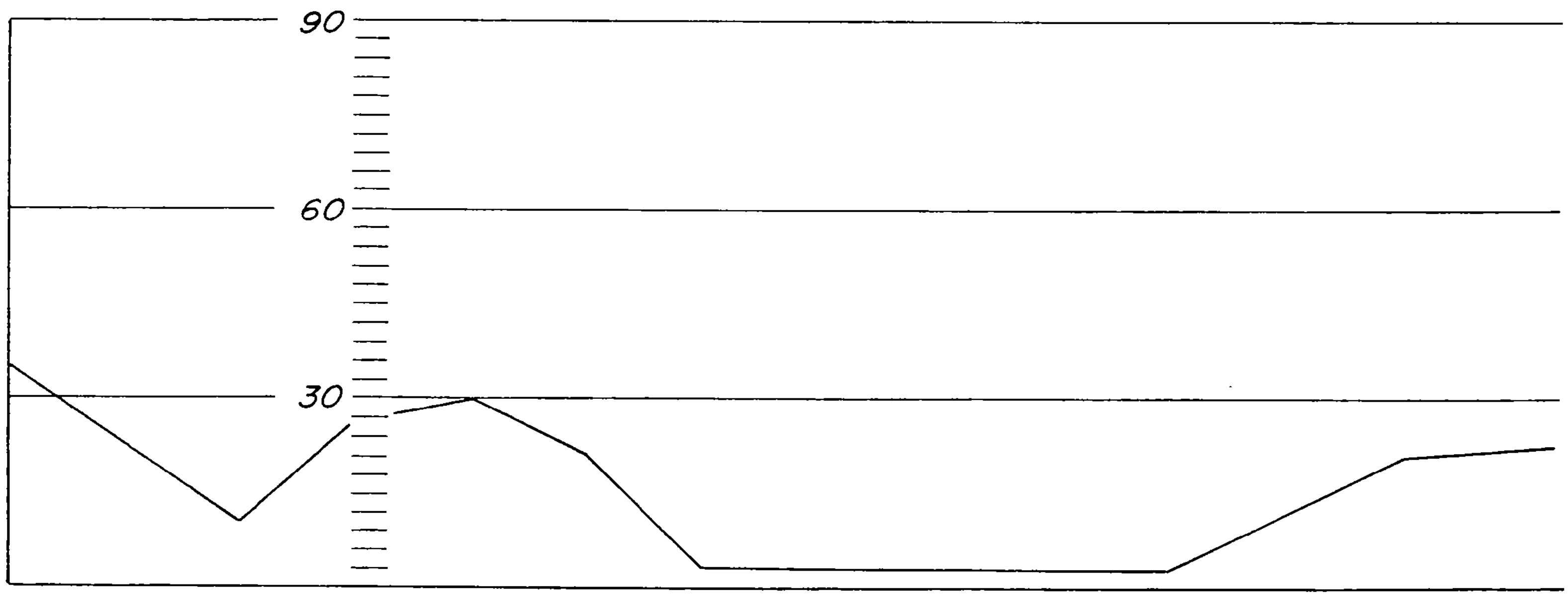

Figure I-11b: Velocities, in cm./sec., at corresponding ice measurement locations on above transect.

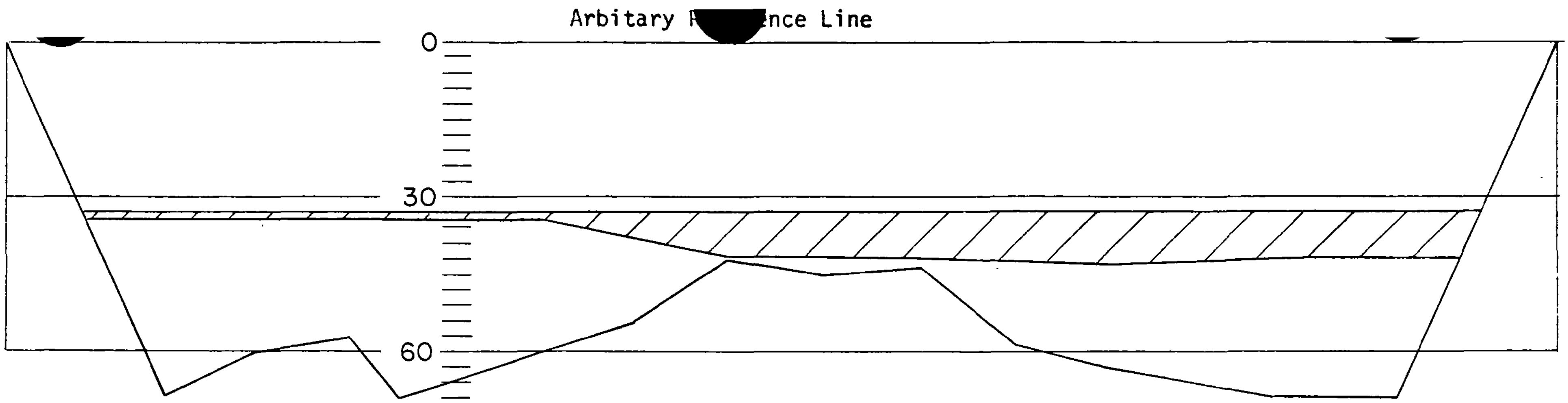

Figure I-12a: Cross-sectional view of channel and surface ice sheet at transect 3, Orcutt Ranch Section, 11/26/75. Vertical scale in cm. below arbitrary datum.

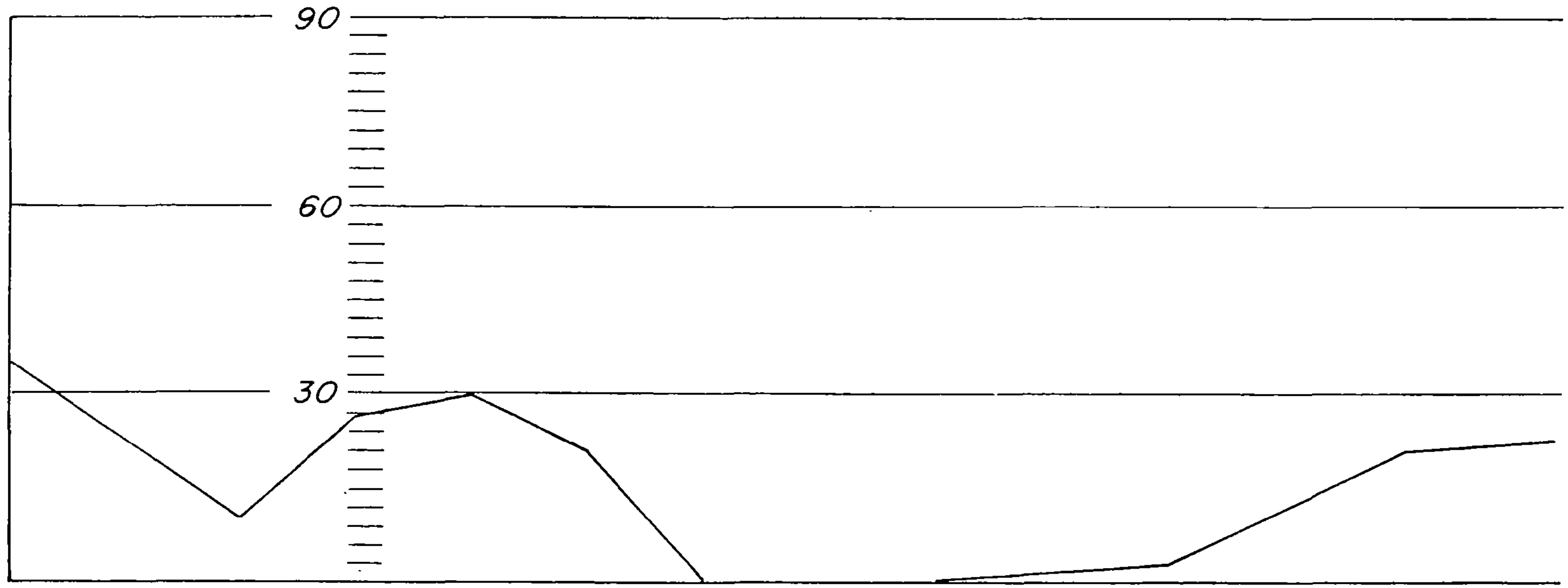

Figure I-12b: Velocities, in cm./sec., at corresponding ice measurement locations on above transect.

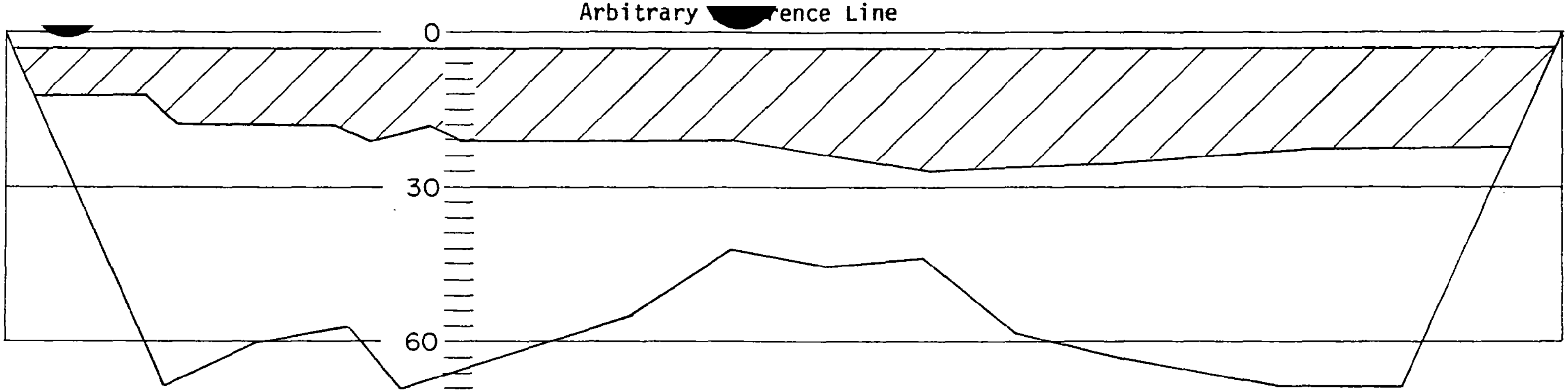

Figure I-13a: Cross-sectional view of channel and surface ice sheet at transect 3, Orcutt Ranch Section, 12/10/75. Vertical scale in cm. below arbitrary datum.

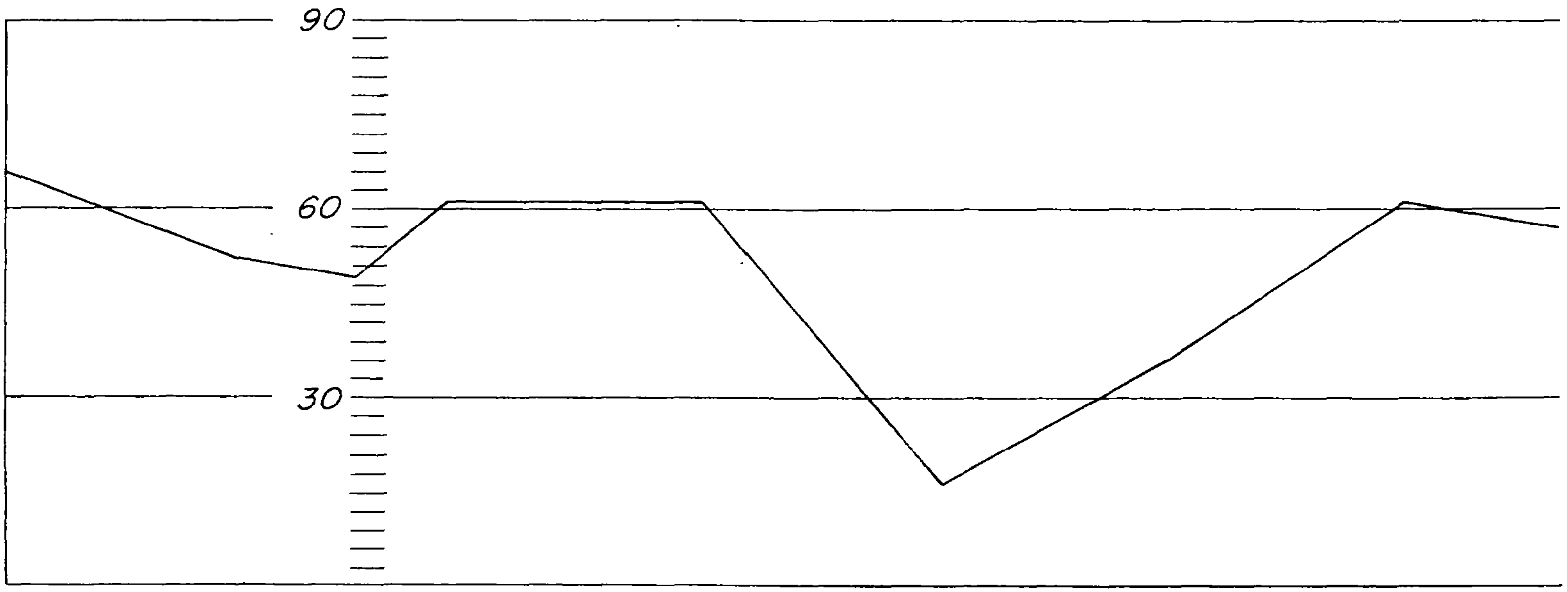

Figure I-13b: Velocities, in cm./sec., at corresponding ice measurement locations on above transect.

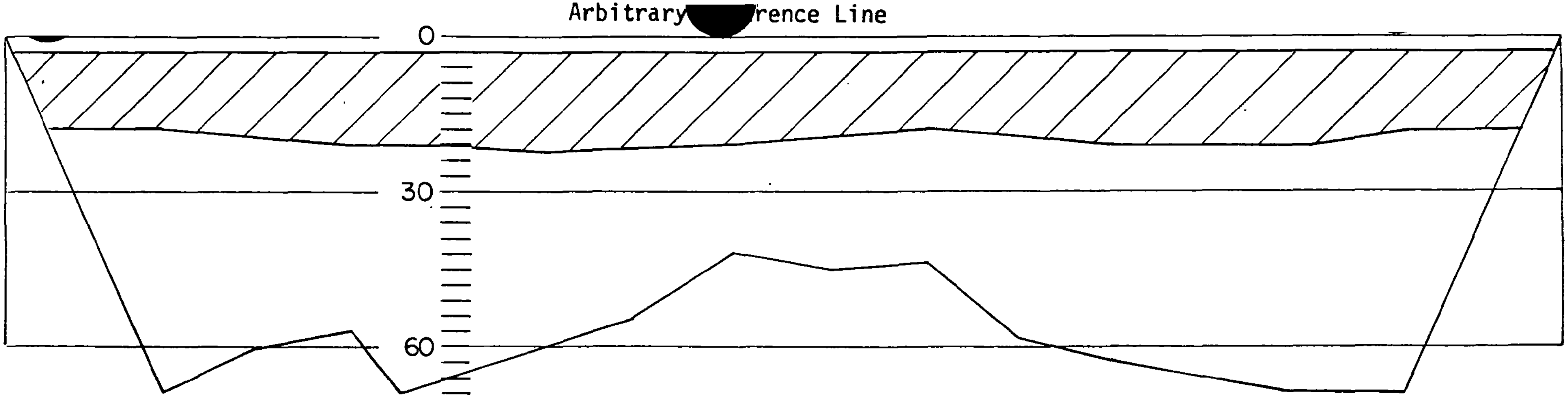

Figure I-14a: Cross-sectional view of channel and surface ice sheet at transect 3, Orcutt Ranch Section, 12/23/75. Vertical scale in cm. below arbitrary datum.

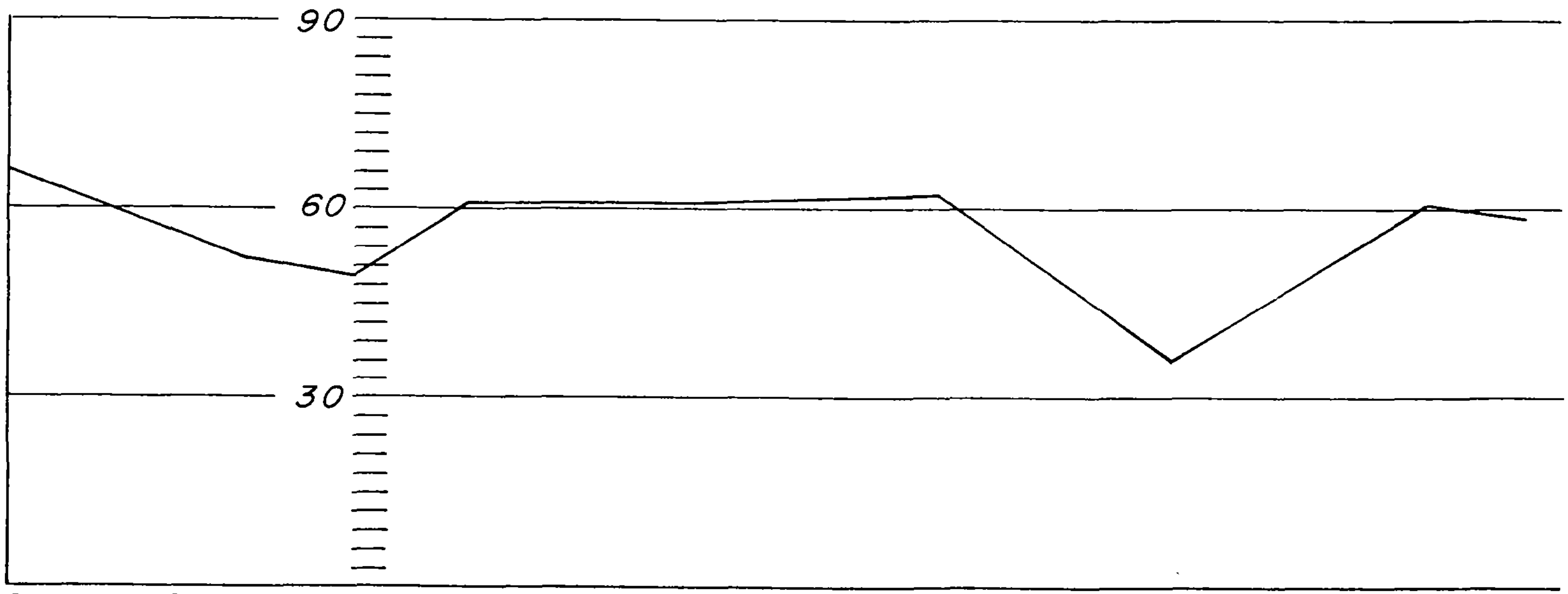

Figure I-14b: Velocities, in cm./sec., at corresponding ice measurement locations on above transect.

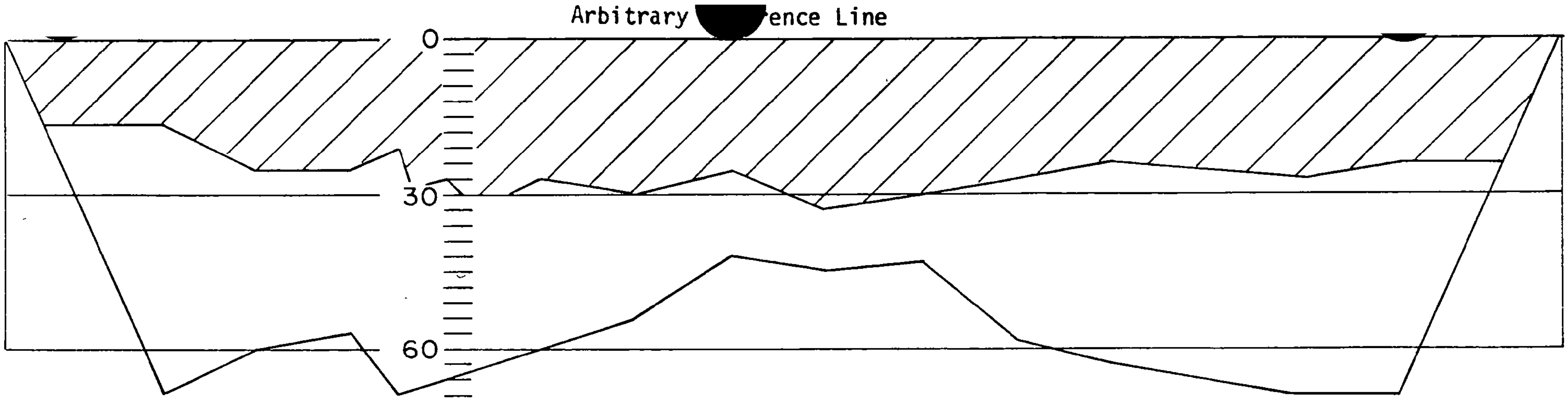

Figure I-15a: Cross-sectional view of channel and surface ice sheet at transect 3, Orcutt Ranch Section, 1/9/76. Vertical scale in cm. below arbitrary datum.

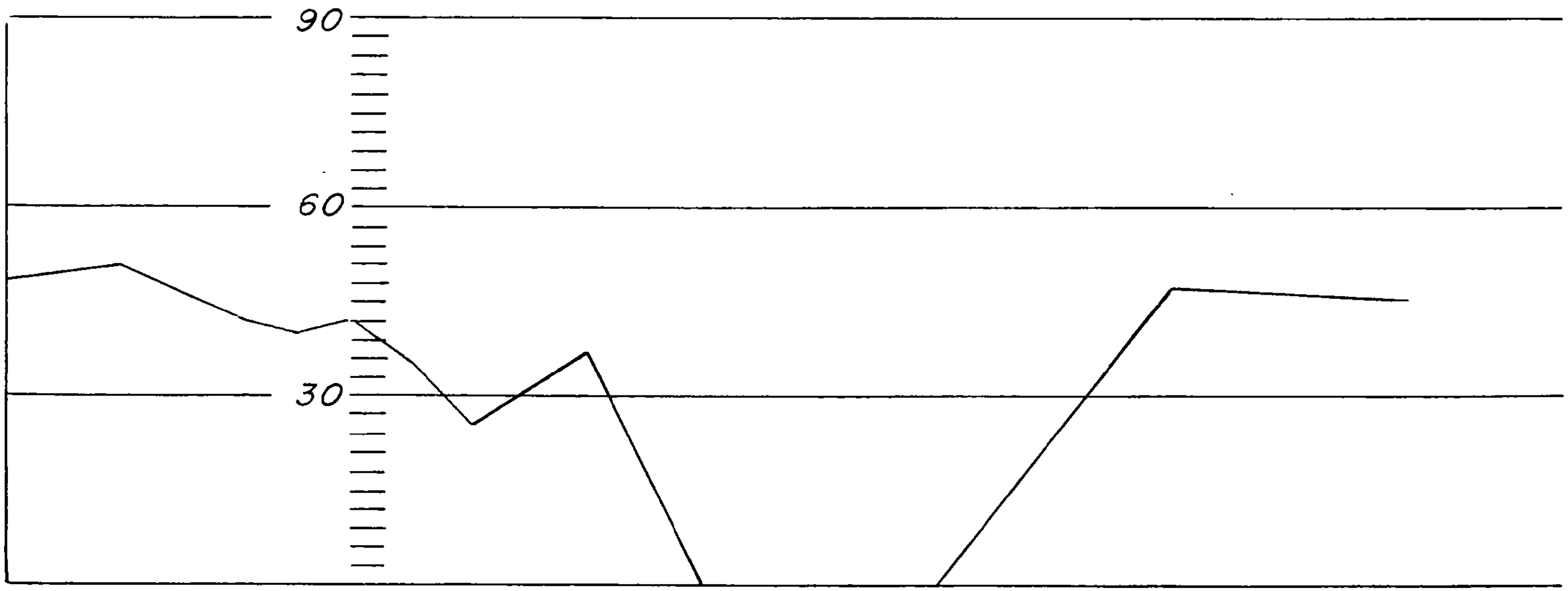

Figure I-15b: Velocities, in cm./sec., at corresponding ice measurement locations on above transect.

APPENDIX J

VEGETATION MAPS OF TONGUE RIVER FLOODPLAIN

LEGEND

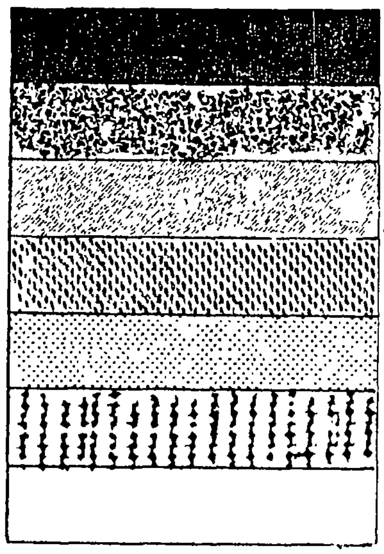

100% Cover
90% Cover
75% Cover
50% Cover
25% Cover
10% Cover
0% Cover

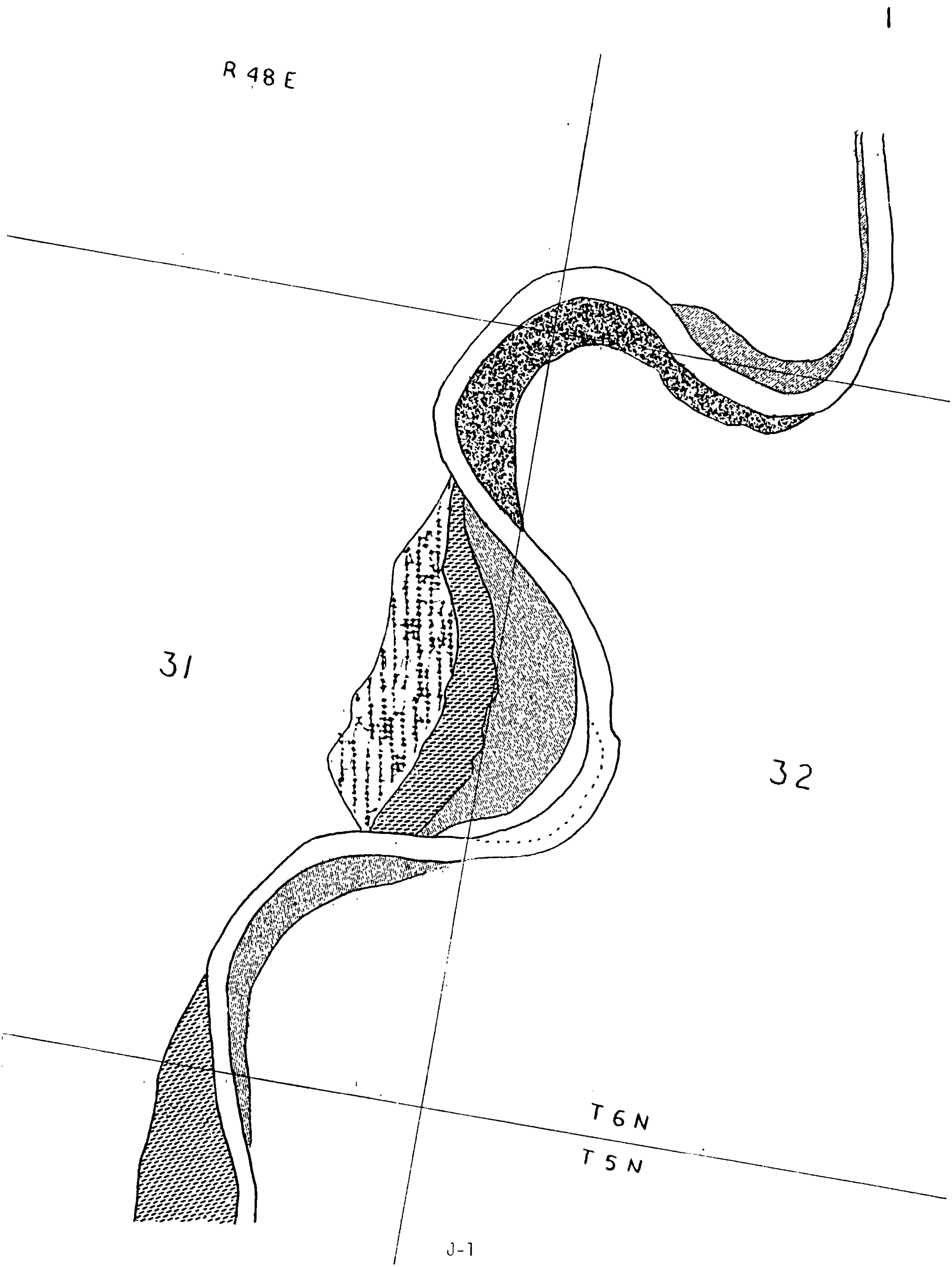
1
R 48 E
31
32
T 6 N
T 5 N

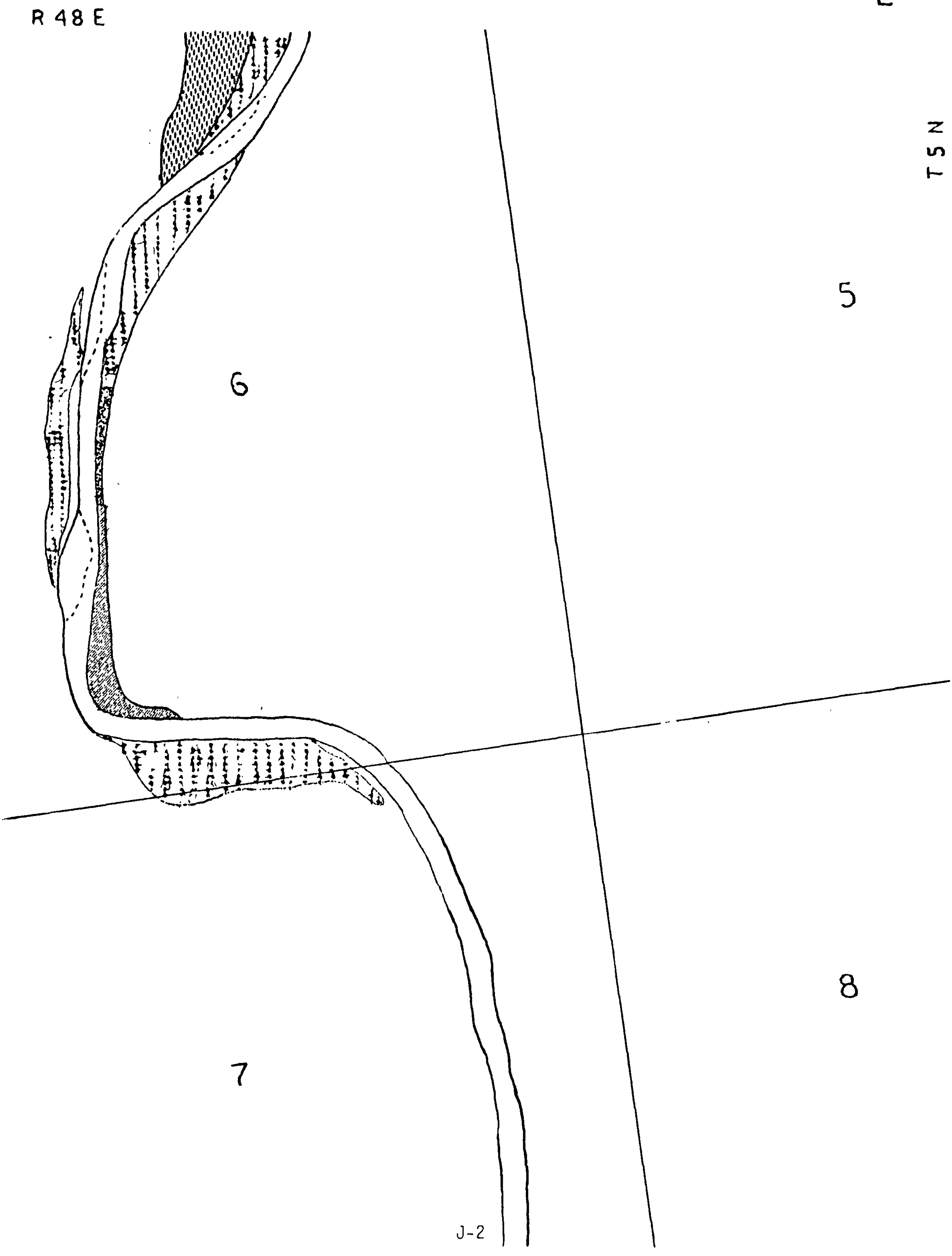
R 48 E
T 5 N
5
6
7
8

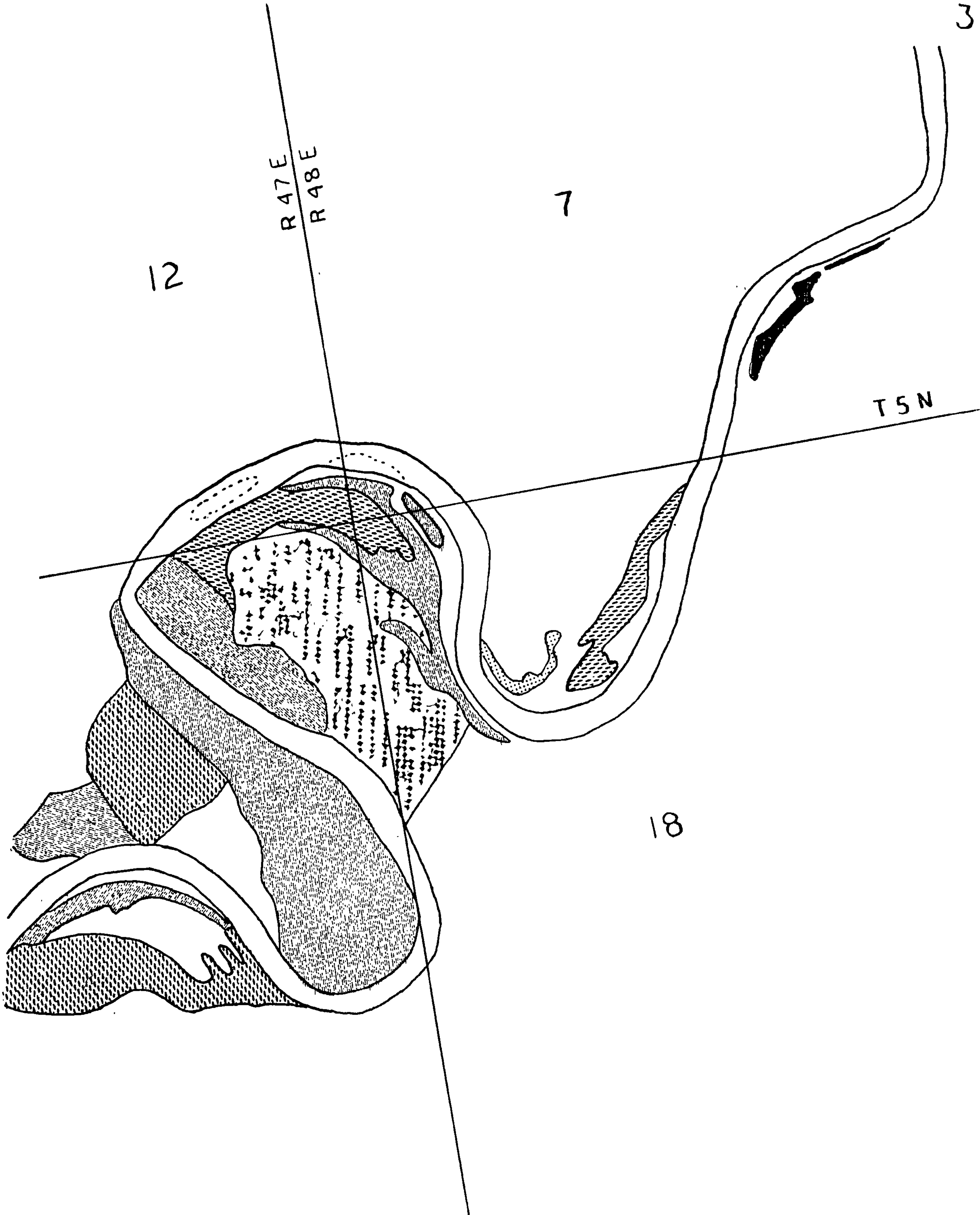
3
R 47 E
R 48 E
7
12
T 5 N
18

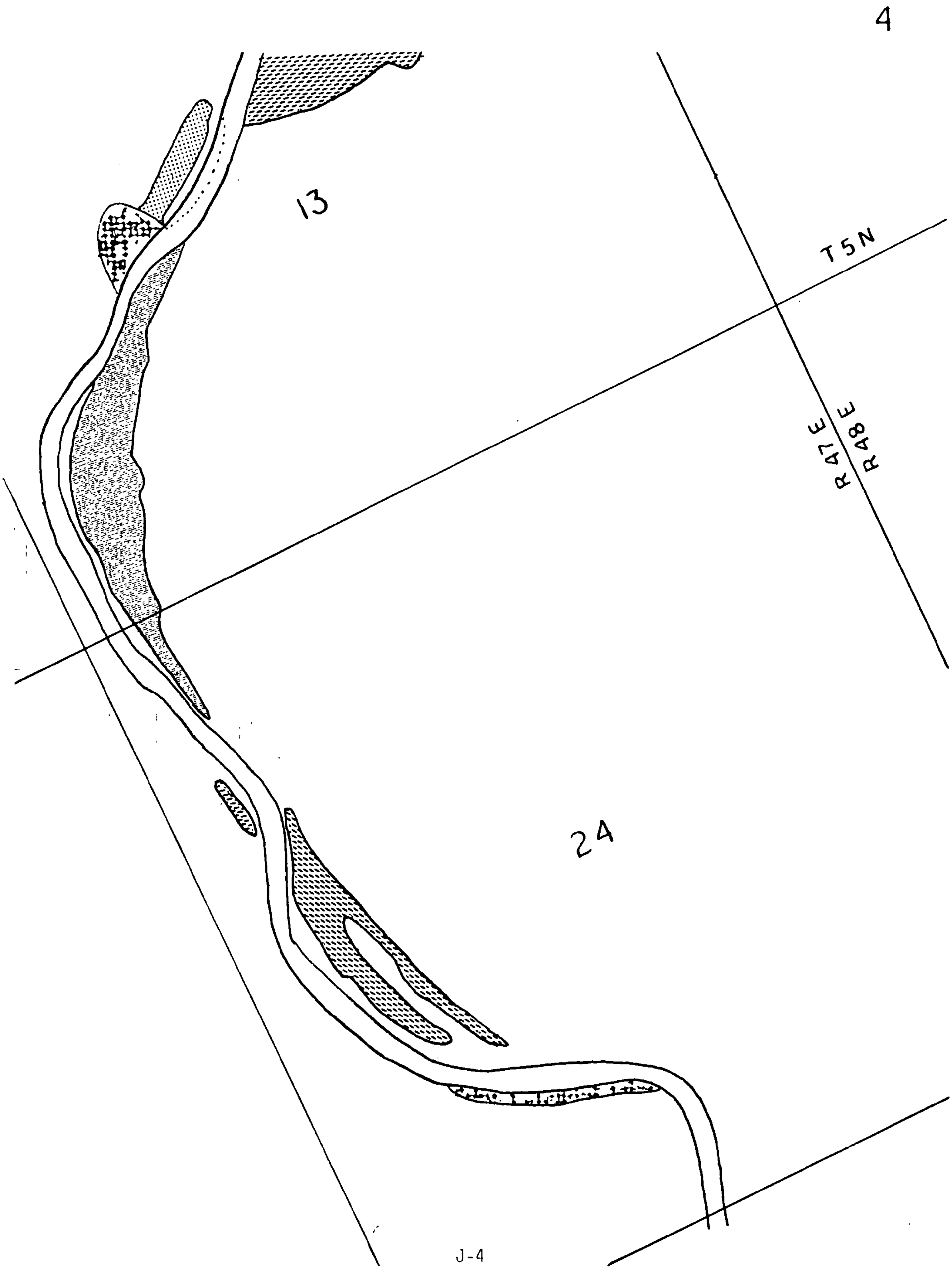

4
13
T5N
R47E
R48E
24

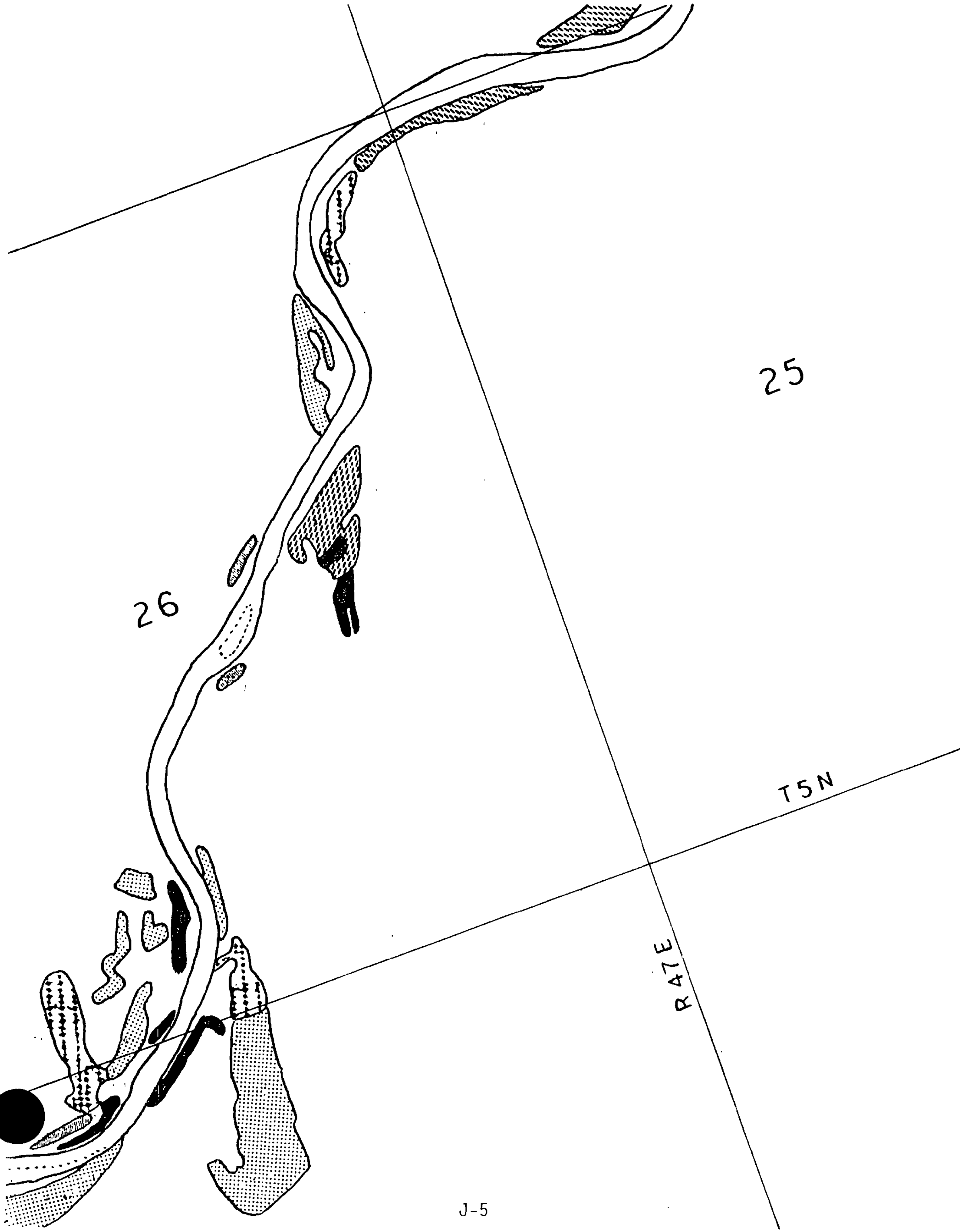
25
26
T5N
R47E

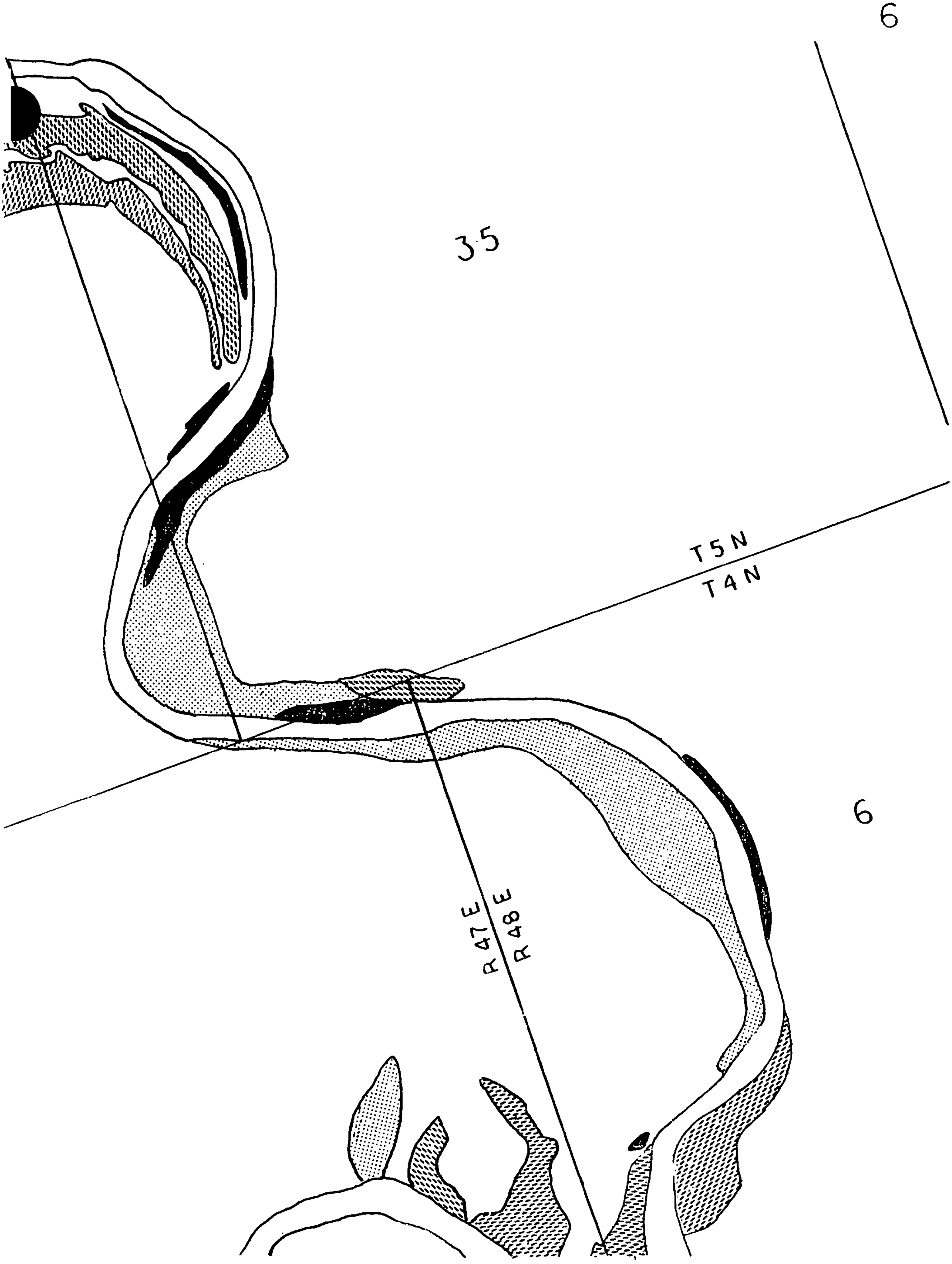

6
35
T5N
T4N
6
R47E
R48E

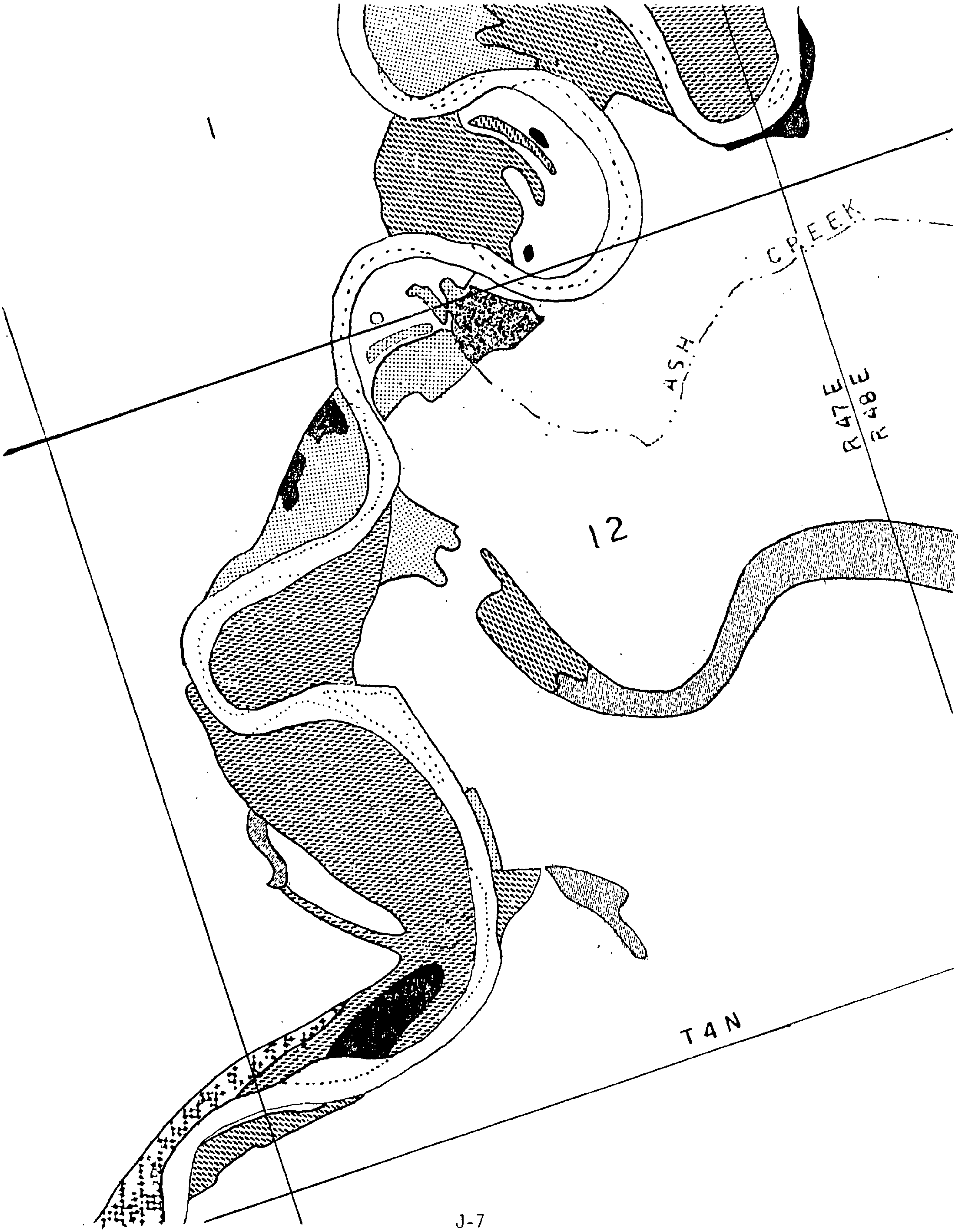
1
ASH CREEK
R 47 E
R 48 E
12
T 4 N

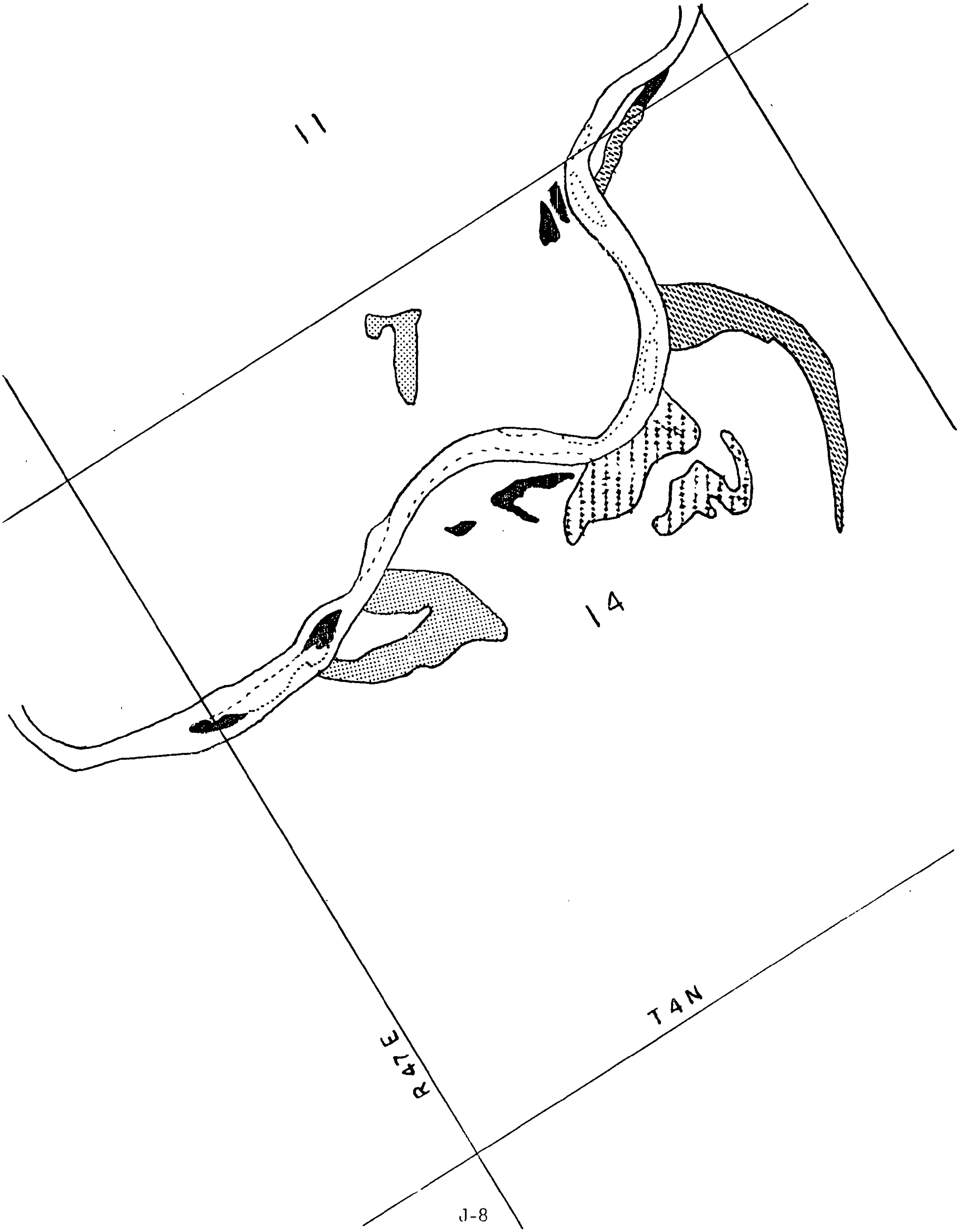
11
14
R47E
T4N


22
21
T 4 N
R 47 E

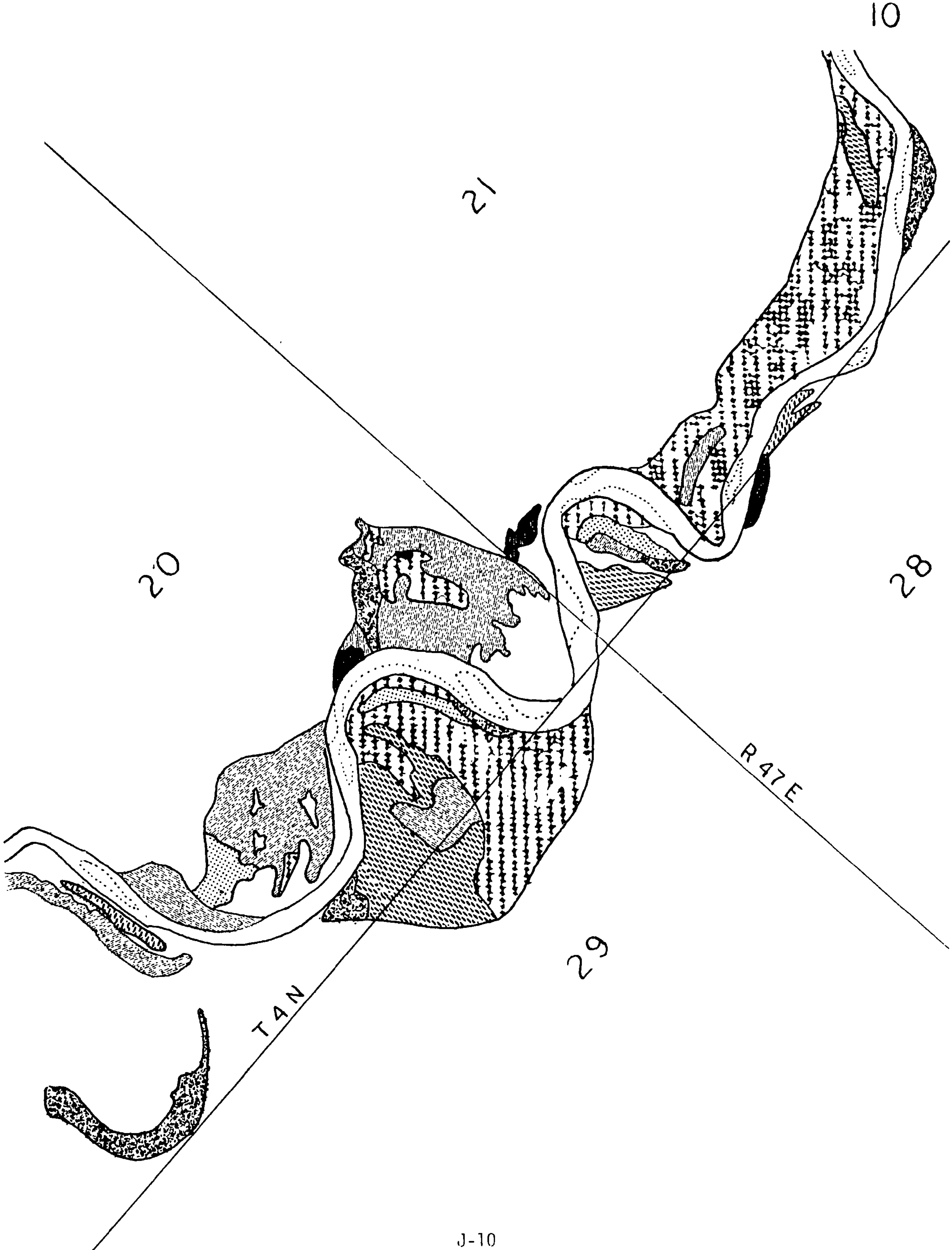
10
21
20
28
R47E
29
TAN

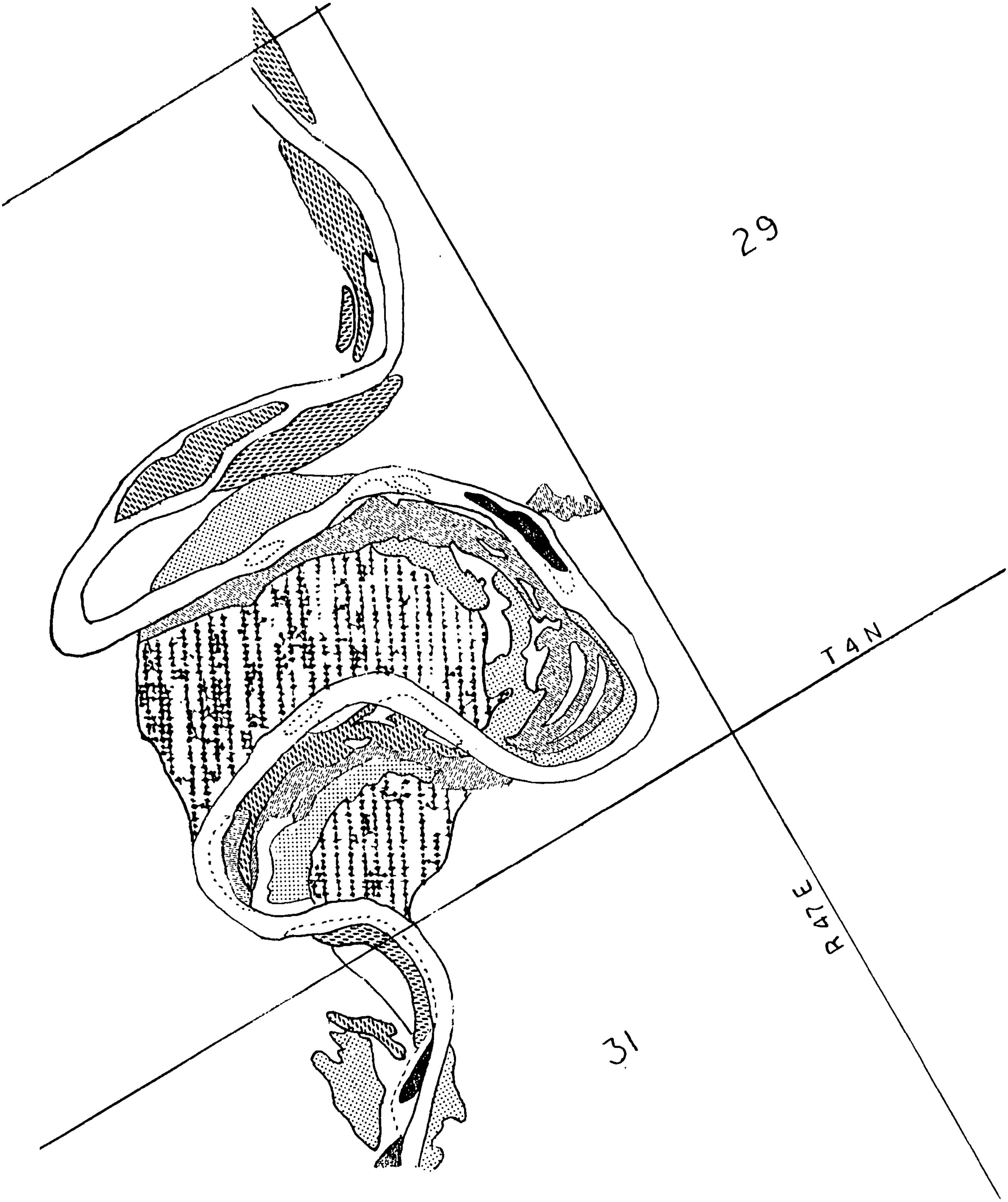
29
T4N
R47E
31


12
HADDOW CREEK
T4N
T3N
6
R46E
R47E
1

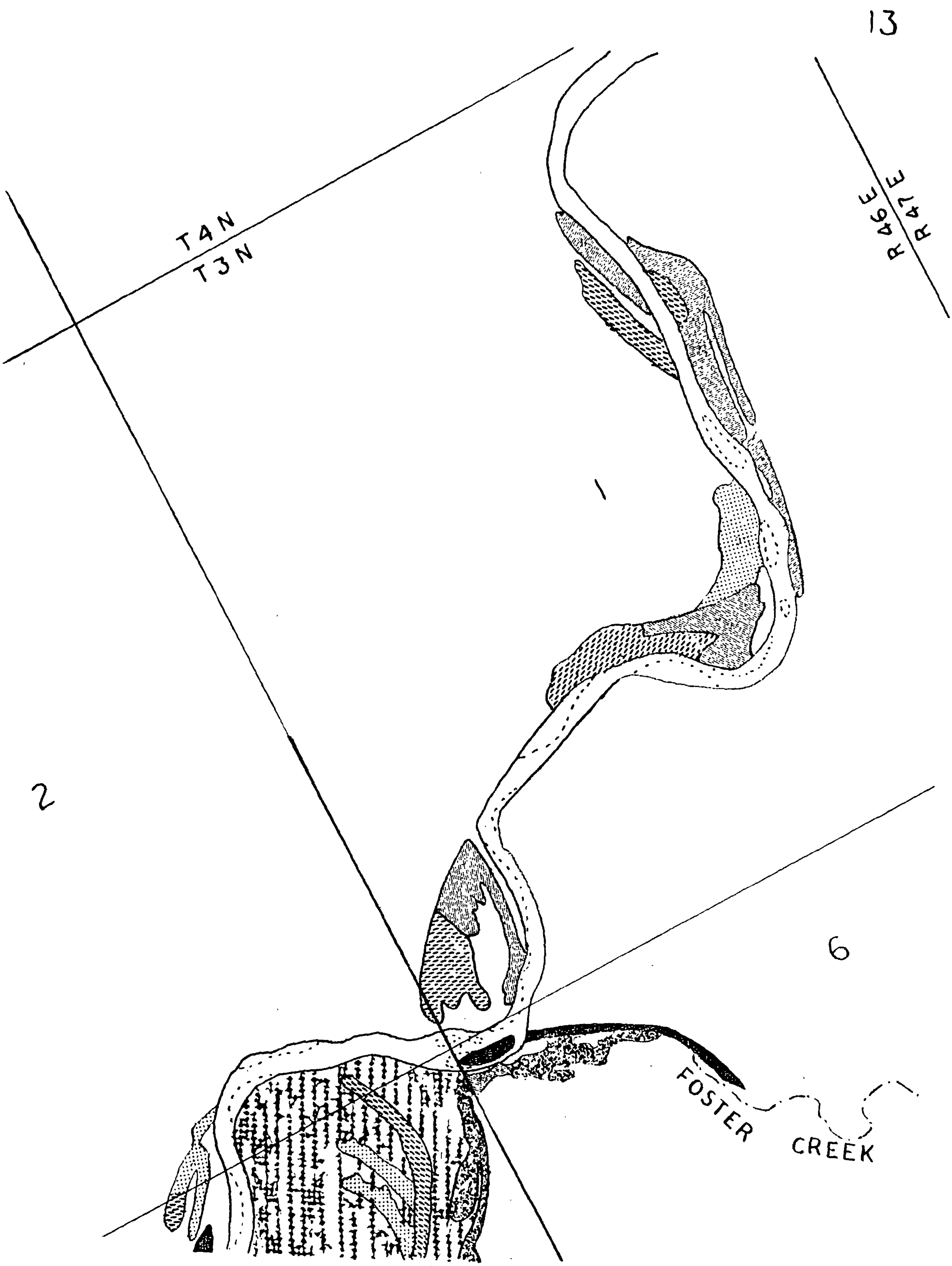

13
T4N
T3N
R46E
R47E
1
2
6
FOSTER
CREEK

GARLAND SCHOOL
11
R46E
T3N
14

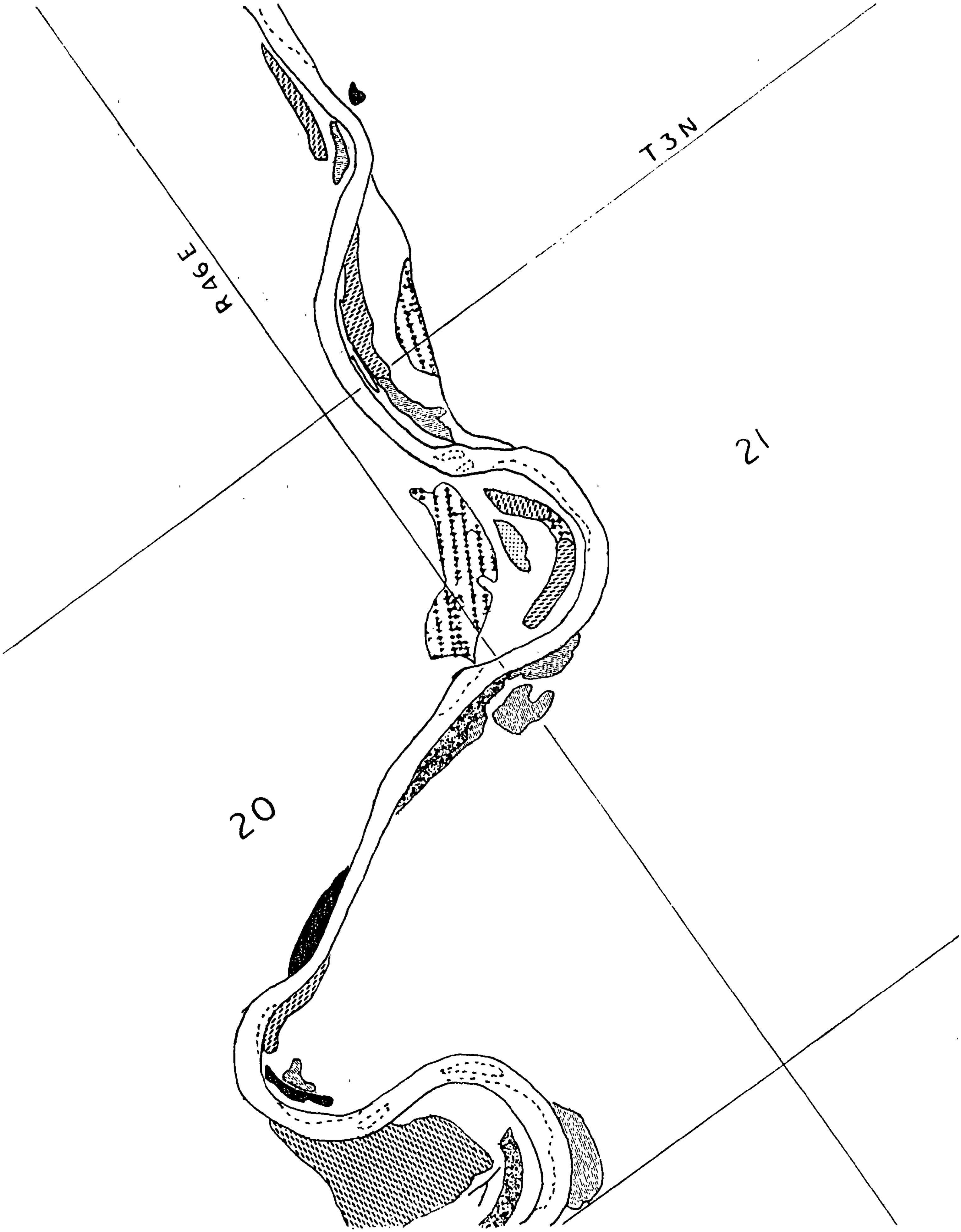
T3N
R46E
21
20

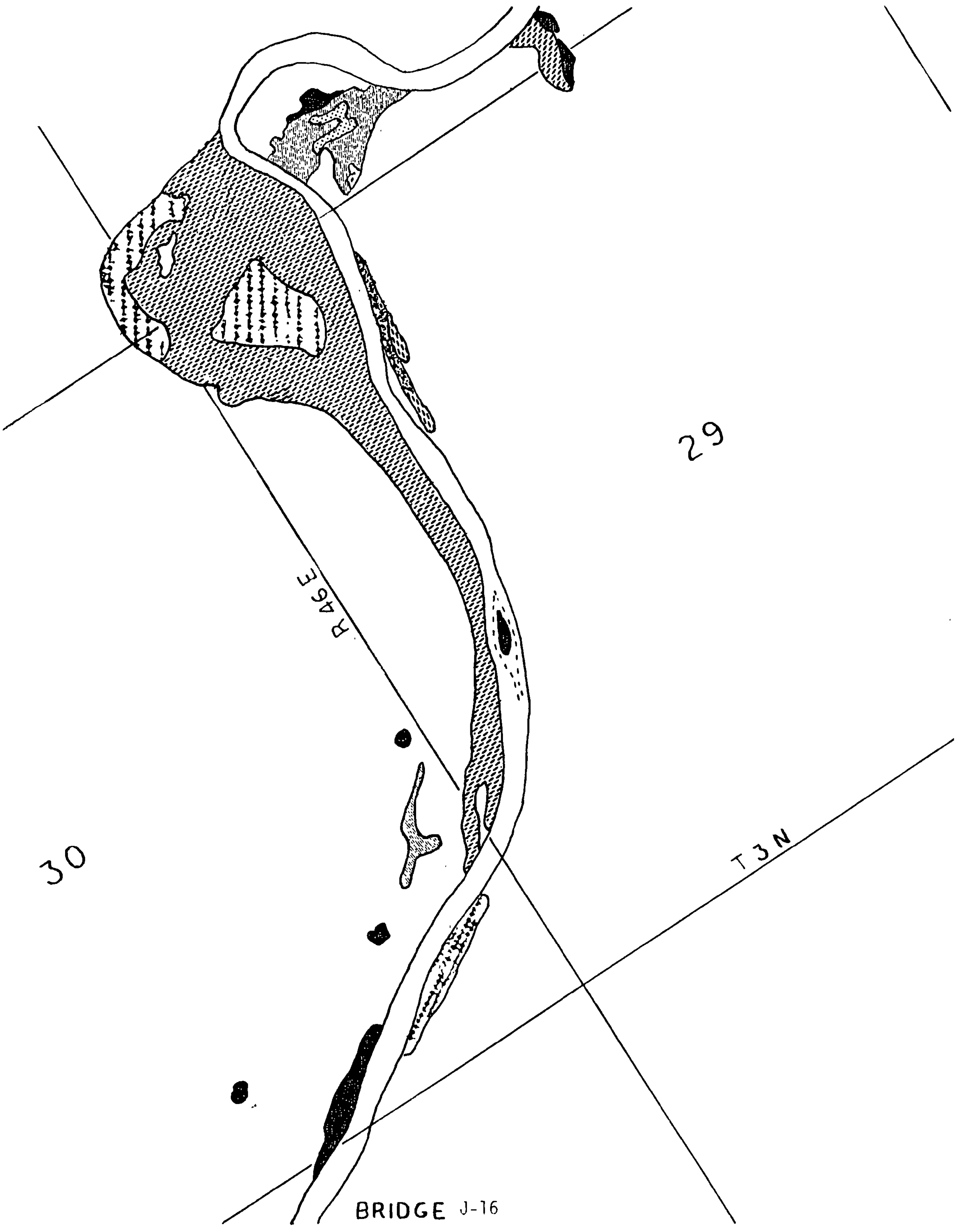
29
R 46 E
30
T 3 N
BRIDGE J-16

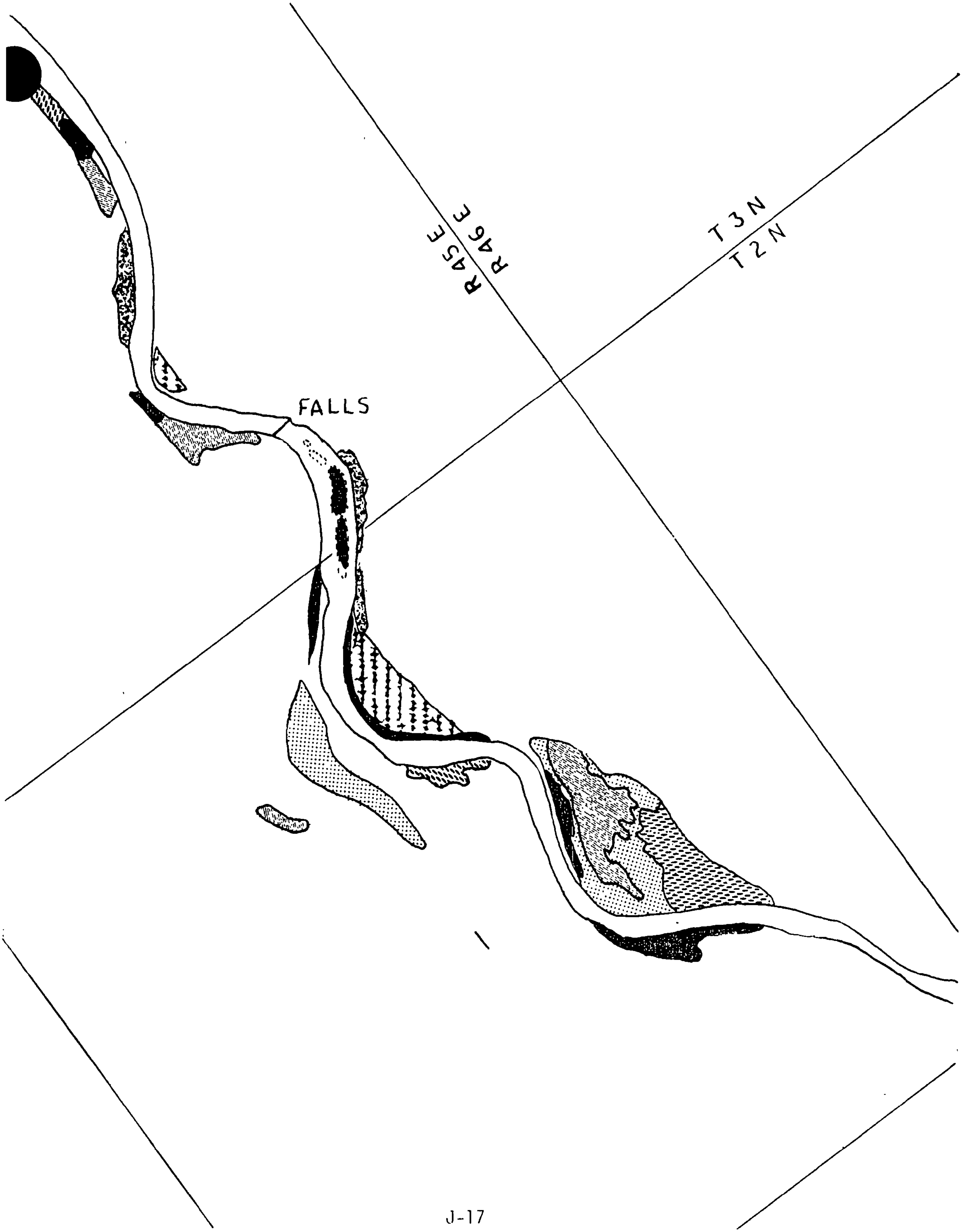
R45E
R46E
T3N
T2N
FALLS

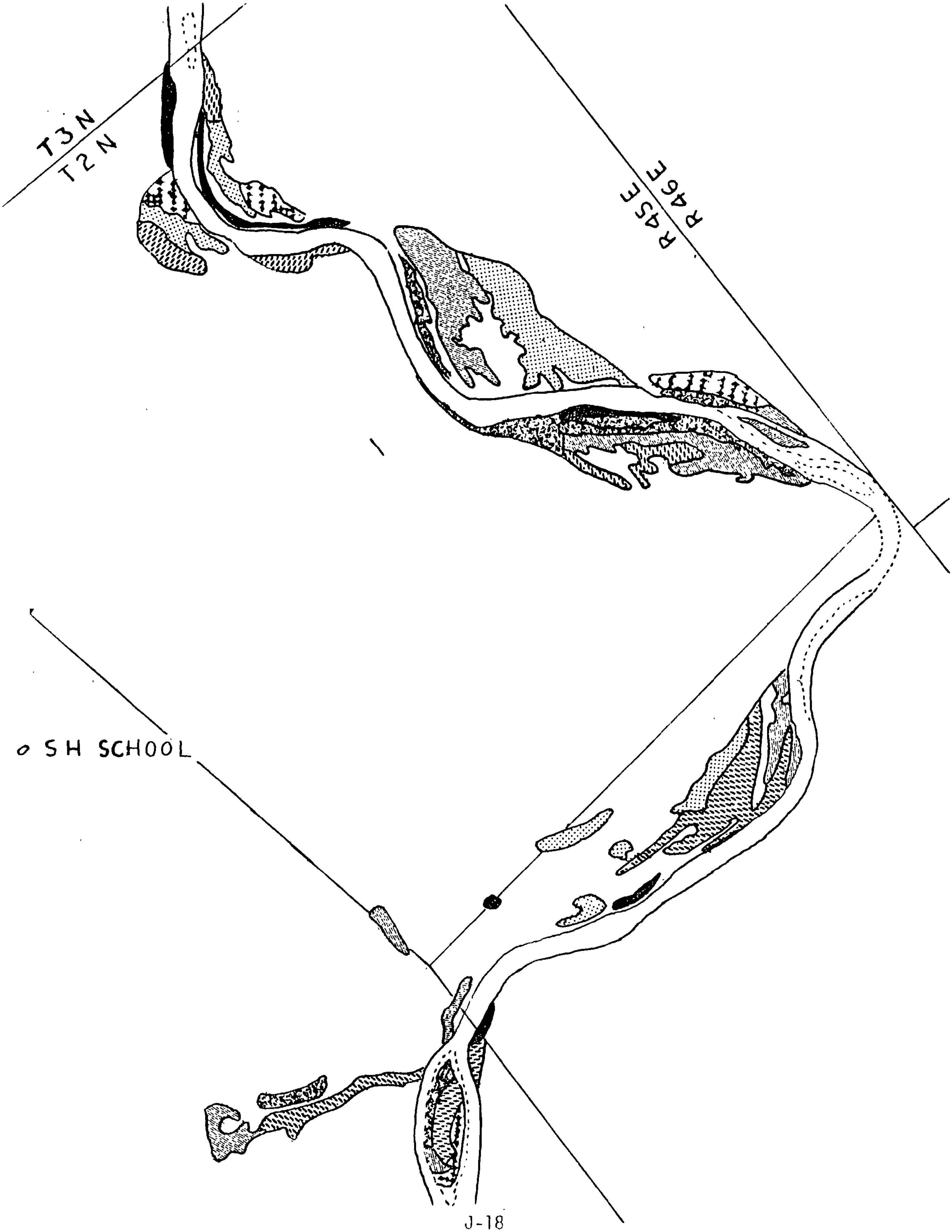
T3N
T2N
R45E
R46E
o SH SCHOOL

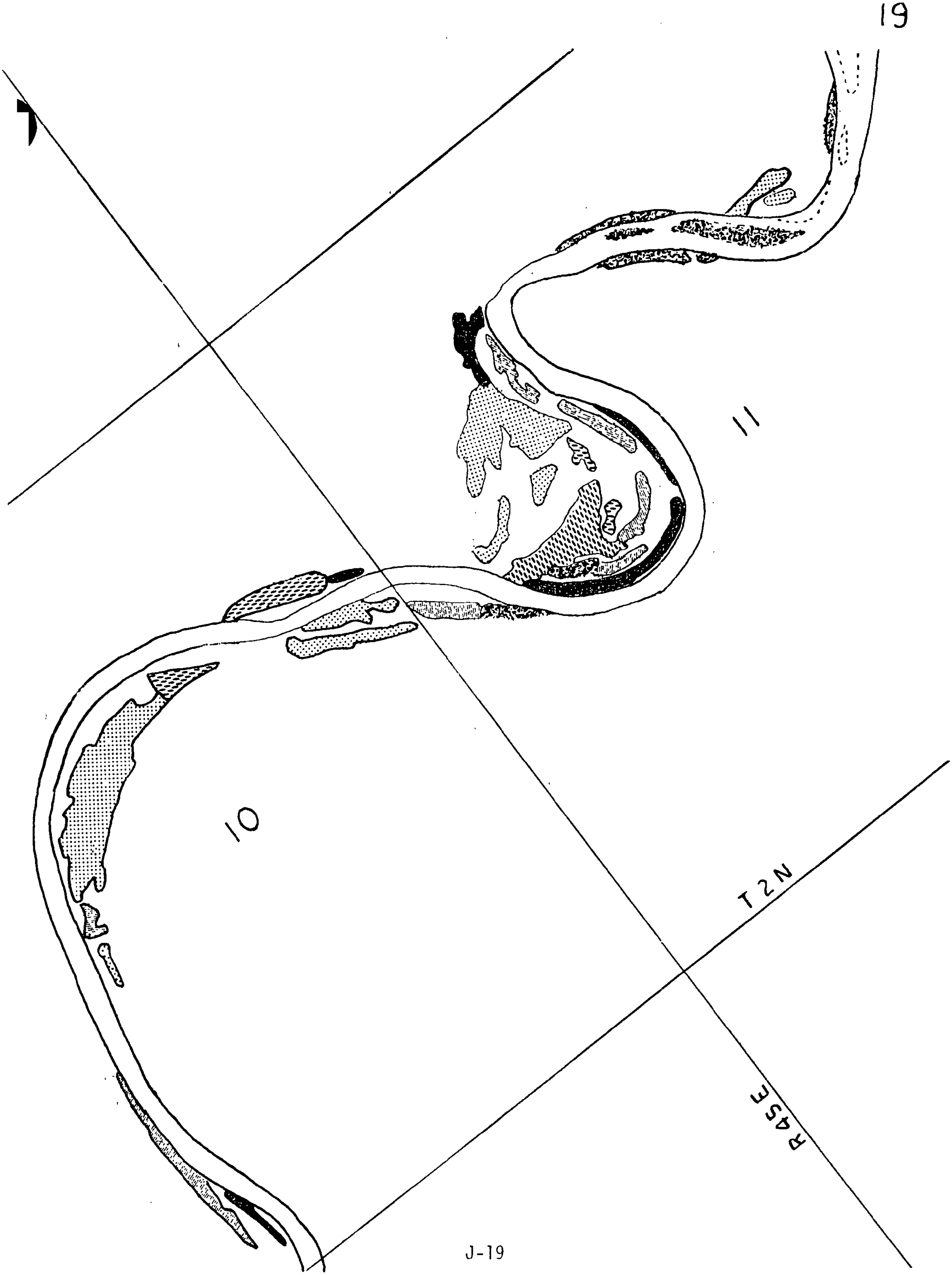
19
11
10
T2N
R45E

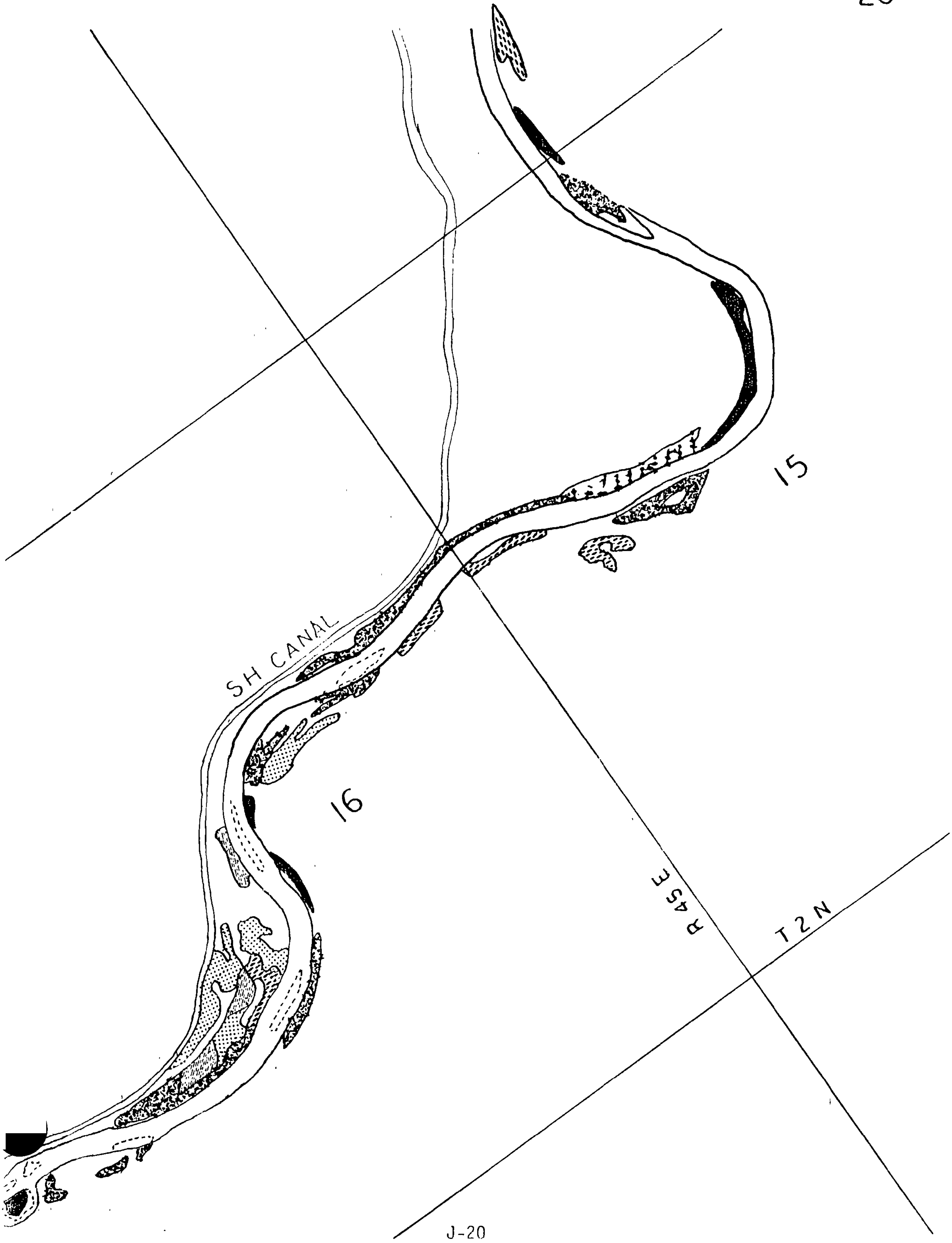
SH CANAL
15
16
R 4 5 E
T 2 N

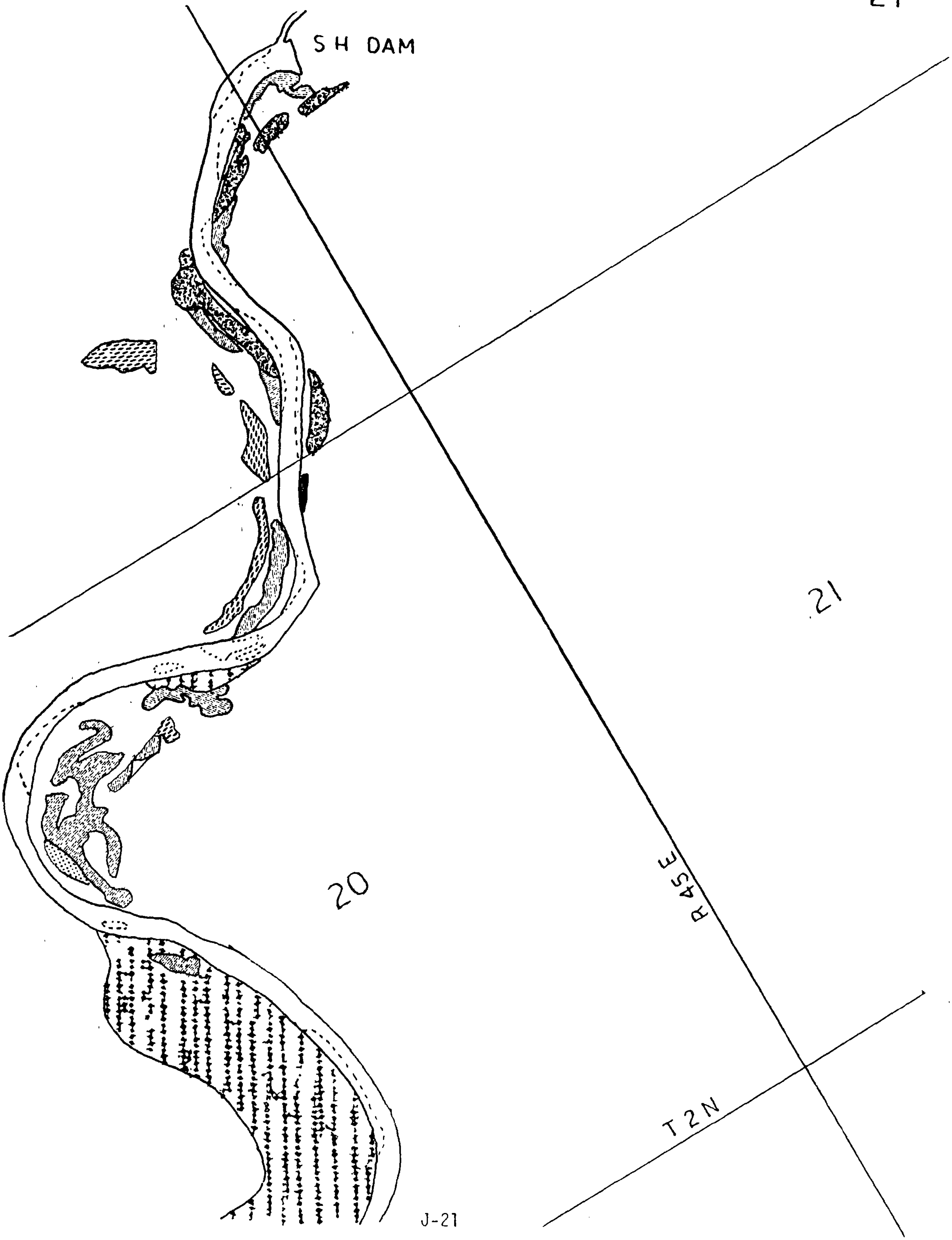
S H DAM
21
20
R 45 E
T 2 N

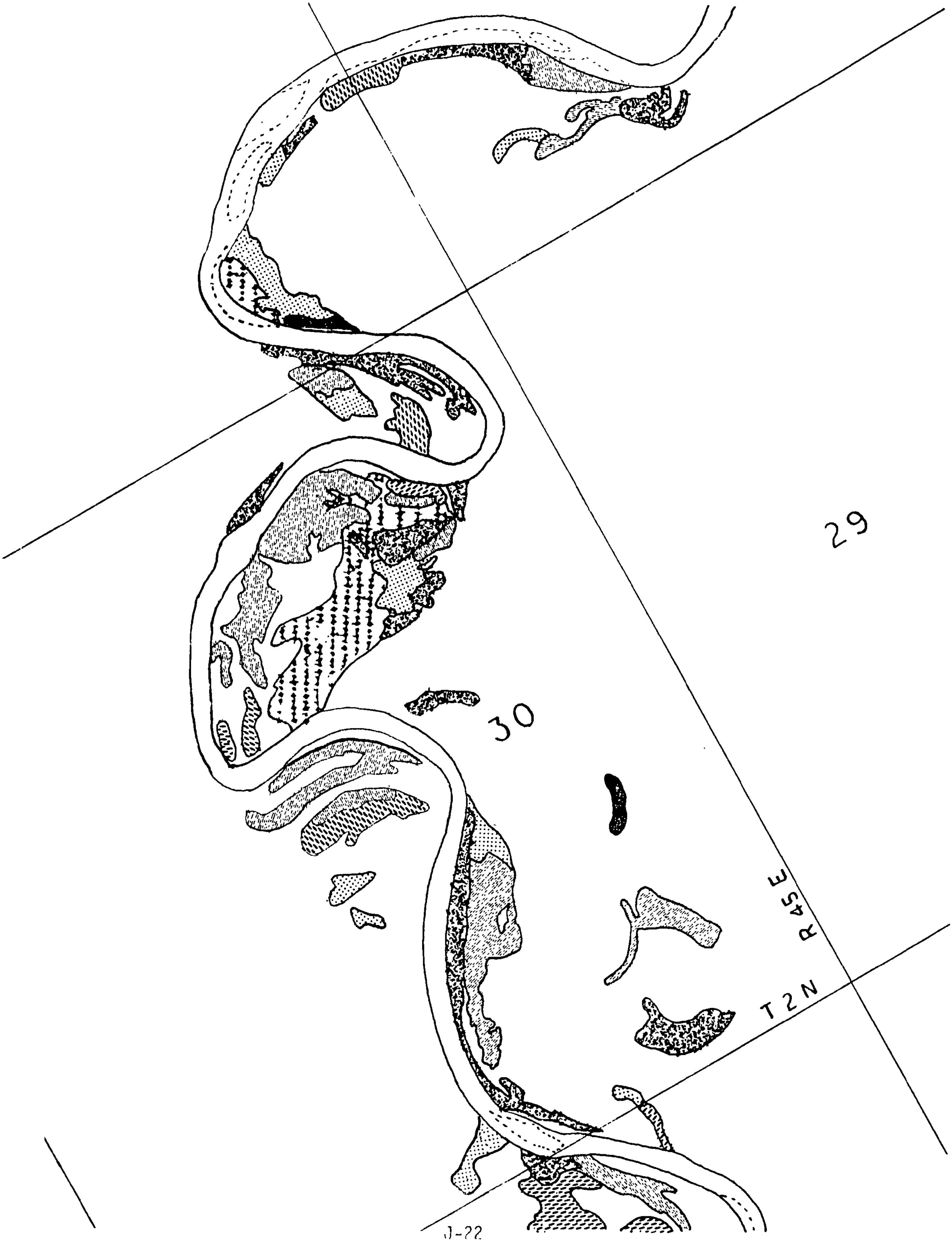
29
30
R 45 E
T 2 N

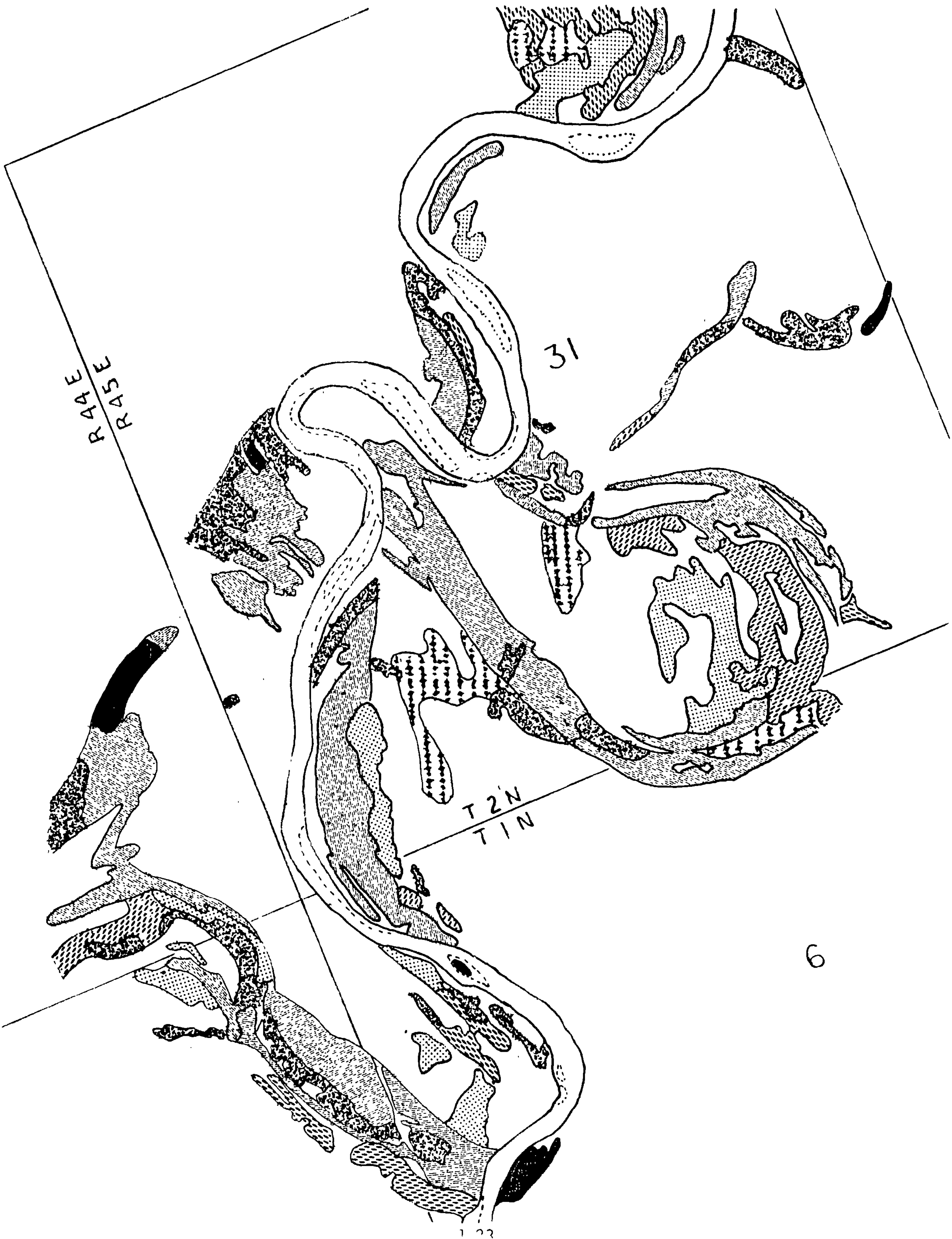
R44E
R45E
31
T2N
T1N
6

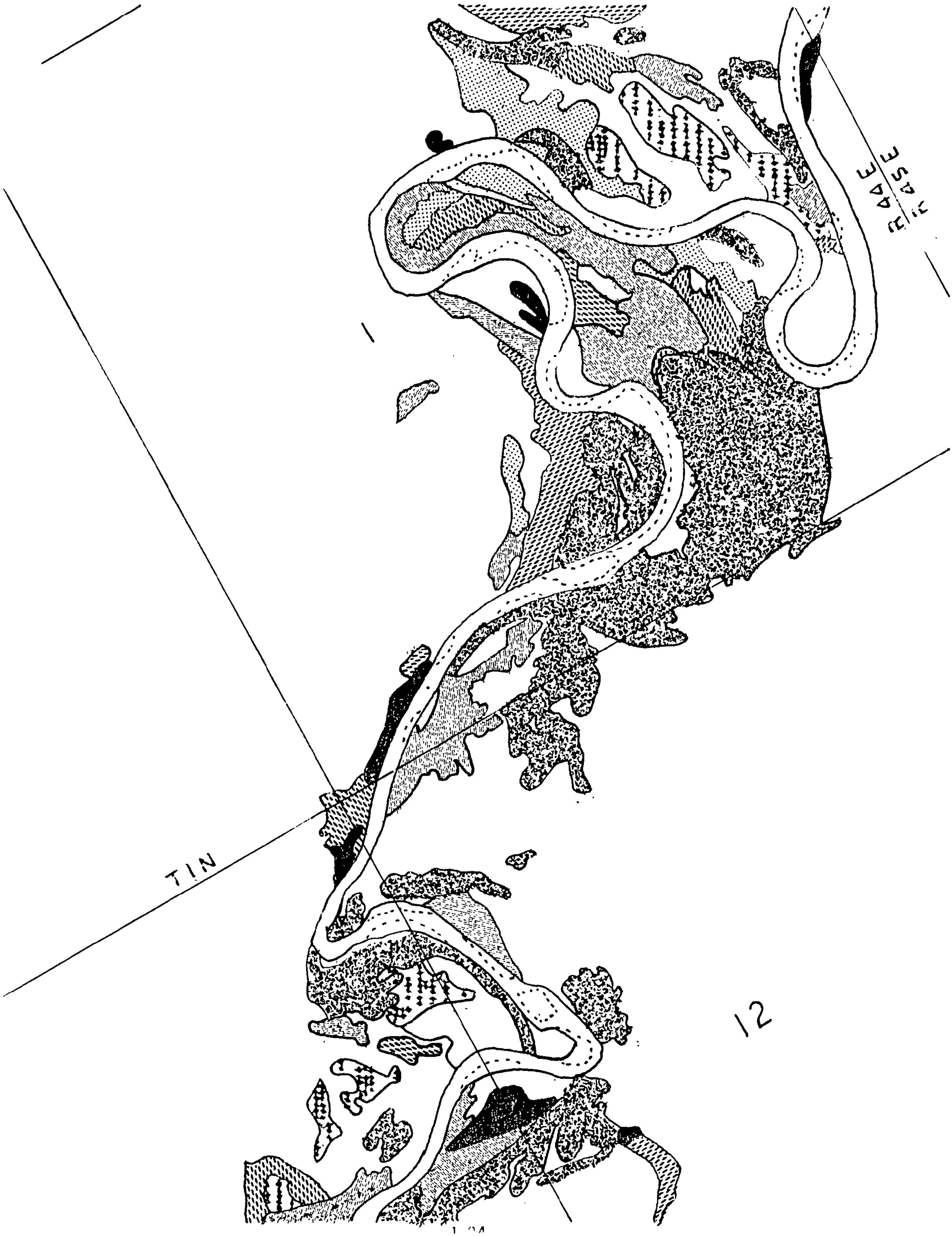
R44E
R45E
1
T1N
12

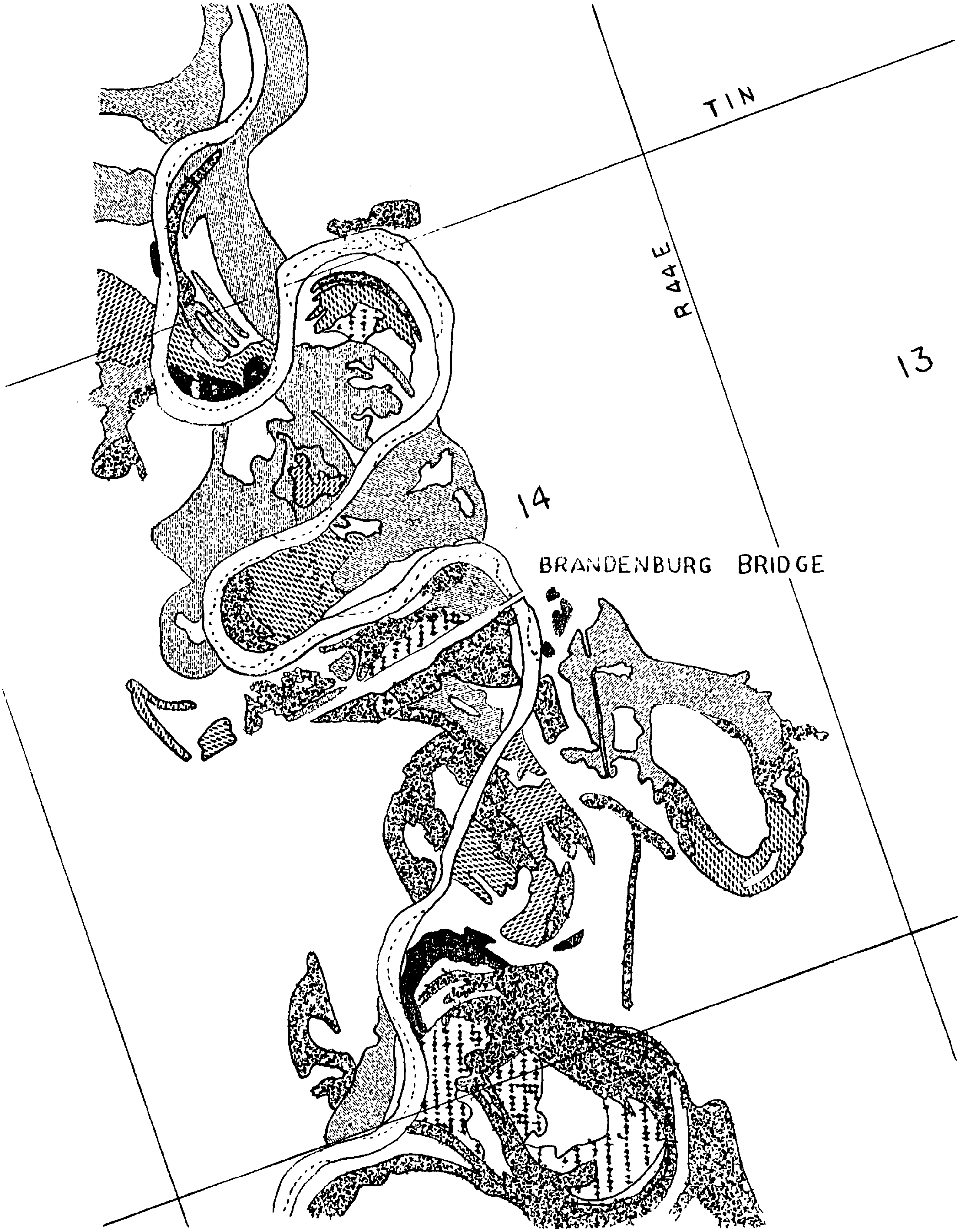
TIN
R44E
13
14
BRANDENBURG BRIDGE

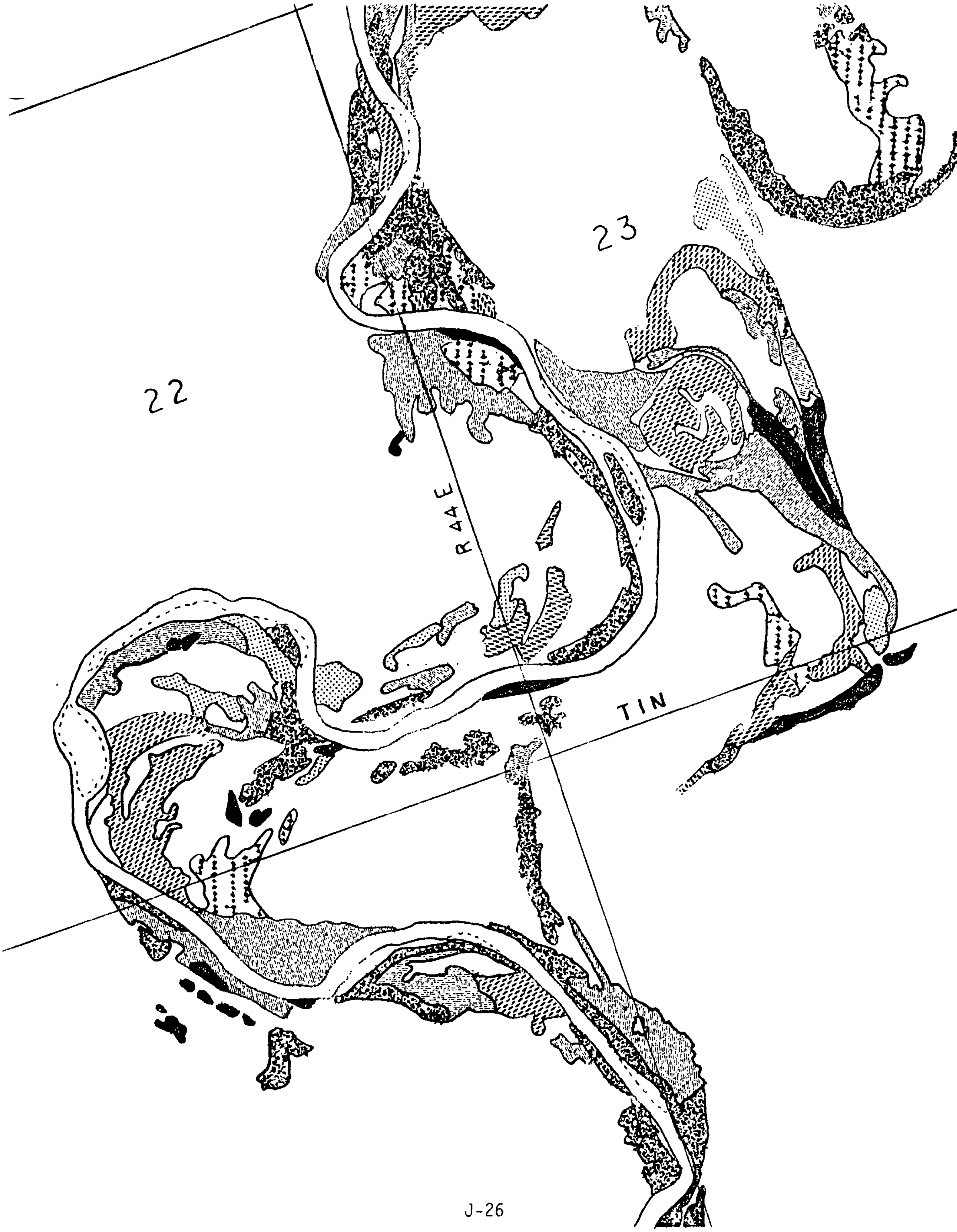
23
22
R 44 E
T1N

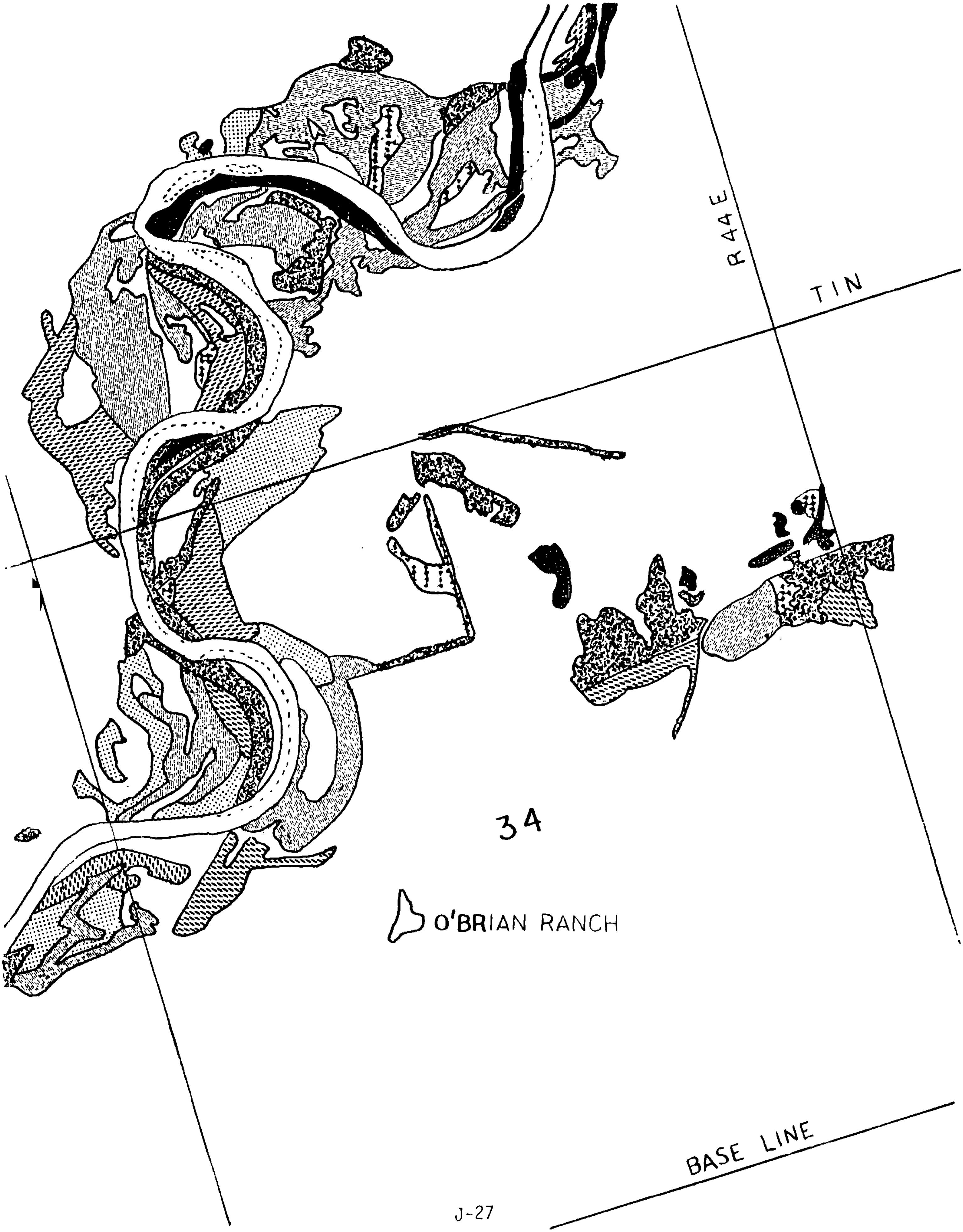
R44E
TIN
34
O'BRIAN RANCH
BASE LINE

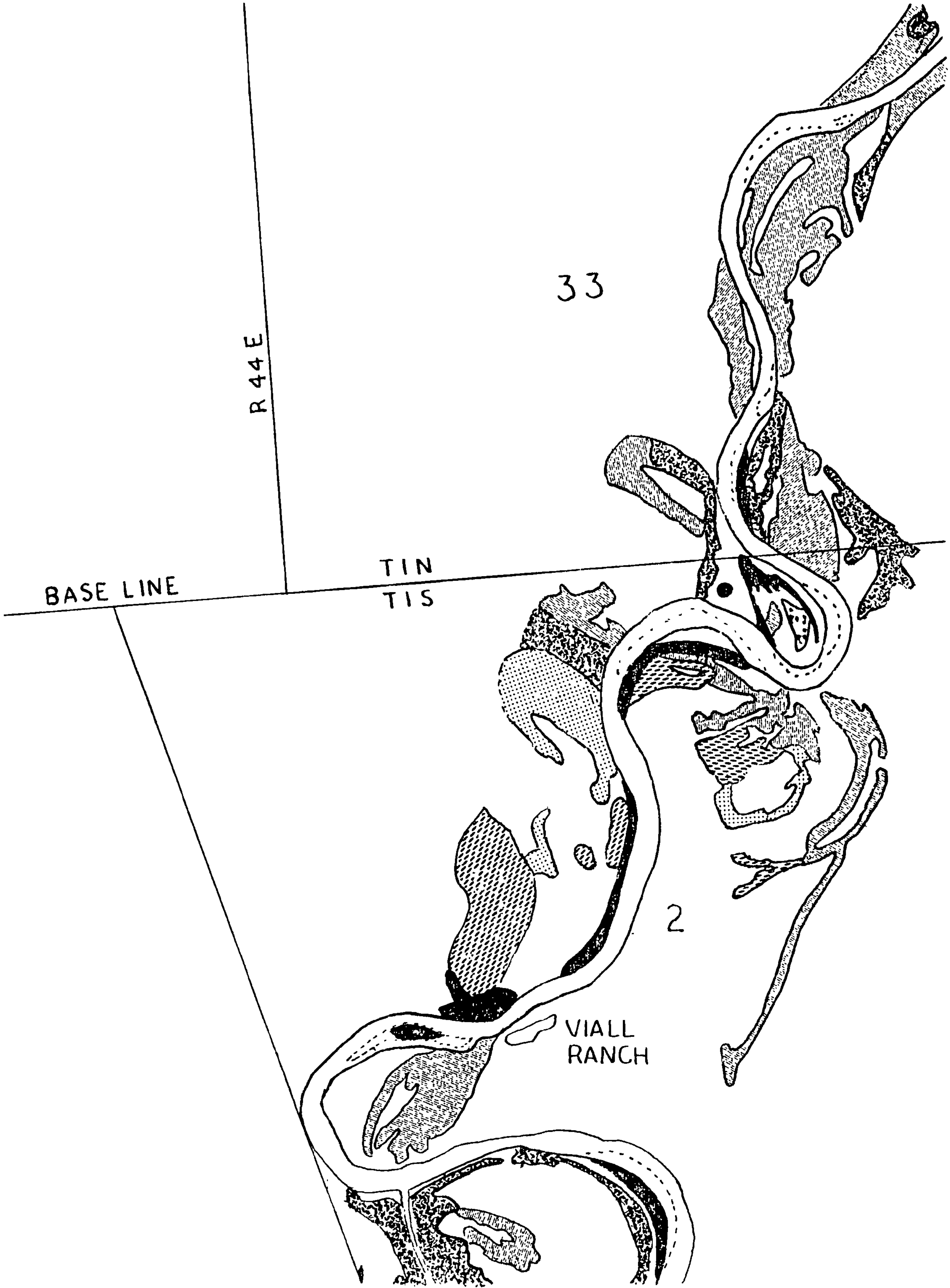
R 44 E
33
BASE LINE
TIN
TIS
2
VIALL
RANCH

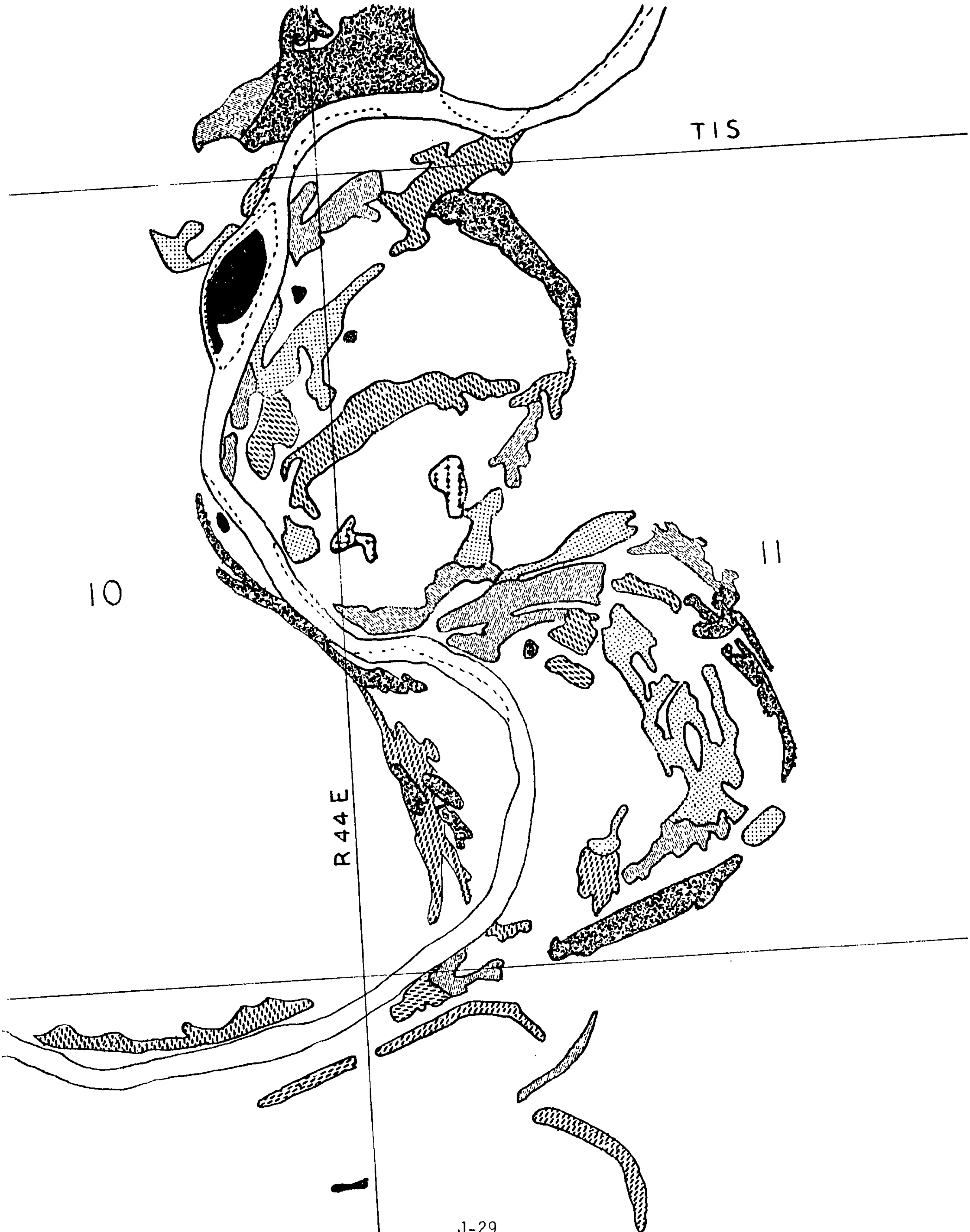
T1S
10
11
R44E

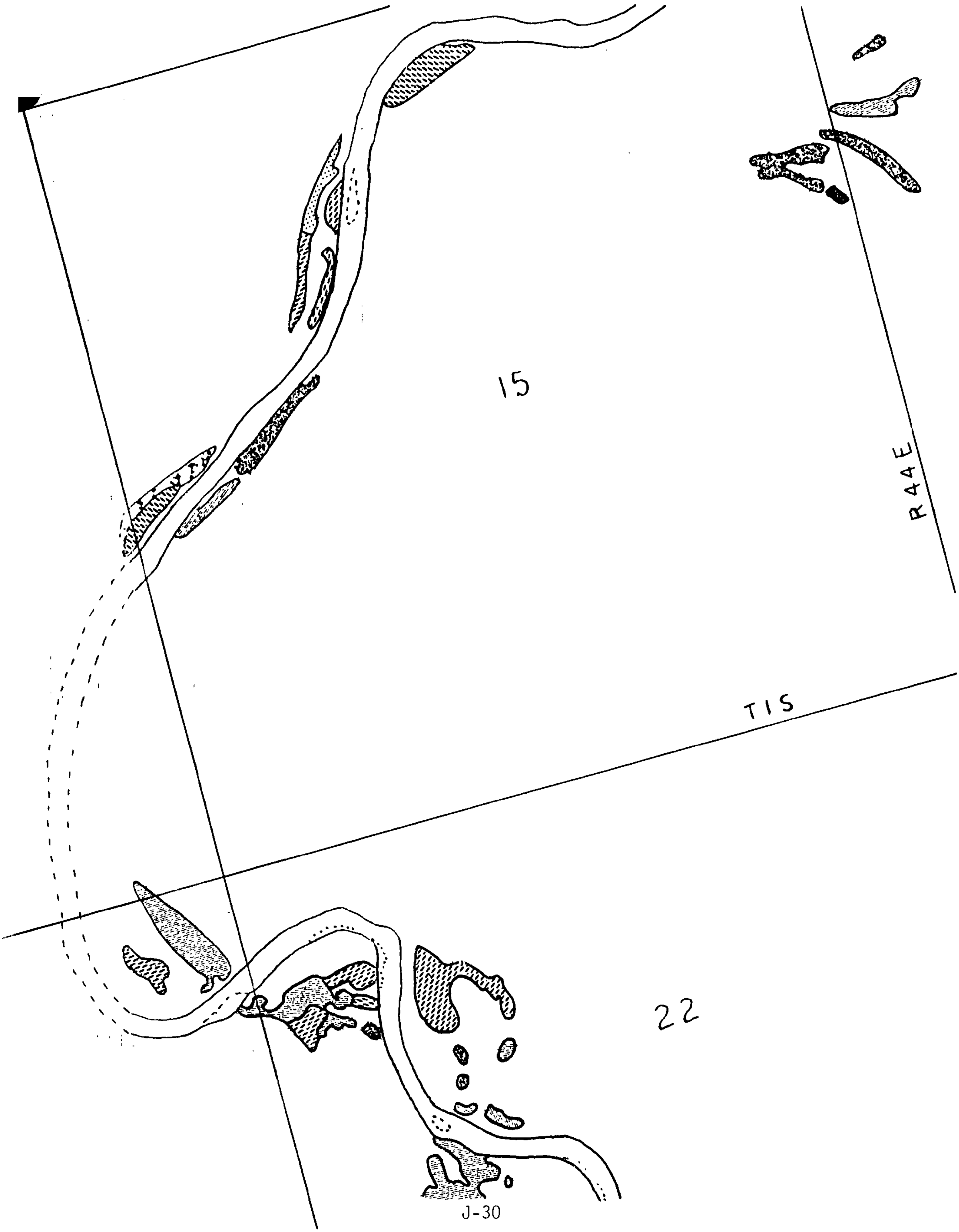
15
R44E
T1S
22

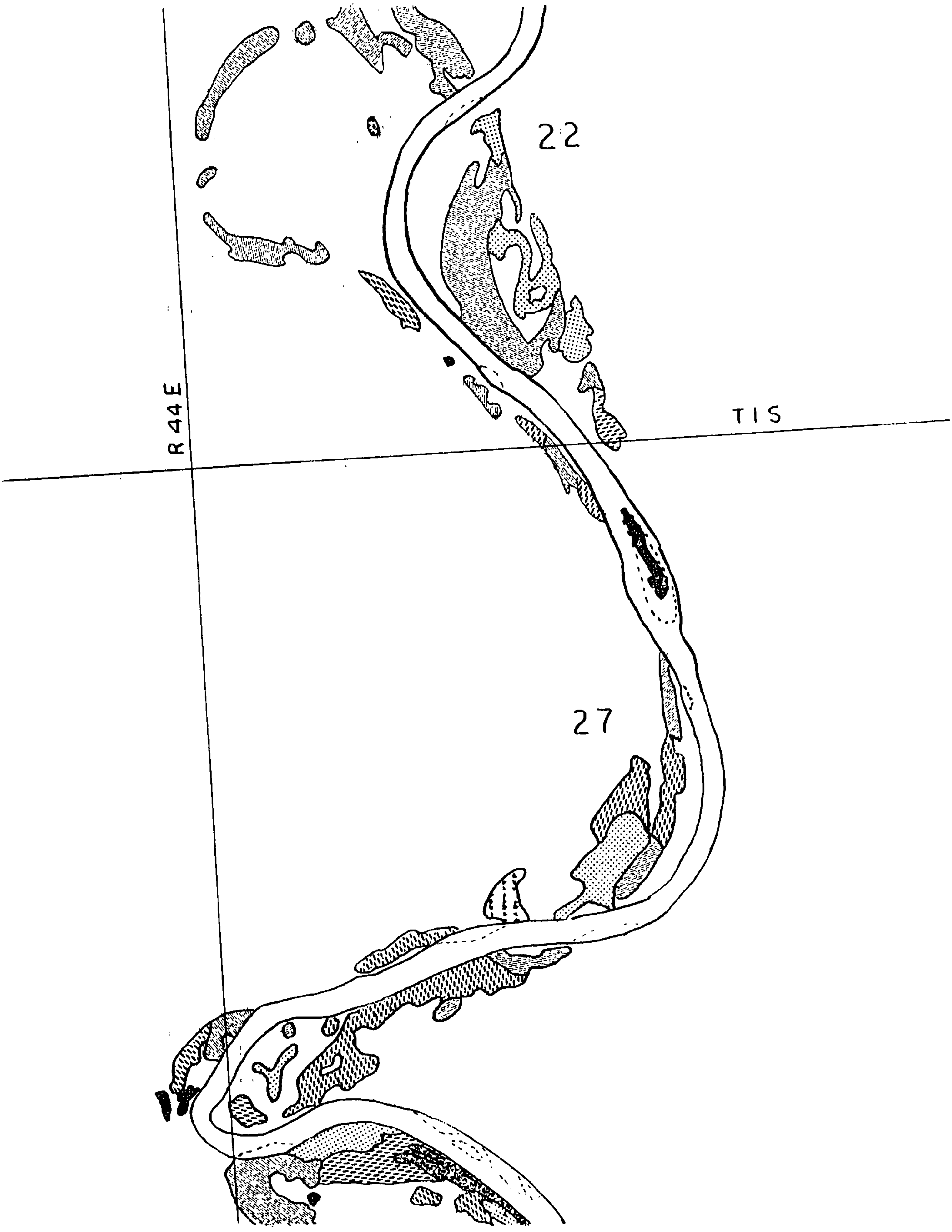
22
T1S
R44E
27

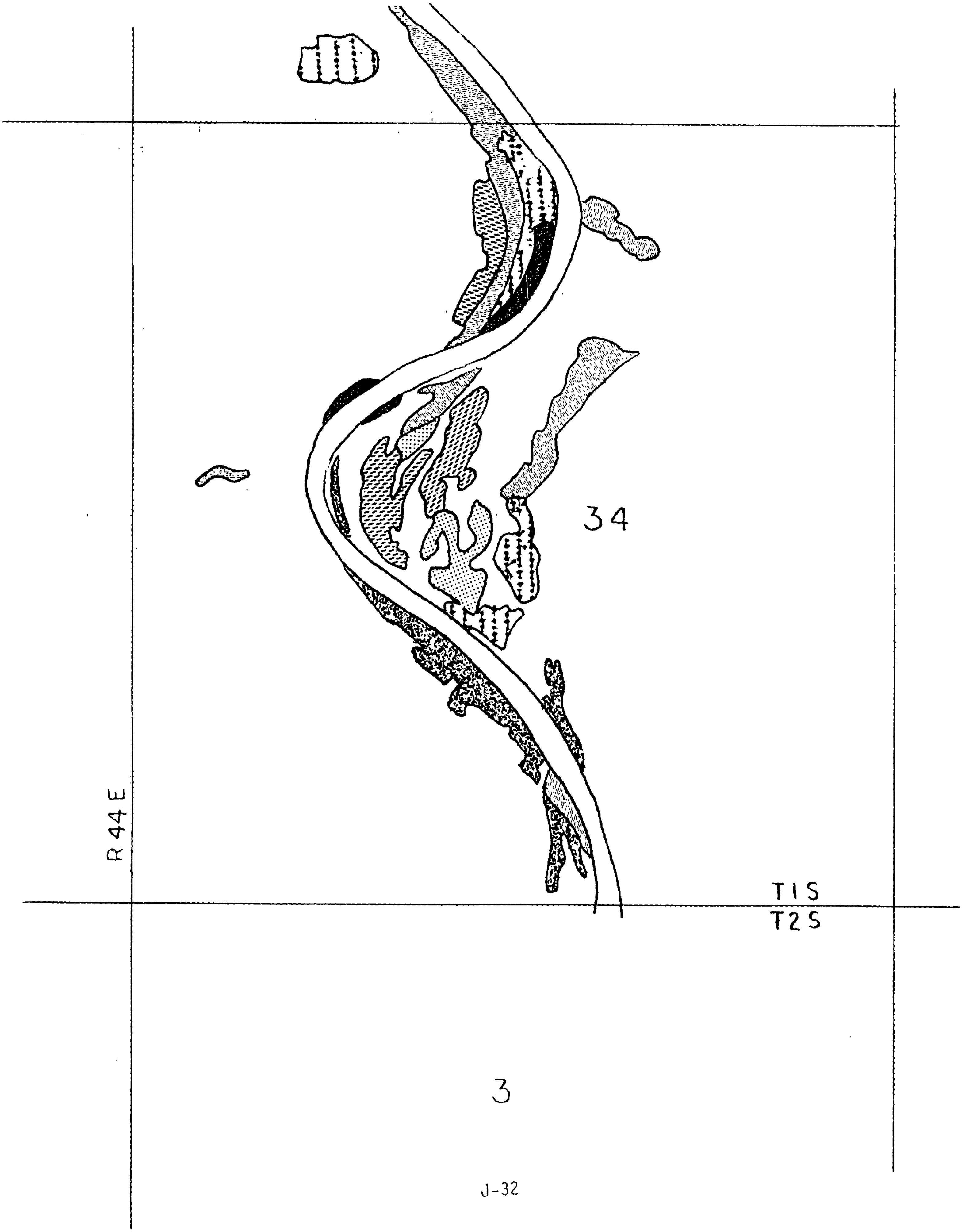
34
R 44 E
T1S
T2S
3

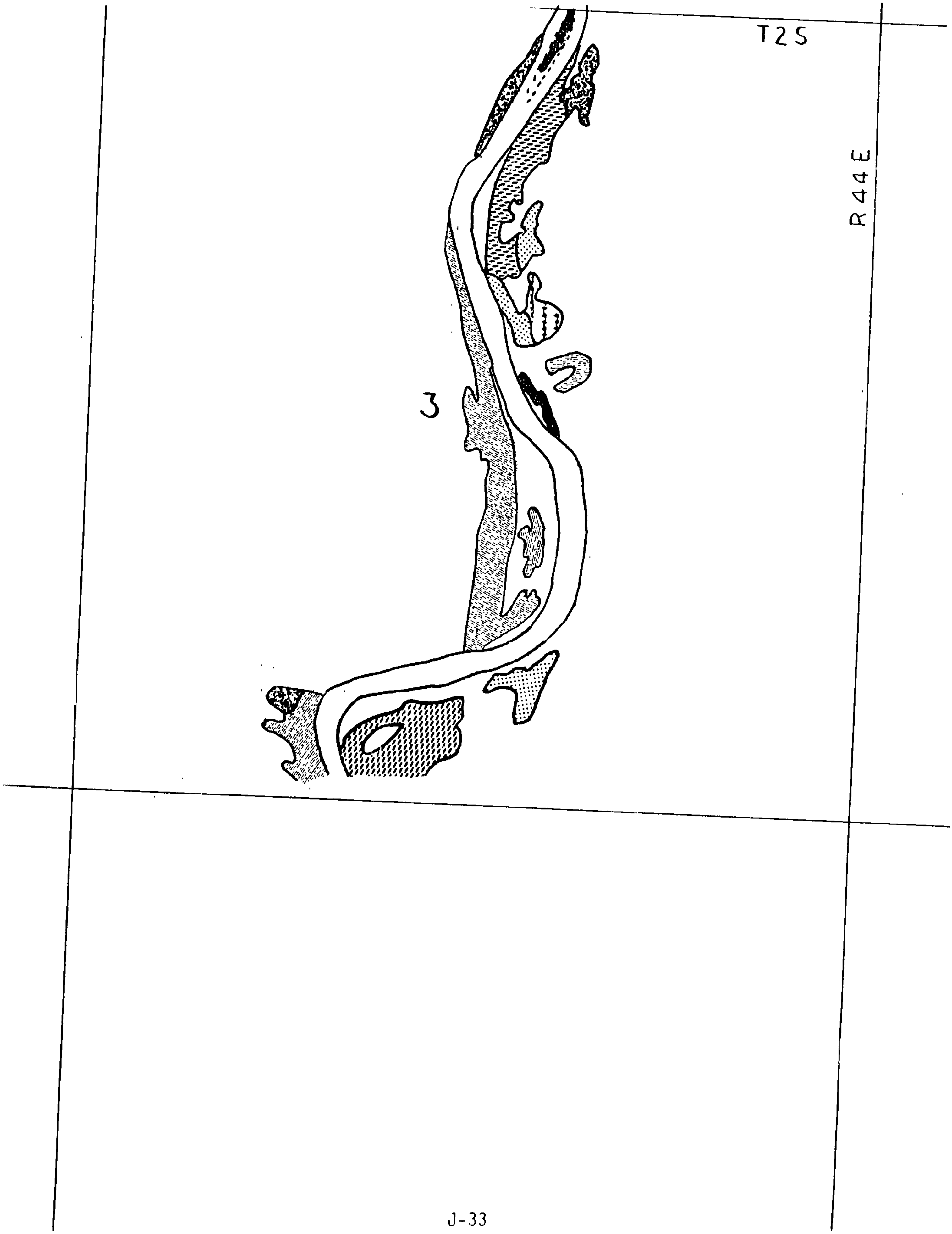
T2S
R44E
3

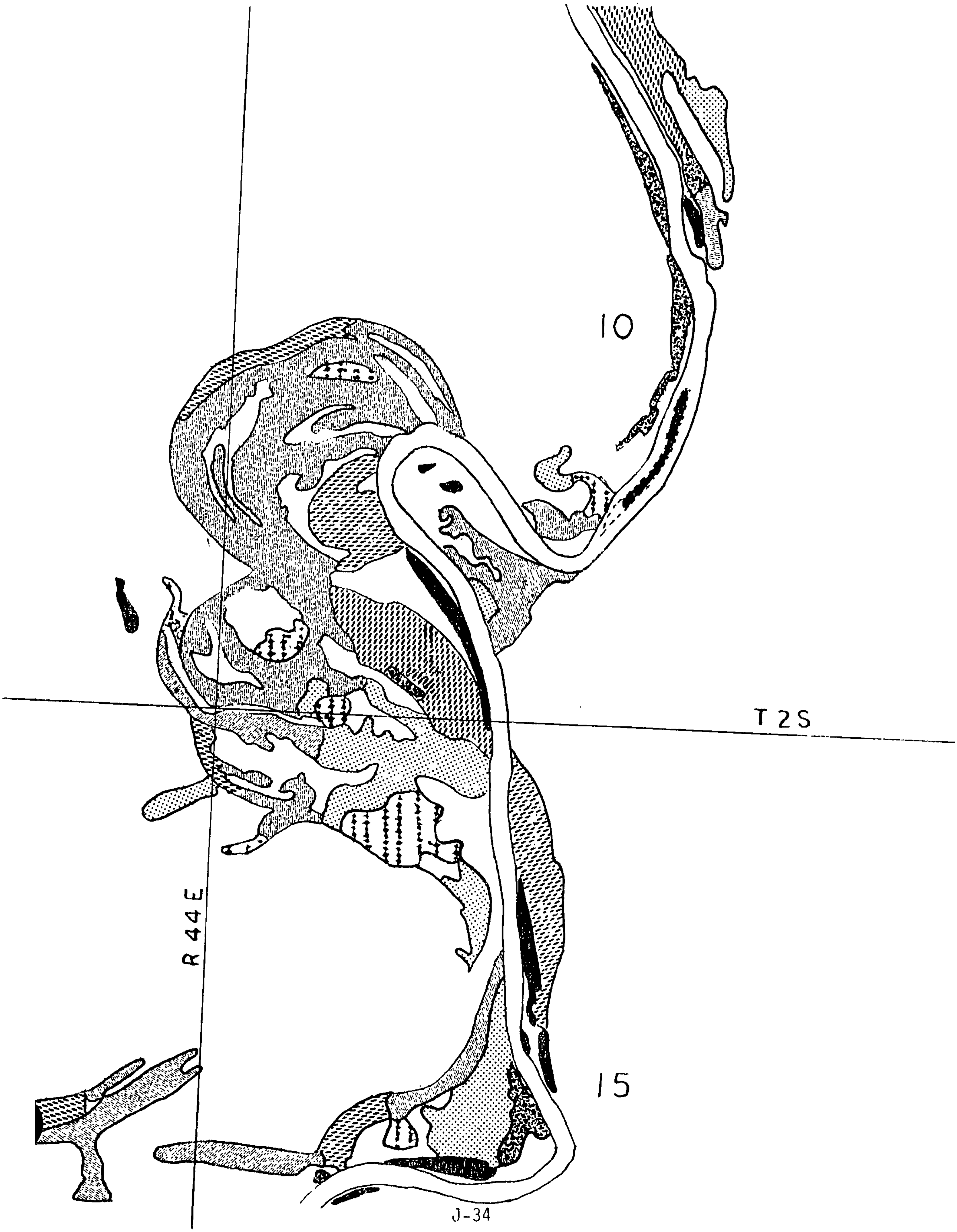
10
T 2 S
R 44 E
15

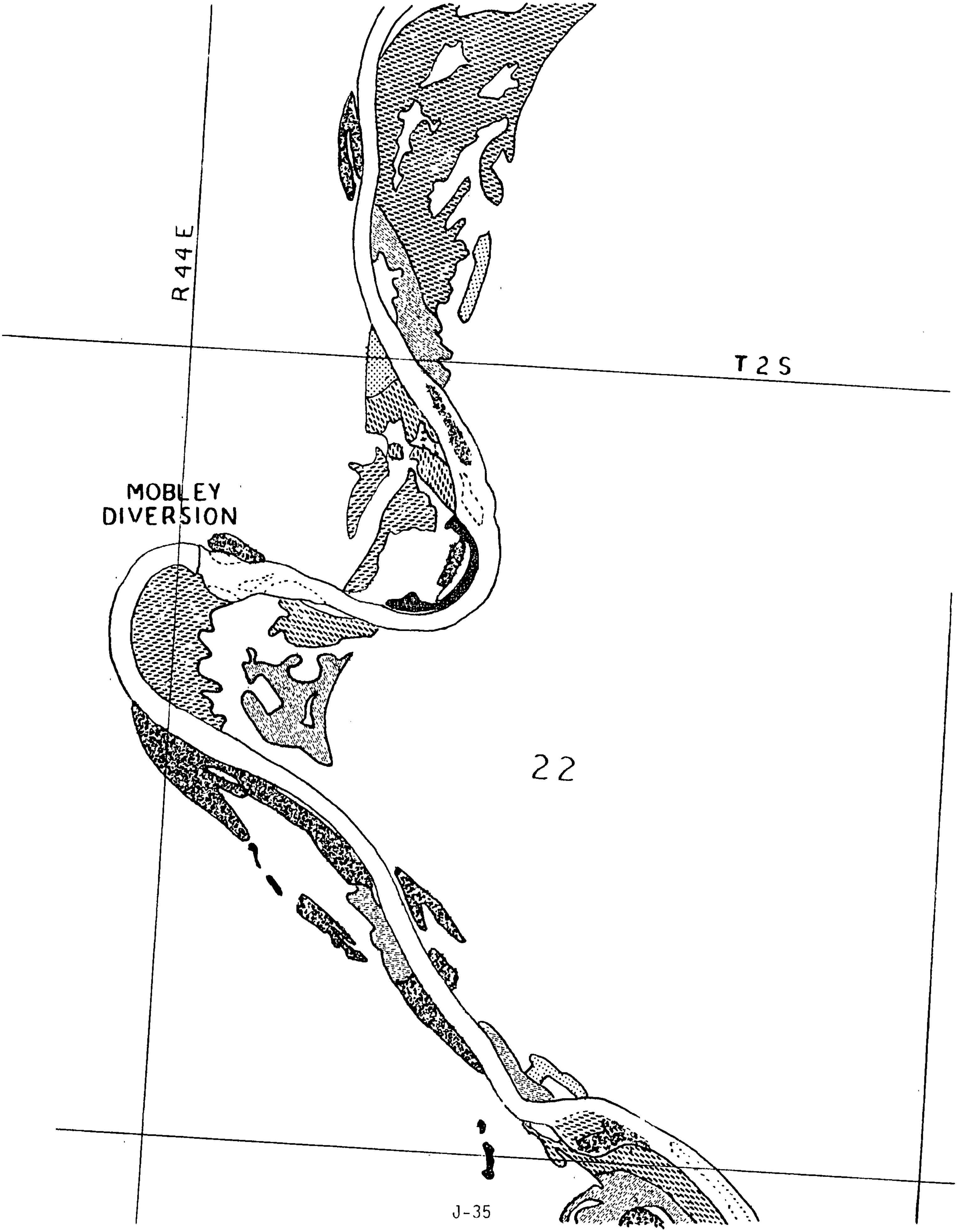
R 44 E
T 2 S
MOBLEY DIVERSION
22

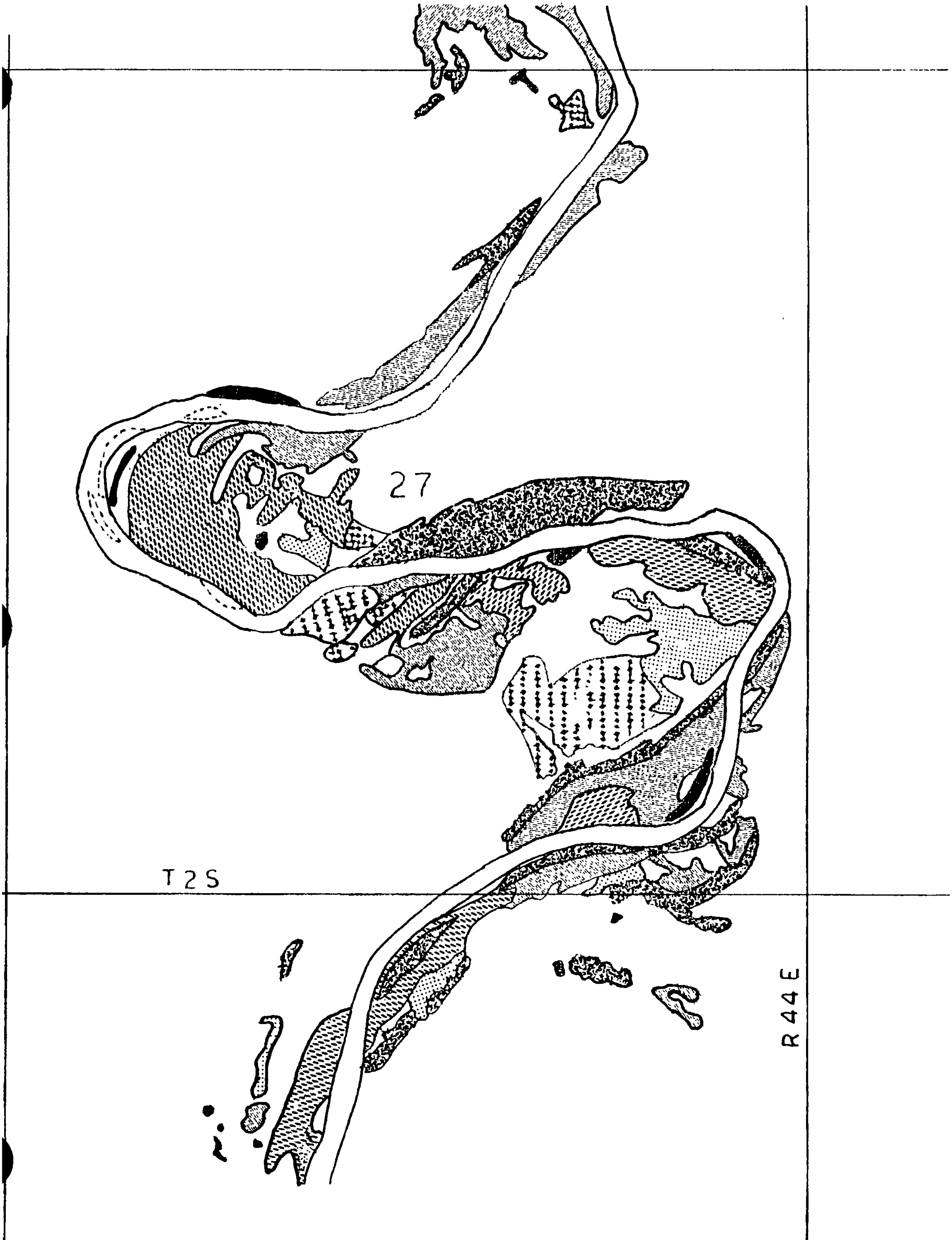
27
T2S
R44E

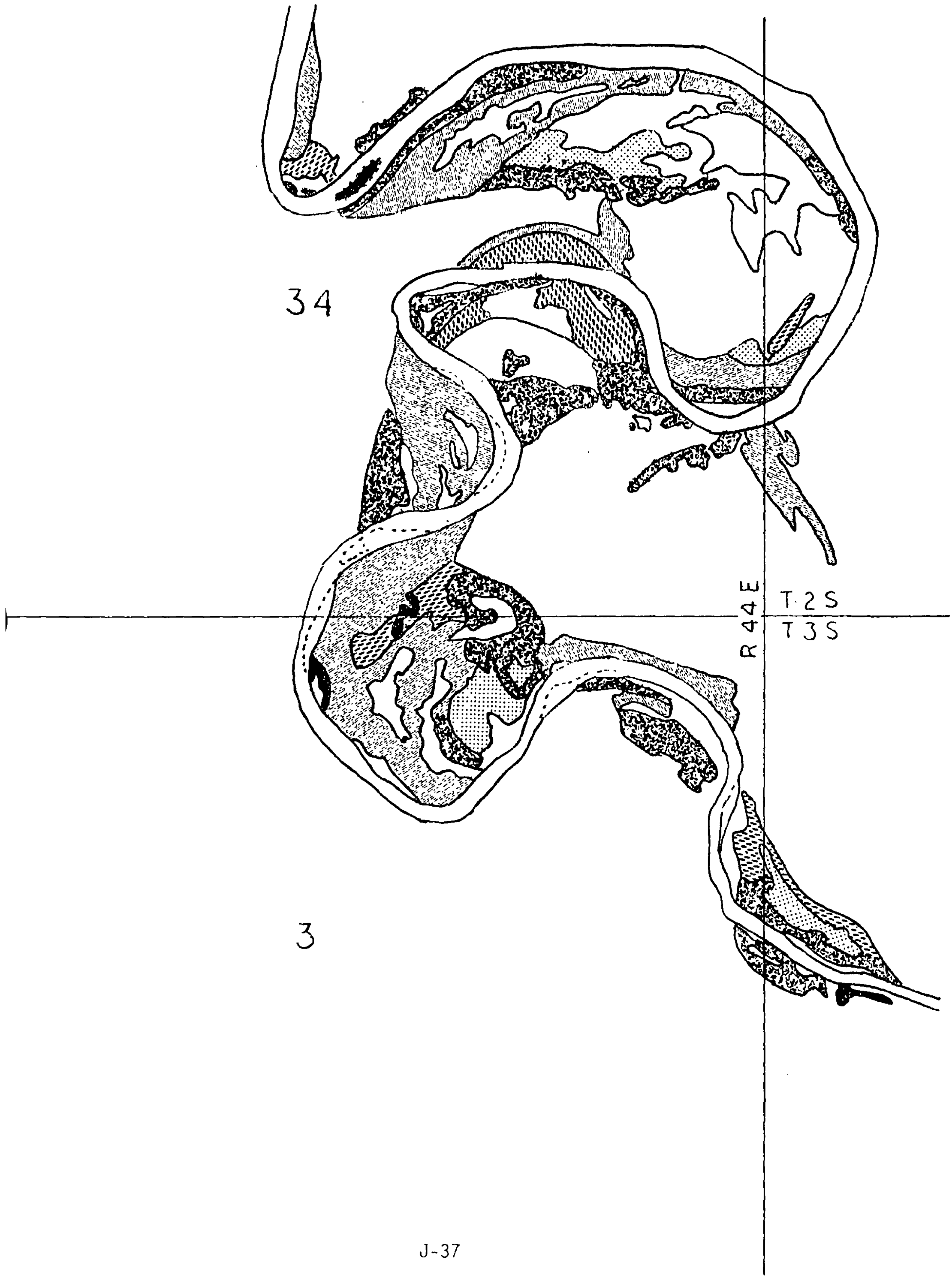
34
3
R 44 E
T 2 S
T 3 S

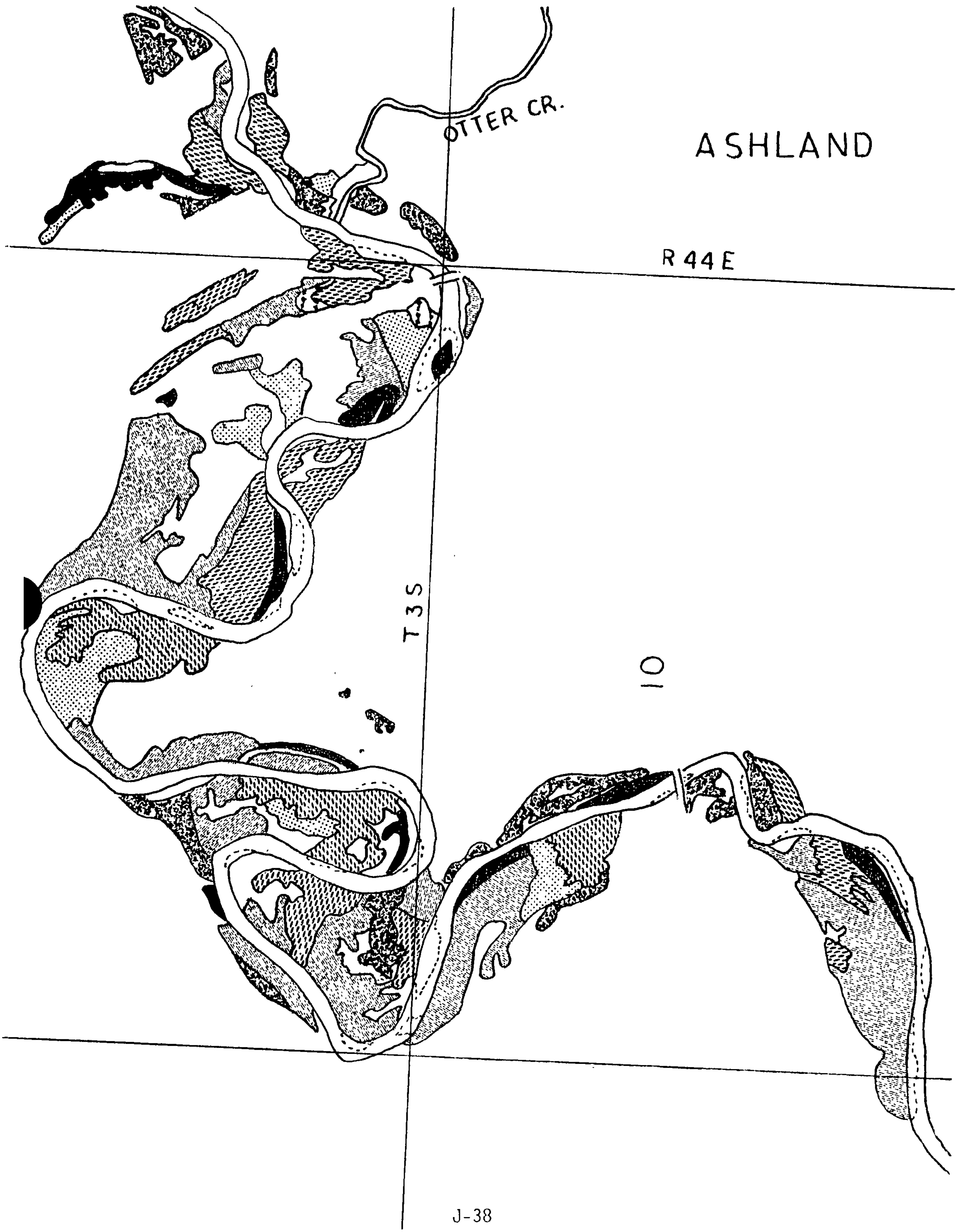
OTTER CR.
ASHLAND
R 44 E
T 3 S
10

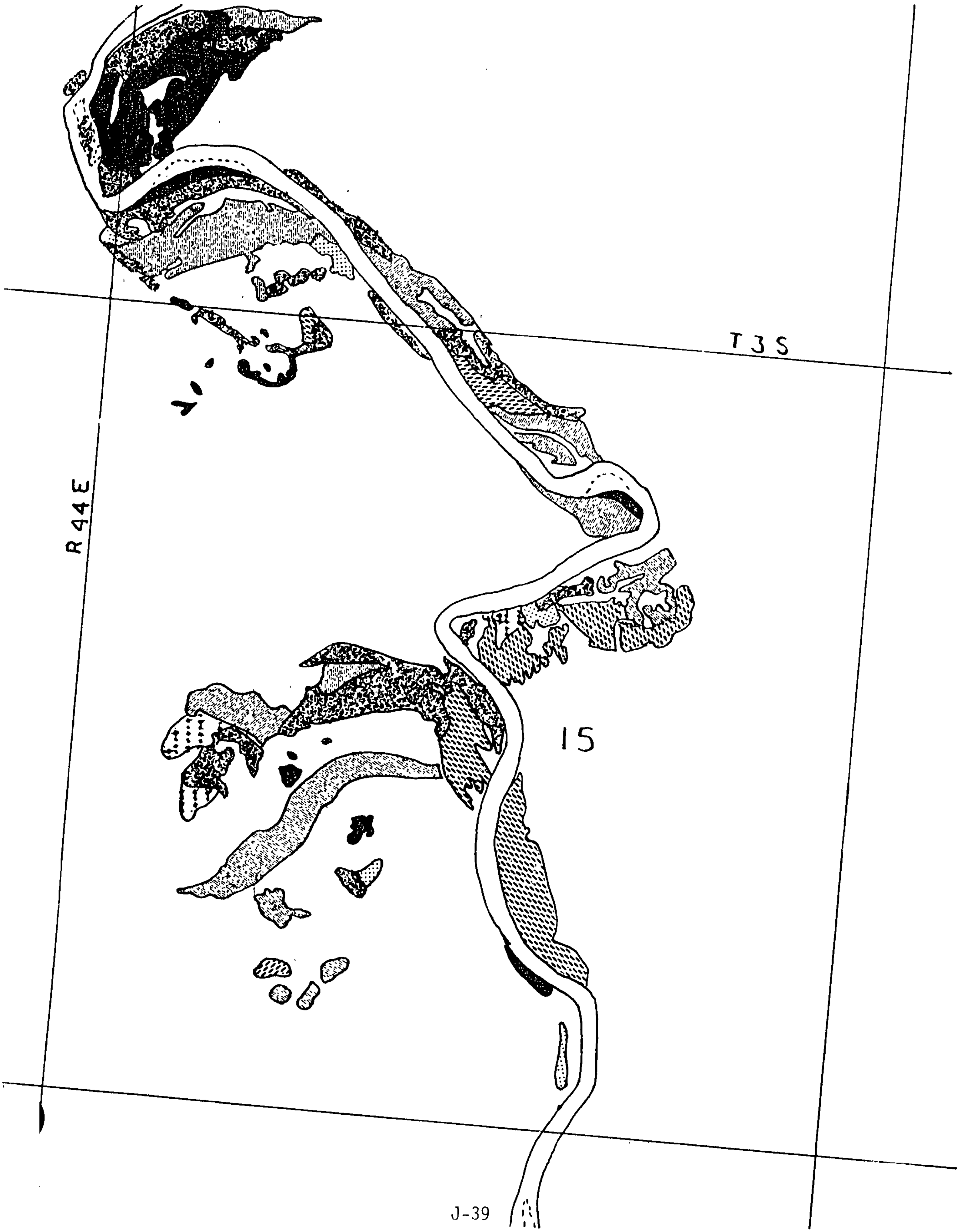
T 3 S
R 44 E
15

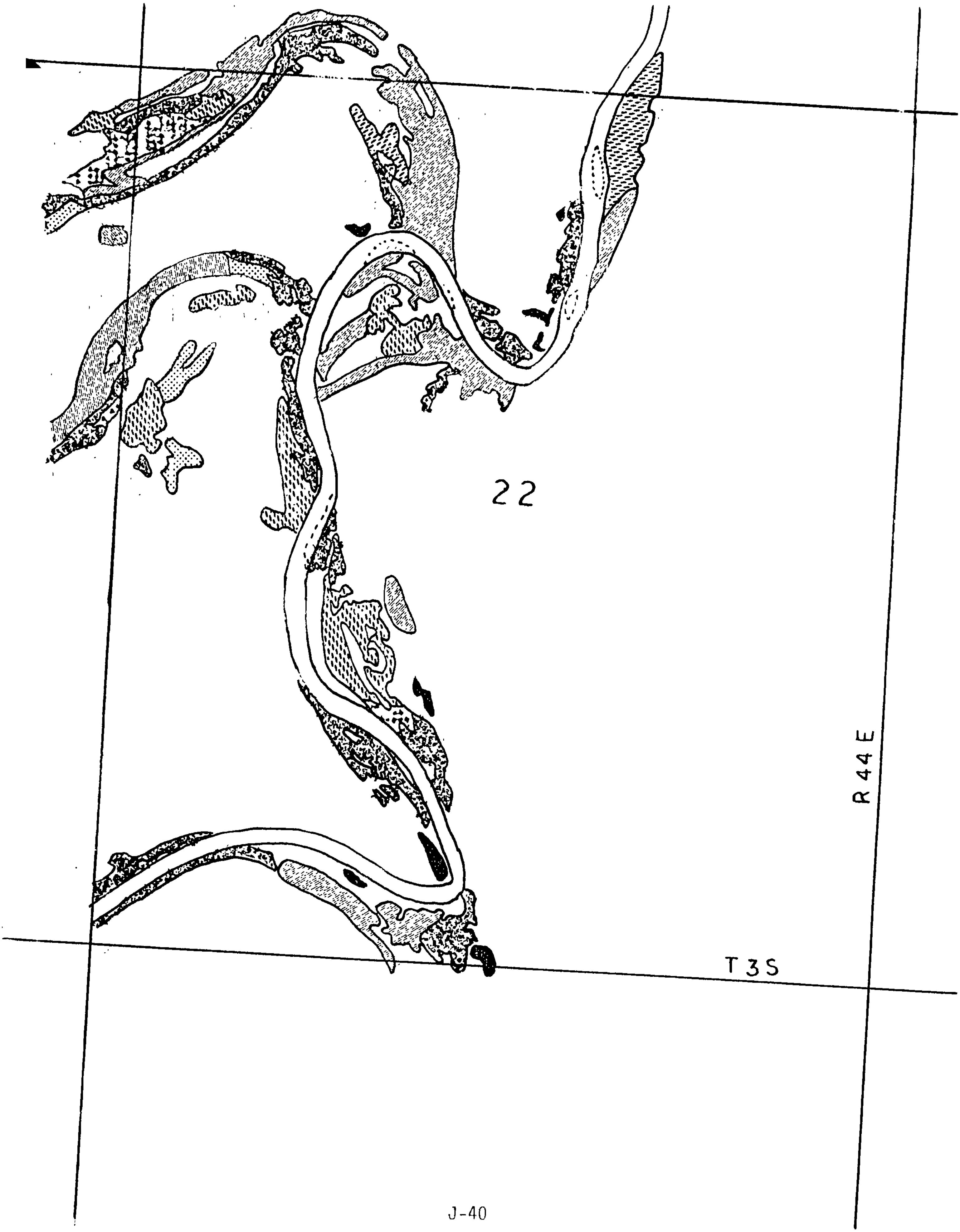
22
R 44 E
T 3 S

APPENDIX K

SEDIMENT-DISCHARGE RATING CURVES

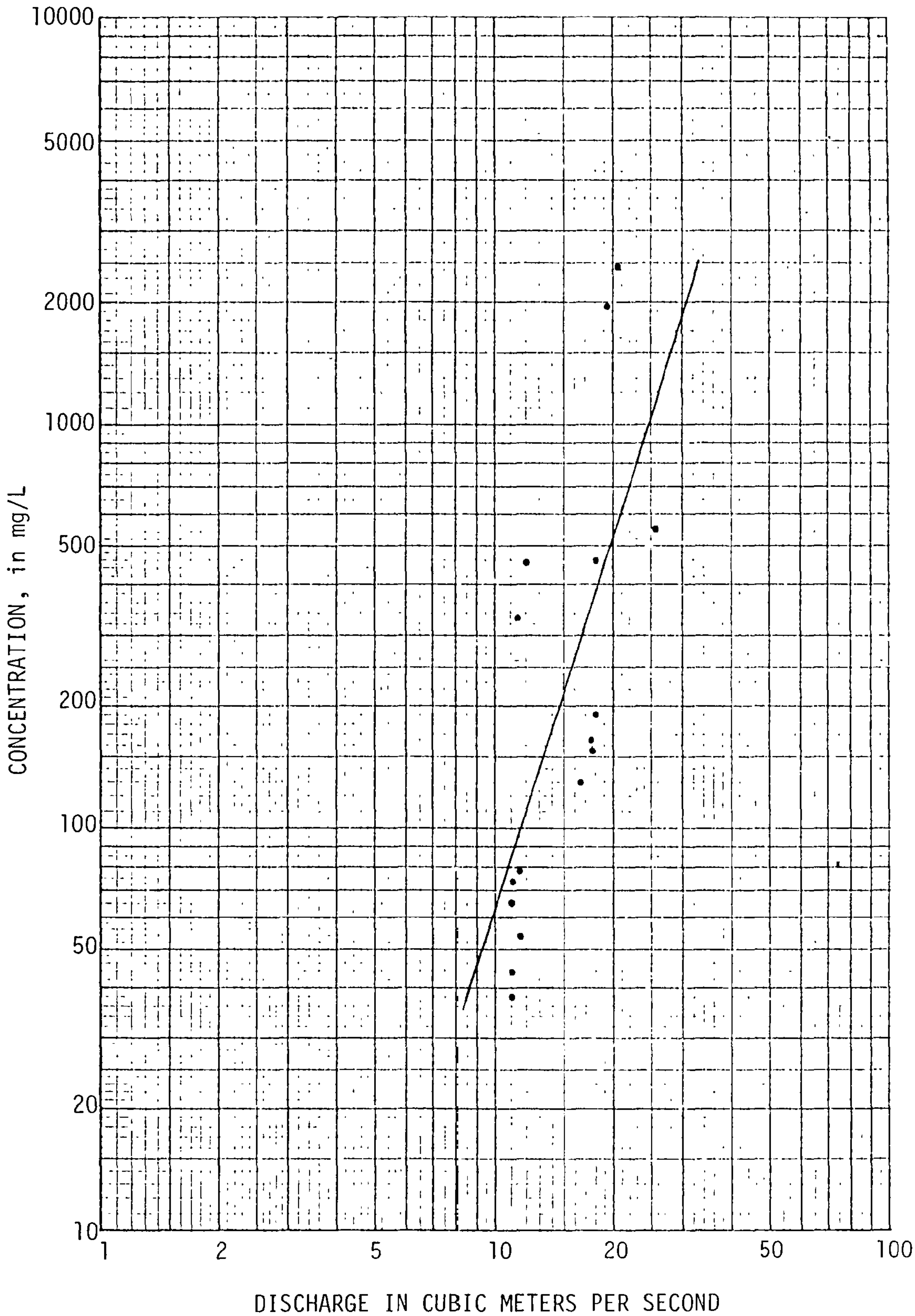

Figure K-1: Total Suspended Sediment Concentration Curve for the Ft. Keogh Section, Tongue River, Montana.

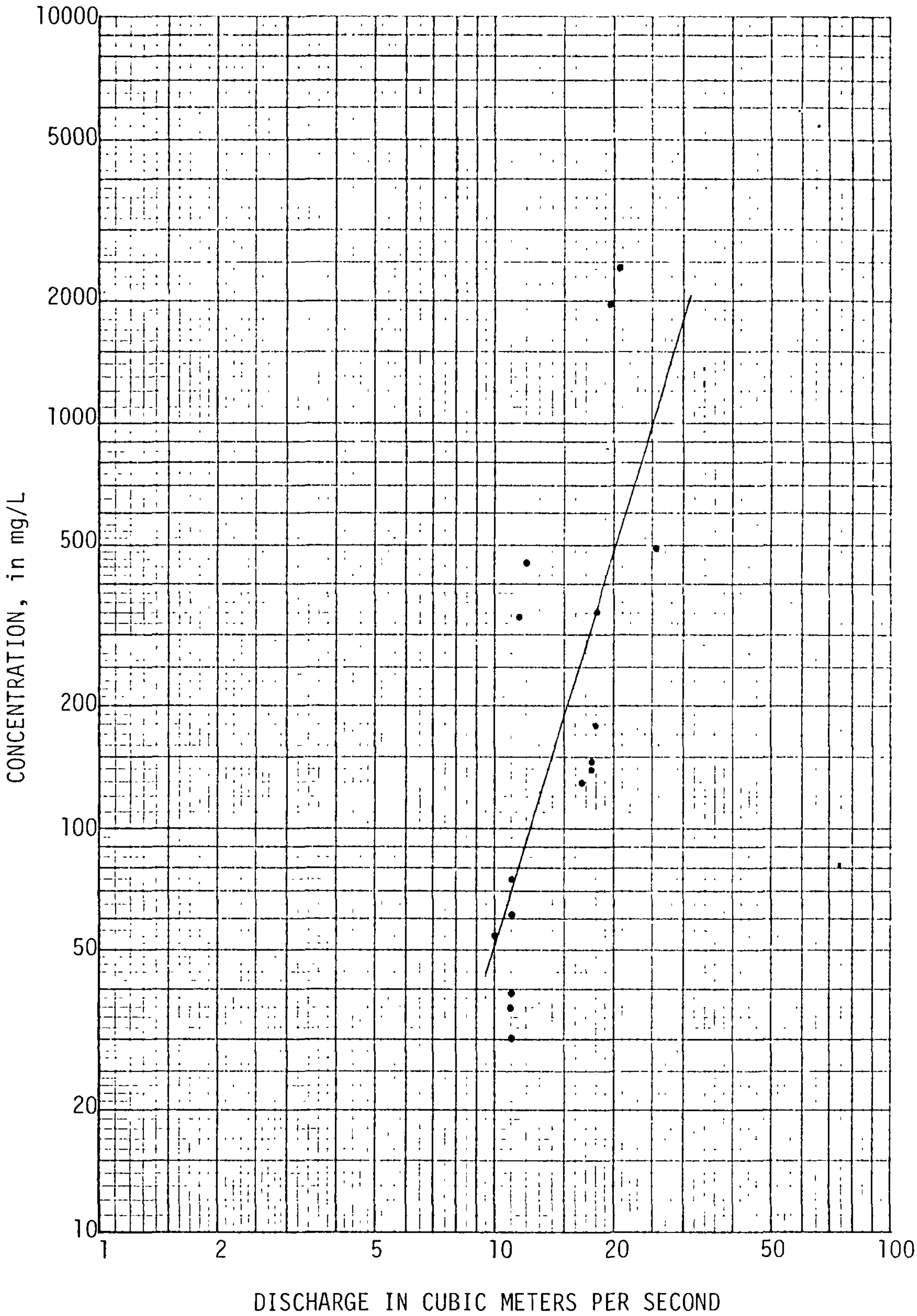

Figure K-2: Concentration of Particles Smaller than 62 Microns (Silt-Clay Fraction) as Suspended Load, Ft. Keogh Section, Tongue River, Montana.

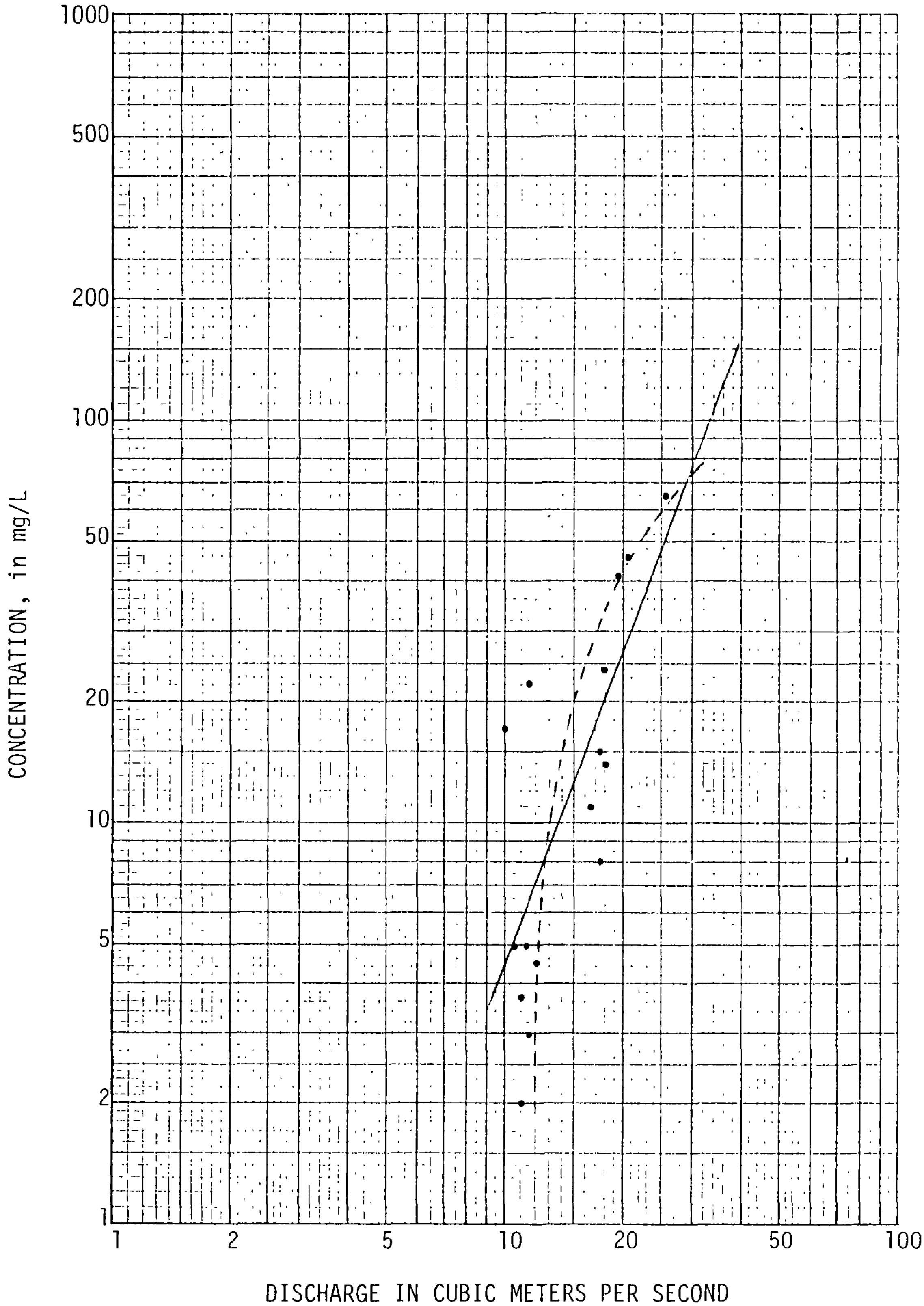

Figure K-3: Concentration of Particles Larger than 62 Microns (Sand Fraction) as Suspended Load, Ft. Keogh Section, Tongue River, Montana.

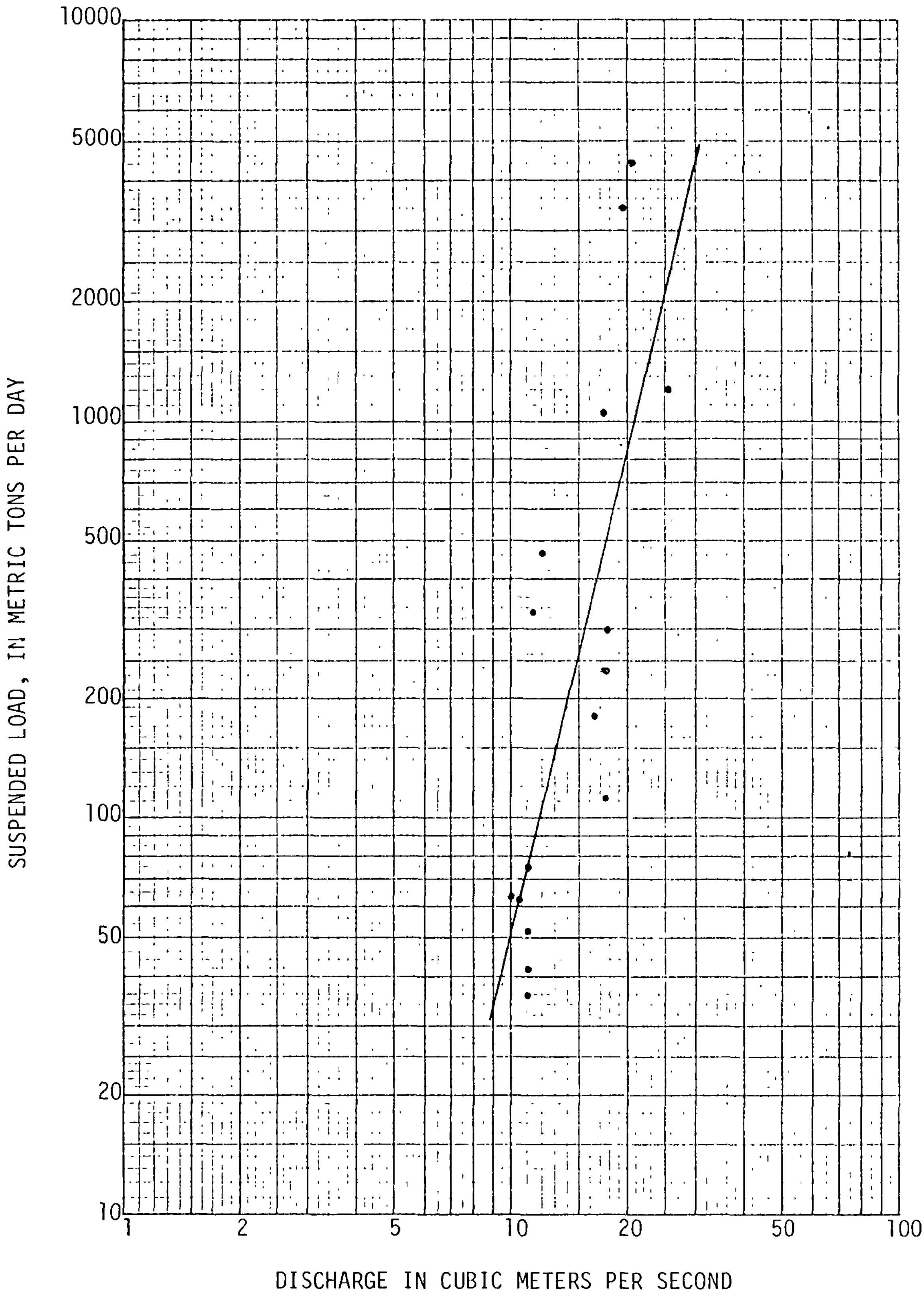

Figure K-4: Total Suspended Sediment Load Curve for the Ft. Keogh Section, Tongue River, Montana.

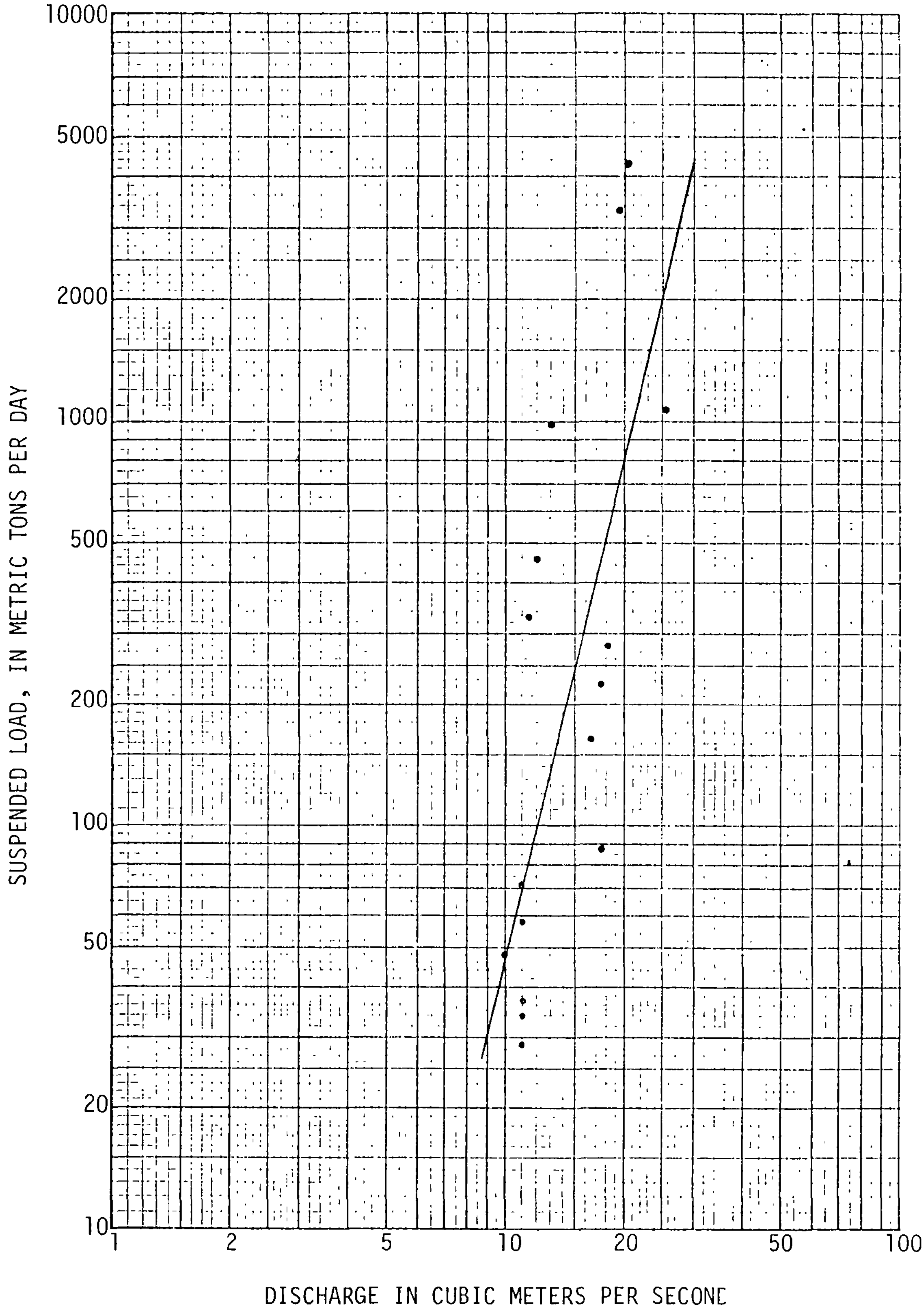

Figure K-5: Total Suspended Load Curve for Particles Smaller than 62 Microns (Silt-Clay Fraction) for the Ft. Keogh Section, Tongue River, Montana.

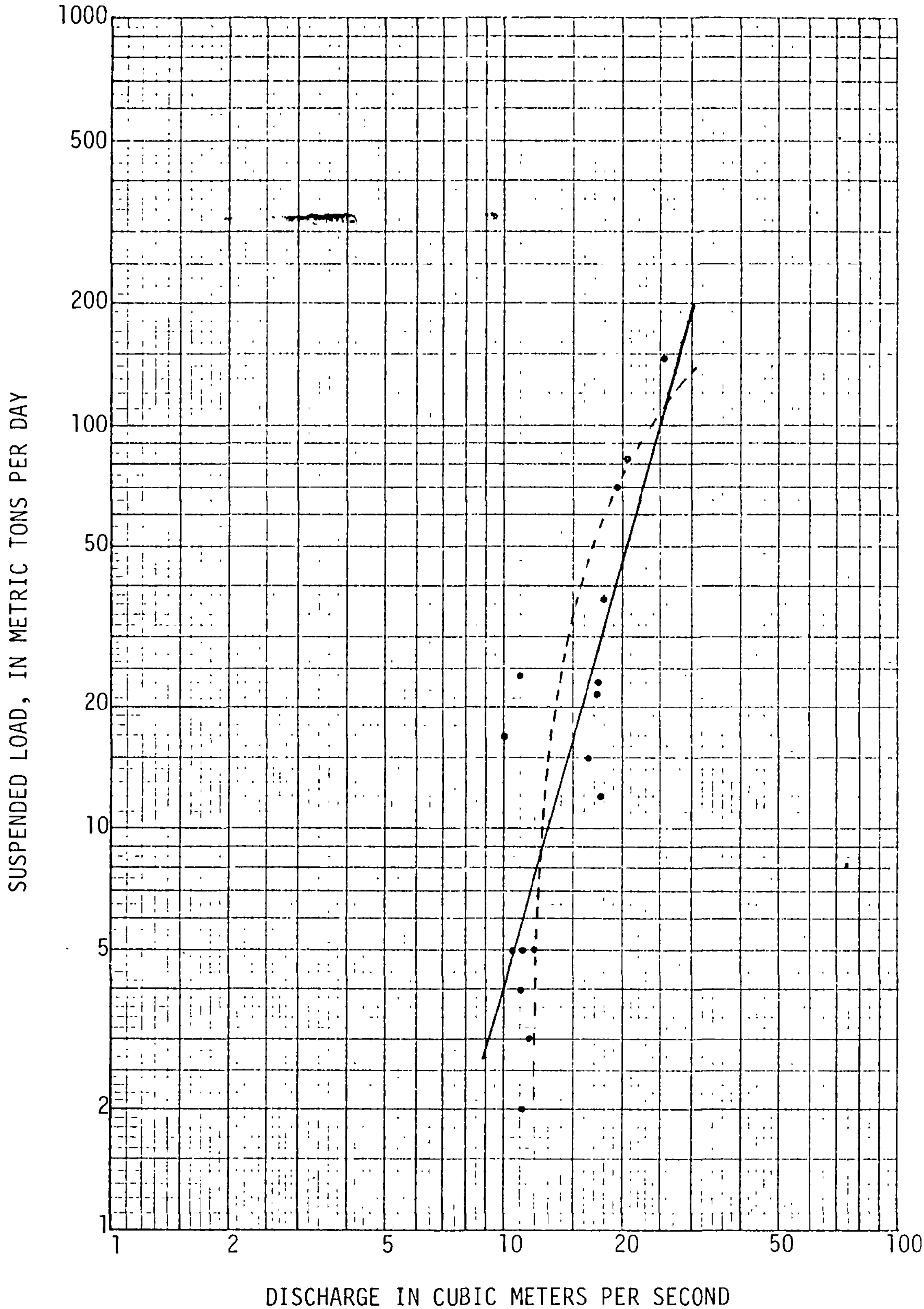

Figure K-6: Suspended Load Curve for Particles Larger than 62 Microns (Sand Fraction) for the Ft. Keogh Section, Tongue River, Montana.

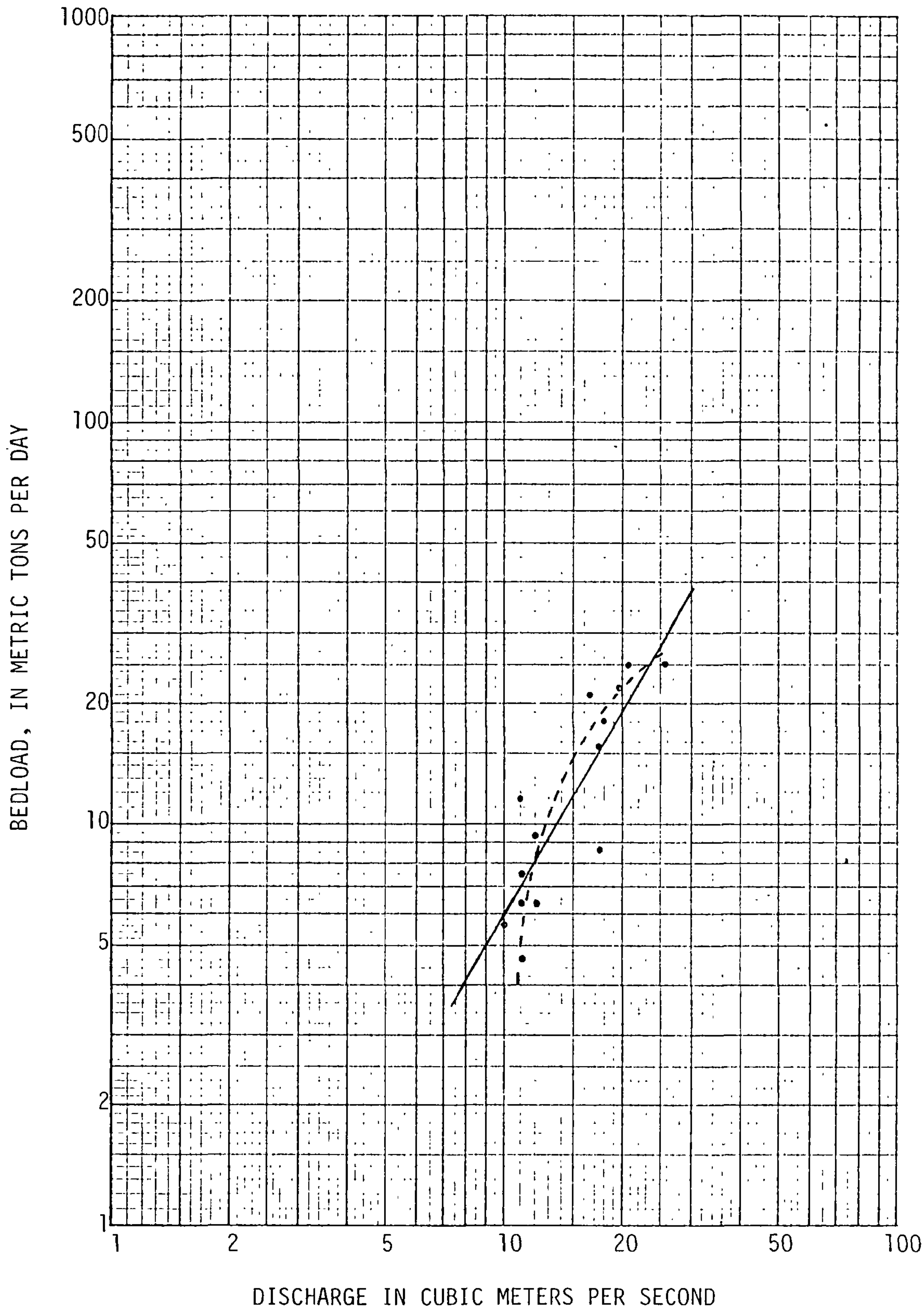

Figure K-7: Total Sediment Bedload Curve for the Ft. Keogh Section, Tongue River, Montana.

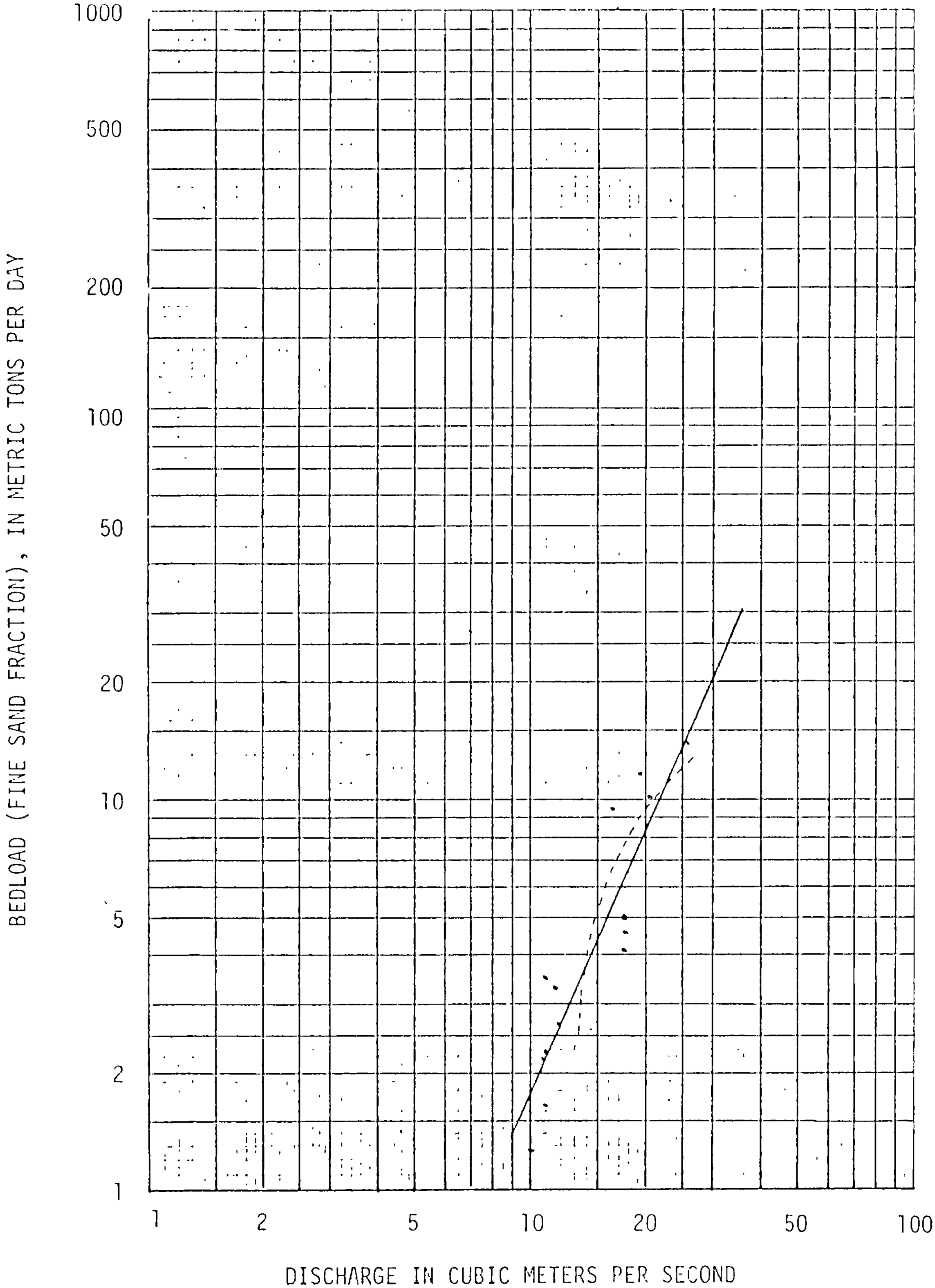

Figure K-8 : Movement of Fine Sand (125 to 250 Microns) as Bedload in the Ft. Keogh Section, Tongue River, Montana

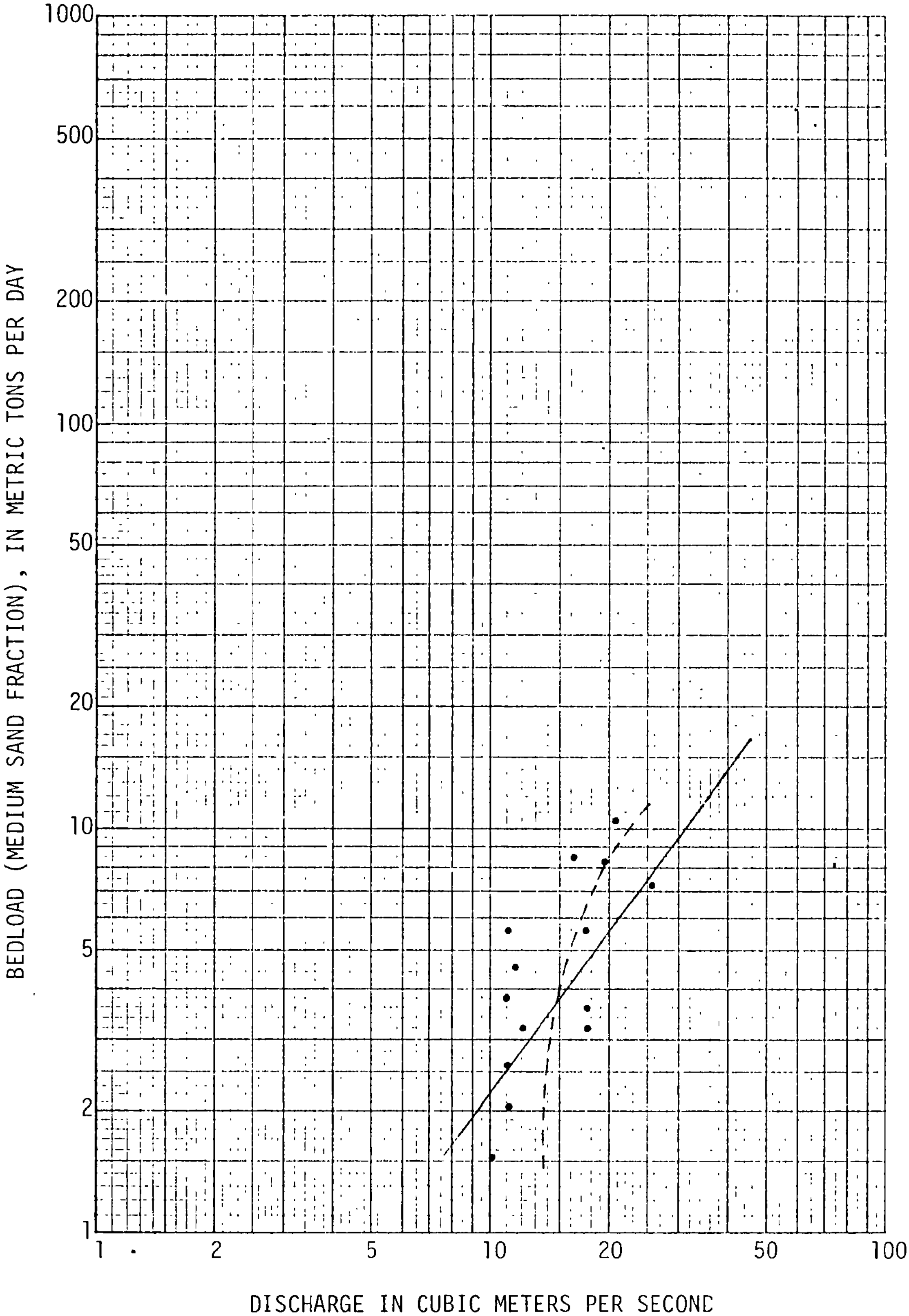

Figure K-9: Movement of Medium Sand (250 to 500 Microns) as Bedload in the Ft. Keogh Section, Tongue River, Montana.

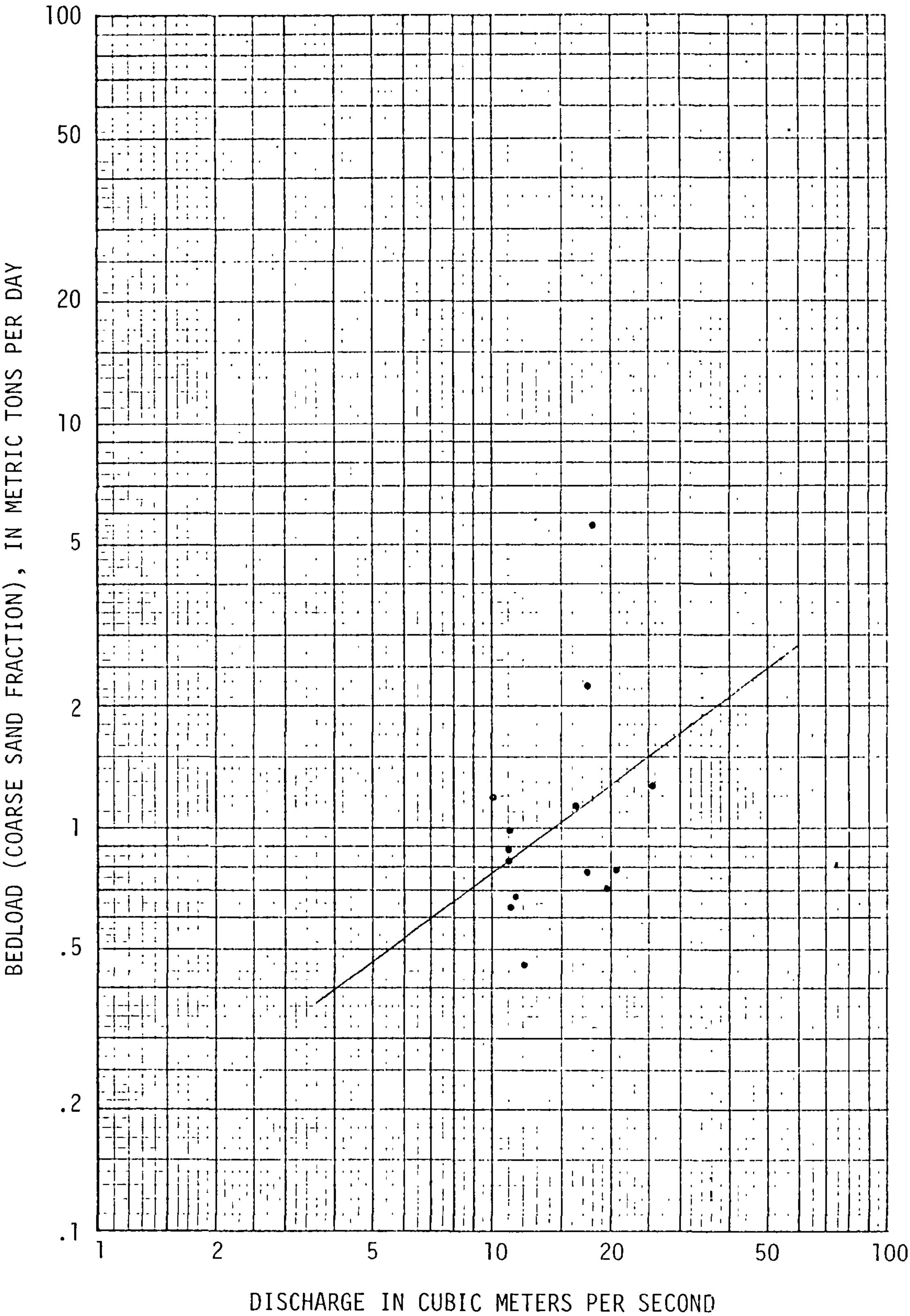

Figure K-10: Movement of Coarse Sand (500 to 1000 Microns) as Bedload in the Ft. Keogh Section, Tongue River, Montana.

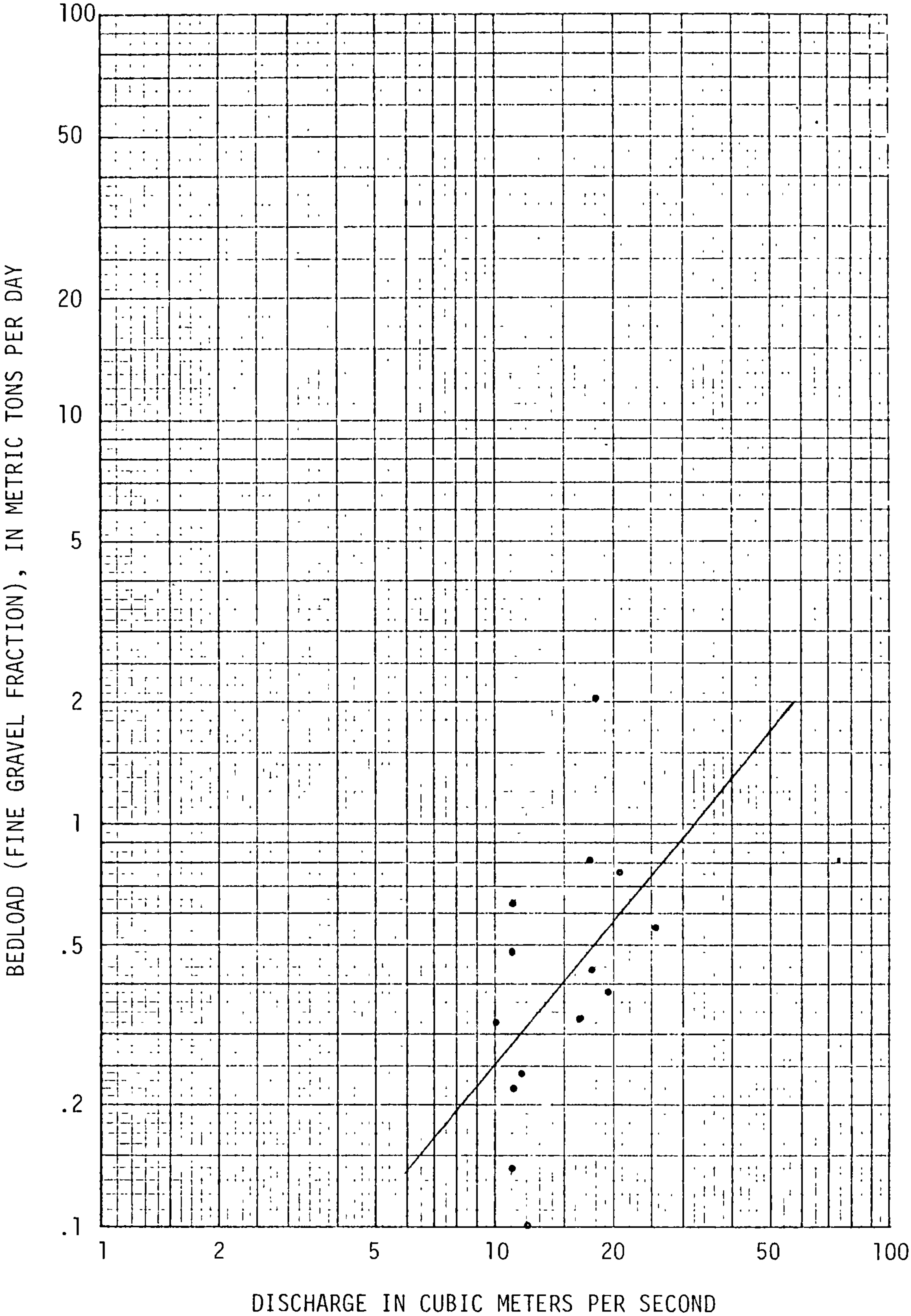

Figure K-11: Movement of Fine Gravel (1 to 2 mm) as Bedload in the Ft. Keogh Section, Tongue River, Montana.

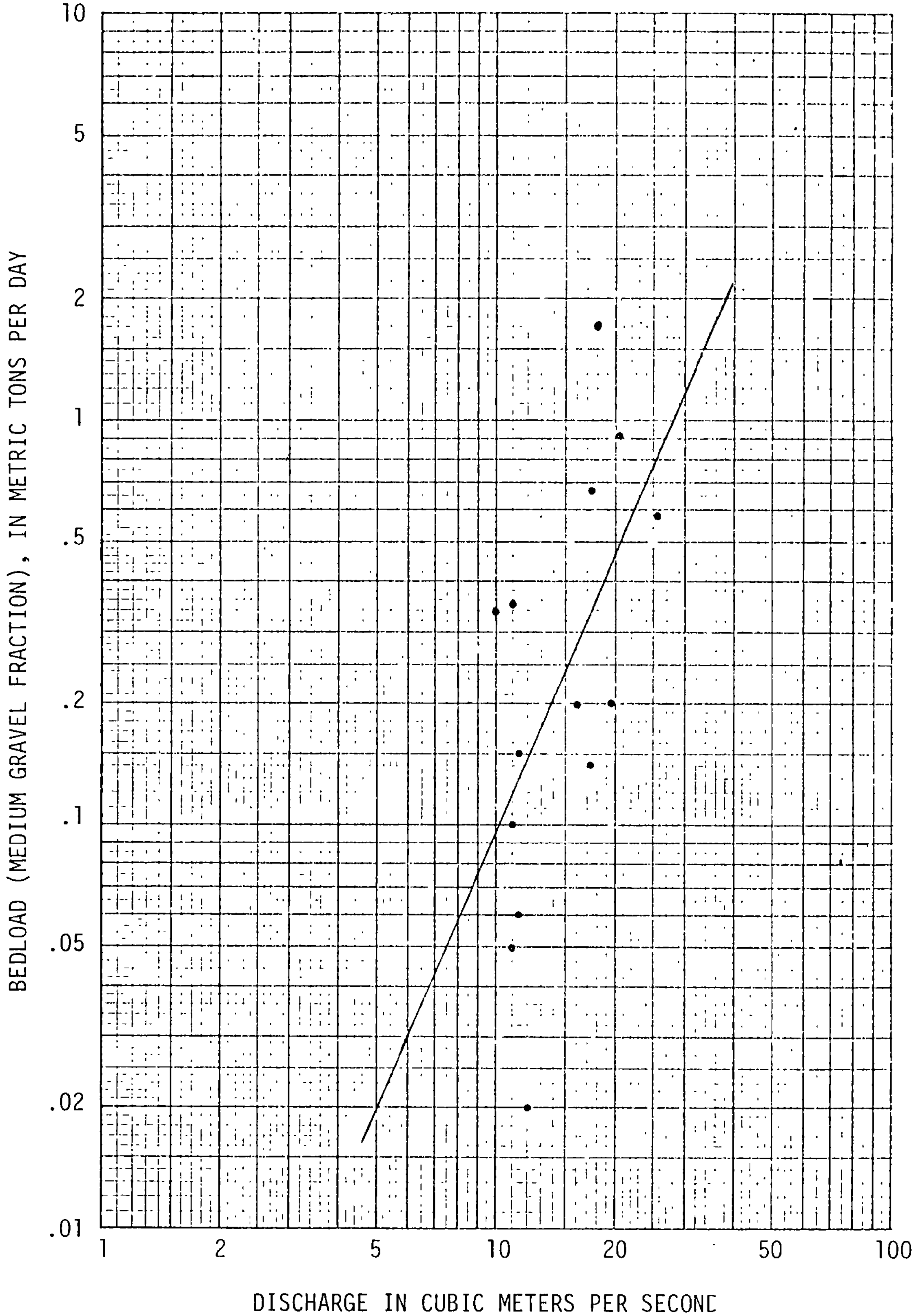

Figure K-12: Movement of Medium Gravel (2 to 4 mm) as Bedload in the Ft. Keogh Section, Tongue River, Montana.

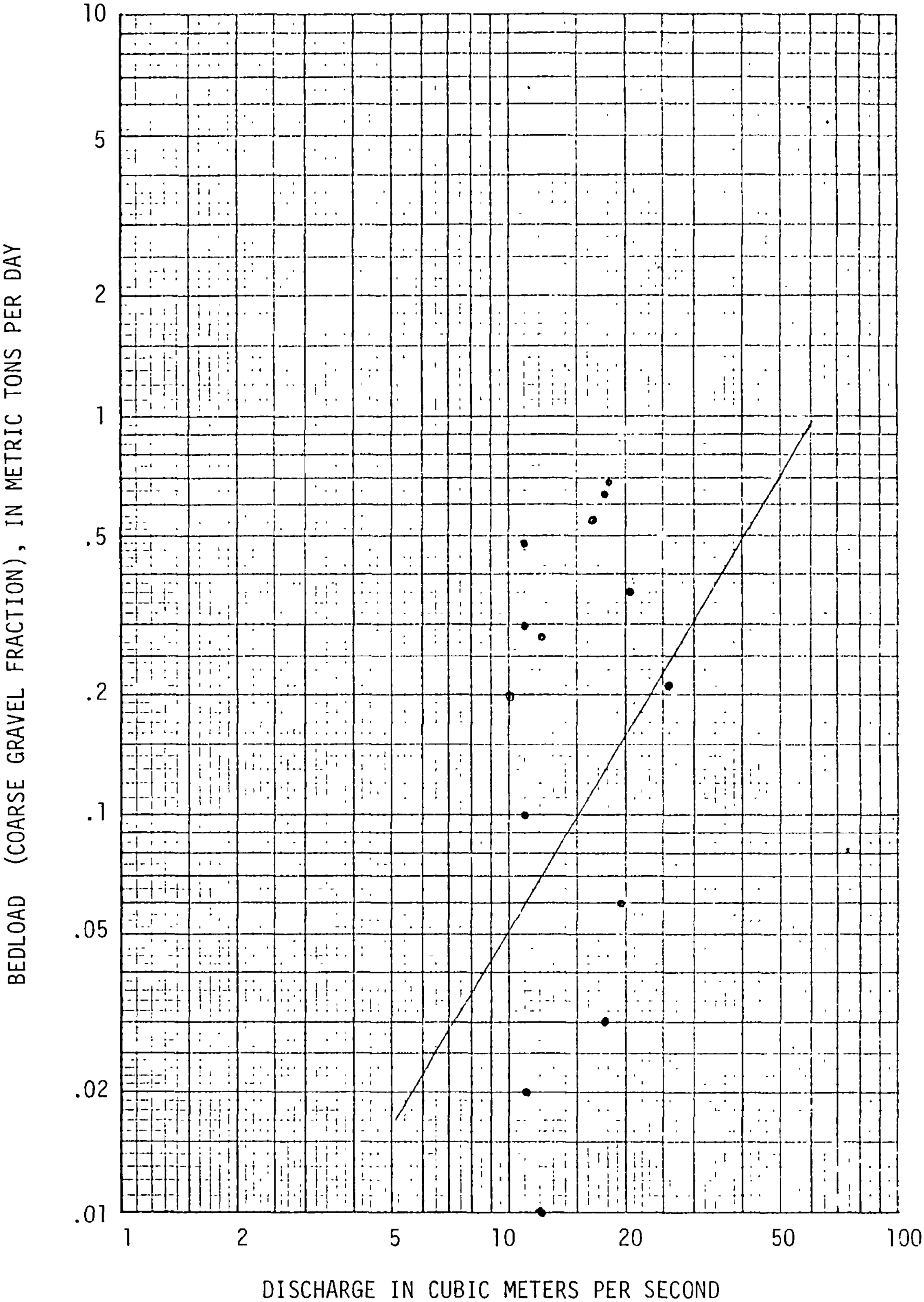

Figure K-13: Movement of Coarse Gravel (4 to 8 mm) as Bedload in the Ft. Keogh Section, Tongue River, Montana.